Frontiers | Research Topics

Efficient nitrogen fertilizer management to improve crop production

Edited by
Li Wang, Ying Zhao and Jianwei Lu

Published in
Frontiers in Plant Science

ISSN 1664-8714
ISBN 978-2-8325-4932-2
DOI 10.3389/978-2-8325-4932-2

About Frontiers

Frontiers is more than just an open access publisher of scholarly articles: it is a pioneering approach to the world of academia, radically improving the way scholarly research is managed. The grand vision of Frontiers is a world where all people have an equal opportunity to seek, share and generate knowledge. Frontiers provides immediate and permanent online open access to all its publications, but this alone is not enough to realize our grand goals.

Frontiers journal series

The Frontiers journal series is a multi-tier and interdisciplinary set of open-access, online journals, promising a paradigm shift from the current review, selection and dissemination processes in academic publishing. All Frontiers journals are driven by researchers for researchers; therefore, they constitute a service to the scholarly community. At the same time, the *Frontiers journal series* operates on a revolutionary invention, the tiered publishing system, initially addressing specific communities of scholars, and gradually climbing up to broader public understanding, thus serving the interests of the lay society, too.

Dedication to quality

Each Frontiers article is a landmark of the highest quality, thanks to genuinely collaborative interactions between authors and review editors, who include some of the world's best academicians. Research must be certified by peers before entering a stream of knowledge that may eventually reach the public - and shape society; therefore, Frontiers only applies the most rigorous and unbiased reviews. Frontiers revolutionizes research publishing by freely delivering the most outstanding research, evaluated with no bias from both the academic and social point of view. By applying the most advanced information technologies, Frontiers is catapulting scholarly publishing into a new generation.

What are Frontiers Research Topics?

Frontiers Research Topics are very popular trademarks of the *Frontiers journals series*: they are collections of at least ten articles, all centered on a particular subject. With their unique mix of varied contributions from Original Research to Review Articles, Frontiers Research Topics unify the most influential researchers, the latest key findings and historical advances in a hot research area.

Find out more on how to host your own Frontiers Research Topic or contribute to one as an author by contacting the Frontiers editorial office: frontiersin.org/about/contact

Efficient nitrogen fertilizer management to improve crop production

Topic editors
Li Wang — Shandong Academy of Agricultural Sciences, China
Ying Zhao — Ludong University, China
Jianwei Lu — Huazhong Agricultural University, China

Citation
Wang, L., Zhao, Y., Lu, J., eds. (2024). *Efficient nitrogen fertilizer management to improve crop production*. Lausanne: Frontiers Media SA.
doi: 10.3389/978-2-8325-4932-2

Table of contents

frontiers | Frontiers in Plant Science

TYPE Original Research
PUBLISHED 08 March 2023
DOI 10.3389/fpls.2023.1124664

Check for updates

OPEN ACCESS

EDITED BY
Li Wang,
Shandong Academy of Agricultural Sciences, China

REVIEWED BY
Puchang Wang,
Guizhou Normal University, China
Baohua Feng,
Chinese Academy of Agricultural Sciences, China

*CORRESPONDENCE
Chunhui Ma
chunhuima@126.com
Man Li
liman570510@126.com
Qianbing Zhang
qbz102@163.com

SPECIALTY SECTION
This article was submitted to Plant Nutrition, a section of the journal Frontiers in Plant Science

RECEIVED 15 December 2022
ACCEPTED 20 February 2023
PUBLISHED 08 March 2023

CITATION
Zhao J, Huang R, Wang X, Ma C, Li M and Zhang Q (2023) Effects of combined nitrogen and phosphorus application on protein fractions and nonstructural carbohydrate of alfalfa.
Front. Plant Sci. 14:1124664.
doi: 10.3389/fpls.2023.1124664

Effects of combined nitrogen and phosphorus application on protein fractions and nonstructural carbohydrate of alfalfa

Jiantao Zhao[1], Rongzheng Huang[1], Xuzhe Wang[1], Chunhui Ma[1*], Man Li[2*] and Qianbing Zhang[1*]

[1]College of Animal Science and Technology, Shihezi University, Shihezi, China, [2]College of Medicine, Shihezi University, Shihezi, China

Nitrogen (N) and phosphorus (P) fertilization significantly affect alfalfa production and chemical composition; however, the effect of combined N and P application on protein fractions and the nonstructural carbohydrate content of alfalfa is not fully understood. This two-year study investigated the effects of N and P fertilization on the protein fractions, nonstructural carbohydrates (NSC), and alfalfa hay yield. Field experiments were carried out using two nitrogen application rates (N60, 60 and N120, 120 kg N ha^{-1}) and four phosphorus application rates (P0, 0; P50, 50; P100, 100; and P150, 150 kg P ha^{-1}), total 8 treatment (N60P0, N60P50, N60P100, N60P150, N120P0, N120P50, N120P100 and N120P150). Alfalfa seeds were sown in the spring of 2019, uniformly managed for alfalfa establishment, and tested in the spring of 2021–2022. Results indicated that P fertilization significantly increased the hay yield (3.07–13.43% ranges), crude protein (6.79–9.54%), non-protein nitrogen of crude protein (fraction A) (4.09–6.40%), and NSC content (11.00–19.40%) of alfalfa under the same treatment of N application ($p < 0.05$), whereas non-degradable protein (fraction C) decreased significantly (6.85–13.30%, $p < 0.05$). Moreover, increasing N application resulted in a linear increase the content of non-protein N (NPN) (4.56–14.09%), soluble protein (SOLP) (3.48–9.70%), and neutral detergent-insoluble protein (NDIP) (2.75–5.89%) ($p < 0.05$), whereas acid detergent-insoluble protein (ADIP) content was significantly decreased (0.56–5.06%, $p < 0.05$). The regression equations for nitrogen and phosphorus application indicated a quadratic relationship between yield and forage nutritive values. Meanwhile, the comprehensive evaluation scores of NSC, nitrogen distribution, protein fractions, and hay yield by principal component analysis (PCA) revealed that the N120P100 treatment had the highest score. Overall, 120 kg N ha^{-1} coupled with 100 kg P ha^{-1} (N120P100) promoted the growth and development of perennial alfalfa, increased soluble nitrogen compounds and total carbohydrate content, and reduced protein degradation, thus improving the alfalfa hay yield and nutritional quality.

KEYWORDS

alfalfa, nitrogen and phosphorus combined, protein fractions, nonstructural carbohydrate, hay yield

1 Introduction

Due to the increasing population, forage quality and yield issues are becoming increasingly important for animal production. Alfalfa is widely planted as high-quality forage because of its good palatability, high crude protein content, and high hay yield (Yuan et al., 2022). In recent years, with the development of large-scale and standardized animal husbandry, the demand for high-quality and yield forage has increased year by year, which has led to an intense increase in the demand for alfalfa. The shortage of high-quality roughage and the quantity of imported alfalfa hay cannot meet the needs of the husbandry, and the situation is getting more and more serious. A low nutritional value of forage could be due to poor soil fertility and the absence or low level of fertilization (Alencar et al., 2018). Xinjiang is in an arid to semi-arid area of the Asian, with little rainfall all year round, an arid climate, and strong evaporation. Alfalfa is widely planted in the region because of its strong nitrogen fixation ability and high drought and cold resistance. Nitrogen (N) and phosphorus (P) play important roles in plant function, which is affected by limiting nutrients in ecosystems (Luo et al., 2013). Previous studies have observed that the improved nutritional quality of forage grasses is due to the fact that N fertilization enhanced crude protein and reduced crude fiber contents (Sun et al., 2022). P is an essential and abundant element that plays a vital role in plant growth and development. It was found that adding P fertilizer improved the quality and yield of alfalfa through three consecutive years of field trials (Zhang et al., 2020a). Studies have shown that the quality and yield of alfalfa are more significantly affected by the combination of N and P than by single N or P fertilization (Gu et al., 2022). However, excessive P application under N-deficient conditions might not be beneficial. Previous studies on the interplay between N and P emphasized a reduction in forage yield induced by N deficit and the reciprocal impact of P deficiency on forage quality (Zhang et al., 2021). Therefore, the balanced application of N and P is important for improving forage yield and quality.

In addition to high yields, excellent forage nutritive value is the most desirable goal because of its direct impact on the profitability of forage production and the livestock enterprises it supports. In forages, the concentration of protein, starch and soluble sugars are essential because, when consumed by the animals, these are supplied to the rumen microbes and therefore affect animal maintenance and production. The nonstructural carbohydrates (NSC), which play different roles in plant energy metabolism, transportation, and storage carbohydrates, are mainly starch and soluble sugars (Hartmann and Trumbore, 2016). The NSC content not only reflects the balance between plant carbon uptake (photosynthetic assimilation) and carbon consumption (respiration and growth) but also indirectly indicates the growth and nutritional value of the plant. Studies on the effects of N fertilizer addition on changes in NSC content have not yet reached a definite conclusion. It was found that the content of starch, soluble sugars, and NSC in *Reaumuria soongorica* leaves was increased by N fertilization (Zhang et al., 2020b). However, it was also found that N fertilizer addition reduces the NSC content of maize leaves (Wu et al., 2020). However, adequate information regarding the nutritional value of grasses in terms to improve the profile of protein fractions with fertilization is lacking. Given the high cost of chemical fertilization and the pollution of agricultural soils by excessive application, it is critical to determine the best fertilization strategy to improve yields and quality and reduce the cost of alfalfa production in semi-arid regions.

Protein and carbohydrates are the most important nutrients in determining animal performance, and their content and availability vary with fertilization levels and management practices. The Cornell Net Carbohydrate and Protein System (CNCPS) is increasingly used to assess the nutritional value of feeds, enabling an accurate representation of the nutrient content of feeds based on the solubility of each fraction in the rumen. CNCPS accurately splits the nutrient content of feed and accurately predicts the nutritional requirements and production performance of ruminants. Reduced animal performance is partly due to different fertilization levels and strategies to reduce the concentration and availability of protein in the forage. Previous studies have observed that the improved nutritional quality of forage grasses is due to N fertilization increasing nitrogen compounds (non-protein nitrogen (NPN) and soluble protein (SOLP)) (Berca et al., 2021). It has been found that applying N fertilization can improve the quality of forage by increasing the total degradable and true protein contents (Leite et al., 2021). However, adequate information regarding the nutritional value of alfalfa in terms of improving the profile of protein fractions by using different combined N and P application strategies is lacking. Therefore, the purpose of this study is to find the optimal ratio of nitrogen and phosphorus to improve the quality and yield of alfalfa high-quality forage, and thus improve the livestock productivity. The present study hypothesized that the concentrations of non-protein nitrogen of crude protein (fraction A) would increase, and the starch and soluble sugar contents would increase with N and P fertilization. Therefore, to test this hypothesis, we conducted a 2-year field trial. The hay yield was used to evaluate plant growth, the starch and soluble sugar contents were used to study the dynamic changes in NSC, and the fraction A and ruminal degradable protein (fraction B) contents were used to study the dynamic changes in CNCPS and to evaluate the quality of alfalfa.

2 Materials and methods

2.1 Experimental site description

The field experiments were conducted in 2021 and 2022 at the Water-saving Irrigation Experiment Station of Shihezi University, Shihezi (44°20′ N, 88°30′ E, 450.8 m above sea level), located in Xinjiang Province, Northwest China. The climate is temperate continental, dry and with little rain. The average annual temperature is 7°C, the frost-free period is 168~171 d, the annual precipitation is 190~260 mm, the annual evaporation is 1000~1500 mm and the average annual sunshine time is 2770 h. Soil properties measured before the experiment were as follows; total nitrogen 1.18 g kg^{-1}, alkaline nitrogen 145.47 mg·kg^{-1}, total phosphorus

0.53 g·kg^{-1}, available phosphorus 19.30 mg·kg^{-1}, potassium 119.8 mg·kg^{-1}, density 1.54 g·cm^{-3}, and organic matter 39.5 g·kg^{-1}.

2.2 Experimental design and treatments management

Alfalfa stand was established in 2019, uniformly managed for alfalfa establishment, and they were tested in spring 2021–2022, with a seeding drill at rate of 18 kg·ha^{-1}, the row spacing of 20 cm, the sowing depth was 2.0 cm and a plot area of 24 m^2 (4 m×6 m). In this way, the experiment comprised of eight treatments, and each was replicated three times in a two-factor completely randomized design. The N application rates were 60 (N60) and 120 (N120) kg·ha^{-1} (as urea equivalent), and the P application rates included 0 (P0), 50 (P50), 100 (P100) and 150 (P150) kg·ha^{-1} (as P_2O_5 equivalent). The N was added as urea (46% total N) and P was added as monoammonium phosphate (with a low amount of N) (52% P_2O_5, 12.2% total N, respectively), because they are the commonly used fertilizers in the study area. After P fertilizer was applied, the imbalance in N treatments was balanced by the additional applications of N fertilizer to maintain the same N application rate in the different P treatments. The fertilizer was added to the fertilizer tank and applied together with water at the green-up stage (19 April 2021 and 25 April 2022) and 3–5 d after the first, second and third clippings (27 May, 3 July, 4 August, 2021, 30 May, 4 July, 3 August 2022).

2.3 Plant material and growth measurements

Alfalfa was harvested at the early flowering stage (10% of blooming), four times per year. However, this trial involved only the first clipping of alfalfa and was harvested on May 27 and 30 in 2021 and 2022, respectively. At harvest, three representative sample squares (1 m × 1 m), cut approximately 5 cm high, were randomly selected in the center of each plot and used to determine alfalfa yield. The samples were oven dried at 105°C for 30 min and then oven dried at 65°C to a constant weight for determining the dry biomass of fodder. Hay yield was determined using dry matter (Fan et al., 2016). Dried plant samples were ground into fine powder to pass through a 0.04 in screen and used for nutritive analyses.

2.4 Nutritional quality

Weigh 0.5g of the crushed and sieved dried sample into a digestion tube, add concentrated sulphuric acid and catalyst, place a small funnel over the mouth of the bottle and place it on the digestion oven. After digestion, the digest was transferred without damage to a 100 ML volumetric flask, the volume was set and cooled, and 10 ML of liquid was taken. The N contents were determined by the automatic Kjeldahl nitrogen analyzer (K9840, Hanon Co., Ltd., Qingdao, China) and crude protein contents (CP) was estimated as N% × 6.25. Neutral detergent fiber (NDF) and acid detergent fiber (ADF) contents were analyzed by the VanSoest et al. (1991) method. Weigh 0.5g of the sample into a fibrous bag and seal it, boil it for 60 minutes in a neutral detergent or acid detergent, soak it in acetone for 30 minutes, wash the bag with water and put it in an oven (60 °) until it reaches a constant weight.

2.5 Analysis for protein fractions (CNCPS)

Soluble protein (SOLP) concentrations were analyzed according to Bradford (1976), some modifications were made to determine the SOLP content. Take 43.5 g of $Na_2HPO_4 \cdot 12H_2O$ (71.64 g L) and 56.5 g of $NaH_2PO_4 \cdot 2H_2O$ (31.2 g L), fix the volume to 1 L, and configure it into Borate-phosphate buffer solution (pH=6.7-6.8), weigh 0.05 g of the ground and dried sample, and place it in a 15 ml centrifuge tube. Add 10 ml Borate-phosphate buffer solution and 1 ml sodium azide solution. After standing for 3 h (20-25°C), the sample was centrifuged at 4000 r min^{-1} for 10 min. The absorbance of the solutions of SOLP after reaction with Coomassie brilliant blue G-250 reagent was measured at 595 nm using a spectrophotometer. The NPN, neutral detergent-insoluble protein (NDIP), and acid detergent-insoluble protein (ADIP) concentrations were analyzed according to Licitra et al. (1996). Determination of NDIP and ADIP: the samples of neutral detergent fiber and acid detergent fiber were dried and digested to determine the residual nitrogen. Determination of NPN: Weigh 0.5 g of sample into a 250 ml conical flask, add 50 ml of distilled water and let stand for 30 min. Add 10 ml of 10% trichloroacetic acid and allow to stand for 30 min. Filter and wash twice with trichloroacetic acid solution. The filter paper was dried and digested to determine the residual nitrogen. The determination of NDIP and ADIP is to digest the samples dried after measuring the medium wash and acid wash and determine the residual nitrogen. The protein fraction were analyzed according to the Cornell Net Carbohydrate and Protein System (CNCPS) (Sniffen et al., 1992; Licitra et al., 1996). The CP content was divided into instantaneously solubilizable protein A (PA), completely undegradable (PC) and potentially degradable true protein (PB). The PB was further sub-divided into rapidly (PB_1), intermediately (PB_2), and slowly (PB_3) degradable true protein. The calculation formula is as follows: PA (% CP) = NPN (%SOLP) × 0.01 × SOLP (% CP); PB_1 = SOLP (% CP)-PA (% CP); PB_2 = 100-PA (% CP)-PB_1 (% CP)-PB_3 (% CP)-PC (% CP); PB_3 = NDIP (% CP)-ADIP (% CP); PC = ADIP (% CP).

2.6 Non-structural carbohydrate determination

NSC concentration was defined as the sum of soluble sugar and starch content. The soluble sugar and starch content were analyzed according to Hajihashemi et al. (2020) and Wang et al. (2021). Precisely weigh 0.2 g of the sample and place it in a 15 ml centrifuge tube. Add 4 ML of 80% ethanol solution to the centrifuge tube and leave it in a water bath at 80°C for 30 minutes. The solution was cooled to room temperature and then centrifuged at 4000 r min^{-1} for 10 min. The extraction process was repeated 3 times. The supernatant was retained for the determination of soluble sugar content. To the precipitate, 2 mL of distilled water was added and boiled for 15 min. After the solution was cooled to room temperature, 3 mL of 9.2 M $HClO_4$ solution was added and shaken for 15 min. 4 mL of distilled water was added and centrifuged at 4800 r min^{-1} for 10 min. The supernatant was retained and further extracted with 3 mL of 4.6 M $HClO_4$. All supernatants were collected for determination of amylose content.

2.7 Statistical analysis

Figures were constructed with Excel 2016 (Microsoft Corp., USA) and Origin 2021 (Origin Corp., USA). Analysis of variance (ANOVA) for the two-year data was performed using the SPSS 20.0 statistical (IBM Corp., USA). Repeated-measures analysis of variance was used to determine the effects of N and P on agronomic traits, protein fractions, nonstructural carbohydrate and hay yield of alfalfa. Tukey's significant difference test was used to compare the significant differences among the treatment means, and interaction effects, wherever found significant were also calculated and presented. The relationships of forage yield and qualitative indexes were checked for normality in relation to treatments in different years using Origin 2021, and linear and nonlinear regression analyses were per formed.

2.3.1 Mathematical model for comprehensive evaluation by principal component analysis:

2.3.1.1 Normalizing raw data

$$\tilde{X}_{ij} / \frac{X_{ij}\ \tilde{X}_j}{S_j} \text{‹} \leftarrow i / 1\text{‹}2\text{‹}\ldots\text{‹}n, j / 1\text{‹}2\text{‹}\ldots\text{‹}m \leftarrow$$

2.3.1.2 Establish the correlation coefficient matrix R between the variables

Related Matrix $R=(r_{ij})_{m\times m}$

$$r_{i\ \ j} = \frac{\sum_{k=1}^{n} \tilde{X}_{ki} \cdot \tilde{X}_{kj}}{n-1}, (i, j = 1, 2, \ldots, m)$$

2.3.1.3 Calculate the eigenvalues and eigenvectors of the correlation coefficient matrix R

$$\begin{cases} y_1 / u_{11}\tilde{x}_1 \rightharpoondown u_{21}\tilde{x}_2 \rightharpoondown \ldots \rightharpoondown u_{n1}\tilde{x}_n \\ y_2 / u_{12}\tilde{x}_1 \rightharpoondown u_{22}\tilde{x}_2 \rightharpoondown \ldots \rightharpoondown u_{n2}\tilde{x}_n \\ \ldots\ldots\ldots\ldots\ldots \Updownarrow \ldots\ldots\ldots\ldots\ldots \\ y_m / u_{1m}\tilde{x}_1 \rightharpoondown u_{2m}\tilde{x}_2 \rightharpoondown \ldots \rightharpoondown u_{nm}\tilde{x}_n \end{cases}$$

2.3.1.4 Calculate the composite score

Calculate the information contribution rate and cumulative contribution rate of the given value $\lambda_j (j=1,2,...,m)$

The information contribution of the principal components is $b_j = \frac{\lambda_j}{\sum_{k=1}^{m} \lambda_k} (j = 1, 2, \ldots, m)$

The cumulative contribution of the principal components is $\alpha_p = \frac{\sum_{k=1}^{p} \lambda_k}{\sum_{k=1}^{m} \lambda_k}$

Calculate the overall score $Z = \sum_{j=1}^{p} b_j y_j (j = 1, 2, \ldots, m)$

3 Results

3.1 Effects of nitrogen and phosphorus combined application on nitrogen distribution

Nitrogen (N) and phosphorus (P) fertilization showed significant effects ($p < 0.05$) on crude protein (CP), soluble protein (SOLP), neutral detergent-insoluble protein (NDIP) and non-protein nitrogen (NPN) content of alfalfa. The CP, SOLP, NDIP and NPN contents showed an increasing and then decreasing trend, while the ADIP content showed a decreasing and then increasing trend with the increase of P application under the same N treatment from 2021 to 2022 (Figure 1). Meanwhile, the CP, SOLP, NDIP and NPN contents were significantly greater in the P100 treatment than P0 treatments (in the 6.79 – 9.54, 11.00 – 19.40, 3.46 – 8.54, and 11.18 – 15.73% ranges, respectively, $p < 0.05$), while the ADIP contents were significantly lower than in the P0 treatment in 2021 (in the 0.22 – 5.99% ranges, $p < 0.05$). In addition, CP, SOLP, NDIP and NPN contents were significantly different under each P treatment ($p < 0.05$), and ADIP contents were not significantly different ($p > 0.05$). Under the same P treatment, the CP, SOLP, NDIP and NPN contents showed an increasing trend with the increase of N fertilization (in the 2.50 – 6.81, 3.48 – 9.70, 2.75 – 5.89, and 4.56 – 14.09% ranges, respectively, $p < 0.05$), while the ADIP content showed a decreasing trend (in the 0.56 –5.06% range, $p > 0.05$). In addition, CP, SOLP, NDIP and NPN contents were significantly different ($p < 0.05$), and ADIP contents were not significant ($p > 0.05$) under N120 treatment than N100 treatment from 2021 to 2022.

3.2 Effects of nitrogen and phosphorus combined application on protein fractions

The contents of PA, PB_1, and PB_3 in the protein fractions showed an increasing trend and then decreased with an increase in P fertilization, while the contents of PB_2 and PC showed a trend of decreasing and then increasing P application (Figure 2). Under N60 conditions, PA and PB_3 contents were significantly increased (4.09–6.40 and 2.81–9.69%, respectively, $p < 0.05$), and PB_2 and PC contents were significantly lower (4.23–6.61% and 6.85–13.30%, respectively, $p < 0.05$) under P100 treatment compared to P0 treatment in 2021 and 2022. Moreover, the PB_1 content was significantly different ($p < 0.05$) after P100 treatment in 2022. Under the same P application treatment, PA and PB_3 contents

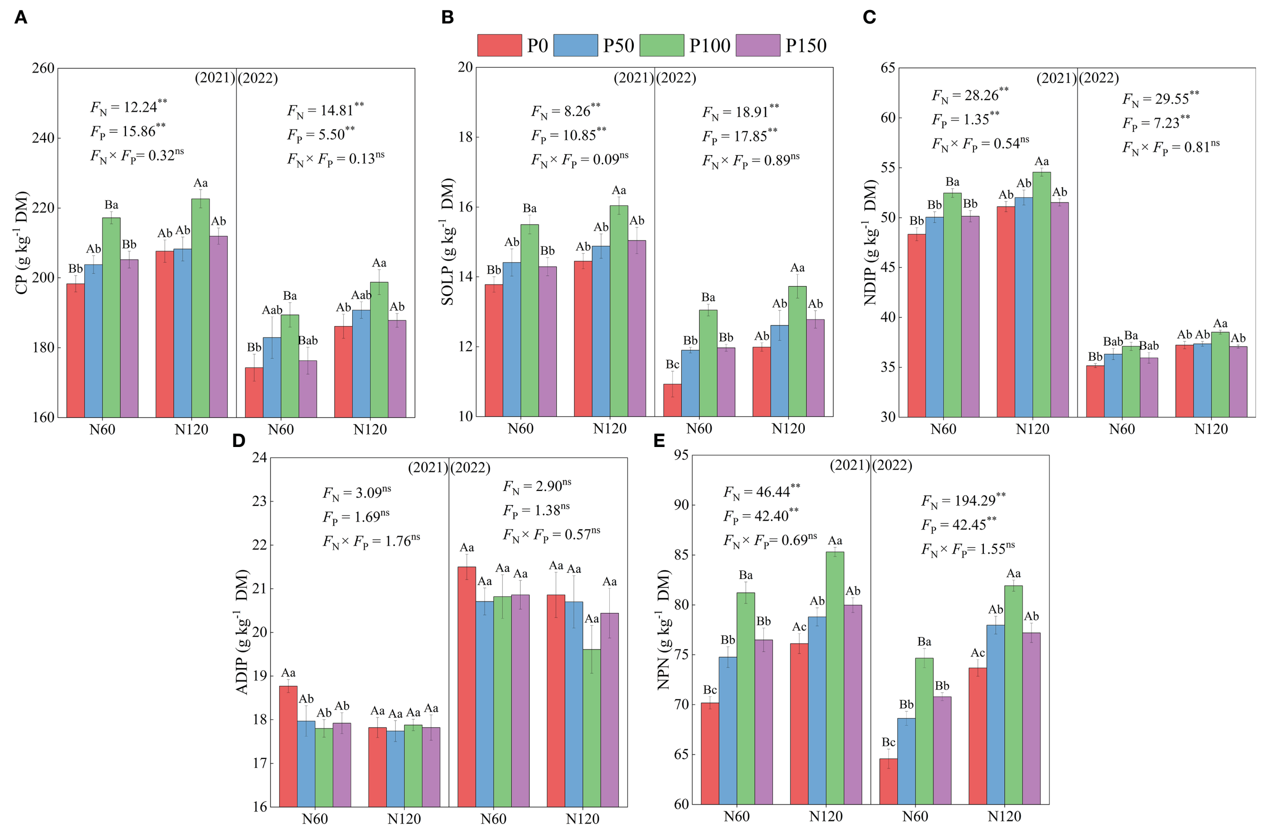

FIGURE 1
CP, crude protein **(A)**, SOLP, soluble protein **(B)**, NDIP, neutral detergent-insoluble protein **(C)**, ADIP, acid detergent-insoluble protein **(D)** and NPN, non-protein nitrogen **(E)** of alfalfa during difference nitrogen and phosphorus combined fertilization in 2021 to 2022. All the values were the means of four replicates with standard errors. Different small letters indicate significant differences between different P fertilizer treatments under the same N application condition (p < 0.05). Different capital letters indicate significant differences between different N fertilizer levels under the same P application condition (p < 0.05). F_N, F_P and $F_N \times F_P$ represent the F value under the N application levels, P application levels and the interaction of N and P application levels, respectively. ns indicates no significant difference (p > 0.05), * indicates significant difference (p < 0.05) and ** indicates extremely significant difference (p < 0.01).

were significantly greater under the N120 treatment than under the N60 treatment (2.37–8.93 and 2.81–9.69%, respectively, p < 0.05), while PB_2 and PC contents were significantly lower than the N60 treatment (1.53–6.98 and 2.07–10.28%, respectively, p < 0.05). In addition, PA, PB_2, PB_3, and PC contents differed significantly (p < 0.05), whereas PB_1 content did not differ significantly between the N treatments in 2021 and 2022 (p > 0.05).

3.3 Effects of nitrogen and phosphorus combined application on non-structural carbohydrate

The soluble sugar (SS), starch (ST), and nonstructural carbohydrate (NSC) contents showed a trend of increasing and then decreasing with an increase in P fertilization under the same N fertilization treatment (Figure 3). Meanwhile, the SS and NSC content of the P100 treatment was significantly higher than that of the P0 treatment (5.68–10.61 and 11.00–19.40%, respectively, p < 0.05), while the difference in starch was not significant in 2021 (p > 0.05). In addition, the difference in NSC between the P treatments was significant (p < 0.05) in 2021 and 2022, and soluble sugar content was significant (p < 0.05) only in 2021. Under the same P treatment, the SS, ST, and NSC content increased with increasing N application, and ST and NSC content was significantly higher in N120 than in the N60 treatment (2.23–6.75, 3.65–6.17, and 3.48–9.70%, respectively, p < 0.05), while soluble sugar content showed no significant difference (p > 0.05).

3.4 Effects of nitrogen and phosphorus combined application on hay yield

Combined nitrogen and phosphorus fertilization showed significant effects (p < 0.05) on the hay yield of alfalfa (Figure 4). Under the same N treatment, alfalfa hay yield showed a trend of increasing and then decreasing with increasing P application, reaching the maximum under P100, and was significantly higher than the P0 treatment (3.07–13.43%, p < 0.05) in 2021 and 2022. Under the same P treatment, alfalfa hay yield increased with increasing N application,

 10.3389/fpls.2023.1124664

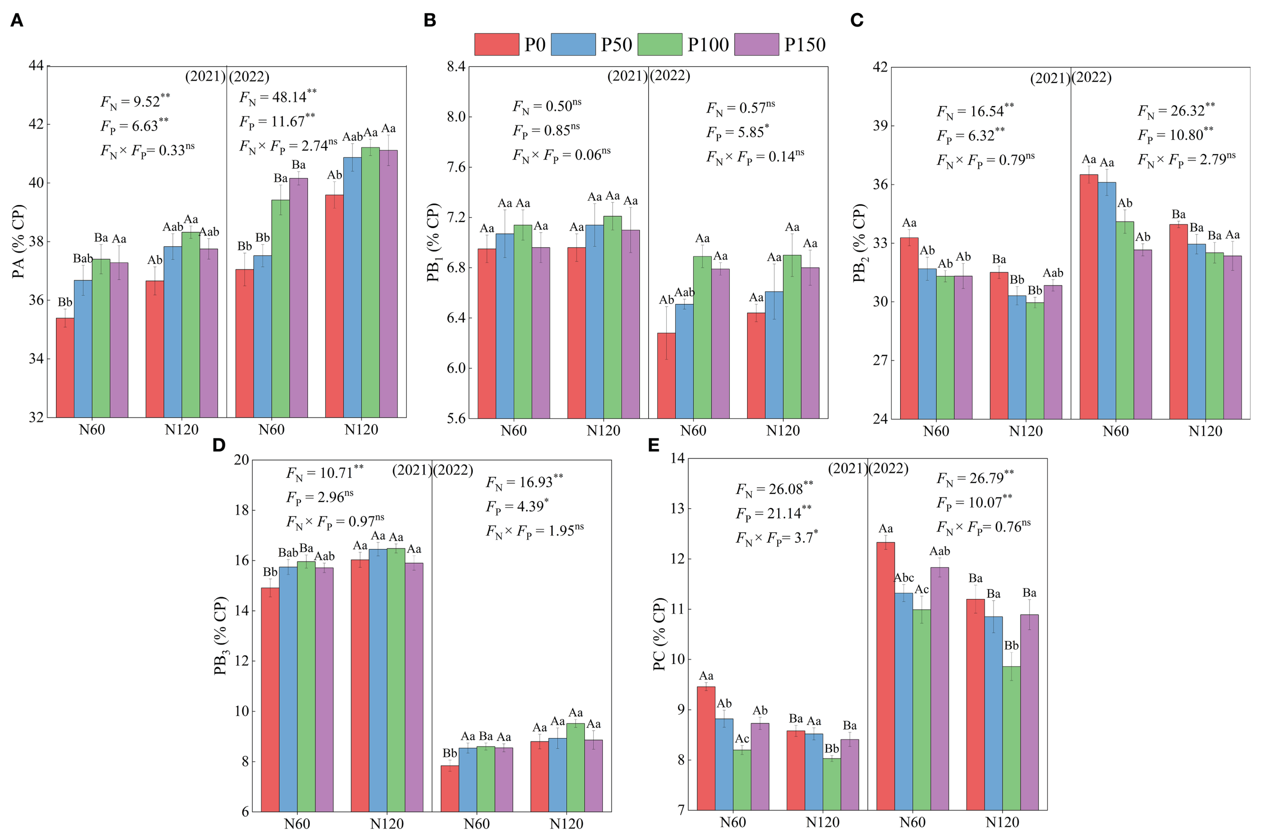

FIGURE 2
Effect of nitrogen and phosphorus combined fertilization on protein fraction of PA = non-protein nitrogen of crude protein **(A)**, PB_1 = easily degradable protein **(B)**, PB_2 = intermediately degradable protein **(C)**, PB_3 = slowly degradable protein **(D)**, and PC = non-degradable protein **(E)** of alfalfa. Different small letters indicate significant differences between different P fertilizer treatments under the same N application condition (p < 0.05). Different capital letters indicate significant differences between different N fertilizer levels under the same P application condition (p < 0.05). F_N, F_P and $F_N \times F_P$ represent the F value under the N application levels, P application levels and the interaction of N and P application levels, respectively. ns indicates no significant difference (p > 0.05), * indicates significant difference (p < 0.05) and ** indicates extremely significant difference (p < 0.01).

with the N120 treatment being significantly higher than the N60 treatment (2.11–8.49%, p < 0.05) in 2021 and 2022.

3.5 Relationship of measured indexes and phosphorus under nitrogen fertilization

Regression analysis of protein components, hay yield, and P application showed that PA, PB_1, PB_2, PB_3, PC and hay yield showed a parabolic relationship with P application under low or high P rates. Under low N conditions, PA, PB_3 and hay yield contents showed significant positive correlations with phosphorus rates, and the coefficient of determination values (R^2) were 0.47, 0.39 and 0.63, respectively. However, PB_2 and PC contents showed significant and negative correlations, and the coefficient determination values (R^2) were 0.45 and 0.76, respectively (Figure 5). Under high N condition, PA and hay yield contents showed significant and positive correlations with phosphorus rates and the coefficient determination values (R^2) were 0.45 and 0.59, respectively. However, PB_2 contents showed significant and negative correlations, and the coefficient of determination values (R^2) was 0.49 (Figure 6).

3.6 Principal component analysis and comprehensive evaluation

To investigate the effect of different N and P combined fertilization strategies on the hay yield and quality of alfalfa at the first flowering stage, we assessed the response of NSC, nitrogen distribution and protein fractions on the hay yield of alfalfa by principal coordinate analysis (PCA). Extracting the principal component eigenvalues greater than 1, two principal components were obtained (Table 1), it was found that the first and second axes explained 90.5% of the total variation (Figure 7A). The results of the analysis can be used to replace the original fourteen indicators with two principal component variables, PCA1 and PCA2, yielding the following eigenvectors for each principal component:

$$\begin{aligned} PC1 = {} & 0.270\ MX1 + 0.275\ MX2 + 0.286\ MX3 - 0.224MX4 + \\ & 0.283\ MX5 + 0.273\ MX6 + 0.249\ MX7 - 0.274\ MX8 + \\ & 0.270\ MX9 - 0.279\ MX10 + 0.274\ MX11 + 0.249\ MX12 + \\ & 0.283\ MX13 + 0.243\ MX14 \end{aligned}$$

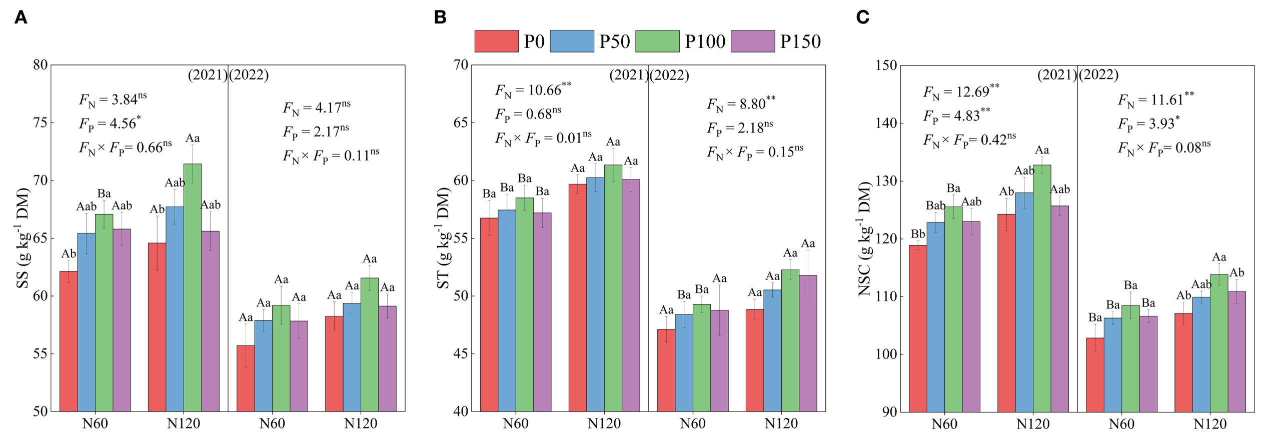

FIGURE 3
SS, soluble sugar **(A)**, ST, starch **(B)** and NSC, non-structural carbohydrate **(C)** of alfalfa during difference nitrogen and phosphorus combined fertilization in 2021 to 2022. Different small letters indicate significant differences between different P fertilizer treatments under the same N application condition (p < 0.05). Different capital letters indicate significant differences between different N fertilizer levels under the same P application condition (p < 0.05). F_N, F_P and $F_N \times F_P$ represent the F value under the N application levels, P application levels and the interaction of N and P application levels, respectively. ns indicates no significant difference (p > 0.05), * indicates significant difference (p < 0.05) and ** indicates extremely significant difference (p < 0.01).

$$
\begin{aligned}
PC2 = {} & 0.293\ MX1 + 0.317\ MX2 + 0.144\ MX3 + 0.637\ MX4 + \\
& 0.122\ MX5 - 0.186\ MX6 + 0.331\ MX7 + 0.281\ MX8 - \\
& 0.333\ MX9 + 0.061 MX10 + 0.153\ MX11 - 0.069\ MX12 + \\
& 0.073\ MX13 + 0.032\ MX14
\end{aligned}
$$

Note: PC1 and PC2 denote the scores of principal components 1 and 2, respectively. MX1 represents CP, MX2 represents SOLP, MX3 represents NDFIP, MX4 represents ADFIP, MX5 represents NPN, MX6 represents PA, MX7 represents PB_1, MX8 represents PB_2, MX9 represents PB_3, MX10 represents PC, MX11 represents SS, MX12 represents ST, MX13 represents NSC and MX14 represents HY.

A comprehensive evaluation model was constructed by using the selected variance contributions of the 1st and 2nd principal components A1 (84.7%) and A2 (5.8%) (Figure 7A) as weights: PC3=A1PC1 + A2PC2.

The principal component analysis revealed that the highest overall score was obtained under the treatment of 100 phosphorus application at 60 or 120 kg N hm^{-2} (Table 2 and Figure 7B). Therefore, 120 kg N ha^{-1} coupled with 100 kg P ha^{-1} showed the most promising effects in terms of achieving optimal forage yield consistent with enhanced forage nutritive values.

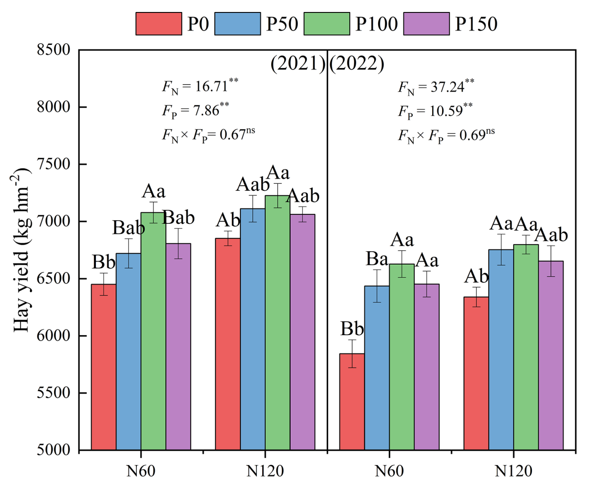

FIGURE 4
Effect of nitrogen and phosphorus combined fertilization on the hay yield (first clipping) of alfalfa in 2021 to 2022. Different small letters indicate significant differences between different P fertilizer treatments under the same N application condition (p < 0.05). Different capital letters indicate significant differences between different N fertilizer levels under the same P application condition (p < 0.05). F_N, F_P and $F_N \times F_P$ represent the F value under the N application levels, P application levels and the interaction of N and P application levels, respectively. ns indicates no significant difference (p > 0.05), * indicates significant difference (p < 0.05) and ** indicates extremely significant difference (p < 0.01).

4 Discussion

4.1 Effects of nitrogen and phosphorus combined application on hay yield

As a perennial legume forage, alfalfa is famous for its high quality and yield, and its hay yield is a representative indicator of production performance. The available literature is inconsistent regarding the effects of fertilization on legume forage yields, particularly in alfalfa. Some studies have found no benefit from nitrogen fertilization in legume crops, as there was no significant increase in biomass yield or quality (Xie et al., 2015). Appropriate N application has been reported to regulate the distribution of photoassimilates in the aboveground parts of plants, thereby increasing the yield and resource use efficiency of alfalfa (Zhang et al., 2021). Therefore, the relationship between N application, resource use efficiency, and biomass differs between nitrogen-fixing plants and those dependent only on mineral nitrogen. There is a

10.3389/fpls.2023.1124664

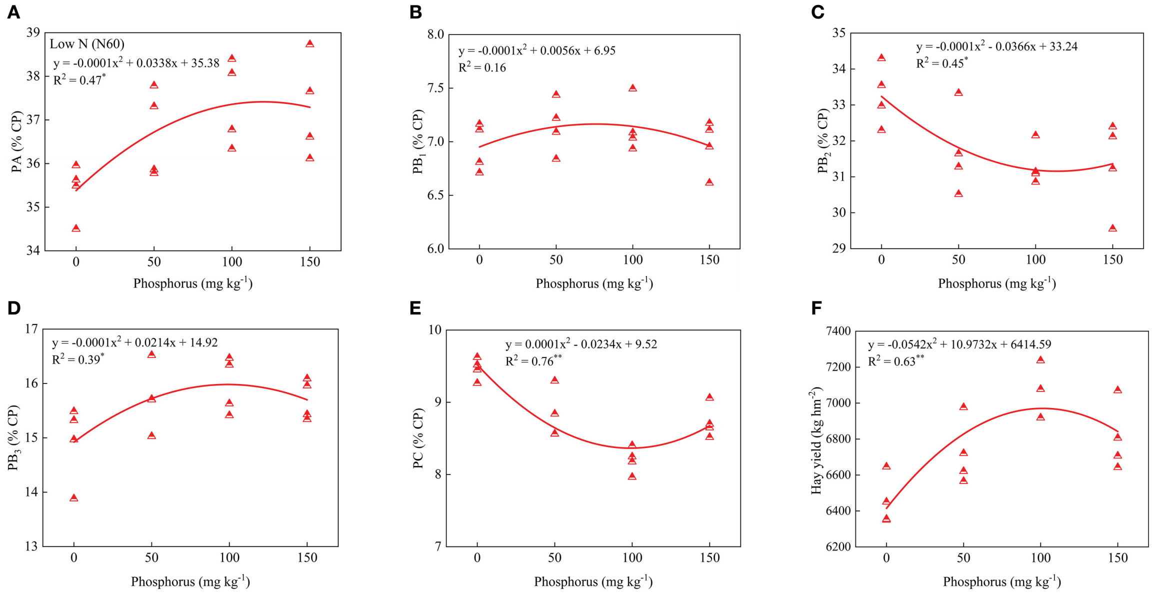

FIGURE 5
Relationship of PA **(A)**, PB_1 **(B)**, PB_2 **(C)**, PB_3 **(D)**, PC **(E)**, and forage yield **(F)** with phosphorus treatments under low nitrogen condition. * and ** indicates the significant level at $p \leq 0.05$ and $p \leq 0.01$, respectively. The X and Y axes were adjusted to minimize the graph's blank areas and highlight the relationship.

certain interaction between N and P fertilization. When a threshold of nitrogen is reached, applying a certain amount of P fertilizer can again improve the yield and quality of forage. Studies have shown that N and P fertilization could shift some ecosystems from N to P limitation or N and P co-limitation (Elser et al., 2010). The results of this study showed that at 60 or 120 kg N ha^{-1}, the perceived third-order polynomial relationship between alfalfa yield and P fertilization was applied. When the P application is too high, the hay yield is inhibited, and there is a positive correlation between hay yield and P application. PCA showed that the highest combined

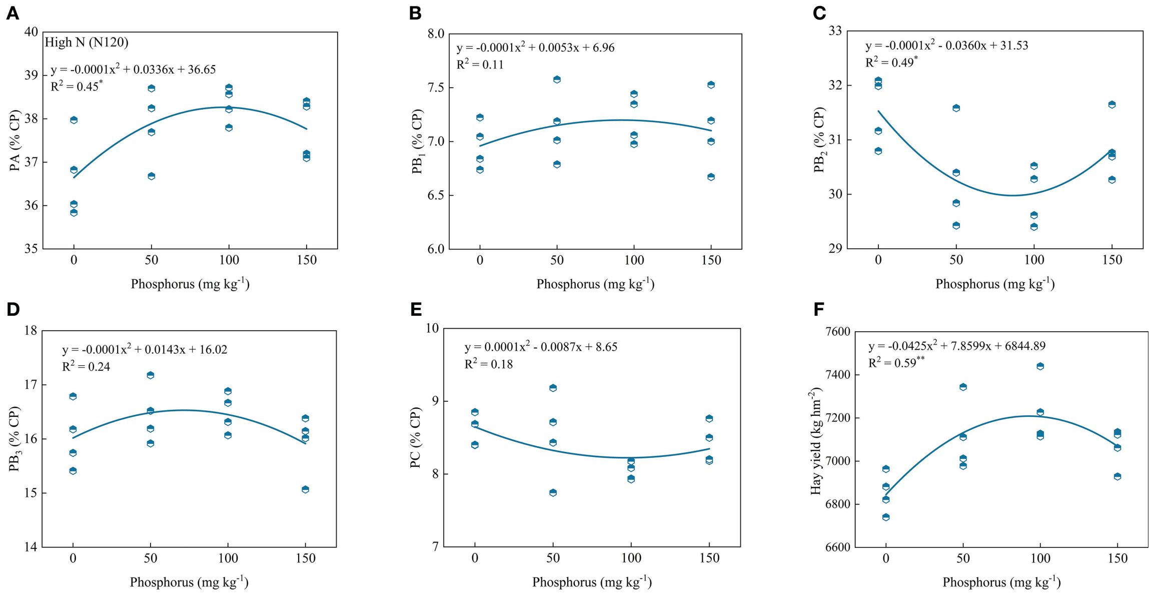

FIGURE 6
Relationship of PA **(A)**, PB_1 **(B)**, PB_2 **(C)**, PB_3 **(D)**, PC **(E)** and forage yield **(F)** with phosphorus treatments under high nitrogen condition. * and ** indicates the significant level at $p \leq 0.05$ and $p \leq 0.01$, respectively. The X and Y axes were adjusted to minimize the graph's blank areas and highlight the relationship.

TABLE 1 Principal component score coefficient matrix.

Index	PC1	PC2
CP (Crude protein)	0.270	0.293
SOLP (Soluble protein)	0.275	0.317
NDFIP (Neutral detergent-insoluble protein)	0.286	0.144
ADFIP (Acid detergent-insoluble protein)	-0.224	0.637
NPN (Non-protein nitrogen)	0.283	0.122
PA (Fraction A)	0.273	-0.186
PB_1 (Fraction B_1)	0.249	0.331
PB_2 (Fraction B_2)	-0.274	0.281
PB_3 (Fraction B_3)	0.270	-0.333
PC (Fraction C)	-0.279	0.061
SS (Soluble sugar)	0.274	0.153
ST (Starch)	0.249	-0.069
NSC (Non-structural carbohydrate)	0.283	0.073
HY (Hay yield)	0.243	0.032

scores for hay yield, agronomic traits, protein fraction, and nonstructural carbohydrates were obtained for alfalfa at 120 kg N ha^{-1} and 100 kg P ha^{-1}. Meanwhile, correlation analysis showed that SS, ST, and NSC were significantly positively correlated with hay yield. Based on these results, we assumed that there is a certain threshold for fertilization uptake by alfalfa below which fertilization can promote growth and development, whereas fertilization above the maximum uptake will negatively affect growth and development and reduce forage yield, as confirmed by previous studies (Fan et al., 2016; Zhang et al., 2021). Therefore, a rational N and P combined fertilization strategy increases the hay yield of alfalfa and improves its nutritional quality.

4.2 Effects of nitrogen and phosphorus combined application on non-structural carbohydrates

Carbohydrate partitioning plays an important role in plant productivity and can vary with specific life forms. Carbohydrates in plants are both structural and nonstructural. Structural carbohydrates are polysaccharides, which are components of the cell wall and provide structural support to the plant (Vorwerk et al., 2004), whereas NSC act as mediators of metabolism, energy transport, and storage in plants. Total nonstructural carbohydrates (NSC) is commonly used as an indicator of quality in forage crops (Jensen et al., 2014). Among them, NSC consist mainly of soluble sugar (SS) and starch (ST), which are reserves in plant tissues (Ishimaru et al., 2004). The total NSC concentration decreased slightly with increasing N application, whereas ST decreased with N addition (Pan et al., 2011). In contrast, plant NSC content increases with the amount of N fertilization (Liu et al., 2016), and either too low or too high N fertilization causes a decrease in ST and NSC content of rice at the tasseling stage (Cao et al., 2020). It was also found that the concentration of NSC decreased slightly with increasing N fertilization, whereas the concentration of ST decreased with the application of foliar urea (Li et al., 2018). However, in this study, it was found that ST and SS increased slightly with increasing N application under the same P treatment, whereas NSC increased significantly. This may be due to the low demand for N fertilization in alfalfa at the first flowering stage and the relatively low consumption of carbohydrates for carbon skeleton and energy by N assimilation (Cheng and Fuchigami, 2002). Therefore, N supply can increase the level of leaf NSC. P is a key element in many plant functions, including carbohydrate metabolism (Vance et al., 2003) and transport (Paponov et al., 2020). Lower P application reduces ST accumulation in flowers and young fruits, which in turn reduces plant NSC content (Hermans et al., 2006). In contrast, the transport

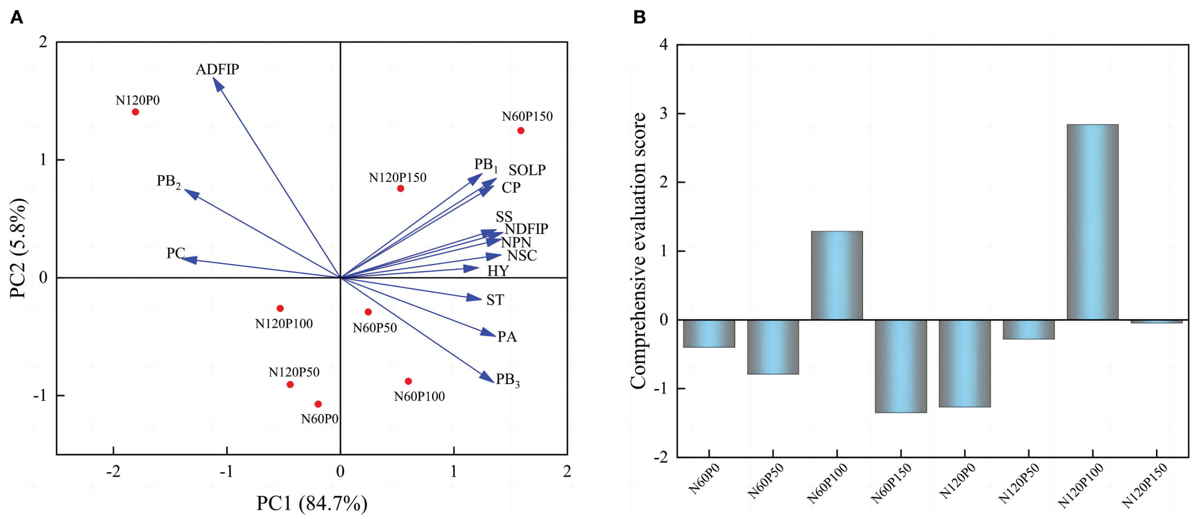

FIGURE 7
Principal component analysis of protein fractions and non-structural carbohydrates of alfalfa. **(A)** Principal component analysis, **(B)** Comprehensive evaluation score.

TABLE 2 Principal components, comprehensive scores and rankings under nitrogen and phosphorus combined application.

Treatment		Principal component 1 (PC1)	Principal component 2 (PC2)	Comprehensive score (PC3)	Rank
N60	P0	-1.8036	1.40531	-0.39829	5
	P50	-0.52905	-0.2602	-0.78925	6
	P100	0.53214	0.75711	1.28925	2
	P150	-0.44164	-0.90612	-1.34776	7
N120	P0	-0.194	-1.07285	-1.26685	8
	P50	0.59907	-0.87913	-0.28006	4
	P100	1.5912	1.24684	2.83804	1
	P150	0.24588	-0.29096	-0.04508	3

PC3 denotes the composite score and A is the weight of each principal component.

of NSC from nutrient organs to reproductive organs under phosphorus-free conditions is greater than that under high P conditions, and the effect of nitrogen on NSC transport is related to P levels (Yan et al., 2018). Interestingly, a mixture of N and P fertilization significantly increased post-flowering leaf SS concentration in oilseed flax, and a relatively high N and P mixture significantly increased post-flowering leaf ST concentration and content. However, the high N and P treatments had the lowest pre-flowering leaf ST concentration and content (Yan et al., 2018). This is consistent with the results of this study, as SS and ST content showed a trend of increasing and then decreasing with the increase of N fertilization. Once the fertilizer application is too high, it will limit the benefits of N and P fertilization to alfalfa, reducing SS, ST, and NSC content. This study also found that SS and NSC contents tended to increase and then decrease with increasing P application under the same N fertilization treatment, whereas ST slightly increased. The accumulation of ST in P-limited would support the proposal that a phosphate-dependent translocator regulates the movement of triosephosphates out of the chloroplast. Thus, when phosphate is limiting, triosephosphates accumulate in the bundle sheath chloroplasts, resulting in a higher PGA/Pi ratio, with a corresponding activation of ADP glucose pyrophosphorylase, resulting in the accumulation of ST (Yan et al., 2018). We hypothesized that a reasonable N and P combined application strategy could help increase the accumulation of SS and ST in alfalfa, and thus increase its hay yield.

4.3 Effects of nitrogen and phosphorus combined application on nitrogen distribution and protein fractions

Nitrogen compounds comprise 40–50% of the protoplasm dry matter and are a constituent of amino acids, the building blocks of proteins (Rosenblueth et al., 2018). In addition, SOLP and favorable growth conditions are improved by N supply (Sugiyama et al., 1984). Previous studies have shown that soluble protein and NPN content increased with increasing levels of N fertilization (Alharbi et al., 2022). In our study, NPN and SOLP content increased with increasing N content at the same P fertilization. This is because the N fertilization levels increased the accumulation of nitrate in plants taken up by plants and reduced to ammonia, a substrate for amino acid and protein synthesis, increasing plant NPN content (Gomes et al., 2018). Among the N treatments, 120 kg N ha^{-1} was the best nutrient quantity for forage. In this study, CP and SOLP contents had a parabolic relationship with increasing P application, and their contents decreased at the highest P application rate. This may be due to the high P treatment had a stressful effect on alfalfa, reducing its nutritional value. A high mineral N rate restricts root system nodule development and decreases 120 kg N ha^{-1} fixation in legumes (Xie et al., 2015), thus limiting nitrogen compound synthesis.

The CNCPS protein fraction system visually reflects the utilization of each protein fraction by forage in the animal's rumen (Fox et al., 1995). True proteins are extensively degraded in the rumen, contribute to the N supply of rumen microorganisms, and are incorporated into the carbon skeleton (Sniffen et al., 1992). However, the easily degradable protein of this fraction can lead to peptide construction and escape into the intestine, as the use of these fraction limits protein degradation. Previous research has indicated that increased levels of N fertilization increase nitrate accumulation in plants, which is a portion of fraction A (Johnson et al., 2001). Our results showed that the content of fractions A, B_1, and B_3 increased with increasing N fertilization, probably because N fertilization increased nitrogen compounds in tissues and protein synthesis in plants (Johnson et al., 2001). Fractions B_1 and B_3 tended to increase and then decrease with the increase in P application, probably because the addition of P promoted the absorption and utilization of N fertilization by alfalfa, which in turn increased the

NPN content in the plant. (Klabi et al., 2018). However, rapid rumen proteolysis of this fraction can lead to peptide construction and escape into the intestine, as the use of these components is limiting to protein degradation. Animal performance depends on the production of microbial proteins, which can be optimized with larger amounts of soluble N. However, high concentrations of fraction A and B_1 are desirable, as this fraction is rapidly degraded in the rumen, thereby affecting rumen homeostasis and possibly the ruminant growth performance. Fraction C corresponds to N linked to lignin, tannin-protein complexes, and merad products, which are highly resistant to enzymes produced by microorganisms in the rumen and are considered unusable for animals (Sniffen et al., 1992). In our study, it was found that fraction C decreased with an increase in N fertilization level, which was consistent with the results of previous studies (Alharbi et al., 2022). However, the fraction C content showed a trend of increasing and then decreasing with an increase in P application because P fertilization decreased the acid detergent fiber content in alfalfa, which in turn decreased the fraction C content (Zhang et al., 2014). Therefore, a good N and P combined application strategy can increase the content of fractions A and B and decrease that of fraction C, and increase the protein effectiveness of alfalfa, which in turn will benefit the growth and development of ruminants.

5 Conclusion

The results of the present study showed that a good N and P combined fertilization strategy could increase the soluble nitrogen compounds and total carbohydrate content of perennial alfalfa. On the other hand, reasonable P fertilization levels were more beneficial for increasing the true protein content and reducing the non-degradable protein, slowly degrading protein content, and crude fiber content of alfalfa. Therefore, the fertilization of 120 kg N ha^{-1} and 100 kg P ha^{-1} to alfalfa for consecutive years promoted its growth and development, increased its protein content, and avoided the accumulation of more structural carbohydrates, thus increasing the hay yield and nutritional quality of alfalfa.

Data availability statement

The original contributions presented in the study are included in the article/supplementary material. Further inquiries can be directed to the corresponding authors.

Author contributions

Conceptualisation, QZ, XW and CM. Software, ML. Validation, JZ and RH. Formal analysis, JZ. Data curation, QZ and JZ. Writing—original draft preparation, JZ. Visualisation, JZ. Supervision, QZ. Funding acquisition, QZ. All authors contributed to the article and approved the submitted version.

Funding

National Natural Science Foundation of China, Grant/Award Number: 32260347; 32001400; Fok Ying Tung Education Foundation of China, Grant/Award Number: 171099; Science and Tech-nology Innovation Key Talent Project of Xinjiang Production and Construction Corps, Grant/Award Number: 2021CB034; China Agriculture Research System of MOF and MARA.

Conflict of interest

The authors declare that the research was conducted in the absence of any commercial or financial relationships that could be construed as a potential conflict of interest.

Publisher's note

All claims expressed in this article are solely those of the authors and do not necessarily represent those of their affiliated organizations, or those of the publisher, the editors and the reviewers. Any product that may be evaluated in this article, or claim that may be made by its manufacturer, is not guaranteed or endorsed by the publisher.

References

Alencar, N. M., Vendramini, J. M. B., dos Santos, A. C., Silveira, M. L., Dubeux, J. C. B.Jr., Sousa, L. F., et al. (2018). Herbage characteristics of *Pintoi peanut and paslisadegrass* established as monoculture or mixed swards. *Crop Sci.* 58, 2131–2137. doi: 10.2135/cropsci2017.09.0538

Alharbi, K., Haroun, S. A., and Gamel, R. M. E. (2022). Physiological studies and ultrastructure of *Vigna sinensis* l. and *Helianthus annuus* l. under varying levels of nitrogen supply. *Plants-Basel* 11, 1884. doi: 10.3390/plants11141884

Berca, A. S., Cardoso, A. D., Longhini, V. Z., Tedeschi, L. O., Boddey, R. M., Reis, R. A., et al. (2021). Protein and carbohydrate fractions in warm-season pastures: Effects of nitrogen management strategies. *Agron.-Basel* 11, 847. doi: 10.3390/agronomy11050847

Bradford, M. M. (1976). A rapid and sensitive method for the quantitation of microgram quantities of protein utilizing the principle of protein-dye binding. *Anal. Biochem.* 72, 248–254. doi: 10.1016/0003-2697(76)90527-3

Cao, P. P., Sun, W. J., Huang, Y., Yang, J. R., Yang, K., Lv, C. H., et al. (2020). Effects of elevated CO_2 concentration and nitrogen application levels on the accumulation and translocation of non-structural carbohydrates in japonica rice. *Sustainability* 12, 5386. doi: 10.3390/su12135386

Cheng, L. L., and Fuchigami, L. H. (2002). Growth of young apple trees in relation to reserve nitrogen and carbohydrates. *Tree Physiol.* 22, 1297–1303. doi: 10.1093/treephys/22.18.1297

Elser, J. J., Fagan, W. F., Kerkhoff, A. J., Swenson, N. G., and Enquist, B. J. (2010). Biological stoichiometry of plant production: metabolism, scaling and ecological response to global change. *New Phytol.* 186, 593–608. doi: 10.1111/j.1469-8137.2010.03214.x

Fan, J. W., Du, Y. L., Wang, B. R., Turner, N. C., Wang, T., Abbott, L. K., et al. (2016). Forage yield, soil water depletion, shoot nitrogen and phosphorus uptake and concentration, of young and old stands of alfalfa in response to nitrogen and phosphorus fertilisation in a semiarid environment. *Field Crops Res.* 198, 247–257. doi: 10.1016/j.fcr.2016.08.014

Fox, D. G., Barry, M. C., Pitt, R. E., Roseler, D. K., and Stone, W. C. (1995). Application of the cornell net carbohydrate and protein model for cattle consuming forages. *J. Anim. Sci.* 73, 267–277. doi: 10.2527/1995.731267x

Gomes, F. K., Oliveira, M. D. B. L., Homem, B. G. C., Boddey, R. M., Bernardes, T. F., Gionbelli, M. P., et al. (2018). Effects of grazing management in brachiaria grass-forage peanut pastures on canopy structure and forage intake. *J. Anim. Sci.* 96, 3837–3849. doi: 10.1093/jas/sky236

Gu, X. D., Zhang, F. J., Wang, T., Xie, X. W., Jia, X. H., and Xu, X. (2022). Effects of nitrogen and phosphorus addition on growth and leaf nitrogen metabolism of alfalfa in alkaline soil in yinchuan plain of *Hetao Basin*. *Peerj* 10, e13261. doi: 10.7717/peerj.13261

Hajihashemi, S., Skalicky, M., Brestic, M., and Vachova, P. (2020). Cross-talk between nitric oxide, hydrogen peroxide and calcium in salt-stressed *Chenopodium quinoa* willd. At seed germination stage. *Plant Physiol. Biochem.* 154, 657–664. doi: 10.1016/j.plaphy.2020.07.022

Hartmann, H., and Trumbore, S. (2016). Understanding the roles of nonstructural carbohydrates in forest trees – from what we can measure to what we want to know. *New Phytol.* 211, 386–403. doi: 10.1111/nph.13955

Hermans, C., Hammond, J. P., White, P. J., and Verbruggen, N. (2006). How do plants respond to nutrient shortage by biomass allocation. *Trends Plant Sci.* 11, 610–617. doi: 10.1016/j.tplants.2006.10.007

Ishimaru, K., Ishimaru, M., Sasaki, H., and Kashiwagi, T. (2004). Leaf contents differ depending on the position in a rice leaf sheath during sink–source transition. *Plant Physiol. Biochem.* 42, 855–860. doi: 10.1016/j.plaphy.2004.10.008

Jensen, K. B., Harrison, P., Chatterton, N. J., Bushman, B. S., and Creech, J. E. (2014). Seasonal trends in nonstructural carbohydrates in cool – and warm-season grasses. *Crop Sci.* 54, 2328–2340. doi: 10.2135/cropsci2013.07.0465

Johnson, C. R., Reiling, B. A., Mislevy, P., and Hall, M. B. (2001). Effects of nitrogen fertilization and harvest date on yield, digestibility, fiber, and protein fractions of tropical grasses. *J. Anim. Sci.* 79, 2439–2448. doi: 10.2527/2001.7992439x

Klabi, R., Bell, T. H., Hamel, C., Iwaasa, A., Schellenberg, M. P., and St-Arnaud, M. (2018). Contribution of *Medicago sativa* to the productivity and nutritive value of forage in semi-arid grassland pastures. *Grass Forage Sci.* 73, 159–173. doi: 10.1111/gfs.12294

Leite, R. G., Cardoso, A. D., Fonseca, N. V. B., Silva, M. L. C., Tedeschi, L. O., Delevatti, L. M., et al. (2021). Effects of nitrogen fertilization on protein and carbohydrate fractions of *Marandu palisadegrass*. *Sci. Rep.* 11, 14786. doi: 10.1038/s41598-021-94098-4

Li, G. H., Hu, Q. Q., Shi, Y. G., Cui, K. H., Nie, L. X., Huang, J. L., et al. (2018). Low nitrogen application enhances starch-metabolizing enzyme activity and improves accumulation and translocation of non-structural carbohydrates in rice stems. *Front. Plant Sci.* 9. doi: 10.3389/fpls.2018.01128

Licitra, G., Hernandez, T. M., and VanSoest, P. J. (1996). Standardization of procedures for nitrogen fractionation of ruminant feeds. *Anim. Feed Sci. Technol.* 57, 347–358. doi: 10.1016/0377-8401(95)00837-3

Liu, J., Wu, N. N., Wang, H., Sun, J. F., Peng, B., Jiang, P., et al. (2016). Nitrogen addition affects chemical compositions of plant tissues, litter and soil organic matter. *Ecology* 97, 1796–1806. doi: 10.1890/15-1683.1

Luo, J., Qin, J. J., He, F. F., Li, H., Liu, T. X., Polle, A., et al. (2013). Net fluxes of ammonium and nitrate in association with h^+ fluxes in fine roots of *Populus popularis*. *Planta* 237, 919–931. doi: 10.1007/s00425-012-1807-7

Pan, J. F., Cui, K. H., Cui, D., Huang, J. L., Xiang, J., and Nie, L. X. (2011). Relationships of non-structural carbohydrates accumulation and translocation with yield formation in rice recombinant inbred lines under two nitrogen levels. *Physiol. Plant* 141, 321–331. doi: 10.1111/j.1399-3054.2010.01441.x

Paponov, I. A., Paponov, M., Sambo, P., and Engels, C. (2020). Differential regulation of kernel set and potential kernel weight by nitrogen supply and carbohydrate availability in maize genotypes contrasting in nitrogen use efficiency. *Front. Plant Sci.* 11. doi: 10.3389/fpls.2020.00586

Rosenblueth, M., Ormeno-Orrillo, E., Lopez-Lopez, A., Rogel, M. A., Reyes-Hernandez, B. J., Martinez-Romero, J. C., et al. (2018). Nitrogen fixation in cereals. *Front. Microbiol.* 9. doi: 10.3389/fmicb.2018.01794

Sniffen, C. J., O'Connor, J. D., Van Soest, P. J., Fox, D. G., and Russell, J. B. (1992). A net carbohydrate and protein system for evaluating cattle diets: II. carbohydrate and protein availability. *J. Anim. Sci.* 70, 3562–3577. doi: 10.2527/1992.70113562x

Sugiyama, T., Mizuno, M., and Hayashi, M. (1984). Partitioning of nitrogen among ribulose-1,5-bisphosphate carboxylase/oxygenase, phosphoenolpyruvate carboxylase, and pyruvate orthophosphate dikinase as related to biomass productivity in maize seedlings. *Plant Physiol.* 75, 665–669. doi: 10.1104/pp.75.3.665

Sun, Y. L., Wang, X. Z., Ma, C. H., and Zhang, Q. B. (2022). Effects of nitrogen and phosphorus addition on agronomic characters, photosynthetic performance and anatomical structure of alfalfa in northern xinjiang, China. *Agron.-Basel* 12, 1613. doi: 10.3390/agronomy12071613

Vance, C. P., Uhde-Stone, C., and Allan, D. L. (2003). Phosphorus acquisition and use: critical adaptations by plants for securing a nonrenewable resource. *New Phytol.* 157, 423–447. doi: 10.1046/j.1469-8137.2003.00695.x

VanSoest, P. J., Robertson, J. B., and Lewis, B. A. (1991). Methods for dietary fiber, neutral detergent fiber, and nonstarch polysaccharides in relation to animal nutrition. *J. Dairy Sci.* 74, 3583–3597. doi: 10.3168/jds.S0022-0302(91)78551-2

Vorwerk, S., Somerville, S., and Somerville, C. (2004). The role of plant cell wall polysaccharide composition in disease resistance. *Trends Plant Sci.* 9, 203–209. doi: 10.1016/j.tplants.2004.02.005

Wang, J. X., Zhang, H. Q., Gao, J., Zhang, Y., Liu, Y. Q., and Tang, M. (2021). Effects of ectomycorrhizal fungi (*Suillus variegatus*) on the growth, hydraulic function, and non-structural carbohydrates of *Pinus tabulaeformis* under drought stress. *BMC Plant Biol.* 21, 171. doi: 10.1186/S12870-021-02945-3

Wu, Y. W., Zhao, B., Li, Q., Kong, F. L., Du, L. J., Zhou, F., et al. (2020). Non-structural carbohydrates in maize with different nitrogen tolerance are affected by nitrogen addition. *PloS One* 14, e0225753. doi: 10.1371/journal.pone.0225753

Xie, K. Y., Li, X. L., He, F., Zhang, Y. J., Wan, L. Q., Hannaway, D. B., et al. (2015). Effect of nitrogen fertilization on yield, n content, and nitrogen fixation of alfalfa and smooth bromegrass grown alone or in mixture in greenhouse pots. *J. Integr. Agric.* 14, 1864–1876. doi: 10.1016/S2095-3119(15)61150-9

Yan, B., Wu, B., Gao, Y. H., Wu, J. M., Niu, J. Y., Xie, Y. P., et al. (2018). Effects of nitrogen and phosphorus on the regulation of nonstructural carbohydrate accumulation, translocation and the yield formation of oilseed flax. *Field Crops Res.* 219, 229–241. doi: 10.1016/j.fcr.2018.01.032

Yuan, Y. Y., Song, T. T., Yu, J. Q., Zhang, W. K., Hou, X. Y., Ling, Z. K., et al. (2022). Genome-wide investigation of the cysteine synthase gene family shows that overexpression of csase confers alkali tolerance to alfalfa (*Medicago sativa* l.). *Front. Plant Sci.* 12. doi: 10.3389/fpls.2021.792862

Zhang, S., Jiang, H., Zhao, H. X., Korpelainen, H., and Li, C. Y. (2014). Sexually different physiological responses of populus cathayana to nitrogen and phosphorus deficiencies. *Tree Physiol.* 34, 343–354. doi: 10.1093/treephys/tpu025

Zhang, Q. B., Liu, J. Y., Liu, X. S., Li, S. Y., Liu, Y. L., Lu, W. H., et al. (2020a). Optimizing water and phosphorus management to improve hay yield and water- and phosphorus-use efficiency in alfalfa under drip irrigation. *Food Sci. Nutr.* 8, 2406–2418. doi: 10.1002/fsn3.1530

Zhang, Q. B., Liu, J. Y., Liu, X. S., Sun, Y. L., Li, S. Y., Lu, W. H., et al. (2021). Optimizing the nutritional quality and phosphorus use efficiency of alfalfa under drip irrigation with nitrogen and phosphorus fertilization. *Agron. J.* 112, 3129–3139. doi: 10.1002/agj2.20267

Zhang, W. T., Shan, L. S., Li, Y., Bai, Y. M., and Ma, J. (2020b). Effects of nitrogen addition and precipitation change on non-structural carbohydrates in *Reaumuria soongorica* seedlings. *Chin. J. Ecol.* 39, 803–811. doi: 10.13292/j.1000-4890.202003.017

frontiers | Frontiers in Plant Science

TYPE Original Research
PUBLISHED 04 April 2023
DOI 10.3389/fpls.2023.1153500

OPEN ACCESS

EDITED BY
Li Wang,
Shandong Academy of Agricultural Sciences, China

REVIEWED BY
Krishan K. Verma,
Guangxi Academy of Agricultural Sciences, China
Elsayed Mansour,
Zagazig University, Egypt

*CORRESPONDENCE
Akbar Hossain
akbarhossainwrc@gmail.com

SPECIALTY SECTION
This article was submitted to Plant Nutrition, a section of the journal Frontiers in Plant Science

RECEIVED 29 January 2023
ACCEPTED 14 March 2023
PUBLISHED 04 April 2023

CITATION
Mitra B, Singha P, Roy Chowdhury A, Sinha AK, Skalicky M, Brestic M, Alamri S and Hossain A (2023) Normalized difference vegetation index sensor-based nitrogen management in bread wheat (*Triticum aestivum* L.): Nutrient uptake, use efficiency, and partial nutrient balance. *Front. Plant Sci.* 14:1153500.
doi: 10.3389/fpls.2023.1153500

Normalized difference vegetation index sensor-based nitrogen management in bread wheat (*Triticum aestivum* L.): Nutrient uptake, use efficiency, and partial nutrient balance

Biplab Mitra[1], Prantick Singha[1], Arnab Roy Chowdhury[1], Abhas Kumar Sinha[2], Milan Skalicky[3], Marian Brestic[3,4], Saud Alamri[5] and Akbar Hossain[6*]

[1]Department of Agronomy, Uttar Banga Krishi Viswavidyalaya, Coochbehar, West Bengal, India, [2]Department of Soil Science and Agricultural Chemistry, Uttar Banga Krishi Viswavidyalaya, Coochbehar, West Bengal, India, [3]Department of Botany and Plant Physiology, Faculty of Agrobiology, Food, and Natural Resources, Czech University of Life Sciences Prague, Prague, Czechia, [4]Institute of Plant and Environmental Sciences, Slovak University of Agriculture, Nitra, Slovak, [5]Department of Botany and Microbiology, College of Science, King Saud University, Riyadh, Saudi Arabia, [6]Division of Soil Science, Bangladesh Wheat and Maize Research Institute, Dinajpur, Bangladesh

The present experiment was conducted to assess the impact of fixed and variable doses (using a normalized difference vegetation index-sensor) of nitrogen (N) on wheat yields, nutrient uptake, nitrogen use efficiency, and soil nitrogen balance through the optimization of nitrogen dose. There were 10 treatments based on fixed and variable doses with different splits, and each treatment was replicated three times under a randomized complete block design. The treatments comprised fixed doses of 120 and 150 kg N ha^{-1} with different splits; variable doses based on sensor readings after application of 60, 90, and 120 kg N ha^{-1}; 225 kg N ha^{-1} as a nitrogen-rich control; and no application of nitrogen as the absolute control. It was revealed that the application of a basal dose of 60 kg N ha^{-1} and another 60 kg N ha^{-1} at the crown root initiation stage followed by a sensor-guided N application significantly improved wheat grain yields and grain nitrogen uptake. However, straw nitrogen uptake was highest in N-rich plots where 225 kg N ha^{-1}was applied. It was found that any curtailment in these doses at basal and crown root initiation stages followed by nitrogen application using a normalized difference vegetation index sensor later could not bring about higher crop yields. On average, wheat crops responded to 152–155 kg N ha^{-1} in both years of the study. Partial factor productivity along with agronomic and economic nitrogen use efficiency showed a declining trend with an increased rate of N application. Apparent N recovery values were comparable between normalized difference vegetation index sensor-based N application treatments and treatments receiving lesser N doses. Soil N status decreased in all the treatments except the nitrogen-rich strip, where there was a marginal increase in soil N status after the wheat crop harvest in the rotation. Partial nitrogen balance was negative for all the treatments except the control. From these 2-year field trials, it can be concluded that applying a normalized difference vegetation index sensor could be an essential tool for the rational management of fertilizer nitrogen in wheat grown in eastern sub-Himalayan plains.

KEYWORDS

wheat, NDVI sensor, variable nitrogen doses, partial nutrient balance, nitrogen uptake, nitrogen use efficiency

1 Introduction

Sustainable crop production remains a significant challenge, and it has drawn increasing attention from scientific communities. The alarming rate of natural resource degradation is a substantial concern for moving forward in agriculture, specifically in developing countries (Clair and Lynch, 2010). The present cultivation practices in the rice–wheat system are degrading the soil and water resources, and thus threatening the sustainability of the system (Chauhan et al., 2012; Kumar et al., 2018). The crop production system is nutrient dependent; in the last five decades, nutrient applications have significantly improved crop yields. However, owing to input mismanagement, biodiversity, soil quality, and air quality have been badly damaged, resulting in a negative impact on the environment (Godfray and Garnett, 2014). However, ideal crop management should always aim to enhance nutrient use efficiency, particularly that of nitrogen (N) as higher nitrogen use efficiency (NUE) is observed chiefly with lower rates (Majumdar et al., 2013; Mondal et al., 2018). Without compromising productivity and profitability, using the optimum quantity of nutrients is vital for agricultural sustainability (Salim and Raza, 2020). That is why to achieve sustainability, yields, economics, and nutrient use efficiency need to be considered with equal weighting (Hulmani et al., 2022).

The rice–wheat (R–W) cropping system occupies around 24 million hectares in Asian sub-tropical countries, including India, China, Bangladesh, China, and Nepal (Singh et al., 2013). The system occupies over 6.22 million hectares in the eastern Gangetic plains alone (Timsina et al., 2018). Most of the farmers in this region are continuing to intensify the cropping system by growing wheat during winter months, owing to high subsidies for agricultural inputs such as power, irrigation water, fertilizer, etc. (Saharawat et al., 2009). However, the rice–wheat system across southern Asia is water-, energy-, capital-, and labor-intensive and becomes less profitable as the availability of resources diminishes (Bhatt et al., 2016). Owing to poor soil fertility status, water and temperature stress, significant pest and disease infestation, groundwater depletion, escalating production costs, labor scarcity, climatic vulnerabilities, and, more importantly, deteriorating soil health caused by imbalanced fertilization, crop yields are suffering and sustainability issues are worsening (Islam et al., 2019; Dhanda et al., 2022). Sub-optimal nutrient management vis-à-vis nutrient mining in these tracts has resulted in production fatigue with poor nutrient use efficiency (Dhawan et al., 2021).

In the entire Indo-Gangetic Plain, wheat is mostly grown after monsoon rice during the dry winter season, with 100% of phosphorous (P) and potassium (K) doses and 50% of N doses being applied before final land preparation. Depending on irrigation events, the remaining N is applied in one or two splits before the maximum tillering stage (Pathak et al., 2006). N fertilizer in wheat is mostly applied in blanket doses without any consideration of existing soil fertility status. The inefficient use of N fertilizers results in poor NUE in wheat grown in the region (Adhikari et al., 1999; Dobermann et al., 2003). To a great extent, NUE suffers because of the large-scale blanket application of fertilizers, particularly nitrogen fertilizers (Majumdar et al., 2013; Mitra et al., 2019). Splitting the N doses might be considered an efficient tool through which NUEs could be significantly increased compared with blanket fertilizer application (Khan and Akma, 2021; Derebe et al., 2022). Inefficient splitting of N doses along with excess N applications may be the reason for lower NUEs; however, controversies still exist regarding N fertilization and maximizing yield with improved NUE in wheat production.

Real-time nitrogen management tools, such as a leaf color chart (LCC) or a soil plant analysis development (SPAD) chlorophyll meter, have shown promising results (Ladha et al., 2005); however, N management based on leaf color alone, without any consideration of crop biomass or photosynthetic rates, is considered to be the chief limitation of these tools. Fertilizer recommendation through these tools does not take into account the target or expected yield. In this context, the use of the optical sensor in agriculture for real-time N management, in which the total biomass or photosynthetic rates are considered, appears to be a promising option (Ma et al., 2001; Raun et al., 2001). Spectral vegetation indexes, such as the normalized difference vegetation index (NDVI), could successfully estimate the photosynthetic efficiency of the crop (Raun et al., 2001) and it is sensitive to the leaf area index and green biomass (Ma et al., 2001). By estimating the mid-season N requirement, the NDVI sensor could act as a framework for rational N management in cereals (Singh et al., 2011). A robust relationship between NDVI and grain yield showed higher NUEs than the conventional approach of N recommendation (Ali et al., 2015; Ali et al., 2020; Singha and Mitra, 2020). Considering the inadequacy of the general recommendation, this experiment has been planned to assess the impact on wheat of using NDVI sensor-based N management to ensure high yields and

NUEs with minimum loss of N from the soil. We expect that N scheduling in wheat based on the NDVI sensor could improve yield performance and NUE through the improved synchronization of N application with proper growth stages, through which the sustainability of the rice–wheat system could be maintained.

2 Materials and methods

2.1 Experimental site

The study was conducted in the research field of Uttar Banga Krishi Viswavidyalaya (UBKV), Coochbehar, West Bengal, India (26°24′02.2″N, 89°23′21.7″E, 43 m above mean sea level) over two consecutive wheat seasons during 2017–18 and 2018–19. The layout was kept undisturbed for the entire experimental period (including the growing of rice crops between wheat seasons under uniform fertility levels). The pH of the experimental site was 5.78 with an organic carbon concentration of 0.83% and 188.16, 27.05, and 141.90 kg ha^{-1} of mineralizable nitrogen, available phosphorus, and available potassium, respectively.

2.2 Meteorological parameters during the crop growing period

The annual precipitation of this area varied between 2800 and 3000 mm with relatively dry winter months. Being a per-humid climate, relative humidity remained very high even during the winter months (above 90% from November to January and around 86%–87% during February). During crop season, there was little variation in the temperature during both years, and, overall, there was a favorable temperature regime for the crop. In general, the temperature showed a rising trend from mid-February and reached its peak during May. A notable amount of rainfall (i.e., 36 mm) was received in March 2018, whereas there was less rain in March 2019 (i.e., 9.62 mm). The prevailing meteorological parameters during the period of experimentation reflected a favorable year for wheat (Figure 1 and Table S1).

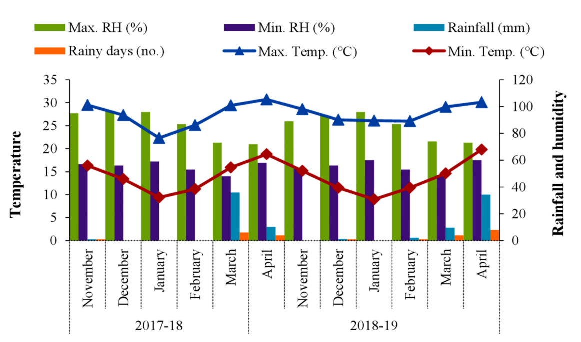

FIGURE 1
Prevailing meteorological data during the experiment.

2.3 Treatment details

The treatments and their combinations (Table 1) were arranged in a randomized complete block design and repeated three times. The size of each experimental plot was 8 m × 5.4 m. The detailed doses and splitting of N under various treatments, particularly the NDVI sensor-guided treatments, are presented in Table 2.

2.4 Crop management practices

The land preparation started with ploughing the site twice using a tractor-drawn cultivator. The soil was exposed would be more appropriate open for the next 10 days to reduce the soil moisture. Afterwards, a rotavator was used in a crisscross pattern to create a desirable tilth. In the second year, the land was prepared with the help of a power tiller within the plot area only without disturbing the previous layout. The crop received nitrogen as per the allocated treatment with 60 kg of P_2O_5 ha^{-1} and 40 kg of K_2O ha^{-1} (P and K levels were uniform for all the treatments), as recommended by the All India Coordinated Research Project on Wheat for this zone. The entire quantity of P and K fertilizers was applied during the final land preparation, while the N fertilizers were applied according to the treatment schedule. Being pH of the soil indicates slight acidity, lime was applied once in 3 years as per the requirement and it was applied during land preparation for the rice crop (i.e., the preceding crop in the rotation). Wheat variety HD 2967, this variety is meant for timely sowing condition under irrigated ecosysytem with a potential yield of 6.5 t ha^{-1}, was used in this experiment. This variety was developed by the Indian Agricultural Research Institute, New Delhi, India, and it has the pedigree ALONDRA/CUCKOO/URES-81/HD-2160-M/HD-2278[4251][4282]; HD-2733/K-9423/K-9351[4281]. After treating the seeds with carbendazim at 2.5 g kg^{-1}, the seeds were line sown, maintaining 20-cm spacing between the lines, with a seed rate of 100 kg ha^{-1}. After seeding, pre-emergence pendimethalin at 30% Emulsifiable Concentrate (EC) was applied at 1 kg ai ha^{-1} to keep the plots free from grassy weeds infestation; thereafter, carfentrazone-ethyl at 40% Dry Flowable (DF) was applied post emergence at 4 weeks after seeding at 20 g ai ha–1 to kill the broad-leaved weeds. There were two applications of boron, once at 35 days and, again, at 55 days after seeding, in the form of Solubor^{TM} (B 20%) at 0.2%. Zn-EDTA 12% at 0.10% was also sprayed at 55 days after seeding. Four irrigations were applied during the crown root initiation (CRI), active tillering, jointing, and milking stages during both years. The check basin method of irrigation was followed, keeping the depth of irrigation at 5 cm. After threshing and drying, grain yield was recorded at 13% moisture.

2.5 Soil and plant analysis

The pH of the experimental soil was determined with a Sorensen's pH meter (1909) using a soil–water suspension (1:2.5) by the potentiometric method. Mineralizable N of the

10.3389/fpls.2023.1153500

TABLE 1 Details of treatment.

Treatment	Dose (kg N ha^{-1})	Details
T1	No application	Absolute control (No N, P, or K)
T2	150	50% as basal + 25% CRI + 25% AT
T3	120	50% as basal + 25% CRI + 25% AT
T4	150	50% as basal + 50% CRI
T5	120	50% as basal + 50% CRI
T6	60 + NDVI	30 kg N each as basal and at CRI + NDVI* sensor
T7	90 + NDVI	30 and 60 kg N as basal and at CRI + NDVI sensor
T8	120 + NDVI	60 kg N each as basal and at CRI + NDVI sensor
T9	90 + NDVI	60 and 30 kg N as basal and at CRI + NDVI sensor
T10	225	50% basal + 50% at CRI

NDVI readings were taken at 45 and 65 days after seeding.
CRI, crown root initiation; AT, active tillering.

soil was measured by the alkaline potassium permanganate method (Subbiah and Asija, 1956). Available phosphorus in the soil was measured by Bray's method (Bray and Kurtz, 1945) with the help of a spectrophotometer at a wavelength of 660 nm. The available potassium in the soil was measured by the ammonium acetate extraction method, which involves extracting the soil with neutral 1(N) ammonium acetate (adjusted to pH 7.0), and the available potassium content was evaluated with the help of a flame photometer (Jackson, 1973). The available organic carbon was measured by the wet digestion method (Walkley and Black, 1934).

For plant analysis, grain and straw portions were crushed and kept separately with suitable descriptions and identification marks. The total N content in plants was determined by the modified micro-Kjeldahl method (Jackson, 1973). The P content of the plant materials was determined by triacid digestion through a vanadomolybdate–orthophosphate complex of yellow color in HNO_3 medium with the help of a spectrophotometer at 420 nm wavelength and by using a standard curve (Jackson, 1973). The potassium content of the plant materials was measured by the triacid digestion method with the help of a flame photometer and by using a standard curve as described by Muhr et al. (1965). The total uptake of N by the wheat at harvest was determined on a dry weight basis by multiplying the total dry matter of the crop with its corresponding content of N. It is expressed in kg N ha^{-1}.

TABLE 2 Nitrogen application at various growth stages under different treatments.

Treatment	N application (kg ha^{-1})									
	2017–18					2018–19				
	Basal	21 DAS	45 DAS	65 DAS	Total	Basal	21 DAS	45 DAS	65 DAS	Total
T1	0	0	0	0	0	0	0	0	0	0
T2	75	37.5	37.5	0	150	75	37.5	37.5	0	150
T3	60	30	30	0	120	60	30	30	0	120
T4	75	75	0	0	150	75	75	0	0	150
T5	40	40	40	0	120	40	40	40	0	120
T6	30	30	44	15	119	30	30	42	16	118
T7	30	60	40	10	140	30	60	35	7	132
T8	60	60	35	0	155	60	60	32	0	152
T9	60	30	42	10	142	60	30	35	5	130
T10	112.5	112.5	0	0	225	112.5	112.5	0	0	225

Treatments detailed in Table 1.
DAS, days after seeding.

TABLE 3 Grain yield, straw yield, and harvest index of wheat as influenced by varying nitrogen scheduling.

Treatment	Grain yield (t ha^{-1})		Straw yield (t ha^{-1})		Harvest index	
	2017–18	2018–19	2017–18	2018–19	2017–18	2018–19
T1	1.757a	1.353a	3.162a	2.382a	0.36b	0.36a
T2	4.725d	4.720d	6.850bc	6.603bc	0.41d	0.42b
T3	4.296bc	4.098b	6.951bc	6.265bc	0.38c	0.40b
T4	4.527cd	4.700d	6.690bc	6.910	0.40d	0.40b
T5	4.140b	4.125b	6.290b	6.395bc	0.40d	0.39b
T6	4.148b	4.030b	6.347b	5.924b	0.40d	0.40b
T7	4.523cd	4.355bc	6.921bc	6.740cd	0.40d	0.39b
T8	4.957d	5.068e	7.192d	7.084d	0.41d	0.42b
T9	4.450bc	4.385c	6.770bc	6.675bc	0.40d	0.40b
T10	4.513cd	4.637d	8.588e	8.763e	0.34a	0.35a
LSD (0.05)	**	**	**	**	**	**

Numbers followed by various lowercase letters within a column are significantly different from each other at a p-value ≤ 0.05 and are otherwise statistically on par; **significant at a 5% level of significance ($p \leq 0.05$). LSD, least significant difference.

2.6 Nitrogen use efficiency indices and partial nitrogen balance

The following NUE indices were calculated, as per the following formulae:

Partial factor productivity (kg grain kg^{-1} nitrogen applied) = yield under treatment (kg ha^{-1}) amount of nitrogen added (kg ha^{-1}). (1)

Agronomic N use efficiency (kg grain kg^{-1} nutrient applied over control) = [yield under test treatment (kg ha^{-1}) – yield under control (kg ha^{-1})][unit of nitrogen applied in the treatment (kg ha^{-1})]. (2)

Agrophysiological efficiency (kg grain kg^{-1} nutrient uptake) = [(grain yield under fertilizer treatment (kg ha^{-1}) – grain yield under control (kg ha^{-1})]/[(N uptake of nutrient in test treatment (kg ha^{-1}) – N uptake of nutrient in control (kg ha^{-1})]. (3)

Apparent N recovery (%) = [(amount of nutrient taken from test treatment plot (kg ha^{-1}) – the amount of nutrient taken from the control plot (kg ha^{-1})]/amount of nutrient added (kg ha^{-1}). (4)

Economic N use efficiency (kg grain ₹$^{-1}$ of investment in N) = yield under treatment (kg ha^{-1})/amount invested in nitrogen (₹ ha^{-1}). (5)

The partial N-balanced approach provides a quantitative framework of N inputs and outputs. Nitrogen addition through both fertilizers and inherent soil N were taken as input. Similarly, N removal from grain and straw was considered as output. The expected N balance was worked out by subtracting the total removal (results) from total inputs (soil plus fertilizer N), and this predicted balance was further compared with the actual soil N status after harvest of the crop to express gain or loss of N (Rana et al., 2017).

2.7 Statistical analysis

Analysis of variance (ANOVA) was used for the randomized complete block design. The significance of various nitrogen scheduling treatments was tested by mean squared error as proposed by the Fisher–Snedecor F-test at a 5% probability level (Cochran and Cox, 1950; Panse and Sukhatme, 1967). A Fisher and Yates's table was consulted for the computation of critical differences and comparisons. Finally, the mean values of each treatment were evaluated by Duncan's multiple range test (DMRT) using IBM SPSS Statistics version 20.0.3 (IBM Corporation, Armonk, NY, USA). In addition, the relationships between the various NUE indices were assessed using bivariate correlation analysis (Pearson's correlation coefficients and a two-tailed significance test).

3 Results

3.1 Changes in nitrogen scheduling influence the grain and straw yields as well as harvest index

Varying N scheduling had a significant effect on wheat grain yields in both years of the experiment (Table 3). The crops receiving 60 kg N ha^{-1} at baseline and 60 kg N ha^{-1} at CRI stages followed by NDVI-based N application (T8) achieved the maximum grain yield, followed by the crops receiving 75 kg N ha^{-1} at baseline along with 37.5 kg ha^{-1} each at the CRI and tillering stages. These two stages (i.e., CRI and active tillering) coincided with the timings of the second and third irrigation events.

In the treatments in which Less nitrogen compared to 150 kg/ha (the optimum dose) was applied (i.e., T2, T5, and T6), the grain yield was recorded as lower than in treatments with higher N application doses. It was noted that higher N application during CRI stages followed by further application based on the NDVI sensor recorded better yields than lower doses of N application at CRI. The N-rich plot did not result in higher yields owing to the lower number of filled grains per spike (data not presented) despite having higher spikes per m^2. However, the maximum straw yield was achieved in the N-rich plots in both years of the experiment. This was followed by treatment T8, in which 60 kg N ha^{-1} at baseline and 60 kg N ha^{-1} at CRI stages was applied, followed by the NDVI-based application of N. The harvest index varied significantly among the various N schedules, although there was little variation in the treatments receiving fixed or variable doses of N through the NDVI sensor with the exception of the absolute control (T1) and N-rich (T10) treatments, in which the harvest index value was much lower in both the years.

3.2 Nitrogen uptake by wheat grain and straw is influenced by changes in nitrogen scheduling

The crops receiving 60 kg N ha^{-1} at baseline along with 60 kg N ha^{-1} at CRI stages followed by NDVI-based N application (T8) also achieved the highest N uptake in its grain (65.9 and 67.9 kg N ha^{-1} during the first and second year of the experiment, respectively). It was closely followed by the N-rich treatment (64.1 and 66.8 kg N ha^{-1} during 2017–18 and 2018–19, respectively). Despite a higher proportion of N in grain and straw in the N-rich treatment, the uptake was somewhat lower in T10 owing to its lower grain yield than T8 (Figure 2 and Table S2). It was evident that there was little variation in grain N uptake between treatments T2, T4, T7, T8, T9, and T10. In contrast to grain N uptake, the straw N uptake was highest (39.5 and 42.1 N kg ha^{-1} during 2017–18 and 2018–19, respectively) in N-rich plots where 225 kg N ha^{-1} was applied in two equal doses, and was significantly higher than in any other treatment in the experiment (Figure 2 and Table S2). The lowest grain and straw N uptake were seen the absolute control treatment (T1).

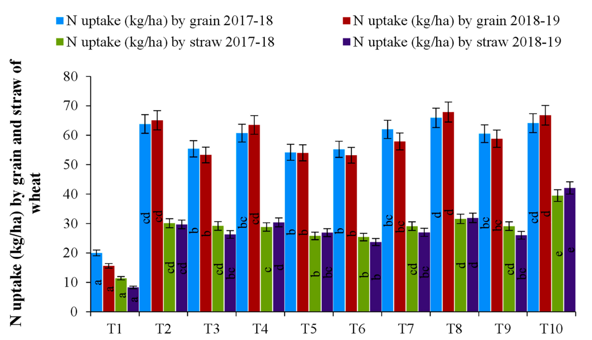

FIGURE 2
Nitrogen uptake by grain and straw of wheat, as influenced by various nitrogen schedules. Lowercase letters within a column are significantly different from each other at a *p*-value ≤ 0.05 and are otherwise statistically similar; **significant at a 5% level of significance ($p \leq 0.05$).

3.3 Nitrogen use efficiency indices are influenced by changes in nitrogen scheduling

Partial factor productivity of nitrogen (PFP_N) and agronomic NUE showed a decreasing trend as the rate of N application increased. We observed a lower PFP_N and agronomic NUE as the dose of N increased from 120 to 150 kg N ha^{-1}. The further increase in N rates from 150 to 225 kg N ha^{-1} in N-rich plots reflected the lowest N response regarding PFP_N and agronomic NUE. It was revealed that the lower rates of N, whether applied through fixed rates or at variable rates using NDVI, resulted in similar PFP_N and agronomic NUE values (Table 4). Irrespective of the number of splits, a dose of 120 kg N ha^{-1} showed the highest PFP_N and agronomic NUE values. As the expenditure towards N fertilizers was lower in treatments with lower rates of application, the economic N use efficiency (ENUE) value was also lower at 120 kg N ha^{-1} than other higher rates of N application. Invariably, the N-rich treatment (T10) showed the lowest ENUE value. It was evident that, except for in the N-rich plots where 225 kg ha^{-1} of N was applied, there was little variation in agrophysiological efficiency (APE) values among the treatments during both years of the experiment. The highest APE value was achieved with the treatment receiving 30 kg N ha^{-1} at baseline along with 30 kg N ha^{-1} at CRI stages, followed by NDVI-based N application (T6). Apparent N recovery (ANR) depends on the congruence between plant nitrogen demand and the quantity of nitrogen released from applied N. In general, ANR values were higher in treatments with lower N rates. It was interesting to note that T8 reflected the highest ANR value during the second year of study, indicating the feasibility of NDVI sensor-based N application.

3.4 Soil nitrogen status after the harvest of each crop is influenced by changes in nitrogen scheduling

Soil N status was estimated twice in each year, i.e., at the end of the wheat crop harvest and the end of the rice crop harvest (taken in the rotation after the wheat), and the changes in soil N status after each crop in the rotation are presented in Table 5.

The initial N status (188.16 kg N ha^{-1}) decreased in all treatments except in the N-rich strip, where there was a marginal increase in soil N (192.72 kg ha^{-1}) after the wheat crop harvest in the rotation. Owing to the changes in N scheduling in wheat, it was seen that even with recommended doses of N application (150 kg N ha^{-1}), the N status of the experimental soil decreased slightly. Even in T8, where 152–

TABLE 4 Nitrogen use efficiency indices in wheat as influenced by changes in nitrogen scheduling.

Treatment	Partial factor productivity of N (kg grain kg^{-1} of N)		Agronomic NUE (kg grain kg^{-1} of N)		Economic efficiency (kg grain ₹$^{-1}$ of investment in N)		Agrophysiological efficiency (kg grain kg^{-1} of N uptake)		Apparent N recovery (%)	
	2017–18	2018–19	2017–18	2018–19	2017–18	2018–19	2017–18	2018–19	2017–18	2018–19
T1	–	–	–	–	–	–	–	–	–	–
T2	31.50bc	31.47b	19.79bc	22.45b	1.91b	1.91b	47.5bc	47.5b	41.7bc	47.3c
T3	35.80d	34.15d	21.16d	22.88b	2.17c	2.07c	47.7bc	49.3bc	44.3c	46.4bc
T4	30.18b	31.33b	18.47b	22.31b	1.83b	1.90b	47.7bc	47.8b	38.7b	46.6bc
T5	34.50cd	34.38d	19.86bc	23.10bc	2.09c	2.08c	49.0c	48.6bc	40.5bc	47.5c
T6	34.86cd	34.15d	20.09cd	22.69b	2.11c	2.07c	48.6c	50.5c	41.3bc	44.9b
T7	32.31bc	32.99bc	19.76bc	22.74b	1.96b	2.00bc	46.4b	49.2bc	42.6c	46.2bc
T8	31.98bc	33.34bc	20.65cd	24.44c	1.94b	2.02bc	48.4bc	49.0bc	42.7c	49.9c
T9	31.34b	33.73bc	18.96b	23.32bc	1.90b	2.04bc	46.2b	49.8bc	41.0bc	46.8bc
T10	20.06a	20.61a	12.25a	14.60a	1.22a	1.25a	38.2a	38.7a	32.1a	37.7a
LSD (0.05)	**	**	**	**	**	**	**	**	**	**

Numbers followed by various lowercase letters within a column are significantly different from each other at a p-value ≤ 0.05 and are otherwise statistically on par; **significant at a 5% level of significance ($p \leq 0.05$). LSD, least significant difference.

155 kg N ha^{-1} was applied based on the NDVI sensor, the soil N concentration decreased. In the treatment where no N was used, the decrease in soil N was the greatest (170.53 kg N ha^{-1}). After the rice harvest (taken after wheat in the rotation), the N status in all treatments (including the control and N-rich treatments) further decreased by 10–17 kg N ha^{-1}. After the second-year wheat crop harvest, the soil N increased slightly (by 2–9 kg N ha^{-1}) in treatments where 150 kg N ha^{-1} or more was applied. For the remaining treatments, the soil N status decreased further, following the trend of the first year.

3.5 Partial nitrogen balance is influenced by changes in nitrogen scheduling

A statement of nitrogen inputs and outputs was expressed through the partial N-balanced approach. The sustainability of a system is examined through the retention of N in the soil. Although N inputs include direct addition through manures and fertilizers, atmospheric deposition, irrigation water, biological N fixation, etc., we have used only N addition through fertilizers and soil-inherent N as inputs. Similarly, we have concentrated on N removal through

TABLE 5 Soil nitrogen status after each crop in the rotation was influenced by various N schedules.

Treatment	Mineralizable N in soil (kg N ha^{-1})			
	2017–18		2018–19	
	End of wheat crop	End of rice crop	End of wheat crop	End of rice crop
T1	170.53	160.42	154.95	143.53
T2	185.38	172.31	181.73	170.25
T3	177.53	168.24	162.51	150.37
T4	182.28	170.25	178.38	166.23
T5	172.94	161.00	165.48	148.73
T6	175.32	160.81	157.31	145.32
T7	178.90	162.35	162.48	154.31
T8	184.00	170.52	172.30	160.38
T9	175.63	158.38	160.48	145.20
T10	192.72	187.34	196.29	188.75
Initial	188.16		171.23	

crop uptake only, although N is also removed through leaching, denitrification, volatilization, etc., which is difficult to measure. The N balance sheet was calculated after the wheat crop harvest in both years. During 2017–18, N balance was recorded as negative for all treatments except the control (which showed a positive balance), which reflected an overall loss of soil N under the various treatments, excluding the control. However, there was variation in the extent of N loss: the smallest losses were achieved when lower doses of N (118–120 kg N ha^{-1}) were used. The greatest losses (−116.84 kg ha^{-1}) were recorded for T10, the N-rich treatment (Table 6). The treatment in which no N was added recorded a positive balance (+13.77 kg N ha^{-1}) after the first-year harvest of the wheat crop. During 2018–19, the N balance sheet showed a similar trend to the first year, with a negative balance for all treatments except the control.

3.6 The correlation matrix

Correlation studies were performed with several NUE indices, viz., PFP_N, Agronomic Nitrogen Use Efficiency (ANUE), APE, ANR, and ENUE for both years (Table 7). The correlation matrix for 2017–18 and 2018–19 suggests a robust positive correlation among the various NUE indices (Table 7). It was observed that an absolute positive correlation existed between PFP_N and ENUE (r = 1) during both years of investigation. Apart from these two, the r-values for the other NUE indices ranged from 0.845 to 0.964 and from 0.845 to 0.985 in 2017–18 and 2018–19, respectively, indicating that the indices were highly correlated. As all these indices were calculated with respect to either grain yield, total biomass production, or total N intake and N rate, any change in N application rate primarily affected all these indices, for which the values showed a high positive correlation.

TABLE 6 Nitrogen balance sheet in wheat as influenced by changes in N scheduling in 2017–18 and 2018–19.

Treatment	Initial soil N (kg N ha^{-1}) (a)	Fertilizer N (kg N ha^{-1}) (b)	Total N (kg N ha^{-1}) (c = a + b)	Total grain + straw N uptake (kg N ha^{-1}) (d)	Expected balance (kg N ha^{-1}) (e = c − d)	Final balance (kg N ha^{-1}) (f)	Net gain or loss (kg N ha^{-1}) (g = f − e)
2017–18							
T1	188.16	0	188.16	31.4	156.76	170.53	+13.27
T2	188.16	150	338.16	93.9	244.26	185.38	−58.88
T3	188.16	120	308.16	84.6	223.56	177.53	−46.03
T4	188.16	150	338.16	89.4	248.76	182.28	−66.48
T5	188.16	120	308.16	80.0	228.16	172.94	−55.22
T6	188.16	119	307.16	80.6	226.56	175.32	−51.24
T7	188.16	140	328.16	91.0	237.16	178.90	−58.26
T8	188.16	155	343.16	97.6	245.56	184.00	−61.56
T9	188.16	142	330.16	89.6	240.56	175.63	−64.93
T10	188.16	225	413.16	103.6	309.56	192.72	−116.84
Treatments	2018–19						
T1	171.23	0	171.23	23.9	147.33	154.95	+17.62
T2	171.23	150	321.23	94.8	226.43	181.73	−44.70
T3	171.23	120	291.23	79.6	211.63	162.51	−49.12
T4	171.23	150	321.23	93.6	227.23	178.38	−48.95
T5	171.23	120	299.23	80.9	210.33	165.48	−44.85
T6	171.23	119	289.23	76.9	212.33	157.31	−55.02
T7	171.23	140	303.23	84.9	218.33	162.48	−55.85
T8	171.23	155	328.23	99.9	223.33	172.30	−51.03
T9	171.23	142	301.23	84.8	2.6.43	160.48	−55.95
T10	171.23	225	396.23	108.8	287.43	196.29	−91.14

TABLE 7 Correlation matrix of various nitrogen use efficiency (NUE) indices during 2017–18 and 2018–19.

Index	2017–18				
	PFP_N	ANUE	APE	ANR	ENUE
PFP_N	1.00				
ANUE	0.963**	1.00			
APE	0.932**	0.947**	1.00		
ANR	0.917**	0.972**	0.845**	1.00	
ENUE	1.000**	0.964**	0.932**	0.918**	1.00
Characters	2018–19				
PFP_N	1.00				
ANUE	0.967**	1.00			
APE	0.985**	0.958**	1.00		
ANR	0.875**	0.963**	0.845**	1.00	
ENUE	1.000**	0.967**	0.985**	0.876**	1.00

** Correlation is significant at the 0.01 level (two-tailed).

4 Discussion

4.1 Changes in nitrogen scheduling influence the grain and straw yields as well as harvest index

This study demonstrated that the crops receiving 60 kg N ha^{-1} at baseline along with 60 kg N ha^{-1} at CRI stages followed by NDVI sensor-based N application (T8) achieved the highest grain yield, although the highest straw yield was obtained in N-rich plots where 225 kg N ha^{-1} was applied. Excessive nitrogen application in the N-rich treatment triggered vegetative growth, and very often depressed the activity of superoxide dismutase and peroxidase and increased the accumulation of reactive oxygen species (ROS) and malondialdehyde. Higher NDVI values at anthesis interfered with N and lipid metabolism through increased lipid peroxidation, thus leading to poor grain filling in wheat (Kong et al., 2017). The activity of certain flag leaf enzymes, which play a crucial role in grain filling, is also disrupted under excess nitrogen application, reducing the number of filled grains (Kong et al., 2017). Singh et al. (2011) observed robust relationships between N application at Feekes's growth stages 5 and 6 and 7 and 8 and actual wheat yields.

In our experiment, the NDVI-based N application coincided with Feekes's growth stages 5 and 6 [45 days after seeding (DAS)] and 7 and 8 (65 DAS). The yield was enhanced, compared with a fixed nitrogen application dose, when N was applied based on the NDVI sensor at 45 and 65 DAS. Our study showed that the crop did not require any application of N at 65 DAS if 60 kg ha^{-1} of N was applied at baseline during the final land preparation stage and again at the CRI stage. Our results indicated that the timing of the nitrogen application and the quantity of nitrogen involved in each split determined the yield. A higher number of divisions may not always result in higher yields if the amount is insufficient during these crucial growth stages. Sobh et al. (2000) and Melaj et al. (2003) also demonstrated an increase in yield with the synchronization of nitrogen application at essential growth stages. Mitra et al. (2014) reported that grain yield was significantly affected by different N rates owing to the effect on spikelets per spike, grains per spike, and 1,000-grain weight.

4.2 Nitrogen uptake by grain and straw of wheat is influenced by changes in nitrogen scheduling

The higher N concentrations in the grain from plots with more applied N may be attributed to a better response to applied N through the translocation of absorbed N to grain. N supply in the soil may also affect the grain N concentration in combination with genetic variability (Lopez-Bellido et al., 2004). Achieving good yields with higher N concentrations in grain resulted in higher grain N uptake in treatment T8. Sinebo et al. (2004) also reported higher N concentrations in wheat grains with increasing N supply. However, the straw yield in the N-rich treatment was far higher than in any other treatments in the experiment. The straw N concentration was also higher in the N-rich treatment, as was the total straw N uptake. Nitrogen uptake depends on the timing of its application (Kumar and Yadav, 2005). Split application of N after the first irrigation significantly increased the N uptake, and N application at critical stages of crop growth resulted in higher yields and, therefore, higher N uptake. Mattas et al. (2011) observed a significant increase in N uptake in three-split applications over two-split applications in Ludhiana, India. Through leaf measurements using an NDVI sensor, N uptake as well as grain yields could be improved by a considerable amount (Ali et al., 2015). Thus, the NDVI sensor could act as a framework for refining nitrogen management in wheat.

4.3 Nitrogen use efficiency indices are influenced by changes in nitrogen scheduling

Most NUE indices showed higher values with lower rates of N application. Increasing yields in wheat with lower PFP_N was previously reported by Haile et al. (2012) and Mondal et al. (2018). These values indicate a higher proportion of yield attainment per unit of N application using lower rates of N application. Our study suggests that the application of N based on an NDVI sensor could be more efficient than a fixed rate of N application applied with two or three splits. Better synchronization, with the timely application of N at the proper doses, may be the key to NDVI-based N applications. Raun et al. (2002) showed that NUEs in wheat were improved by more than 15% when N fertilization was based on an in-season estimate of yield (INSEY) calculated from an optically measured NDVI. PFP_N and agronomic NUE are essential tools for judging N management's nutrient use efficiency and developing environmentally sound nutrient management strategies. Partial factor productivity increases with precise fertilizer application, better crop management practices, and an increased nutrient conversion ratio in plant systems. In the treatments in which N was applied based on the NDVI sensor (T6–T9), there was a slight variation in ENUE. More importantly, these values were statistically on par with the highest values recorded during 2018–19. Regarding economic N use efficiency (ENUE), higher values were recorded in treatments with lower rates of N application than higher rates. This indicates that investment in N was lower in those treatments for which there was an increased ENUE value, owing to the lesser use of N. The yields obtained with higher N doses may not always be economically feasible. These indices suggest that the use of an NDVI sensor could have the potential to achieve both higher yields and increased ENUE values. Biermacher et al. (2006) showed significant nitrogen savings under variable-rate N applications. Higher ENUE values have been reported in wheat using site-specific nutrient management practices with precise N application in the sub-Himalayan plains of West Bengal, India (Mondal et al., 2018; Mitra et al., 2019).

As APE is related to grain yield only, it was a powerful tool in assessing the effect of N application on grain yields. Here also, the values were slightly higher in treatments with less applied N, although there was some slight variation. Achieving higher grain yields with lower rates of N application brought about an increase in APE values under both fixed and (using the NDVI sensor) variable rates of N application. There was no evidence that the APE values increased steadily with an increasing number of splits. Higher APE values in wheat with lower rates of N application have been previously reported (Gauer et al., 1992).

In general, the apparent nitrogen recovery (ANR) of crops was higher in treatments receiving less N. From this trend, it was evident that the N-rich plots recorded the lowest ANR values. It was further noted that the ANR values were comparable in NDVI-based N application treatments with those of lower-N treatments. It is interesting to note that T8 recorded the highest ANR value (49.9%) in 2018–19, reflecting more effective N splitting in terms of a higher N uptake value (comparable with N-rich plots). This suggests that site-specific adjustments to nutrient management guidelines could achieve higher yield performances and an increase in profit.

The correlation matrix in both seasons suggested a robust positive correlation among the various NUE indices (Table 7). An absolute positive correlation was observed between PFP_N and ENUE, (r = 1). Apart from these two, the r-values for the other NUE indices ranged from 0.845 to 0.964 and from 0.845 to 0.985 in 2017–18 and 2018–19, respectively, indicating that the indices were highly correlated. As all these indices were calculated with regard to grain yield, total biomass production, or total N intake and N rate, any change in N rate primarily affected all these indices, for which the values showed a high positive correlation. The findings of our current study in relation to NUE indices were also confirmed by several earlier studies (Fageria and Baligar, 2005; Chuan et al., 2016), which confirmed that the application of higher amounts of fertilizer N than the required quantities leads to high N losses and low NUEs. On the other hand, other findings stated that a site-specific nutrient management strategy based on synchronizing fertilizer N supply with the N demand of the crop and supply of N from soil sources could cause soil N to increase, as confirmed by Ali et al. (2015) and Ali et al. (2020), who also reported that the use of an NDVI sensor could optimize the N dose to improve NUEs with reduced environmental risks.

4.4 Soil nitrogen status after the harvest of each crop is influenced by changes in nitrogen scheduling

Soil N status decreased after the wheat harvest, even with the application of 150 kg N ha^{-1} to the crop. The N status of the experimental soil suggests that N scheduling in the wheat–rice rotation has to be restructured more precisely to maintain the overall N status of the soil and the sustainability of the system. In fact, N application of 150 kg N ha^{-1} or more in wheat did not decrease the overall N status of the experimental soil to a greater extent than lower-N applications, as reflected in the data after the wheat harvest. However, after the rice harvest, the decrease in soil N was very high. As there was no treatment difference in the rice crops concerning N nutrition, the extent of the decrease in soil N status was similar across all treatments. While studying the rice–wheat system in the Tailake region of China, Xue et al. (2014) noted that increased fertilizer N input was primarily responsible for the low NUE. The authors also found higher losses after the rice harvest, possibly owing to higher losses of N through leaching and runoff. N loss could be minimized with reduced chemical inputs combined with organic inputs. We feel that a more thorough understanding of N dynamics in this rotation is required to maintain the system's sustainability.

4.5 Partial nitrogen balance is influenced by changes in nitrogen scheduling

The partial N balance showed that the extent of N losses was slightly smaller in the second year than in the first year. The greatest negative balance was recorded in the N-rich plot (–91.14 kg N ha^{-1}). The control treatment recorded a positive balance (+7.62 kg N ha^{-1}) after the harvest of the second-year wheat. The negative balance indicated that the soil itself is a source of (and not a drain on) N—a result of increased mineralization of crop residues and the conversion of organic N into inorganic N, which has taken up the plants. N balance studies are always beneficial for long-term experiments (Ross et al., 2008; Pieri et al., 2011). Long-term nutrient management significantly affected the N-uptake and NUE indices. The reduced N losses combined with balanced N management could improve productivity with a lesser degree of environmental pollution (Dhawan et al., 2021). Minimum loss of N was previously reported in some studies in which organic manures were used with NPK fertilizers (Dhawan et al., 2021; Fazal et al., 2022). There are complexities in measuring a range of inputs and outputs and, depending on the climate and soil features, environments can undergo long-term change in just a few years (Watson and Atkinson, 1999). Sainju (2017) advocated that balancing N over 5-year cycles is highly beneficial for managing N.

5 Conclusions

From this 2-year field trial, it can be concluded that applying the normalized difference vegetation index sensor could be an essential tool for the rational management of fertilizer nitrogen in wheat grown in eastern sub-Himalayan plains. A dose of 60 kg N ha^{-1} at baseline and 60 kg N ha^{-1} at crown root initiation followed by nitrogen application controlled by the sensor (32–35 kg N ha^{-1}) resulted in a significant improvement in yield parameters and nutrient uptake, although lower nitrogen doses (118–120 kg ha^{-1}) resulted in higher values of various NUE parameters. Apparent nitrogen recovery values were comparable between sensor-based nitrogen application treatments and treatments receiving lower N doses. Despite the application of 150–155 kg N ha^{-1} in wheat, a negative balance of soil nitrogen suggested the need for further precision in nitrogen scheduling to maintain the system's sustainability for this region.

Data availability statement

The raw data supporting the conclusions of this article will be made available by the authors, without undue reservation.

Author contributions

Conceptualization: BM, PS, AR, and AS; methodology: BM, PS, AR, and AS; formal analysis: MS, MB, SA, and AH; data curation: MS, MB, SA, and AH; statistical expertise: MS, MB, SA, and AH; writing—original draft preparation: MS, MB, SA, and AH; writing—review and editing: SA and AH; visualization: BM, PS, AR, and AS; supervision: BM and AS; and funding acquisition: SA and AH. All authors contributed to the article and approved the submitted version.

Funding

This work was financially supported by the Department of Agronomy, Uttar Banga Krishi Viswavidyalaya, Pundibari, Coochbehar 736165, West Bengal, India. The research was also partially funded by the Researchers Supporting Project (number RSP2023R194), King Saud University, Riyadh, Saudi Arabia.

Acknowledgments

The authors would like to extend their sincere appreciation to the Researchers Supporting Project (number RSP2023R194), King Saud University, Riyadh, Saudi Arabia.

Conflict of interest

The authors declare that the research was conducted in the absence of any commercial or financial relationships that could be construed as a potential conflict of interest.

Publisher's note

Supplementary material

The Supplementary Material for this article can be found online at: https://www.frontiersin.org/articles/10.3389/fpls.2023.1153500/full#supplementary-material

References

Adhikari, C., Bronson, K. F., Panaullah, G. M., Regmi, A. P., Saha, P. K., Dobermann, A., et al. (1999). On-farm n supply and n nutrition in the rice-wheat system of Nepal and Bangladesh. *Field Crops Res.* 64, 273–286. doi: 10.1016/S0378-4290(99)00063-5

Ali, A. M., Ibrahim, S. M., and Singh, B. (2020). Wheat grain yield and nitrogen uptake prediction using atLeaf and GreenSeeker portable optical sensors at jointing growth stage. *Inf. Process Agric.* 7, 375–383. doi: 10.1016/j.inpa.2019.09.008

Ali, A. M., Thind, H. S., Singh, V., and Singh, B. A. (2015). A framework for refining nitrogen management in direct seed rice using GreenSeeker optical sensor. *Comput. Electron Agric.* 110, 114–120. doi: 10.1016/j.compag.2014.10.021

Amer, M. M. (2017). *Response of wheat yield to fertilization by nitrogen, potassium and biofertilizers in salt affected soils*. [Doctoral thesis, Department of Soil Science, Kafr EL-Sheikh]. doi: 10.13140/RG.2.2.17572.88963

Bhatt, R., Kukal, S. S., Busari, M. A., Arora, S., and Yadav, M. (2016). Sustainability issues on rice-wheat cropping system. *Int. Soil Water Conserv. Res.* 4 (1), 64–74. doi: 10.1016/j.iswcr.2015.12.001

Biermacher, J. T., Epplin, F. M., Brorsen, B. W., Solie, J. B., and Raun, W. R. (2006). Maximum benefit of a precise nitrogen application system for wheat. *Precis. Agric.* 7, 193–204. doi: 10.1007/s11119-006-9017-6

Bray, R. H., and Kurtz, L. T. (1945). Determination of total organic and available forms of phosphorus in soils. *Soil Sci.* 59, 39–45. doi: 10.1097/00010694-194501000-00006

Clair, S. B., and Lynch, J. (2010). The opening of Pandora's Box:climate change impacts on soil fertility and crop nutrition in developing countries. *Plant Soil* 335, 101–115.

Chauhan, B. S., Mahajan, G., Sardana, V., Timsina, J., and Jat, M. L. (2012). Productivity and sustainability of the rice–wheat cropping system in the indo-gangetic plains of the Indian subcontinent: problems, opportunities, and strategies. *Adv. Agron.* 117, 315–369. doi: 10.1016/B978-0-12-394278-4.00006-4

Chuan, L., He, P., Zhao, T., Zheng, H., and Xu, X. (2016). Agronomic characteristics related to grain yield and nutrient use efficiency for wheat production in China. *PloS One* 11 (9), e0162802. doi: 10.1371/journal.pone.0162802

Cochran, W. G., and Cox, G. M. (1950). *Experimental designs* (New York: John Wiley and Sons).

Derebe, B., Bitew, Y., Asargew, F., and Chakrlie, G. (2022). Optimizing time and split application of nitrogen fertilizer to harness grain yield and quality of bread wheat (Triticum aestivum l.) in northwestern Ethiopia. *PloS One* 17 (12), e0279193. doi: 10.1371/journal.pone.0279193

Dhanda, S., Yadav, A., Yadav, D. B., and Chauhan, B. S. (2022). Emerging issues and potential opportunities in rice-wheat cropping system of north-western India. *Front. Plant Sci.* 13. doi: 10.3389/fpls.2022.832683

Dhawan, D., Dheri, G. S., and Gill, A. A. S. (2021). Nitrogen budgeting of rice-wheat cropping system under long-term nutrient management in an inceptisols of north India. *Eur. J. Agron.* 130, 126376. doi: 10.1016/j.eja.2021.126376

Dobermann, A., Witt, C., Abdulrachman, S., Gines, H. C., Nagarajan, R., Son, T. T., et al. (2003). Soil fertility and indigenous nutrient supply in irrigated domains of Asia. *Agron. J.* 95, 913–927. doi: 10.2134/agronj2003.0913

Fageria, N. K., and Baligar, V. C. (2005). Enhancing nitrogen use efficiency in crop plants. *Adv. Agron.* 88, 97–185. doi: 10.1016/S0065-2113(05)88004-6

Fazal, A., Khan, A., Anjum, A., Khan, S., Khan, A. A., and Akbar, H. (2022). Wheat production and partial nitrogen budget in response to herbicide and nitrogen application. *J. Plant Nutr.* 45 (8), 1253–1263. doi: 10.1080/01904167.2021.2003391

Gauer, L. E., Grant, C. A., Gehl, D. T., and Bailey, L. D. (1992). Effects of nitrogen fertilization on grain protein content, nitrogen uptake, and nitrogen use efficiency of six spring wheat (*Triticum aestivum* l.) cultivars, in relation to estimated moisture supply. *Can. J. Plant Sci.* 72, 235–241. doi: 10.4141/cjps92-026

Godfray, H. C. J., and Garnett, T. (2014). Food security and sustainable intensification. *Phil. Trans. R. Soc. B.* 369, 20120273. doi: 10.1098/rstb.2012.0273

Haile, D., Nigussie, D., and Ayana, A. (2012). Nitrogen use efficiency of bread wheat: Effects of nitrogen rate and time of application. *J. Soil Sci. Plant Nutr.* 12 (3), 389–410. doi: 10.4067/S0718-95162012005000002

Hulmani, S., Salakinkop, S. R., and Somangouda, G. (2022). Productivity, nutrient use efficiency, energetic, and economics of winter maize in south Asia. *PloS One* 17 (7), e0266886. doi: 10.1371/journal.pone.0266886

Islam, S., Gathala, M. K., Tiwari, T. P., Timsina, J., Liang, A. M., Maharajan, S., et al. (2019). Conservation agriculture based sustainable intensification: Increasing yields and water productivity for smallholders of the Eastern gangetic plains. *Field Crops Res.* 238, 1–17. doi: 10.1016/j.fcr.2019.04.005

Jackson, M. L. (1973). *Soil chemical analysis* (New Delhi: Prentice Hall of India Pvt. Ltd.), 498.

Khan, G. R., and Akma, M. (2021). Nitrogen application rate and timing management for improved grain quality parameters of wheat crop. *Pak. J. Agric. Sci.* 58, 1141–1153. doi: 10.21162/PAKJAS/21.102

Kong, L., Xie, Y., Hu, L., Si, J., and Wang, Z. (2017). Excessive nitrogen application dampens anti-oxidant capacity and grain filling in wheat as revealed by metabolic and physiological analyses. *Sci. Rep.* 7, 43363. doi: 10.1038/srep43363

Kumar, R., and Yadav, D. S. (2005). Effect of zero and minimum tillage in conjunction with nitrogen management in wheat (*Triticum aestivum*) after rice (*Oryza sativa*). *Ind. J. Agron.* 50 (1), 54–57.

Kumar, V., Jat, H. S., Sharma, P. C., Gathala, M. K., Malik, R., Kamboj, B. R., et al. (2018). Can productivity and profitability be enhanced in intensively managed cereal systems while reducing the environmental footprint of production? assessing sustainable intensification options in the breadbasket of India. *Agric. Ecosyst. Environ.* 252, 132–147. doi: 10.1016/j.agee.2017.10.006

Ladha, J. K., Pathak, H., Krupnik, T. J., Six, J., and Van Kessel, C. (2005). Efficiency of fertilizer nitrogen in cereal production: retrospect and prospects. *Adv. Agron.* 87, 85–156. doi: 10.1016/S0065-2113(05)87003-8

Lopez-Bellido, R., Shepherd, C., and Barraclough, P. (2004). Predicting post-anthesis n requirements of bread wheat with a minolta SPAD meter. *Eur. J. Agron.* 20, 313–320. doi: 10.1016/S1161-0301(03)00025-X

Ma, B. L., Dwyer, L. M., Costa, C., Cober, E. R., and Morrison, M. J. (2001). Early prediction of soybean yield from canopy reflectance measurements. *Agron. J.* 93, 1227–1234. doi: 10.2134/agronj2001.1227

Majumdar, K., Jat, M. L., Pampolino, M., Satyanarayana, T., Dutta, S., and Kumar, A. (2013). Nutrient management in wheat: Current scenario, improved strategies and future research needs in India. *J. Wheat Res.* 4, 1–10.

Mattas, K. K., Uppal, R. S., and Singh, R. P. (2011). Effect of varieties and nitrogen management on the growth, yield and nitrogen uptake of durum wheat. *Res. J. Agric. Sci.* 2 (2), 376–380.

Melaj, M. A., Echeverría, H. E., López, S. C., Studdert, G., Andrade, F., and Bárbaro, N. O. (2003). Timing of nitrogen fertilization in wheat under the conventional and no-tillage system. *Agron. J.* 95, 1525–1531. doi: 10.2134/agronj2003.1525

Mitra, B., Mookherjee, S., and Das, S. (2014). Performances of wheat under various tillage and nitrogen management in sub-Himalayan plains of West Bengal. *J. Wheat Res.* 6 (2), 150–153.

Mitra, B., Majumdar, K., Dutta, S. K., Mondal, T., Das, S., Banerjee, H., et al. (2019). Nutrient management in wheat (*Triticum aestivum*) production system under conventional and zero tillage in eastern sub-Himalayan plains of India. *Ind. J. Agric. Sci.* 89 (5), 775–784. doi: 10.56093/ijas.v89i5.89657

Mondal, T., Mitra, B., and Das, S. (2018). Precision nutrient management in wheat (*Triticum aestivum* l.) using nutrient expert: Growth phenology, yield, nitrogen use efficiency and profitability under eastern sub-Himalayan plains. *Ind. J. Agron.* 63 (2), 174–180.

Muhr, G. R., Datta, N. P., Sankarasubramoney, H., Dever, F., Laley, V. K., and Donahue, R. L. (1965). "Critical test value for available n, p and K in different soils," in *Soil testing in India*, *2nd Edition* (New Delhi: U.S Agency for International Development).

Panse, V. G., and Sukhatme, P. V. (1967). *Statistical methods for agricultural workers. 2nd Edition* (New Delhi: Indian Council of Agricultural Research).

Pathak, H., Li, C., Wassman, R., and Ladha JK, J. K. (2006). Simulation of nitrogen balance in rice-wheat systems of the indo-gangetic plains. *Soil Sci. Soc. Am. J.* 70, 1612–1622. doi: 10.2136/sssaj2005.0165

Pieri, L., Ventura, F., and Vignudelli, P. R. (2011). Nitrogen balance in a hilly semi-agricultural watershed in northern Italy. *Ital. J. Agron.* 6, 67–75. doi: 10.4081/ija.2011.e12

Rana, L., Banerjee, H., Dutta, S. K., Ray, K., Majumdar, K., and Sarkar, S. (2017). Management practices of macronutrients for potato for smallholder farming system at alluvial soils of India. *Arch. Agron. Soil Sci.* 63, 1963–1976. doi: 10.1080/03650340.2017.1317922

Raun, W. R., Johnson, G. V., Stone, M. L., Solie, J. B., Lukina, E. V., Thomason, W. E., et al. (2001). In-season prediction of potential grain yield in winter wheat using canopy reflectance. *Agron. J.* 93, 131–138. doi: 10.2134/agronj2001.931131x

Raun, W. R., Solie, J. B., Johnson, G. V., Stone, M. L., Mullen, R. W., Freeman, K. W., et al. (2002). Improving nitrogen use efficiency in cereal grain production with optical sensing and variable rate application. *Agron. J.* 94, 815–820. doi: 10.2134/agronj2002.8150

Ross, S. M., Izaurralde, R. C., Janzen, H. H., Robertsa, J. A., and McGill, W. B. (2008). The nitrogen balance of three long-term agroecosystems on a boreal soil in Western Canada. *Agric. Ecosyst. Environ.* 127, 241–250. doi: 10.1016/j.agee.2008.04.007

Saharawat, Y. S., Gathala, M. K., Ladha, J. K., Malik, R. K., Singh, S., Jat, M. L., et al. (2009). "Evaluation and promotion of integrated crop and resource management in the rice–wheat system in north-west India," in *Integrated crop and resource management in the rice–wheat system of south Asia*. Eds. J. K. Ladha, Y.-. Singh, O. Erenstein and B. Hardy (Los Banos, Philippines: International rice research institute (IRRI), 133–150.

Sainju, U. M. (2017). Determination of nitrogen balance on agroecosystems. *Methods X.* 4, 199–208. doi: 10.1016/j.mex.2017.06.001

Salim, N., and Raza, A. (2020). Nutrient use efficiency (NUENUE) for sustainable wheat production: a review. *J. Plant Nutr.* 43, 297–315. doi: 10.1080/01904167.2019.1676907

Sinebo, W., Gretzmacher, R., and Edelbauer, A. (2004). Genotypic variation for nitrogen use efficiency in Ethiopian barley. *Field Crop Res.* 85, 43–60. doi: 10.1016/S0378-4290(03)00135-7

Singh, B., Sharma, R. K., Kaur, J., Jat, M. L., Martin, K. L., Singh, Y., et al. (2011). Assessment of nitrogen management strategy using an optical sensor for irrigated wheat. *Agron. Sustain Dev.* 31, 589–603. doi: 10.1007/s13593-011-0005-5

Singh, V. K., Dwivedi, B. S., Buresh, R. J., Jat, M. L., Majumdar, K., Gangwar, B., et al. (2013). Potassium fertilization in the rice-wheat system across northern India: Crop performance and soil nutrients. *Agron. J.* 105, 471–481. doi: 10.2134/agronj2012.0226

Singha, P., and Mitra, B. (2020). Nitrogen scheduling in wheat (*Triticum aestivum* l.) using a NDVI sensor under sub-Himalayan plains of West Bengal. *J. Crop Weed* 16, 49–55. doi: 10.22271/09746315.2020.v16.i3.1364

Subbiah, B. V., and Asija, G. L. (1956). A rapid procedure for the estimation of available nitrogen in soils. *Curr. Sci.* 25, 259–260.

Timsina, J., Wolf, J., Guilpart, N., van Bussel, L., Grassini, P., Wart, J., et al. (2018). Can Bangladesh produce enough cereals to meet future damand? *Agric. Syst.* 163, 36–44. doi: 10.1016/j.agsy.2016.11.003

Walkley, A. J., and Black, C. A. (1934). Estimation of soil organic carbon by the chromic acid titration method. *Soil Sci.* 37, 29–38. doi: 10.1097/00010694-193401000-00003

Watson, C. A., and Atkinson, D. (1999). Using nitrogen budgets to indicate nitrogen use efficiency and losses from whole farm systems: a comparison of three methodological approach. *Nutr. Cycl. Agroecosyst.* 53, 259–267. doi: 10.1023/A:1009793120577

Xue, L., Yu, Y., and Yang, L. (2014). Maintaining yields and reducing n loss in rice-wheat rotation system in taihu lake region with proper fertilizer management. *Environ. Res. Newslett.* 9, 115010. doi: 10.1088/1748-9326/9/11/115010

frontiers | Frontiers in Plant Science

TYPE Original Research
PUBLISHED 11 April 2023
DOI 10.3389/fpls.2023.1144461

Check for updates

OPEN ACCESS

EDITED BY
Ying Zhao,
Ludong University, China

REVIEWED BY
Krishan K. Verma,
Guangxi Academy of Agricultural Sciences, China
Zhenwei Song,
Institute of Crop Sciences (CAAS), China

*CORRESPONDENCE
Yixiang Sun
sunyixiang@126.com

SPECIALTY SECTION
This article was submitted to Plant Nutrition, a section of the journal Frontiers in Plant Science

RECEIVED 14 January 2023
ACCEPTED 24 February 2023
PUBLISHED 11 April 2023

CITATION
Yuan M, Sun Y, Wu G, Wang J, Liu C, Tang T, Zhang X, Wang W and Jing Y (2023) The optimum economic nitrogen rate of blended controlled-release nitrogen fertilizer for rice in the Chanoyu watershed in the Yangtze River Delta, China. *Front. Plant Sci.* 14:1144461. doi: 10.3389/fpls.2023.1144461

The optimum economic nitrogen rate of blended controlled-release nitrogen fertilizer for rice in the Chanoyu watershed in the Yangtze River Delta, China

Manman Yuan[1], Yixiang Sun[1*], Gang Wu[1], Jiabao Wang[1], Chuang Liu[1], Tongtong Tang[2], Xiangming Zhang[1], Wenjun Wang[2] and Yudan Jing[2]

[1]Key Laboratory of Nutrient Cycling, Resources and Environment of Anhui, Institute of Soil and Fertilizer, Anhui Academy of Agricultural Sciences, Hefei, China, [2]School of Biological Science and Food Engineering, Chuzhou University, Chuzhou, China

Introduction: The application of controlled-release nitrogen fertilizer (CRN) has become an important production method to achieve high crop yield and ecological safety. However, the rate of urea-blended CRN for rice is usually determined by conventional urea, and the actual rate is still unclear.

Methods: A five-year field experiment was carried out in the Chaohu watershed in the Yangtze River Delta to study rice yield, N fertilizer utilization efficiency (NUE), ammonia (NH3) volatilization and economic benefit under the four urea-blended CRN treatments with a 4:3:3 ratio applied at one time (60, 120, 180, 240 kg/hm2, CRN60, CRN120, CRN180, CRN240), four conventional N fertilizer treatments (N60, N120, N180, N240) and a control without N fertilizer (N0).

Results and Discussion: The results showed that the N released from the blended CRNs could well satisfy the N demand of rice growth. Similar to the conventional N fertilizer treatments, a quadratic equation was used to model the relationship between rice yield and N rate under the blended CRN treatments. The blended CRN treatments increased rice yield by 0.9-8.2% and NUE by 6.9-14.8%, respectively, compared with the conventional N fertilizer treatments at the same N application rate. The increase in NUE in response to applied blended CRN was related to the reduction in NH3 volatilization. Based on the quadratic equation, the five-year average NUE under the blended CRN treatment was 42.0% when rice yield reached the maximum, which was 28.9% higher than that under the conventional N fertilizer treatment. Among all treatments, CRN180 had the highest yield and net benefit in 2019. Considering the yield output, environmental loss, labor and fertilizer costs, the optimum economic N rate under the blended CRN treatment in the Chaohu watershed was 180-214 kg/

hm2, compared with 212-278 kg/hm2 under the conventional N fertilizer treatment. The findings suggest that blended CRN improved rice yield, NUE and economic income while decreasing NH3 volatilization and negative environmental outcomes.

KEYWORDS

optimum economic nitrogen rate, nitrogen release, rice, yield, NH3 volatilization, environmental loss

1 Introduction

Rice provides food for approximately half of the world's population and is a major source of calories and protein for poor people in Asia and Africa (Muthayya et al., 2015). According to the estimate of the Food and Agriculture Organization of the United Nations, the world population will reach 9 billion by 2050, and food production will need to increase by at least 70% to meet the demand due to population growth (Niggli, 2015). Nitrogen (N) is an essential nutrient for rice growth. High rates of N fertilizer are applied to achieve a high yield of rice. China consumes more than one-third of the world's total N fertilizer and is currently the largest N fertilizer user in the world (IFA, 2021). The Chaohu watershed in the Yangtze River Delta in China is one of the major rice production areas in China. The maximum application rate of chemical N fertilizer during the rice growing period can reach 300 kg/hm^2. The N fertilizer utilization efficiency (NUE) of rice was reported to be 39% in this area (Yu and Shi, 2015), which is 20–30 percentage points lower than the levels in developed countries such as Europe and the United States (Lassaletta et al., 2014). Excessive application of N fertilizer not only increases the cost of rice production, reduces NUE, and leads to the eutrophication of water bodies and soil compaction (Congreves et al., 2021), but also causes the volatilization of nitrogen oxides and ammonia (NH_3) into the air, and these gases have become the main components of haze and reduced atmospheric quality (Wang et al., 2016). NH_3 volatilization from agricultural production was estimated to account for more than 50% of global NH_3 emissions (Gronwald et al., 2018). Therefore, to control the contribution of N loss in paddy fields to environmental emissions, research on nutrient reduction technology in agricultural fields has become a current research hotspot.

To reduce N use and loss, fertilization measures such as deep application, split application, and N fertilizer setback are often used in rice production (Emran et al., 2019; Wang et al., 2019; Ju et al., 2021), but they still present existing problems in actual production. On the one hand, topdressing in a split application is often spread on the soil surface, which can cause nutrient runoff, leaching, and NH_3 volatilization (Wang et al., 2019; Zhan et al., 2020; Song et al., 2021). On the other hand, due to the rapid development of rice farming intensification and the decrease in the agricultural labor force, rice farmers with large land areas generally face the problems of labor shortages and increasing labor costs (Luo, 2021; Xu et al., 2021). The study of light and simplified fertilizer application technology for rice is important to improve labor efficiency and reduce the cost of fertilizer application.

Controlled-release N fertilizer (CRN) has the advantages of a high synchronization rate between nutrient release and crop nutrient uptake and high fertilizer efficiency, which allows for one-time fertilization of rice, solving the difficult problem of topdressing rice, decreasing N loss, improving NUE, and reducing environmental risks (Chen et al., 2020; Guo et al., 2019; Li et al., 2015; Zhang et al., 2018). It was found that different types of CRNs could reduce N loss in paddy fields compared with the split application of conventional N fertilizer at the same N application rate, and the effect was better when blended CRN and conventional N fertilizer were applied at different ratios (Lyu T. et al., 2021). However, the current application rates of blended CRN are mainly determined by the application rate of urea (Lyu Y. et al., 2021), while the appropriate rate of blended CRN to further reduce the environmental risk based on ensuring rice yield is still unclear.

Therefore, based on five consecutive years of rice field location trials in the Chaohu watershed, this study compared the differences in rice yield, NUE, and NH_3 volatilization between the split application of urea and the one-time application of blended CRNs and urea under different N rates. The optimum economic N application rate for rice was evaluated using an environmental and economic evaluation method that considered the reduction in the N rate while guaranteeing a high rice yield. This study is expected to provide a scientific basis for the determination of an ecologically suitable fertilization technology for rice in the Chaohu watershed.

2 Materials and methods

2.1 Experimental materials

Field experiments were conducted over five years from 2016 to 2020 in Zhonghan village, Hefei city, Anhui Province, located in the Chaohu watershed in the Yangtze River Delta, China (N 31°39′14″, E117°46′34″), with a long history of rice cultivation and a northern subtropical monsoon climate (Figure 1; Figure S1). The annual average temperature and precipitation are 16.1°C and 1,030 mm, respectively. The soil type is gleyed paddy soil, and the main initial properties of the top-layer soil (0–20 cm) were as follows: pH, 7.1

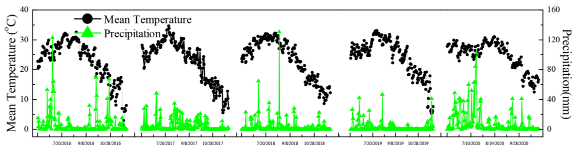

FIGURE 1
Mean temperature and precipitation in the rice season from 2016 to 2020.

(1:2.5, soil/water); total N, 1.9 g/kg; available phosphorus, 9.0 mg/kg; available potassium, 198.8 mg/kg; and organic matter, 29.1 g/kg.

The controlled-release nitrogen fertilizer (CRN, 44.5% N) was obtained from Anhui Moith Agricultural Technology Co., Ltd. (Anhui, China), the center of which was a urea pellet coated with polyurethane. In this experiment, the periods of CRN were 40 and 90 days, represented by CRN1 and CRN2, respectively. The N release durations of CRN1 and CRN2 in 25°C water and paddy fields were measured at 42 and 100 days in 2019 (Figures 2A–D, 3A–D).

Conventional N, phosphorus, and potassium fertilizers were applied in the form of urea (46% N), heavy granular superphosphate (42% P_2O_5), and potassium chloride (60% K_2O).

2.2 Experimental design

The experiment was conducted in a split-plot block design: the main plot was the type of N fertilizer and its application method, and the subplot was the amount of nitrogen fertilizer. There were nine treatments and three replications. The plot area was 30 m^2 (5 m × 6 m). The specific treatments were as follows: control without N fertilizer (N0); four blended CRN treatments with a 4:3:3 ratio [60 kg/hm^2 (CRN60), 120 kg/hm^2 (CRN120), 180 kg/hm^2 (CRN180), and 240 kg/hm^2 (CRN240)] applied at one time but with conventional N fertilizer, CRN1 and CRN2; and four conventional N fertilizer treatments [60 kg/hm^2 (N60), 120 kg/hm^2 (N120), 180 kg/hm^2 (N180), and 240 kg/hm^2 (N240)] in accordance with a 5:3:2 ratio of the N rate with three applications of basal, tillering, and panicle fertilizer. Phosphorus (P_2O_5) and potassium (K_2O) fertilizers were applied at one time as basal fertilizers, at rates of 90 and 75 kg/hm^2, respectively.

The rice variety and timing of planting and management operations in this study are shown in Table 1. The spacing of transplanted rice was 0.30 m (length) by 0.13 m (width).

2.3 Sample processing and measurements

NH_3 volatilization was measured by the semi-open static cylinder system (Kissel et al., 1977; Jantalia et al., 2012; Feng et al., 2017), which was a plexiglass enclosure 20 cm in diameter and 15 cm in height with ventilation holes at the top. Volatilized NH_3 was absorbed with a 20 g/L boric acid solution and titrated with standard acid ($C_{1/2H2SO4}$ = 0.020678 mol/L) at the end of each collection. Air extraction was performed from 9:00 to 11:00 am and from 14:00 to 17:00 pm each day after fertilization. The air exchange frequency was 16 to 20 times/min. The amount of NH_3 volatilized throughout the day was calculated based on this average value (Yu et al., 2013). NH_3 volatilization was determined continuously after fertilizer was applied until it was not detected.

At maturity, the tiller number of rice per square meter was investigated in each subplot. Based on the mean tiller number per hill, rice from three representative hills was selected and destructively sampled. The samples were separated into plants

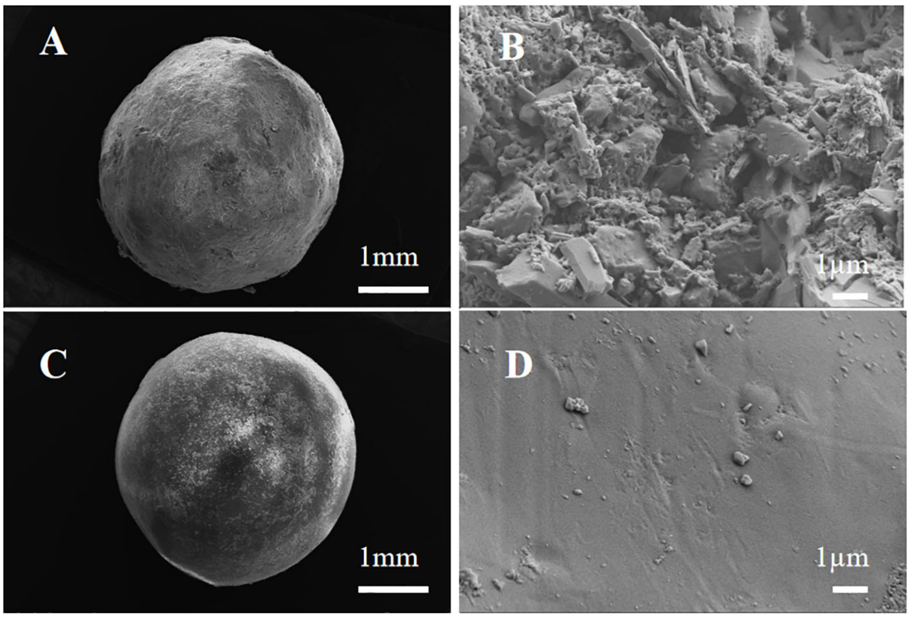

FIGURE 2
Surface scanning electron microscopy (SEM) of controlled-release N fertilizers (CRNs) with release periods of 40 d **(A, B)** and 90 d **(C, D)**.

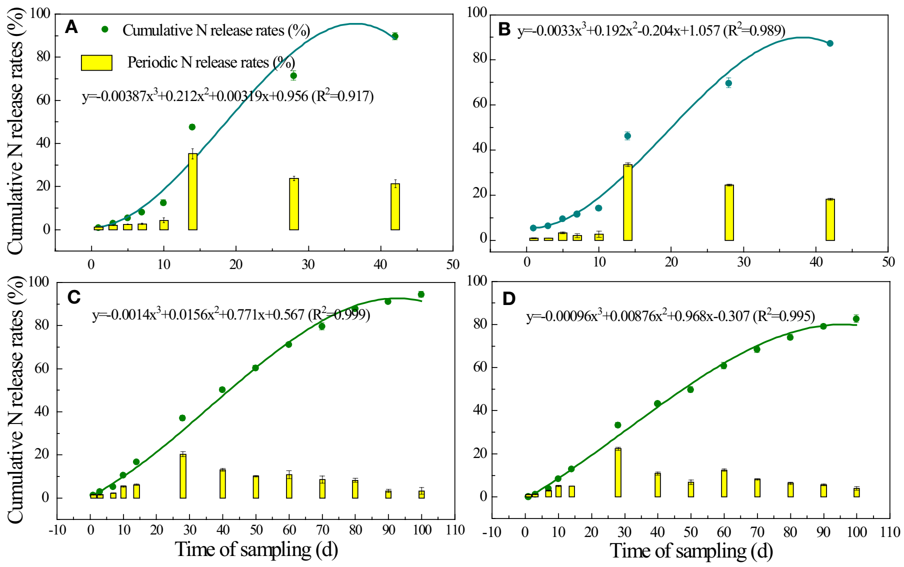

FIGURE 3
Cumulative N release rates (curves) and periodic N release rates (bars) of CRNs with periods of 40 d **(A, B)** and 90 d **(C, D)** incubated in paddy fields **(A, C)** and water (25°C) **(B, D)** in 2019.

(including leaves and stems) and panicles. Then, the samples were oven-dried at 105°C for 2 h and then at 70°C for 72 h, and the dry matter was measured. The N concentrations of the samples were determined by the Kjeldahl method (Bremner & Mulvaney, 1982). Grain yield was manually determined based on all plants within an area of 5 m × 3 m within each subplot after the grain moisture content at the time of harvest was adjusted to 0.14 g/g fresh weight.

The release curves of the CRNs with release periods of 40 and 90 days were determined both in paddy fields and in the laboratory using the method reported by Geng et al. (2015), as described below.

CRN1 and CRN2 (10 g) were placed in a nylon bag with an aperture of 0.15 mm and sealed. When rice was transplanted in 2019, the fertilizer materials were buried in the paddy soil without fertilizer near the experimental site, at a depth of 10 cm. In the laboratory, the samples were placed in a 300-ml plastic bottle to which 250 ml of laboratory-pure water was added, and then the bottle was sealed and placed in a biochemical thermostatic incubator at 25 °C. Samples of CRN1 were collected every 24 h and then on the 3rd, 7th, 10th, 14th, 28th, and 42nd days, respectively. Samples of CRN2 were collected at 24 h on the 3rd, 7th, 10th, 14th, 28th, 40th, 50th, 60th, 70th, 80th, 90th, and 100th days, respectively. Three bags of each fertilizer were collected each time. For the samples of paddy soil, after the cultivation bag was opened, all the soil and fertilizer were transferred to a sieve with an aperture of 1 mm and slowly washed with laboratory-pure water to clean up the soil. Then, the fertilizer film was removed. The fertilizer that was removed was filtered into a 250-ml volumetric flask. The N concentrations of the fertilizer solution were determined by the Kjeldahl method (Bremner & Mulvaney, 1982). For the samples in the laboratory, during sampling, the bottle was inverted up and down three times to ensure a homogeneously mixed solution. Subsequently, the fertilizer solution was transferred into another bottle to determine the N concentration, after which 250 ml of laboratory-pure water was added to the bottle containing the fertilizer bag, and then the bottle was sealed and placed in a biochemical thermostatic incubator at 25 °C for further incubation.

TABLE 1 Rice variety and timing of the planting and management operations.

Year	Rice variety	Sowing	Transplanting	Basal fertilization	Tillering topdressing	Heading topdressing	Harvest
2016	Huang hua zhan	5/26	6/29	6/29	7/7	8/10	10/22
2017	Chaoyou 1000	5/12	6/14	6/14	6/24	7/23	10/1
2018	Chaoyou 1000	5/20	6/21	6/21	7/3	8/1	10/9
2019	Chaoyou 1000	5/25	6/29	6/29	7/6	8/2	10/8
2020	Chaoyou 1000	5/20	6/22	6/22	6/30	7/29	10/10

The surface morphology of the CRNs was determined by a scanning electron microscope (SEM, ZEISS Sigma 300 EDS: Model Smart EDX, Britain).

2.4 Calculation and statistics

NH_3 volatilization flux was calculated according to the following equation (Jantalia et al., 2012; Feng et al., 2017).

$$F = \frac{V \times C \times 0.014 \times 12 \times 10^{-3}}{\pi \times r^2 \times 10^{-4}} \quad (1)$$

where F is the NH_3 volatilization flux (kg/hm^2/d); V is the volume of standard acid for titration (mL); 10^{-3} is the conversion of mL to L; C is the calibration concentration of standard acid for titration (mol/L); 0.014 is the relative atomic mass of N atoms (kg/mol); 10^4 is the conversion of m^2 to hm^2; r is the radius of the airtight chamber (m); and 12 is the conversion to NH_3 volatilization flux over a one-day period.

Cumulative NH_3 emissions were calculated according to the following equation (Jantalia et al., 2012; Feng et al., 2017).

$$E_{NH_3} = \sum_{i=1}^{n} \left(\frac{F_i + F_{i+1}}{2}\right) \times (t_{i+1} - t_i) \quad (2)$$

E_{NH_3} represents the cumulative NH_3 emissions (kg/hm^2); Fi is the NH_3 volatilization flux (kg/hm^2/d) on sampling day i; i represents the ith sampling day; and $t_{i+1} - t$represents the time interval (d) between two sampling measurements.

The NH_3 emission factor (EF_{NH_3} .) as calculated according to the following equation (Huang et al., 2016).

$$EF_{NH_3} = \frac{E_{NH_3-\text{fertilizer}} - E_{NH_3-N0}}{F_N} \quad (3)$$

E_{NH_3}–fertilizer represents the cumulative NH_3 emissions under N application (kg/hm^2), E_{NH_3}–N0 presents the cumulative NH_3 emissions under the N0 treatment (kg/hm^2), and F_N is the N application rate (kg/hm^2).

Yield-scale NH_3 emissions [kg/t(grain)] were calculated according to the following equation (Huang et al., 2016).

$$E_{NH3}yield - scale = \frac{E_{NH_3}}{Y} \quad (4)$$

E_{NH_3} represents the cumulative NH_3 emissions (kg/hm^2), and Y is the rice grain yield under each treatment (t/hm^2).

Nitrogen use efficiency (NUE) was calculated according to the following equation (Sun et al., 2012):

$$NUE(\%) = \frac{U_N - U_0}{F_N} \quad (5)$$

U_N is rice grain and plant N accumulation under N application (kg/hm^2); U_0 is grain and plant N accumulation under N0 treatment (kg/hm^2); F_N is the N application rate (kg/hm^2).

According to the Eco-indicator 95 transformation procedure, 1 kg NH_3 volatilization flux is equivalent to the eutrophication effect of 0.33 kg PO_4^{3-} and the acid rain effect of 1.88 kg SO_2 (Goedkoop, 1995). However, 4% of the Chaohu watershed is natural wetlands (rivers, lakes, marshes, etc.) (Wu et al., 2020). Therefore, 96% of NH_3 volatilization will cause acidification through wet and dry deposition on the soil surface. The NH_3 deposited on the water surface has a eutrophication effect on the water body. The marginal environmental loss (M_1, yuan/hm^2) for the acid rain effect and the marginal environmental loss (M_2, yuan/hm^2) for the eutrophication effect of NH_3 volatilization from N application can be expressed by the following equations (Xia and Yan, 2012):

$$M_1 = 96\% \times 1.88 \times E_{NH_3} P_a \times 17/14 \quad (6)$$

$$M_2 = 4\% \times 0.33 \times E_{NH_3} P_e \times 17/14 \quad (7)$$

In the equation, 1.88 is the conversion factor of the acid rain effect of 1 kg cumulative NH_3 emission equivalent SO_2; P_a is the acid rain loss caused per kg SO_2 (yuan/kg), which was 5 yuan/kg in this study; P_e is the loss of the eutrophication effect caused per kg PO_4^{3-} (yuan/kg), which was 3.88 yuan/kg in this study; E_{NH_3} represents the cumulative NH_3 emissions (kg/hm^2); and 17/14 is the conversion factor of N to NH_3.

The environmental loss caused by NH_3 volatilization (M_{loss}, yuan/kg) was calculated according to the following equation.

$$M_{loss} = M_1 + M_2 \quad (8)$$

The net benefit from rice planting in the Chaohu watershed (M_{net}, yuan/kg) was calculated according to the following equation.

$$M_{net} = M_Y - M_L - M_F - M_{loss} \quad (9)$$

M_Y is the output value of rice yield (yuan/hm^2), and the price of rice sold in 2019 was 2.5 yuan/kg; M_L is the labor cost of rice fertilization, and the labor cost of rice fertilization per event was 900 yuan/hm^2; and M_F is the fertilizer cost. The prices of urea, CRN, potassium, and phosphorus fertilizer were 2.0, 2.8, 2.0 and 0.6 yuan/kg, respectively, in 2019; M_{loss} is the environmental loss of NH_3 volatilization.

2.5 Statistical analysis

SPSS 22.0 software (IBM Corp., Armonk, NY, USA) was used to perform multivariate analyses based on a general linear model. Pearson's correlation was used to analyze the relationships between parameters. Origin 2022 (OriginLab Corp., Northampton, MA, USA) was used to plot the figures.

3 Results

3.1 Release characteristics of CRNs

Scanning electron microscopy images clearly showed the coating materials and fertilizer particles of CRN1 and CRN2 (Figures 2A–D). When magnified 44 times, the surfaces of both CRN1 and CRN2 were smooth (Figures 2A, C). When magnified 20,000 times, the surface of CRN2 was still smooth. However, the surface of CRN1 with a N release period of 40 days was somewhat loose compared with that of CRN2 (Figures 2B, D).

The N release curves of CRN1 and CRN2 showed a steady release rate in the paddy field and 25°C water, which fit cubic binomial curves (Figures 3A–D). The cumulative N release rate of CRN1 in the paddy field was 89.7% of the supplemental N released within 40 days (Figure 3A), while that of CRN2 was 91.2% within 90 days (Figure 3C). The N release characteristics in 25°C water were slightly slower (Figures 3B, D), with 86.7% of N released in 40 days for CNR1 and 87.4% of N released in 90 days for CNR2; the maximum periodic N release rate was approximately 1/3 of their release periods. In the paddy field, the cumulative N release rate of CRN1 was 33.5% in 14 days, and that of CRN2 was 22.3% in 28 days. The results were similar in water.

3.2 Rice yield

The rates and types of N fertilizers and their application methods had a significant effect on rice yield. The yield results for five consecutive years from 2016 to 2020 showed consistent trends. The rice yields under the N application treatments were significantly higher than those under N0 (P<0.01) (Figures 4A–E). Under the blended CRN treatments, yields increased with increasing N application rates of 60–180 kg/hm^2. However, the yield under CRN240 decreased by 1.5%–5.8% compared with that under CRN180 from 2016 to 2020. Under the conventional N fertilizer treatments, yields increased with increasing N application rates of 60–240 kg/hm^2. At the same N application rate of 60 to 180 kg/hm^2, the yield was significantly higher under the blended CRN treatments than under the conventional N fertilizer treatments (P<0.05). The results of the five-year experiment showed that yield increased by 0.9%–4.3% under CRN60 compared to N60, by 2.4%–6.3% under CRN120 compared to N120, and by 5.6%–8.2% under CRN180 compared to N180. In contrast, the yields of CRN240 and N240 were not significantly different (P >0.05), with an average increase of 0.9% over 5 years.

The relationship between rice yield and the N application rate was modeled by a quadratic equation (Figures 4A–E). As simulated by the equation, the highest yield of rice in the five years under the blended CRN treatments was 8,295–11,347 kg/hm^2, and the corresponding N application rate was 191–214 kg/hm^2 (Figures 4A–E). The average highest yield was 9,844 kg/hm^2 with an N application rate of 194 kg/hm^2 under CRN treatments (Figure 5). Under conventional N fertilizer treatments, the highest yield of rice in the five years was 8,137–11,038 kg/hm^2, corresponding to 212–278 kg/hm^2 of N applied (Figures 4A–E). The average highest yield was 9,499 kg/hm^2 with an N application rate of 222 kg/hm^2 (Figure 5). The highest yield under the blended CRN treatments increased by 1.8%–5.6% in the five years compared with that under the conventional N fertilizer treatments, with an average increase of 3.6%, and the corresponding N application rate decreased by 21–60 kg/hm^2, with an average decrease of 12.5%.

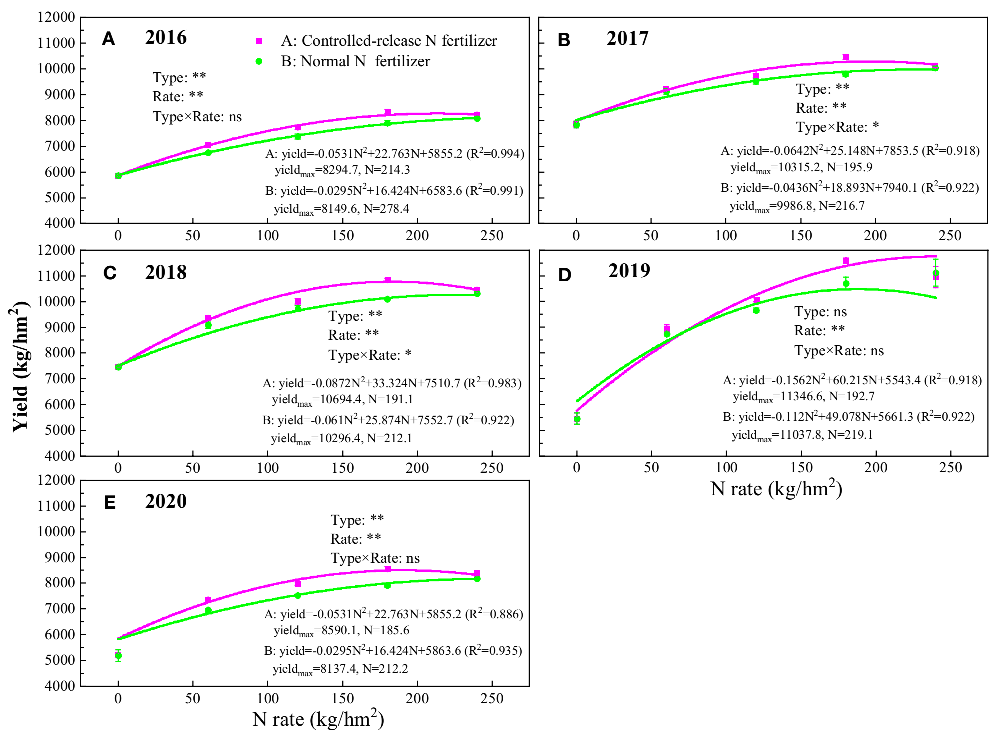

FIGURE 4
Rice yield under the blended CRN treatments (red square) and conventional N fertilizer treatments (green circle) with applied N rates of 0, 60, 120, 180, and 240 kg/hm^2 from 2016 to 2020 **(A–E)**. Statistically significant differences (**P<0.01; *P<0.05) and no significant differences (P >0.05, ns) are shown. Values are the means ± SEs (n = 3).

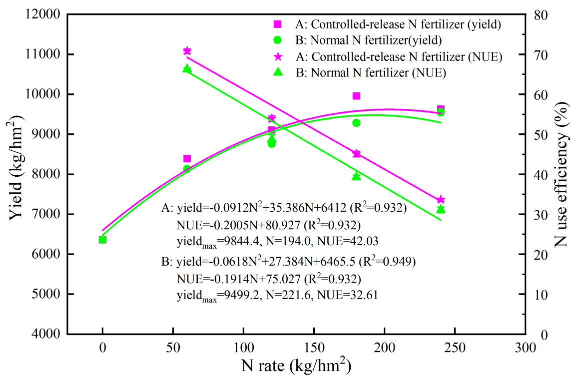

FIGURE 5
Average yield and N use efficiency (NUE) of rice from 2016 to 2020 under the blended CRN treatments (red graph) and conventional N fertilizer treatments (green graph) with applied N rates of 0, 60, 120, 180, and 240 kg/hm^2.

3.3 Rice NUE

The trend of the rice NUE was consistent for five consecutive years from 2016 to 2020, with NUE showing a negative correlation with the N application rate (Figure 5; Table 2). The NUE of the blended CNR treatments was significantly higher than that of the conventional N fertilizer treatments at the same N application rate (P<0.01). The increases were 0.5%–7.8%, 8.9%–15.4%, 10.3%–16.7%, and 4.9%–11.5% at N rates of 60, 120, 180, and 240 kg/hm^2 over 5 years, with average increases of 6.9%, 10.7%, 14.8%, and 8.2%, respectively (Table 2). According to the simulation based on the quadratic equation, when the average rice yield was the highest over the five years, the NUE of the blended CNR treatments was 42.0% and that of the conventional N fertilizer treatments was 32.6%, which was an increase of 28.9% compared with the NUE under the conventional N fertilizer treatments (Figure 5).

3.4 NH_3 volatilization

The NH_3 volatilization flux was affected by the rates and types of N fertilizers and their application methods. In 2019, the NH_3 volatilization flux under conventional N fertilizer treatments and blended CRN treatments was 0.08–5.90 and 0.10–6.61 kg/hm^2/d, with averages of 1.28 and 0.80 kg/hm^2/d, respectively (Figures 6A–D). The NH_3 volatilization flux peaked on the first to third day after N fertilizer application, followed by a rapid decline. The NH_3 volatilization flux under conventional N fertilizer treatment was close to the background value 7 days after N fertilizer application. The NH_3 volatilization flux in the blended CRN treatments was always higher than that in N0 during the rice growth period, and the increase was greater with the increase in N application. After basal fertilizer application at the same N rate, the NH_3 volatilization flux increased under the blended CRN treatments compared with the conventional N fertilizer treatments, with average increases of 31.3%, 17.6%, 18.9%, and 32.9% at N rates of 60, 120, 180, and 240 kg/hm^2, respectively. However, after tillering and panicle fertilization, the average decrease under the blended CRN treatments was 65.9% and 75.4%, 63.7% and 66.5%, 70.0% and 80.2%, and 79.7% and 77.6% at N rates of 60, 120, 180, and 240 kg/hm^2, respectively, compared with that under the conventional N fertilizer treatments. Throughout the whole growing period of rice, the average reductions in the NH_3 volatilization flux under the blended CRN treatments were 15.9%, 42.6%, 38.0%, and 40.7% compared with those under the conventional N fertilizer treatments (Figures 6A–D).

With an increase in the N rate, the cumulative NH_3 emissions under different N fertilizer treatments gradually increased, but the ratio of NH_3 emissions to the N application rate gradually decreased (Table 3). Cumulative NH_3 emissions under conventional N fertilizer treatments ranged from 17.0 to 47.7 kg/km^2, accounting for 19.9% to 28.3% of the N application rate. Cumulative NH_3 emissions under CRN treatments ranged from 14.3 to 28.3 kg/km^2,

TABLE 2 N fertilizer utilization efficiency (NUE) of rice under different N fertilizer treatments from 2016 to 2020 (%).

Treatment	2016	2017	2018	2019	2020	Average NUE
CRN60	66.3 ± 1.27	69.9 ± 1.14	69.8 ± 1.46	76.1 ± 0.81	72.0 ± 4.17	70.8 ± 0.58
CRN120	51.2 ± 1.23	54.3 ± 2.92	56.1 ± 3.18	56.1 ± 2.87	51.8 ± 3.23	53.9 ± 0.71
CRN180	42.3 ± 0.44	43.7 ± 1.61	48.3 ± 0.44	49.2 ± 0.20	41.9 ± 2.31	45.1 ± 0.69
CRN240	31.3 ± 0.89	33.0 ± 1.14	36.4 ± 0.95	36.4 ± 2.91	31.1 ± 1.94	33.6 ± 0.37
N60	66.0 ± 2.09	64.8 ± 1.93	65.6 ± 1.12	72.5 ± 1.43	62.3 ± 4.31	66.2 ± 0.36
N120	46.0 ± 0.41	50.2 ± 1.43	51.1 ± 1.03	48.6 ± 3.91	47.6 ± 2.90	48.7 ± 1.25
N180	36.3 ± 0.79	37.8 ± 0.53	41.5 ± 0.96	42.6 ± 0.72	38.1 ± 2.27	39.3 ± 0.53
N240	28.6 ± 0.40	29.6 ± 0.09	33.2 ± 0.88	34.5 ± 3.08	29.6 ± 2.36	31.1 ± 0.71
Type	**	**	**	**	*	**
Rate	**	**	**	**	**	**
Type × Rate	ns	ns	ns	ns	ns	ns

Statistically significant differences (**P<0.01; *P<0.05) and no significant differences (P >0.05, ns) are shown. Values are the means ± SEs (n = 3).

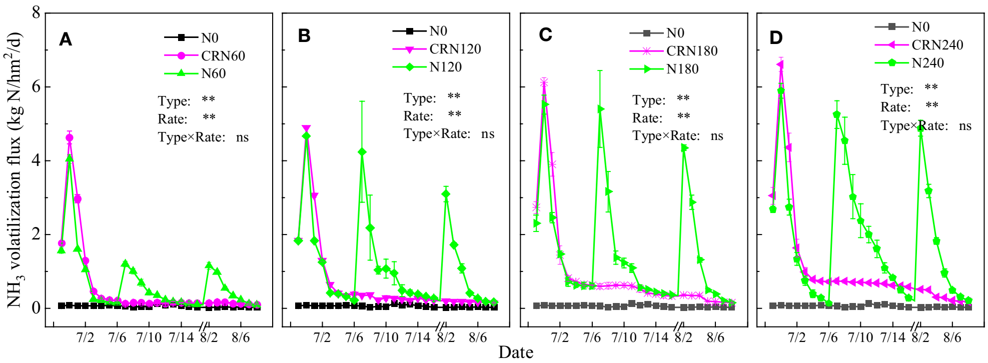

FIGURE 6
NH_3 volatilization flux under the blended CRN treatments (red graph) and conventional N fertilizer treatments (green graph) with applied N rates of 0, 60, 120, 180, and 240 kg/hm^2 in the 2019 rice season **(A–D)**.

accounting for 11.8% to 23.8% of the N application rate. At the same N rate, the blended CRN treatments significantly increased the cumulative NH_3 emissions compared with the conventional N fertilizer treatments after the basal fertilizer application. When the N rate was 60, 120, 180, and 240 kg/hm^2, the cumulative NH_3 emissions under the blended CRN treatment increased by 31.2%, 17.6%, 18.9%, and 32.9%, respectively. However, after tillering and panicle fertilization, the cumulative NH_3 emissions under the blended CRN treatment decreased by 66.0% and 73.0%, 75.4% and 82.5%, 63.7% and 82.4%, and 66.5% and 81.7% at N rates of 60, 120, 180, and 240 kg/hm^2, respectively. During the whole rice growth period, cumulative NH_3 emissions under the blended CRN treatment decreased by 15.9%, 42.5%, 38.0%, and 40.7% at respective N rates of 60, 120, 180, and 240 kg/hm^2.

The NH_3 emission factors under different N fertilizer treatments gradually decreased with increasing N application rates (Figure 7A). The NH_3 emission factors were 19.3%–25.9% and 11.2%–21.4% under conventional N fertilizer treatments and blended CRN treatments, respectively. At the same N rate, the NH_3 emission factors under blended CRN treatments were significantly lower than those under conventional N fertilizer treatments (P<0.01). When the N rate was 60, 120, 180, and 240 kg/hm^2, the NH_3 emission factors decreased by 17.4%, 44.8%, 39.5%, and 42.0%, respectively.

Yield-scale NH_3 emissions are driven by the effect of fertilizer management on both crop yields and NH_3 emissions. With an increasing N application rate, yield-scale NH_3 emissions gradually increased under the different N fertilizer treatments (Figure 7B).

TABLE 3 Cumulative NH_3 emissions and the ratio of NH_3 emissions under different N fertilizer treatments in the 2019 rice season.

Treatment	Basal fertilization		Tillering topdressing		Heading topdressing		Rice growing season	
	Cumulative NH_3 emission kg/hm^2	Ratio of NH_3 emission %	Cumulative NH_3 emission kg/hm^2	Ratio of NH_3 emission %	Cumulative NH_3 emission kg/hm^2	Ratio of NH_3 emission %	Cumulative NH_3 emission kg/hm^2	Ratio of NH_3 emission %
N0	0.6 ± 0.05	–	0.7 ± 0.02	–	0.2 ± 0.01	–	1.5 ± 0.08	–
CRN60	11.8 ± 0.20	19.9 ± 0.33	1.5 ± 0.02	2.6 ± 0.03	0.9 ± 0.01	1.5 ± 0.01	14.3 ± 0.20	23.8 ± 0.33
CRN120	12.9 ± 0.15	10.7 ± 0.12	2.8 ± 0.21	2.4 ± 0.17	1.2 ± 0.00	1.0 ± 0.00	16.9 ± 0.34	14.1 ± 4.65
CRN180	17.0 ± 0.24	9.5 ± 0.13	5.4 ± 0.33	3.0 ± 0.18	1.7 ± 0.07	1.0 ± 0.04	24.1 ± 0.41	13.4 ± 2.99
CRN240	18.8 ± 0.64	7.9 ± 0.27	7.3 ± 0.05	3.1 ± 0.02	2.2 ± 0.03	1.0 ± 0.01	28.3 ± 0.07	11.8 ± 3.02
N60	9.0 ± 0.10	15.0 ± 0.17	4.5 ± 0.14	7.6 ± 0.24	3.45 ± 0.05	5.8 ± 0.09	17.0 ± 0.09	28.3 ± 0.16
N120	10.9 ± 0.01	9.1 ± 0.01	11.6 ± 2.76	9.6 ± 2.30	6.9 ± 0.13	5.8 ± 0.11	29.4 ± 2.63	24.5 ± 7.95
N180	14.3 ± 0.79	8.0 ± 0.44	14.9 ± 1.58	8.3 ± 0.88	9.8 ± 0.22	5.4 ± 0.12	38.9 ± 2.46	21.6 ± 5.01
N240	14.2 ± 0.21	5.9 ± 0.09	21.7 ± 0.83	9.0 ± 0.35	11.6 ± 0.08	4.9 ± 0.03	47.7 ± 0.92	19.9 ± 4.83
Type	**	**	**	**	**	**	**	**
Rate	**	**	**	ns	**	**	**	**
Type × Rate	*	**	**	ns	**	**	**	*

Statistically significant differences (**P<0.01; *P<0.05) and no significant differences (P >0.05, ns) are shown. Values are the means ± SEs (n = 3).

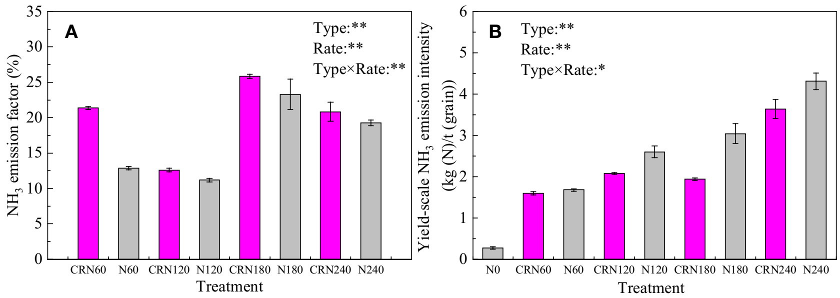

FIGURE 7
NH_3 emission factors **(A)** and yield-scale NH_3 emission intensity **(B)** under the blended CRN treatments (red graph) and conventional N fertilizer treatments (gray graph) with applied N rates of 0, 60, 120, 180, and 240 kg/hm^2 in 2019.

The yield-scale NH_3 emissions were 1.6%–2.6% and 1.9%–3.0% under conventional N fertilizer treatments and blended CRN treatments, respectively. The blended CRN treatments significantly reduced these emissions compared with conventional N fertilizer treatments at the same N application rates of 60, 120, 180, and 240 kg/hm^2 (P<0.01), with decreases of 17.9%, 44.8%, 42.7%, and 39.8%, respectively.

Pearson correlation analysis showed that rice yield was positively and significantly correlated with NH_3 volatilization flux and cumulative NH_3 emissions but negatively correlated with the NH_3 emission factors (P<0.01; Table 4). NUE was negatively correlated with NH_3 volatilization flux and cumulative NH_3 emissions and significantly positively correlated with the NH_3 emission factors and yield-scale NH_3 emissions (P<0.05; Table 4).

3.5 Economic benefit

With the use of the economic benefit data for rice in 2019 as an example, fertilizer costs and environmental loss gradually increased with increasing N fertilizer application. CRN180 had the highest output value and net benefit of rice among all treatments (Figure 8). At the same N rate, the blended CRN treatments increased the fertilizer cost and net benefit compared with the conventional N fertilizer treatments; the specific increases were 42 and 2,329, 84 and 2,848, 126 and 4,026, and 168 and 1,412 yuan/hm^2 at N applications of 60, 120, 180, and 240 kg/hm^2, respectively. However, the environmental loss under the blended CRN treatments was lower than that under the conventional N fertilizer treatments at the same N application rates of 60, 120, 180, and 240 kg/hm^2, with decreases of 30, 138, 171, and 214 yuan/hm^2.

The relationship between output value, net benefit, and N application rate was simulated by the binary quadratic equation. When the net benefit of rice was the highest, the N application rate of the blended CRN treatment was 185 kg/hm^2. In addition, the output value of rice was 25,569 yuan/hm^2. The fertilizer cost and environmental loss were 1,608 and 260 yuan/hm^2, respectively. The N application rate for conventional N treatment was 225 kg/hm^2, with the highest net benefit. At the same time, the net benefit of rice was 22,730 yuan/hm^2. The fertilizer cost and environmental loss were 1,650 and 507 yuan/hm^2, respectively (Figure 8). Therefore, when the net benefit of rice was highest, the blended CRN treatment decreased the N fertilizer rate by 40 kg/hm^2, increased the rice income by 2,839 yuan/hm^2, and reduced the fertilizer cost and environmental loss by 43 and 247 yuan/hm^2, compared with the conventional N treatment.

When the highest rice yield was achieved in 2019, the N rates of the blended CRN treatments and the conventional N fertilizer treatments were 193 and 219 kg/hm^2, and the net benefit, fertilizer cost, and environmental loss were 25,548; 1,645; and 267 yuan/hm^2 and 20,287; 1,634; and 496 yuan/hm^2, respectively. When the corresponding rice yield under the two types of N fertilizer reached its maximum, the net benefit decreased, and the N application rate, fertilizer cost, and environmental loss increased compared with the highest net output of rice under these types of N fertilizer application.

TABLE 4 Pearson corrections among yield, NUE, cumulative NH_3 emissions, NH_3 emission factors, and yield-scale NH_3 emission intensity in the 2019 rice season (n = 24).

Index	Yield	NUE	Cumulative NH3 emissions	NH3 emission factor	Yield-scale NH3 emission intensity
Yield	1	−0.726**	0.568**	−0.622**	0.395
NUE	−0.726**	1	−0.781**	0.450*	−0.721**
Cumulative NH3 emissions	0.568**	−0.781**	1	0.075	0.978**
NH3 emission factor	−0.622**	0.450*	0.075	1	0.218
Yield-scale NH3 emission intensity	0.395	−0.721**	0.978**	0.218	1

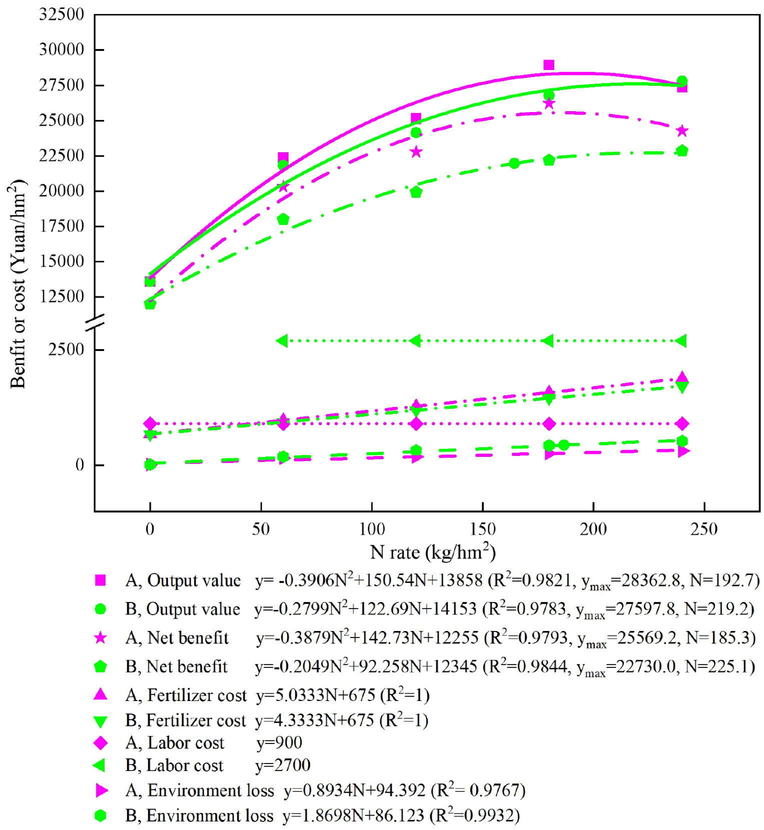

FIGURE 8
Output value, net benefit, fertilizer cost, labor cost, and environmental loss under the blended CRN treatments (red graph) and conventional N fertilizer treatments (green graph) with applied N rates of 0, 60, 120, 180, and 240 kg/hm^2 in the 2019 rice season.

4 Discussion

4.1 N release characteristics of CRNs

Temperature and moisture are important factors affecting the nutrient release of CRNs (Grant et al., 2012; Tong et al., 2018). Soil moisture was not a limiting factor for the N release of CRNs in paddy soil, which was generally in a flooded state. The average daily temperature during the rice season in 2019 was 28°C, which was 3°C higher than the temperature in the laboratory. Furthermore, the average daily temperature within 82 days after transplanting was higher than 25°C (Figure 1). As a result, the cumulative N release rate and the period during which N was released from CRNs with release periods of 40 and 90 days in paddy fields were higher than those in laboratory tests.

N is one of the main nutrients for rice growth. CRNs can provide N for rice growth by controlling the rate of N release (Zhang et al., 2018). Many researchers have used a single release period for CRNs throughout the whole rice growing period (Yu et al., 2013; Guo et al., 2019; Chen et al., 2020). In contrast, in this study, CRNs with different release periods were blended with conventional N for one-time fertilization. CRNs with release periods of 40 and 90 days played the roles of tillering fertilizer and panicle fertilizer, respectively, under conventional fertilization. Within 10 days after fertilization, the cumulative N release rate and the period during which N was released from the CRNs in these two release periods were low. The N required for rice growth was mainly supplied by conventional N during this period (Figures 3A–D). On the 14th day after fertilizer application, the cumulative N release rate of CRN1 with a release period of 40 days peaked to satisfy the tillering growth of rice (Figures 3A, B). On the 28th day after fertilizer application, the cumulative N release rate of CRN2, with a release period of 90 days, peaked. The cumulative N release rate of CRN2 decreased slowly from the 28th day to the 90th day, providing N for the booting, heading, and filling stages of rice (Figures 3C, D). The blended CRNs and normal N fertilizer treatments had similar biomass accumulation and N accumulation characteristics during the rice growth period in 2019 (Figures S2A, B, S3A, B). This indicated that blended CRNs with conventional N can achieve the effect of split fertilization with conventional N to meet the rice growth demand.

4.2 Blended CRN reduced NH_3 volatilization

NH_3 volatilization is one of the main methods of N loss in agricultural fields (He et al., 2018), and this loss can account for 10%–30% of the applied N rate (Yu et al., 2019). The NH_3 volatilization loss in rice fields was closely related to the N rate and application time, which increased with an increased N application rate. This is mainly because an increase in the N rate greatly increases the NH_4^+-N concentration in field surface water (Yu et al., 2013). The results of this study are consistent with this finding (Figures 6A–D, 7A, B; Table 3). However, coated controlled-release N fertilizer can retard the N dissolution process by blocking the movement of water into and out of the coated fertilizer, so that the NH_4^+-N concentration in the paddy soil and surface water is low (Li et al., 2018; Yang et al., 2019). Consequently, the ratio of NH_3 emissions under the blended CRN treatments was lower than that under conventional N fertilizer treatments. Guo et al. (2018) found that there was no obvious peak of NH_3 volatilization flux during the whole rice growth period after the one-time application of CRN as a basal fertilizer, which was consistently maintained at lower levels. Therefore, cumulative NH_3 emissions under the one-time application of CRN were 57.7%–70.5% lower than those under conventional split N application in early and late rice at the same N rate (Guo et al., 2018). The effect of CRN on reducing NH_3 volatilization loss was better than that in this study. NH_3 volatilization loss was concentrated after basal fertilization under the blended CRN treatments in this study. Compared with the conventional N fertilizer treatments, the blended CRN treatments after basal fertilization increased the N application rate by 50% and the cumulative NH_3 emissions by 17.6%–32.9%. However, after tillering and panicle fertilization, the cumulative NH_3 emissions under the blended CRN treatments decreased by 63.7%–75.4% and 73.0%–82.5%, respectively. This result indicated that the contribution of blended CRNs to the reduction in NH_3 volatilization loss was mainly after rice tillering.

4.3 The optimum economic application rate of blended CRNs

The relationship between the N application rate and rice yield is not a simple linear relationship. A linear plus platform model is commonly used to fit the relationship between crop yield and the N application rate (Alivelu et al., 2003; Li et al., 2015). A quadratic equation can also describe the relationship well (Kim et al., 2019; Ju et al., 2021). In this study, the results of five consecutive years of location experiments showed that the relationship between the N application rate and rice yield in both the blended CRN treatments and the conventional N fertilizer treatments could be simulated using a binary quadratic equation (Figures 4A–E, 5). The maximum yield under the blended CRN treatments reached 8,295–11,347 kg/hm^2, which was only 1.8%–5.6% higher than that under conventional N fertilizer treatments. When the controlled-release N fertilizer treatment reached its maximum yield, the corresponding N rate under the blended CRN treatments was 191–214 kg/hm^2, which was 12.5% lower than the average N rate under conventional N fertilizer treatments. Li et al. (2015) showed that the N rate under the conventional N fertilizer treatments was 197 kg/hm^2 when rice reached the maximum yield in Zhejiang Province using the linear plus platform method, i.e., the N rate was decreased by more than 32.9%. The results of this study showed that the N rate for the highest rice yield was like that reported in the study by Li et al. (2015), but the reduction in N was lower, mainly due to the higher N rate in Zhejiang Province, where the N rate can reach 360 kg/hm^2.

Conventional split-application urea can result in high N losses through NH_3 volatilization, runoff, and other ways, leading to a lower NUE compared with that of CRN applied one time (Chen et al., 2020; Guo et al., 2018; Li et al., 2015; Zhang et al., 2018). In this study, the results of five consecutive years of location experiments showed that the blended CRN treatments increased NUE by 6.9%–14.8% on average compared with the conventional N fertilizer treatments at the same N application rate. The N application rate had a significant effect on NUE, which was significantly higher at the low N rate than at the high N rate (Table 2; Figure 5).

Developing countries face the dual challenges of food security and environmental friendliness (Chen et al., 2011). Therefore, the Ministry of Agriculture of the People's Republic of China (MOA) (2015) issued a policy toward a zero increase in fertilizer use. With the collaborative efforts of the government, scientific research departments, and rice growers under the guidance of the government, the N fertilizer rate in the Chaohu watershed is decreasing (Wu et al., 2020). However, the task of achieving high green high rice yields in the Chaohu watershed remains daunting. The economic benefit of rice production should also be considered (Emran et al., 2019).

In this study, among the nine treatments, the net benefit of the blended CRN treatments increased by 6.2%–18.1% compared with the N conventional fertilizer treatments, considering labor cost, fertilizer cost, and other environmental losses. CRN at a N rate of 180 kg/hm^2 achieved the highest net benefit for rice. The NUE was 49.2%. A N rate of 180 kg/hm^2 is also recommended for rice in the middle and lower Yangtze River basins (Liu et al., 2016). The N application rate under the blended CRN treatments was 193 kg/hm^2, reaching the highest yield of rice. The corresponding NUE was 42.4%, which is 3.4 percentage points higher than that in the Chaohu watershed (Yu and Shi, 2015), which resulted in yield priority. Based on the binary quadratic equation to simulate the relationship between the N rate and net benefit of rice, it was found that the net benefit was the highest when the N rate under the blended CRN treatments was 185 kg/hm^2. Under this condition, the NUE was 43.8%. The N rate and NUE were negatively correlated (Figure 5). Considering rice yield, environmental benefit, and economic benefit, the N application rate of blended CRNs was compared. The lowest N rate was achieved when the environmental benefit was prioritized, which could be used as the lower limit of the optimum N rate for blended CRNs. Prior to considering yield, the highest N rate could be used as the upper limit of the optimum N rate for blended CRNs. With priority consideration of the economic benefit, the N rate was between the lower and upper limits of the optimum N rate. The results for five consecutive years showed that the N rate under the blended CRN treatments was 191–214 kg/hm^2, giving priority to yield consideration. Therefore, the optimum economic N rate of blended CRN was 180–214 kg/hm^2 considering yield, environmental benefit, and economic benefit. Under the conventional N fertilizer treatments, the N rate was 212–278 kg/hm^2, giving priority to yield consideration. Among the four conventional N fertilizer treatments, the N rate with the highest net benefit was 240 kg/hm^2. Prior to considering the economic benefit, the N rate was 225 kg/hm^2 under conventional N fertilizer treatments. Therefore, the optimum economic N rate of the conventional N fertilizers was 212–278 kg/hm^2 considering yield, environmental benefit, and economic benefit. The optimum economic N rate of the blended CRN was significantly lower than that of conventional N fertilizer.

5 Conclusions

Urea-blended CRNs with a 4:3:3 ratio according to the N rate and release periods of 40 and 90 days adequately satisfied the N demand of rice during the whole growing period. Like the conventional N fertilizer treatments, the binary quadratic equation simulated the relationship between rice yield and N rate under the CRN treatments. The results showed that the N rate was 191–214 and 212–278 kg/hm^2 for the highest yield under the blended CRN treatments and the conventional N fertilizer treatments, respectively, from 2016 to 2020. The rice net benefit of CNR180 was the highest among all treatments, and that of N240 was the highest among the four conventional N fertilizer treatments in 2019. NH_3 volatilization increased with increasing N rates, but NUE decreased with increasing N rates. The blended CRN treatments reduced NH_3 volatilization after tillering fertilizer and increased NUE compared with conventional N fertilizer treatments at the same N rate. Considering the yield output value, fertilizer cost, labor cost, and environmental loss, the optimum economic N rate was 180–214 kg/hm^2 for the blended CRN treatments and 212–278 kg/hm^2 for the conventional N fertilizer treatments in the Chaohu watershed in the Yangtze River Delta, China. Therefore, urea-blended CRNs are a promising measure to improve the NUE and economic income of rice because these CRNs can decrease NH_3 volatilization and adverse environmental outcomes.

Data availability statement

The raw data supporting the conclusions of this article will be made available by the authors, without undue reservation.

Author contributions

MY: conceptualization, resources, data curation, and writing-original draft. YS: conceptualization and funding acquisition. GW: supervision and resources. JW: investigation and data curation. CL: methodology and software. TT: writing-review and editing. XZ: data curation. WW: visualization. YJ: sample measurement. All authors contributed to the article and approved the submitted version.

Funding

This research was supported by the National Key Research and Development Program of China (Nos. 2022YFD2301403 and 2016YFD0200806) and the Natural Science Foundation of Anhui Province (No. 2108085QC124).

Conflict of interest

The authors declare that the research was conducted in the absence of any commercial or financial relationships that could be construed as a potential conflict of interest.

Publisher's note

All claims expressed in this article are solely those of the authors and do not necessarily represent those of their affiliated organizations, or those of the publisher, the editors and the reviewers. Any product that may be evaluated in this article, or claim that may be made by its manufacturer, is not guaranteed or endorsed by the publisher.

Supplementary material

The Supplementary Material for this article can be found online at: https://www.frontiersin.org/articles/10.3389/fpls.2023.1144461/full#supplementary-material

SUPPLEMENTARY FIGURE 1
The location and treatments of the experiment.

SUPPLEMENTARY FIGURE 2
Biomass accumulation under the blended CRN treatments **(A)** and conventional N fertilizer treatments **(B)** with applied N rates of 0, 60, 120, 180, and 240 kg/hm^2 in the 2019 rice season.

SUPPLEMENTARY FIGURE 3
N accumulation under the blended CRN treatments **(A)** and conventional N fertilizer treatments **(B)** with applied N rates of 0, 60, 120, 180, and 240 kg/hm^2 in the 2019 rice season.

References

Alivelu, K., Srivastava, S., Subba Rao, A., Singh, K. N., Selvakumari, G., and Raju, N. S. (2003). Comparison of modified mitscherlich and response plateau models for calibrating soil test based nitrogen recommendations for rice on typic ustropept. *Commun. Soil Sci. Plant* 34, 2633–2643. doi: 10.1081/CSS-120024790

Bremner, J. M., and Mulvaney, C. S. (1982). "Total nitrogen," in *Methods SSSAJ*, vol. 328 . Eds. T. Page, J. M. Miller and D. R. Keeney (Madison, W. I., USA John Wiley & Sons, Ltd.), 595–642.

Chen, X. P., Cui, Z. L., Vitousek, P. M., Cassman, K. G., Matson, P. A., Bai, J. S., et al. (2011). Integrated soil-crop system management for food security. *P. Natl. Acad. Sci. U.S.A.* 108, 6399–6404. doi: 10.1073/pnas.1101419108

Chen, Z., Wang, Q., Ma, J., Zou, P., and Jiang, L. (2020). Impact of controlled-release urea on rice yield, nitrogen use efficiency and soil fertility in a single rice cropping system. *Sci. Rep.* 10, 10432. doi: 10.1038/s41598-020-67110-6

Congreves, K. A., Otchere, O., Ferland, D., Farzadfar, S., Williams, S., and Arcand, M. M. (2021). Nitrogen use efficiency definitions of today and tomorrow. *Front. Plant Sci.* 12. doi: 10.3389/fpls.2021.637108

Emran, S. A., Krupnik, T. J., Kumar, V., Ali, M. Y., and Pittelkow, C. M. (2019). Agronomic, economic, and environmental performance of nitrogen rates and source in bangladesh's coastal rice agroecosystems. *Field Crop Res.* 241, 107567. doi: 10.1016/j.fcr.2019.107567

Feng, Y. F., Sun, H. J., Xue, L. H., Liu, Y., Gao, Q., Lu, K. P., et al. (2017). Biochar applied at an appropriate rate can avoid increasing NH_3 volatilization dramatically in rice paddy soil. *Chemosphere* 168, 1277–1284. doi: 10.1016/j.chemosphere.2016.11.151

Geng, J. B., Ma, Q., Zhang, M., Li, C. L., Liu, Z. G., Lyu, X. X., et al. (2015). Synchronized relationships between nitrogen release of controlled-release nitrogen fertilizers and nitrogen requirements of cotton. *Field Crop Res.* 184, 9–16. doi: 10.1016/j.fcr.2015.09.001

Goedkoop, M. (1995). The eco-indicator 95: Weighting method for environmental impact analysis for clean design. *Comput. Chem. Eng.* 20, 1377–1382.

Grant, C. A., Wu, R., Selles, F., Harker, K. N., Clayton, G. W., Bittman, S., et al. (2012). Crop yield and nitrogen concentration with controlled release urea and split applications of nitrogen as compared to non-coated urea applied at seeding. *Field Crop Res.* 127, 170–180. doi: 10.1016/j.fcr.2011.11.002

Gronwald, M., Helfrich, M., Don, A., Fu, B. R., Well, R., and Flessa., H. (2018). Application of hydrochar and pyrochar to manure is not effective for mitigation of ammonia emissions from cattle slurry and poultry manure. *Bio. Fer. Soils* 54, 451–465. doi: 10.1007/s00374-018-1273-x

Guo, C., Ren, T., Li, P., Wang, B., Zou, J., Hussain, S., et al. (2019). Producting more grain yield of rice with less ammonia volatilization and greenhouse gases emission using slow/controlled-release urea. *Environ. Sci. Pollut. .R.* 26, 2569–2579. doi: 10.1007/s11356-018-3792-2

He, T. H., Liu, D. Y., Yuan, J. J., Ni, K., Zaman, M., Luo, J. F., et al. (2018). A two years study on the combined effects of biochar and inhibitors on ammonia volatilization in an intensively managed rice field. *Agr. Ecosyst. Environ.* 264, 44–53. doi: 10.1016/j.agee.2018.05.010

Huang, S., Lv, W., Bloszies, S., Shi, Q., Pan, X., and Zeng, Y. (2016). Effects of fertilizer management practices on yield-scaled ammonia emissions from croplands in China: A meta-analysis. *Field Crop Res.* 192, 118–125. doi: 10.1016/j.fcr.2016.04.023

IFA (2021). *IFADATA statstics* (Paris: International Fertilizer Industry Association). Available at: http://www.fertilizer.org/ifa/HomePage/STATISTICS[EB/OL.

Jantalia, C. P., Halvorson, A. D., Follett, R. F., Rodrigues Alves, B. J., Polidoro, J. C., and Urquiaga, S. (2012). Nitrogen source effects on ammonia volatilization as measured with semi-static chambers. *Agron. J.* 104, 1595–1603. doi: 10.2134/agronj2012.0210

Ju, C., Zhu, Y., Liu, T., and Sun, C. (2021). The effect of nitrogen reduction at different stages grain yield and nitrogen use efficiency for nitrogen efficient rice varieties. *Agronomy* 11, 462. doi: 10.3390/agronomy11030462

Kim, G. W., Gutierrez-Suson, J., and Kim, P. J. (2019). Optimum n rate for grain coincides with minimum greenhouse gas intensity in flooded rice fields. *Field Crop Res.* 237, 23–31. doi: 10.1016/j.fcr.2019.04.011

Kissel, D. E., Brewer, H. L., and Arkin, G. F. (1977). Design and test of a field sampler for ammonia volatilization. *Soil Sc. Soc Am. J.* 41, 1133–1138. doi: 10.2136/sssaj1977.03615995004100060024x

Lassaletta, L., Billen, G., Grizzetti, B., Anglade, J., and Garnier, J. (2014). 50 year trends in nitrogen use efficiency of world cropping systems: the relationship between yield and nitrogen input to cropland. *Environ. Res. Lett.* 9, 105011. doi: 10.1088/1748-9326/9/10/105011

Li, Y., Chen, Y., Wu, C., Tang, X., and Ji, X. (2015). Determination of optimum nitrogen application rates in zhejiang province, China, base on rice yields and ecological security. *JIA.* 14, 2426–2433. doi: 10.1016/S2095-3119(15)61168-6

Li, P., Lu, J., Wang, Y., Wang, S., Hussain, S., Ren, T., et al. (2018). Nitrogen losses, use efficiency, and productivity of early rice under controlled-release urea. *Agric. Ecosyst. Environ.* 251, 78–87. doi: 10.1016/j.agee.2017.09.020

Liu, X., Xu, S., Zhang, J., Ding, Y., Li, G., Wang, S., et al. (2016). Effect of continuous reduction of nitrogen application to a rice-wheat rotation system in the middle-lower Yangtze river region, (2013-2015). *Field Crop Res.* 196, 348–356. doi: 10.1016/j.fcr.2016.07.003

Luo, X. (2021). Changing trend and influencing factors of rice production cost in China. *ASIAN* 13, 317685. doi: 10.22004/ag.econ.317685

Lyu, T., Shen, J., Ma, J., Ma, P., Yang, Z., Wu, J, et al. (2021). Hybrid rice yield response to potted-seedling machine transplanting and slow-release nitrogen fertilizer application combined with urea topdressing. *Crop J.* 9, 915–923. doi: 10.1016/j.cj.2020.08.013

Lyu, Y., Yang, X., Pan, H., Zhang, X., Cao, H., Ulgiati, S., et al. (2021). Impact of fertilization schemes with different ratios of urea to controlled release nitrogen fertilizer on environmental sustainability, nitrogen use efficiency and economic benefit of rice production: A study case from southwest China. *J. Clean. Prod.* 293, 126198. doi: 10.1016/j.jclepro.2021.126198

Ministry of Agriculture of the People's Republic of China (MOA) (2015) *Zero growth action plan for the use of chemical fertilizers by 2020*. Available at: http://www.zzys.moa.gov.cn/gzdt/201503/t20150318_6309945.htm..

Muthayya, S., Sugimoto, J. D., Montgomery, S., and Maberly, G. F. (2015). An overview of global rice production, supply, trade, and consumption. *Ann. NY Acad. Sci.* 1324, 7–14. doi: 10.1111/nyas.12540

Niggli, U. (2015). Sustainability of organic food production: Challenges and innovations. *P. Nutr. Soc* 74, 83–88. doi: 10.1017/S0029665114001438

Song, X., Zhang, J., Peng, C., and Li, D. (2021). Replacing nitrogen fertilizer with nitrogen-fixing cyanobacteria reduced nitrogen leaching in red soil paddy fields. *Agric. Ecosyst. Environ.* 312, 107320. doi: 10.1016/j.agee.2021.107320

Sun, Y., Ma, J., Sun, Y., Xu, H., Yang, Z., Liu, S., et al. (2012). The effects of different water and nitrogen managements on yield and nitrogen use efficiency in hybrid rice of China. *Field Crop Res.* 127, 85–98. doi: 10.1016/j.fcr.2011.11.015

Tong, X., Huang, J., Mei, J., Ge, J., Han, L., and Huang, G. (2018). Characterization of controlled release fertilizer by infrared microspectroscopy. *Anal. Lett.* 51, 2252–2270. doi: 10.1080/00032719.2017.1419364

Wang, D., Ye, C., Xu, C., Wang, Z., Chen, S., Chu, G., et al. (2019). Soil nitrogen distribution and plant nitrogen utilization in direct-seeded rice in response to deep placement of basal fertilizer-nitrogen. *Rice Sci.* 26, 404–405. CNKI:SUN:SDKE.0.2019-06-008 doi: 10.1016/j.rsci.2018.12.008

Wang, G., Zhang, R., Gomez, M. E., Yang, L., Zamora, M. L., Hu, M., et al. (2016). Persistent sulfate formation from London fog to Chinese haze. *P. Natl. Acad. Sci. U.S.A.* 113, 13630–13635. doi: 10.1073/pnas.1616540113

Wu, H., Tao, Y., Liu, X., Li, H., Gao, L., Yang, J., et al. (2020). Towards an integrated nutrient management in crop species to improve nitrogen and phosphorus use efficiencies of chaohu watershed. *J. Clean. Prod.* 272, 122765. doi: 10.1016/j.jclepro.2020.122765

Xia, Y. Q., and Yan, X. Y. (2012). Ecologically optimal nitrogen application rates for rice cropping in the taihu lake region of China. *Sustain. Sci.* 7, 33–44. doi: 10.1007/s11625-011-0144-2

Xu, F., Zhang, L., Zhou, X., Guo, X., and Jiang, P. (2021). The ratoon rice system with high yield and high efficiency in China: Progress, trend of theory and technology. *Field Crop Res.* 272, 108282. doi: 10.1016/j.fcr.2021.108282

Xu, H., Zhong, G., Lin, J., Ding, Y., Li, G., Wang, S., et al. (2015). Effect of nitrogen management during the panicle stage in rice on the nitrogen utilization of rice and succeeding wheat crops. *Eur. J. Agron.* 70, 41–47. doi: 10.1016/j.eja.2015.06.008

Yang, Y., Li, N., Ni, X., Yu, L., Yang, Y., Wang, Q., et al. (2019). Combining deep flooding and slowrelease urea to reduce ammonia emission from rice fields. *J. Clean. Prod.* 244, 1–11. doi: 10.1016/j.jclepro.2019.118745

Yu, C. Q., Huang, X., Chen, H., Godfray, H. C. J., Wright, J. S., Hall, J. W., et al. (2019). Managing nitrogen to restore water quality in China. *Nature* 567, 516–520. doi: 10.1038/s41586-019-1001-1

Yu, F., and Shi, W. M. (2015). Nitrogen use efficiencies of major grain crops in China in recent 10 years. *Acta Pedologica Sinica.* 52, 1311–1324. doi: 10.11766/trxb201501270058

Yu, Q., Ye, J., Yang, S., Fu, J., Ma, J., Sun, W., et al. (2013). Effects of nitrogen application level on rice nutrient uptake and ammonia volatilization. *Rice Sci.* 20, 139–147. doi: 10.1016/S1672-6308(13)60117-1

Zhan, X., Zhang, Q., Zhang, H., Hussain, H. A., and Yang, Z. (2020). Pathways of nitrogen loss and optimized nitrogen management for a rice cropping system in arid irrigation region, northwest China. *J. Environ. Manage.* 268, 110702. doi: 10.1016/j.jenvman.2020.110702

Zhang, S., Shen, T., Yang, Y., Li, Y. C., Wan, Y., Wan, Y., et al. (2018). Controlled-released urea reduced nitrogen leaching and improved nitrogen use efficiency and yield of direct-seeded rice. *J. Environ. Manage.* 220, 191–197. doi: 10.1016/j.jenvman.2018.05.010

frontiers | Frontiers in Plant Science

TYPE Original Research
PUBLISHED 08 May 2023
DOI 10.3389/fpls.2023.1171331

Check for updates

OPEN ACCESS

EDITED BY
Li Wang,
Shandong Academy of Agricultural Sciences, China

REVIEWED BY
Krishan K. Verma,
Guangxi Academy of Agricultural Sciences, China
Guanjun Huang,
Jiangxi Agricultural University, China

*CORRESPONDENCE
Liyong Hu
liyonghu@mail.hzau.edu.cn
Lijun Luo
lijun@sagc.org.cn

†These authors have contributed equally to this work and share first authorship

RECEIVED 22 February 2023
ACCEPTED 13 April 2023
PUBLISHED 08 May 2023

CITATION
Liu J, Zhang K, Bi J, Yu X, Luo L and Hu L (2023) Mesophyll conductance and N allocation co-explained the variation in photosynthesis in two canola genotypes under contrasting nitrogen supply.
Front. Plant Sci. 14:1171331.
doi: 10.3389/fpls.2023.1171331

Mesophyll conductance and N allocation co-explained the variation in photosynthesis in two canola genotypes under contrasting nitrogen supply

Jiahuan Liu[1†], Kangkang Zhang[2†], Junguo Bi[2], Xinqiao Yu[2], Lijun Luo[2*] and Liyong Hu[1*]

[1]Ministry of Agriculture and Rural Affairs (MARA) Key Laboratory of Crop Ecophysiology Farming System in the Middle Reaches of the Yangtze River, College of Plant Science Technology, Huazhong Agricultural University, Wuhan, China, [2]Shanghai Agrobiological Gene Center, Shanghai, China

The application of nitrogen fertilizer within a normal range has been found to increase the leaf nitrogen content and photosynthetic rate of canola plants (*Brassica napus* L.). Despite numerous studies on the separate effects of CO_2 diffusion limitation and nitrogen allocation trade-off on photosynthetic rate, few have examined both these factors in relation to the photosynthetic rate of canola. In this study, two genotypes of canola with varying leaf nitrogen content were analyzed to determine the impact of nitrogen supply on leaf photosynthesis, mesophyll conductance, and nitrogen partitioning. The results showed that the CO_2 assimilation rate (A), mesophyll conductance (g_m), and photosynthetic nitrogen content (N_{psn}) increased with an increase in nitrogen supply in both genotypes. The relationship between nitrogen content and A followed a linear-plateau regression, while A had linear relationships with both photosynthetic nitrogen content and g_m, indicating that the key to enhancing A is increasing the distribution of leaf nitrogen into the photosynthetic apparatus and g_m, rather than just increasing nitrogen content. Under high nitrogen treatment, the genotype (QZ) with high nitrogen content had 50.7% more nitrogen than the other genotype (ZY21), but had similar A, which was primarily due to ZY21's higher photosynthetic nitrogen distribution ratio and stomatal conductance (g_{sw}). On the other hand, QZ showed a higher A than ZY21 under low nitrogen treatment as QZ had higher N_{psn} and g_m compared to ZY21. Our results indicate that, in selecting high PNUE rapeseed varieties, it is important to consider the higher photosynthetic nitrogen distribution ratio and CO_2 diffusion conductance.

KEYWORDS

canola, genotype, photosynthetic nitrogen use efficiency, mesophyll conductance, N allocation, photosynthetic N, nitrogen

Introduction

In the past century, the invention of ammonia synthesis technology and its application in agriculture has resulted in an increase in crop yield (Bouchet et al., 2016). However, this advancement has also caused environmental problems such as water eutrophication and soil acidification due to excess nitrogen not being absorbed by crops (Lassaletta et al., 2014). Optimizing agricultural productivity while minimizing environmental impact has become increasingly important, and as a result, improving crop nitrogen use efficiency (NUE) has emerged as a long-term research priority. The definition of NUE is diverse and complex, and in plant ecophysiology, it is generally defined as the CO_2 assimilation rate per unit leaf N concentration (PNUE). Increasing PNUE is crucial for improving NUE (Garnier et al., 1995).

Leaf CO_2 assimilation rate (*A*) is closely linked to leaf nitrogen content, as much of the leaf N is involved in the photosynthetic reaction process (Evans, 1989; Terashima et al., 2011; Yamori et al., 2011; Xiong et al., 2015c). Different forms of nitrogen are present in leaves, including free amino acids, nitrates, soluble proteins, cell-wall binding proteins, and membrane proteins. The allocation pattern of leaf nitrogen to each nitrogen component varies among species (Onoda et al., 2017). A trade-off exists between nitrogen allocation to photosynthetic proteins and non-photosynthetic proteins to maintain a high carbon assimilation rate in plant leaves. For instance, deciduous plants have a higher PNUE than evergreen plants as deciduous plants allocate more nitrogen to the photosynthetic system. However, evergreen species allocate more nitrogen into the cell wall to maintain a longer leaf lifespan (Takashima et al., 2004). A study on *Polygonum cuspidatum* Sieb. et Zucc. showed that the smaller allocation of nitrogen to the cell walls in late germinators was associated with a higher CO_2 assimilation rate, primarily due to a greater fraction of nitrogen allocated to the photosynthetic apparatus (Onoda et al., 2004). The invasive plant, *Ageratina adenophora*, appears to have evolved to allocate a higher fraction of nitrogen to photosynthesis and reduced cell wall allocation (Feng et al., 2009). However, this trade-off is not widely accepted, as other studies in sclerophyllous leaves, between different plant species (Hikosaka and Shigeno, 2009) and among native and invasive species (Funk et al., 2013), did not find this trend. Additionally, the fraction of nitrogen not involved in the metabolic process and structure construction in leaves is referred to as storage nitrogen. It accounts for approximately 50% of the total nitrogen content in plant leaves (Xu et al., 2012; Liu et al., 2018) and plays a crucial role in maintaining leaf expansion and photosynthetic protein synthesis (Lehmeier et al., 2013; Liu et al., 2018). However, a high proportion of storage nitrogen will reduce the PNUE of leaves.

In C_3 plants, the CO_2 assimilation rate is mainly limited by Rubisco carboxylation capacity and CO_2 diffusion efficiency (von Caemmerer and Evans, 2010). Rubisco, the most abundant enzyme in plants, is essential for fixing CO_2 in the Calvin cycle and uses up to 20% of the plant's nitrogen to maintain high photosynthetic rates in leaves (Evans, 1989; Evans and Clarke, 2019). Under natural conditions, the actual carboxylation reaction of Rubisco is much lower than its potential capacity, particularly in leaves with high nitrogen content, because a large number of Rubisco enzymes are inactive due to a lack of CO_2 (Cheng and Fuchigami, 2000; Yamori et al., 2011; Li et al., 2013). During the diffusion of CO_2 from the atmosphere to chloroplasts, the CO_2 encounters several resistances, and its reciprocal is called CO_2 diffusion efficiency, including the leaf boundary layer conductance, stomatal conductance to CO_2 (g_{sc}), and mesophyll conductance (g_m). Despite many studies showings that increasing nitrogen supply increases g_{sc} and g_m in various C_3 crops (Li et al., 2009; Yamori et al., 2011; Xiong et al., 2015b), the increase in g_m is much smaller than the increase in Rubisco enzyme content. As a result, the CO_2 concentration at chloroplast carboxylation sites (C_c) remains insufficient to meet the saturation needs of Rubisco enzymes in high N conditions (Li et al., 2009; Yamori et al., 2011).

There have been numerous studies examining the independent effects of CO_2 diffusion limitation and N allocation trade-off on *A* and PNUE. However, these two hypotheses are not mutually exclusive and need to be considered together to fully understand their effects on *A* and PNUE (Onoda et al., 2017). Our previous study found that, although two canola varieties (Quanzi & Zheyou 21) showed significant differences in leaf nitrogen content, they had a similar maximum CO_2 assimilation rate under high light intensity (Liu et al., 2021). Based on this, we hypothesized that the two genotypes might differ in N allocation trade-off and CO_2 diffusion. To test this hypothesis, we conducted a pot experiment with two canola genotypes under different N supplies. The objective of the study was to (1) Evaluate the impact of different N supplies on *A* and PNUE in the two canola genotypes; (2) Examine the effects of different N supplies on photosynthetic limitation and N partitioning in two canola genotypes; (3) Determine the main cause of the reduction in PNUE under high N supply, whether it is due to CO_2 diffusion limitation or N allocation trade-off.

Materials and methods

Plant materials and N treatments

Two canola genotypes, Quanzi (QZ) and Zheyou 21 (ZY21), were selected. Seeds were provided by the National Key Laboratory of Crop Genetic Improvement and sawed in 0.5 L pots filled with a 0.85 kg mixture of corn soil and sand (1:1, w/w) on the campus of Huazhong Agriculture University, Wuhan, China (114°22'E, 30° 29'N). KH_2PO_4 was mixed into the mixture at the rate of 275 mg per pot. For high N (HN) and low N (LN) treatments, Urea was applied at 144 mg per pot and 29 mg per pot, respectively. Plants were grown in a growth chamber with 14h day/10h night. The light intensity (photosynthetic photon flux density) was 400-420 μmol m^{-2} s^{-1} at the canopy level, and the temperatures were set to 25/20° C (day/night).

Gas exchange and chlorophyll fluorescence measurements

After one month of growth, we used an open-flow gas exchange system (Li-Cor 6800; Li-Cor Inc., Lincoln, NE, USA) with a Multiphase Flash™ Fluorometer (6800-01 A) apertures with 6 cm^2. To avoid plant rhythm on gas exchange measurements, all plants were measured between 9:00 to 16:00. To minimize leaf position and age effects, measurements were taken on the newest fully expanded leaves. In the leaf chamber, CO_2 concentration was set at 400 μmol mol^{-1} with a CO_2 mixer, leaf temperature was maintained at 25 °C, PPFD was 1000 μmol m^{-2} s^{-1} with a blue: red (10:90) light, the leaf-to-air vapor pressure deficit (VPD) was 1.2 kPa. After A and stomatal conductance (g_{sw}) reached the steady-state stage, usually after 20 min, the gas exchange parameters and fluorescence parameters were simultaneously recorded. CO_2 response curves measurements were performed on three plants for each treatment, and the CO_2 concentrations in the reference chamber were set across a series of 400, 300, 200, 150, 100, 50, 400, 600, 800, 1000, 1500, 2000 μmol mol^{-1}. Then, the maximum carboxylation rate ($V_{c,\ max}$) and maximum electron transport rate (J_{max}) were calculated using an R package "*plantecophys*" (Duursma, 2015) from the A/C_c response curves according to the FvCB model (Farquhar et al., 1980).

Estimation of mesophyll conductance

The actual photochemical efficiency of photochemical efficiency of PSII (Φ_{PSII}) was calculated as follows:

$$\Phi_{PSII} = \frac{(F_m' - F_s)}{F_m'} \quad (1)$$

Where, F'_m is the maximum fluorescence and F_s represents the steady-state fluorescence. Then, the electron transport rate (ETR) was calculated as follows:

$$ETR = \Phi_{PSII} \times PPFD \times \alpha \times \beta \quad (2)$$

Where PPFD is photosynthetic photon flux density, α is leaf absorbance, β represents the distribution ratio of electrons in PSII. The $\alpha\beta$ was estimated from light response curves in a low O_2 environment (O_2<2%). Specifically, under low O_2 supply conditions, simultaneous measurement of the response of leaf gas exchange, and chlorophyll fluorescence to PPFD. During the measurements, the leaf chamber conditions were the same as those described above, except that the PPFD was set across a series of 1500, 1000, 800, 400, 250, 150, 100, 50, 20, and 0 μmol m^{-2} s^{-1}. Then, the slope of the relationship between Φ_{PSII} and Φ_{CO2} is regarded as the value of $\alpha\beta$ (Valentini et al., 1995).

The variable J method described by Harley et al. (1992) was used to calculate CO_2 concentration in the chloroplast (C_c) and then to estimate g_m. The g_m was calculated as follows:

$$C_c = \frac{\Gamma^* \ (ETR + 8\,(A + R_d))}{ETR - 4\,(A + R_d)} \quad (3)$$

$$g_m = \frac{A}{C_i - C_c} \quad (4)$$

$$\Gamma^* = C_i^* + \frac{R_d}{g_m} \quad (5)$$

Where A, C_i, and ETR were determined as previously described, and day respiration rate (R_d) and the CO_2 compensation point in the absence of mitochondrial respiration (Γ^*) were calculated by the Laisk method (Harley et al., 1992). Briefly, the response of A to C_i was performed, with CO_2 concentrations in the reference chamber set across a series of 110, 90, 70, and 50 μmol mol^{-1}, at three PPFD of 250, 100, 50 μmol m^{-2} s^{-1}, respectively. The intersection point of three A/C_i curves on the x-axis was C_i*, and on the y-axis was R_d. There was no difference in R_d values between treatments leaves, thus the average value (0.78 μmol m^{-2} s^{-1}) of all the treatments were used in the current study.

Photosynthetic limitation analysis

Relative limitations of photosynthesis, including stomatal (l_s), mesophyll (l_m), and biochemical (l_b) relative limitations, were calculated as follows Grassi and Magnani (2005):

$$l_s = \frac{g_t/g_{sc} \cdot \partial A/\partial C_c}{g_t + \partial A/\partial C_c} \quad (6)$$

$$l_m = \frac{g_t/\ g_m \cdot \partial A/\partial C_c}{g_t + \partial A/\partial C_c} \quad (7)$$

$$l_b = \frac{g_t}{g_t + \partial A/\partial C_c} \quad (8)$$

Where g_t is the total conductance to CO_2 ($g_t = 1/(1/g_{sc} + 1/g_m)$), g_{sc} is stomatal conductance to CO_2 ($g_{sc} = g_{sw}/1.6$), and A/C_c is the slope of A versus C_c response curve. In the current study, A/C_c was calculated according to the FvCB model (Farquhar et al., 1980):

$$\partial A/\partial C_c = V_{c,\ max} \frac{\Gamma^* + K_c(1 + O/K_o)}{(C_c + K_c(1 + O/K_o))^2} \quad (9)$$

Where K_c and K_o are the Rubisco Michaelis-Menten constants for CO_2 and O_2, respectively.

N partitioning by function

The leaf N is divided into photosynthetic N, respiration N, structural N, and storage nitrogen based on the LUNA model described by (Xu et al., 2012; Ali et al., 2016). Photosynthetic N is further divided into three major classes of proteins, including carboxylation system protein (N_{cb}), electron transport system protein (N_{et}), and light capture system protein (N_{lc}). Respiration N is the respiratory enzyme located in the mitochondria to generate the energy required for plant growth. Structural N (N_{str}) represents the N used to build cell walls and DNA. In the current study, structural N was measured by SDS-insoluble protein N. Leaf structural N was measured according to the method of (Takashima et al., 2004) with minor modifications. Leaf tissue was harvested about 0.1g and immersed in liquid N and stored in an ultracold storage freezer (-80). The frozen leaf samples were ground with a Mixer Mill (MM 400, Retsch, Haan, Germany) and homogenized with 1 ml of 100 mM Na phosphate buffer [PH 7.4 and containing 0.4M D-sorbitol, 2 mM $MgCl_2$, 10 mM NaCl, 5 mM iodoacetate, 5 mM phenylmethylsulphonyl fluoride, and 5 mM DTT], then washed into a centrifuge tube with 4 ml of phosphate buffer. The samples were centrifuged at 15 000 g, 4 for 15 min; after that, 1 ml of phosphate buffer containing 3% sodium dodecyl sulfate (SDS) was added to the residue, followed by heating at 90 for 5 min. And then, the mixture was separated by centrifugation at 4500 g for 10 min. This procedure was repeated four times, and the residue (regarded as SDS-insoluble protein) was washed to the quantitative filter paper with ethanol. The samples on the filter papers were dried naturally in a fume hood. And then, the structural N on the quantitative filter paper was dried and digested with H_2SO_4-$HClO_4$ according to the method of Gallaher et al. (1976). The N concentration in the digestion solution was measured by a discrete analyzer (SmartChem 200, Unity Scientific, Brookfield, CT). The blank quantitative filter paper was used as blank control. Besides, about 0.1 g dry matter was used to determine the total leaf N concentration with the same method described above. Storage N is equal to the total leaf N minus photosynthetic N, respiration N, and structural N. The calculation formulas for each form of N are given below.

The carboxylation N content (N_{cb}) is:

$$N_{cb} = \frac{V_{c,\max}}{6.25 \text{ ñ } V_{cr}} \quad (10)$$

Where 6.25 [g Rubisco (g^{-1} N)] represents the proportion of N allocated to Rubisco, V_{cr} is the maximum rate of RUBP carboxylation per unit Rubisco protein [20.8 μmol CO_2 (g Rubisco)$^{-1}$$s^{-1}$ at 25] (Niinemets and Tenhunen, 1997).

The electron transport N (N_{et}) content is:

$$N_{et} = \frac{J_{max}}{8.06 \text{ ñ } J_{mc}} \quad (11)$$

J_{mc} is the maximum electron transport rate per unit cytochrome f [155.65 μmol e^{-1} μmol cytochrome f s^{-1} at 25].

The light capture N (N_{lc}) content:

$$N_{lc} = \frac{C_{Chl}}{C_B} \quad (12)$$

C_{Chl} is the leaf chlorophyll concentration (mmol m^{-2}), and C_B is the ratio of chlorophyll to organic N in light-harvesting components (2.15 mmol g^{-1}).

The photosynthetic N content (N_{psn}) is:

$$N_{psn} = N_{cb} + N_{et} + N_{lc} \quad (13)$$

The respiratory N content (N_{resp}) is:

$$N_{resp} = \frac{R_n}{33.69} \quad (14)$$

R_n is the leaf dark respiration rate (μmol CO_2 m^{-2} s^{-1}), which was assumed to be twice that of R_d (Yamori et al., 2005), and 33.69 is the leaf N use efficiency for respiration at 25 (μmol CO_2 g^{-1} N s^{-1}).

The storage N content (N_{store}) is:

$$N_{store} = N_a - N_{psn} - N_{resp} - N_{str} \quad (15)$$

N_a is the leaf total N concentration based on the area, N_{str} is the leaf structural N content, which is also the SDS-insoluble N content in the current study (Takashima et al., 2004).

Data analysis

Two-way ANOVA was used on two canola varieties to test the trait response to nitrogen treatments. Linear-plateau regression and linear regression were performed to test the correlations between trait parameters. All analyses and figures were performed in R version 4.2.2 (R Core Team, 2020).

Results

Leaf morphological and physiological traits

The results of our study indicated that the application of high levels of nitrogen significantly enhanced the growth parameters of both QZ and ZY21 varieties. The dry matter weight (DMW), shoot weight (SW), and root weight (RW) of both varieties increased by 120.5% and 184.5%, 141.3% and 194.6%, and 92% and 168.7%, respectively, under high N treatment compared to low N treatment (Table 1). The results showed that ZY21 had a higher response to high N treatment, with 65.6%, 72.5%, and 54.9% higher DMW, SW, and RW, respectively, compared to QZ. The leaf nitrogen concentration (N_a) of plants under high N treatment was found to be 1.5-fold and 1.6-fold higher in QZ and ZY21, respectively, compared to plants under low N treatment. Under low N treatment, the difference in N_a between the two varieties was not statistically significant, but under high N treatment, the N_a of QZ was found to be significantly higher than that of ZY21 (by 50.7%). Our results also demonstrate that high N treatment increased the SPAD value and chlorophyll content based on leaf area (C_{Chl}) in both QZ and ZY21, with an increase of 18.3% and 22.0% in SPAD value, and 80.3% and 78.4% in C_{Chl}, respectively (Table 2).

Effect of N concentration on photosynthesis and CO_2 diffusion efficiency

The results of our study indicated that the supply of nitrogen has a significant impact on CO_2 response curves (Figure 1) and photosynthetic parameters (Table 3). Compared with high N treatment, the CO_2 assimilation rate (A), mesophyll conductance of CO_2 (g_m), maximum carboxylation rate ($V_{c,\max}$), and maximum electron transport rate (J_{max}) of the two varieties were significantly

TABLE 1 Effects of N supply on canola (Brassica napus L.) growth.

Nitrogen	Variety	DMW	SW	RW
		g	g	g
HN	QZ	3.66 ± 1.56	2.22 ± 1.30	1.44 ± 0.38
	ZY21	6.06 ± 1.49	3.83 ± 1.04	2.23 ± 0.66
LN	QZ	1.66 ± 0.42	0.92 ± 0.21	0.75 ± 0.30
	ZY21	2.13 ± 0.69	1.3 ± 0.40	0.83 ± 0.34
ANOVA				
Nitrogen (N)		**	**	**
Variety (V)		*	*	*
N * V		ns	ns	ns

HN, high nitrogen treatment; LN, low nitrogen treatment; DMW, dry matter weight; SW, shoot weight; RW, root weight. Data are presented as mean ± SD (n = 3). Stars denote a significant change in values (ns, no significant; *P< 0.05; **P< 0.01).

different in response to low N treatment. Specifically, as compared to plants supplied with high N level, A, $V_{c,\ max,}$ and J_{max} of QZ supplied with low N level decreased by 18.0%, 36.2%, and 30.6% whereas, those of ZY21 supplied with low N level decreased by 37.7%, 35.5%, and 27.6%. Besides, the g_m of QZ is hardly affected by nitrogen fertilizer supply, but that of ZY21 is significantly reduced under low nitrogen conditions. This result indicated that the photosynthetic parameters of ZY21 were more sensitive to the

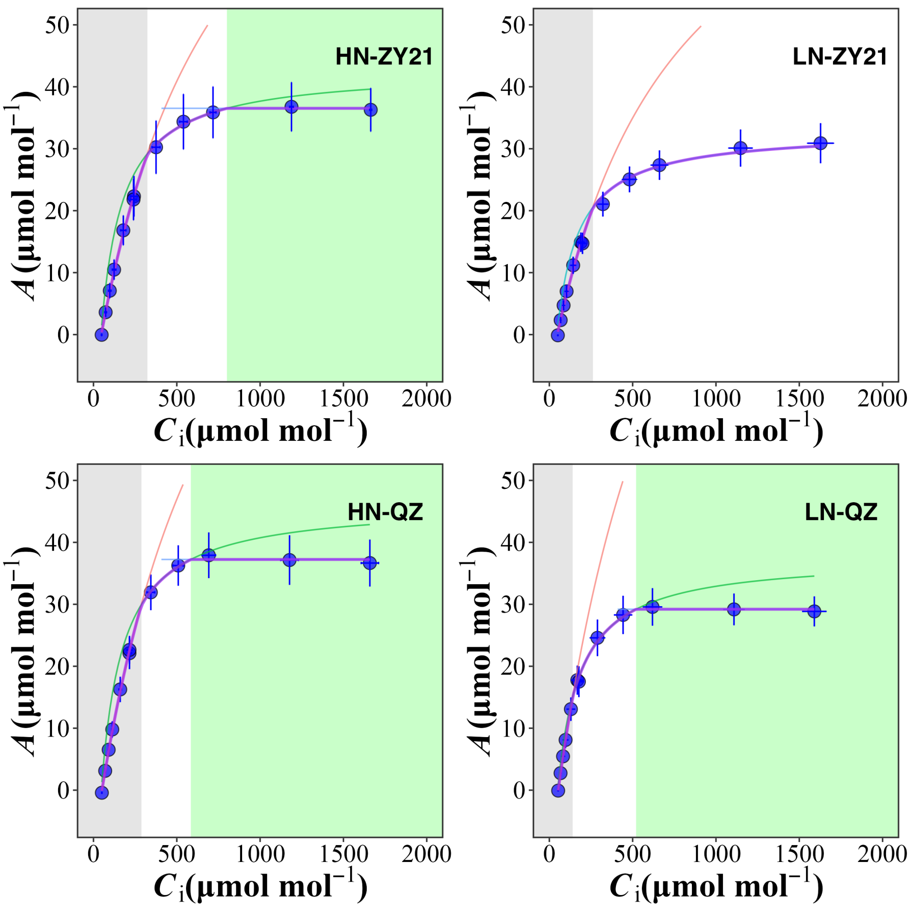

FIGURE 1
Chloroplast CO_2 concentration (C_c) response of the net photosynthetic rate (A) for *Brassica napus* L. under different nitrogen supplies. *A* is limited by RuBP carboxylation (grey shaded area), RuBP regeneration (white area), and triose-phosphate utilization (green area). RuBP carboxylation rate (red lines), RuBP regeneration rate (green lines), and triose-phosphate utilization rate (blue lines) were estimated using FvCB leaf photosynthesis model. The red dots represent the net photosynthetic rate when the ambient CO_2 concentration is 400 μmol mol^{-1}.

TABLE 2 Leaf SPAD value, chlorophyll content (C_{Chl}), and area-based leaf N content N_a) of *Brassica napus* L. under different N supply.

Nitrogen	Variety	SPAD	$C_{Chl.}$ (mg m^{-2})	N_a (g m^{-2})
HN	QZ	65.2 ± 1.1	858 ± 110	3.03 ± 0.63
	ZY21	56.6 ± 0.7	591 ± 46	2.01 ± 0.10
LN	QZ	55.1 ± 1.6	476 ± 21	1.49 ± 0.07
	ZY21	46.4 ± 4.4	331 ± 14	1.25 ± 0.23
ANOVA				
Nitrogen (N)		**	**	**
Variety (V)		**	**	*
N * V		ns	ns	ns

Note. HN, high nitrogen treatment; LN, low nitrogen treatment. Data are presented as mean ± SD (n = 3). Stars denote a significant change in values (ns, no significant; *P< 0.05; **P< 0.01).

change of nitrogen supply than that of QZ. High nitrogen fertilizer supply decreased the C_c at process transition between Rubisco carboxylation-limited (W_c) and RuBP regeneration-limited (W_j) photosynthetic rate. Compared with ZY21, QZ had lower *Cc* at the process transition between W_c to W_j, especially under a low nitrogen fertilizer supply. Furthermore, increasing the N supply significantly reduced the photosynthetic nitrogen use efficiency (PNUE) of QZ by 39.1%, whereas the PNUE of ZY21 was less affected by N supplies (Table 3). Compared with QZ, ZY21 had a higher PNUE under high N treatment; the PNUE of ZY21 is 53.0% higher than QZ.

The quantitative limitation analysis showed that, on average, *A* was mainly limited by biochemical factors (l_b, 60.9%), followed by stomatal conductance (l_s, 21.9%), and mesophyll conductance limitation (l_m, 17.2%) was the lowest (Figure S1). The results also suggested that the *A* of QZ is primarily limited by CO_2 diffusion efficiency, whereas ZY21 is predominantly constrained by biochemical factors.

Effect of N concentration on leaf N partitioning by function

The results of our study demonstrated the impact of increasing nitrogen supply on the allocation of nitrogen in both QZ and ZY21 varieties. The photosynthetic N (N_{psn}), respiratory N (N_{resp}), structural N (N_{str}), and storage N (N_{store}) for leaves developed by plants grown under HN were higher than those for plants grown under LN (Figure 2). QZ allocated more nitrogen to storage N than ZY21 under high N treatment, while the opposite was observed under low N conditions. The allocation of N_{psn} into three major classes of proteins, including carboxylation system protein (N_{cb}), electron transport system protein (N_{et}), and light capture system

TABLE 3 Effects of different N supplies on the CO_2 assimilation rate(A), stomatal conductance (g_{sw}), mesophyll conductance of CO_2 (g_m), intercellular CO_2 concentration (C_i), CO_2 concentration in the chloroplast (C_C), maximum carboxylation rate ($V_{c,\ max}$), maximum electron transport rate (J_{max}) and photosynthetic N use efficiency (PNUE) of *Brassica napus* L.

Nitrogen	Variety	A (µmol m^{-2} s^{-1})	>g_{sw} (mol m^{-2} s^{-1})	g_m (mol m^{-2} s^{-1})	>C_i (µmol mol^{-1})	>C_c (µmol mol^{-1})	>$V_{c,\ max}$ (µmol m^{-2} s^{-1})	>J_{max} (µmol m^{-2} s^{-1})	PNUE (µmol g^{-1})
HN	QZ	21.7 ± 2.3	0.320 ± 0.072	0.261 ± 0.026	253 ± 14	149 ± 14	138.9 ± 6.0	233.9 ± 22.8	7.3 ± 0.9
	ZY21	22.3 ± 3.3	0.512 ± 0.052	0.464 ± 0.075	292 ± 8	243 ± 21	98.7 ± 17.4	200.2 ± 31.6	11.1 ± 1.2
LN	QZ	17.8 ± 2.2	0.367 ± 0.153	0.288 ± 0.096	285 ± 19	219 ± 33	88.6 ± 3.8	162.1 ± 13.6	11.9 ± 1.0
	ZY21	13.9 ± 0.5	0.348 ± 0.032	0.234 ± 0.039	309 ± 7	248 ± 16	63.6 ± 2.6	148.6 ± 18.1	11.4 ± 2.1
ANOVA									
Nitrogen (N)		**	ns	*	ns	ns	**	**	*
Variety (V)		ns	ns	ns	ns	**	**	ns	ns
N * V		ns	ns	**	ns	ns	ns	ns	*

Note. HN, high nitrogen treatment; LN, low nitrogen treatment. Data are presented as mean ± SD (n = 3). Stars denote a significant change in values (ns, no significant; *P< 0.05; **P< 0.01).

protein (N_{lc}), was also analyzed. The results showed that with the increase of nitrogen rate, the absolute N_{cb}, N_{et}, and N_{lc} increased in both varieties (Figure 2). However, the relative content of N_{cb}, N_{et}, and N_{lc} decreased with the rise of nitrogen rate, except for the N_{lc} of ZY21. In addition, our results showed that the decrease in the relative content of N_{cb} was greater in QZ compared to ZY21 with the increase of nitrogen application (from 46% to 36% in QZ compared to 40.1% to 37.7% in ZY21).

Correlations between leaf traits

The relationship between photosynthetic rate (A) and the concentration of nitrogen based on leaf area (N_a) was found to be positive at N_a values below 2.12 g m^{-2}, and stabilized at the highest value of 22.6 µmol m^{-2} s^{-1} when N_a exceeded that level (Figure 3A). Our analysis also revealed that the photosynthetic N (N_{psn}), stomatal conductance (g_{sw}), and mesophyll conductance (g_m) were significantly correlated with A in a linear manner (Figures 3B–D). The photochemical N utilization efficiency (PNUE) was primarily influenced by the allocation of N in the plant. The results showed that the relative content of N allocated to the carboxylation system protein ($N_{cb\%}$), electron transport system protein ($N_{et\%}$), photosynthetic N ($N_{psn\%}$), and respiratory N ($N_{resp\%}$) were positively correlated with PNUE. In contrast, the relative content of N allocated to storage ($N_{store\%}$) was negatively correlated with PNUE. These findings suggested that a higher allocation of N to the photosynthetic and respiratory systems is beneficial for improving PNUE (Figure S2).

Discussion

N supplement enhanced canola photosynthetic capacity and growth

In the present study, A was improved by more N fertilizer supply, which results in larger biomass in both canola genotypes (Table 1). Previous studies have observed a strong correlation between N_a and A across a wide range of species (Cheng and Fuchigami, 2000; Yamori et al., 2011; Xiong et al., 2015c) and under different N supplements (Li et al., 2009; Xiong et al., 2015c; Hou et al., 2019). We also found that increasing N fertilizer application significantly increased the A in both canola genotypes, but the difference in N_a between the two genotypes under high nitrogen supply did not cause changes in A. Our results suggested that N_a is not the main limiting factor for A under normal fertilizer supply conditions, but canola genotypes with high N_a have a higher A under a low N supply.

Effects of N partitioning trade-off on A and PNUE

The distribution of nitrogen within the cellular organelles of a C_3 plant can vary significantly. In mature leaves, the average distribution is 75% in chloroplasts, 10% in cell walls, and the remaining 25% is mainly found in mitochondria, peroxisome, and cytosol (Evans and Clarke, 2019). Several previous studies have shown a strong correlation between the allocation ratio of N in the

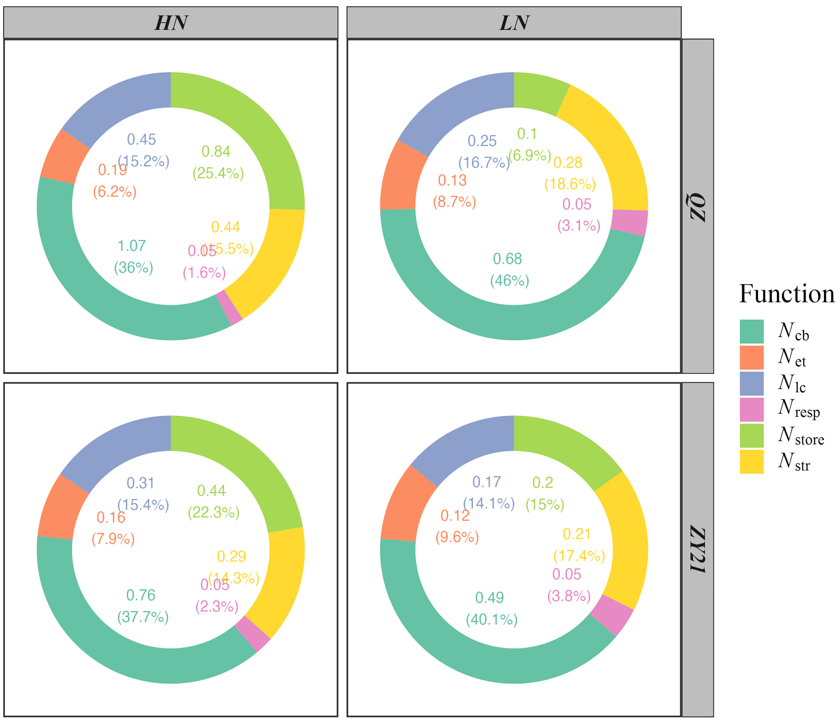

FIGURE 2
Effects of N supply on N partitioning by the function of two canola (*Brassica napus* L.) varieties (QZ and ZY21).

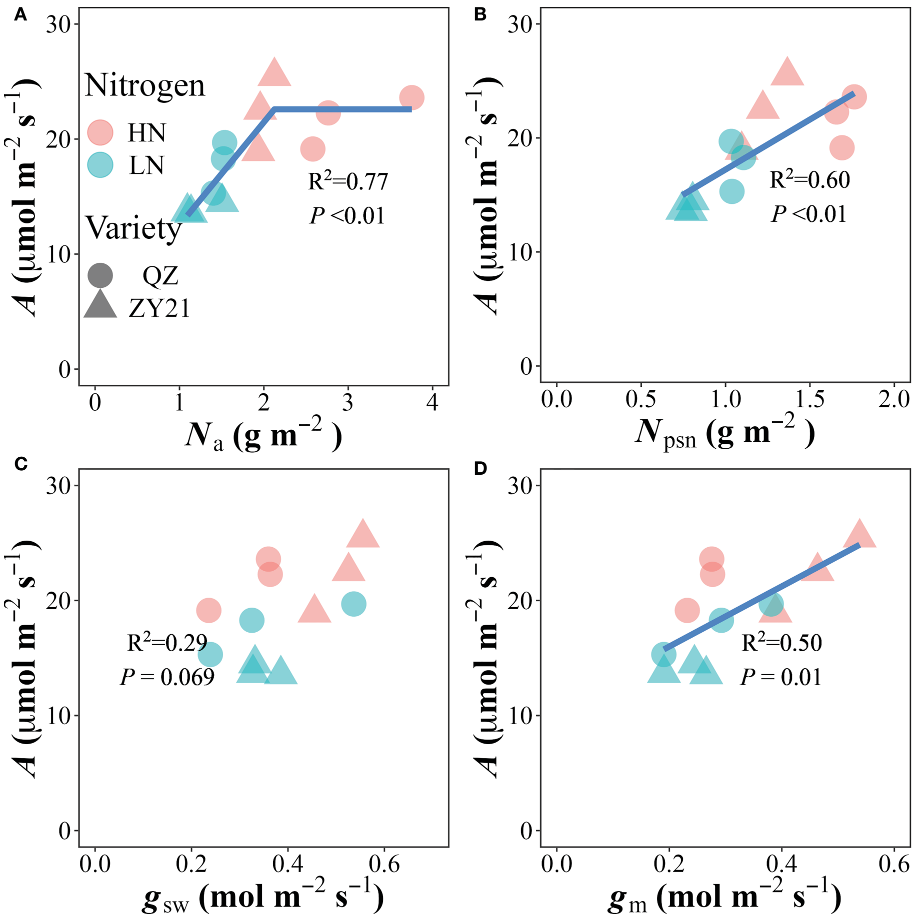

FIGURE 3
Correlations of **(A)** leaf nitrogen content (N_a), **(B)** photosynthetic nitrogen content (N_{psn}), **(C)** stomatal conductance (g_{sw}) and **(D)** mesophyll conductance (g_m) with the CO_2 assimilation rate (*A*). The data from all treatments are used together for correlation analysis and fitted by linear-plateau **(A)** and linear regression, respectively.

photosynthetic apparatus and *A* (Onoda et al., 2004; Takashima et al., 2004; Hou et al., 2019). Our current study supports this correlation (Figure 3B) and shows that the partitioning ratio of nitrogen into the photosynthetic apparatus increased under a low nitrogen supply. As described in the material and method, photosynthetic N is divided into three fractions based on their function, namely: N_{cb}, N_{et}, and N_{lc}. Compared with the low N treatment, the leaf N partitioning ratio into the three components was decreased under high N supply (Figure 2), in general, which was recognized as the primary reason for the low PNUE of plants under high N supply (Takashima et al., 2004; Li et al., 2009; Onoda et al., 2017). The results of our study showed that ZY21 demonstrates a comparable net photosynthetic rate due to its efficient distribution of N_a into N_{cb}, despite having lower N_a than QZ. Consequently, ZY21 had a higher PNUE than QZ under high N treatment. These findings highlight the importance of the distribution pattern of N_a within the photosynthetic apparatus on PNUE in plants (Poorter and Evans, 1998; Takashima et al., 2004; Liu et al., 2018; Hou et al., 2019).

Structural N is thought to make up a significant portion of leaf N, with estimates ranging from 2% to 20% across different species (Takashima et al., 2004; Feng et al., 2008; Harrison et al., 2009). Previous studies on canola have reported that the proportion of N in cell walls ranges from 3% (Hou et al., 2019) to 8% (Liu et al., 2018). The current study found that, on average for all N treatments of both canola genotypes, 16% of leaf N was allocated to structure, which is higher than previous studies and highlights the significant intraspecific variation in structural N. A trade-off between N allocation to cell walls and photosynthetic apparatus has been reported in deciduous herb species such as *Polygonum cuspidatum* (Onoda et al., 2004), *Ageratina adenophora* (Feng et al., 2009), and *Pinus massoniana* (Guan and Wen, 2011). However, not all studies support this trade-off, as some (Harrison et al., 2009; Hikosaka and Shigeno, 2009; Funk et al., 2013) including the current study did not observe such a trend.

Storage N is not involved in any biochemical processes and serves mainly as a buffer pool to support leaf growth and synthesize photosynthetic enzymes (Lehmeier et al., 2013; Liu et al., 2018). In canola, storage N has been found to constitute 30-45% of leaf N (Liu et al., 2018; Hou et al., 2019), while this value was 17.4% on average for both canola genotypes in the current study. Another reason for the numerical differences, in addition to the difference in N_{str} measurement values, is that neither study accounted for the potential impact of g_m on $V_{c,\ max}$, and J_{max} during the fitting of the A/C_c curves, resulting in an underestimation of both values (Sun et al., 2014). The relative content of N_{psn} was negatively correlated with the relative content of N_{store} in both genotypes under two N supplies (Figure S2), indicating a trade-off between N_{store} and N_{psn}. Under N deficiency, new leaves require more N for growth and expansion, leading to a decrease in N_{store} (Liu et al., 2018). There, an adequate amount of N_{store} can delay leaf senescence and promote leaf expansion, but a higher proportion of N_{store} can be disadvantageous for leaf photosynthesis when soil nitrogen is limited.

Effects of CO_2 diffusion resistance on A and PNUE

The CO_2 diffusion pathway is composed of three components: boundary layer conductance, stomatal conductance (g_s), and mesophyll conductance (g_m). The boundary layer has very little resistance to CO_2 diffusion when plants grow without stress, its limitation on A is often ignored in the studies. Our result showed that nitrogen deficiency had little effect on g_s (Table 3), which is in line with previous studies on canola (Hu et al., 2019), rice (Li et al., 2009), and wheat (Veres et al., 2017). However, the generalization of this effect is not yet apparent, as some studies have found that increasing N supply increases g_s in rice (Xiong et al., 2015b), wheat (Zhang et al., 2017), and oak (Zhu et al., 2020). This discrepancy may be due to differences in the response of g_s to nitrogen starvation between species or varieties. The duration of nitrogen starvation and the plant size during nitrogen starvation treatment maybe also affect the relationship between nitrogen fertilizer and g_{sw}.

Leaf anatomy is believed to play a crucial role in determining mesophyll conductance (g_m). Generally, decreasing cell wall thickness (T_{cw}) or increasing the chloroplast surface area facing the intercellular airspace per unit leaf area (S_c) has been shown to increase g_m (Evans et al., 2009; Terashima et al., 2011; Muir et al., 2014). Previous studies have demonstrated that increasing leaf nitrogen content can decrease T_{cw} and increase S_c, thereby increasing the efficiency of CO_2 transport across the membrane (Li et al., 2009; Li et al., 2013). We can infer that cell wall thickness is positively correlated with structural protein N, as various structural proteins are closely associated with the cell wall. In both genotypes studied, leaves under low N treatment allocated more N to structural protein N compared to high N treatment, leading to thickening of the cell walls (Figure 2). This increase in T_{cw} is a likely reason for the decrease in g_m under N deficiency. Generally, S_c is related to the chloroplast size and number. Although we did not study chloroplast structure, our results showed that chlorophyll content decreased significantly under N starvation conditions, which is closely related to the number of chloroplasts (Xiong et al., 2015a). These changes in S_c also explain the decrease in g_m under low N supply. Besides, in the present study, the response of the photosynthetic nitrogen use efficiency (PNUE) of two canola genotypes to nitrogen fertilizer treatment was different. The N supplement significantly decreased the PNUE of QZ, but had little effect on ZY21 (Table 3). This result is probably due to the increase in g_m of QZ under high N treatment being lower than the increase in Rubisco enzyme content of leaves, which resulted in a lower CO_2 concentration in the chloroplast (C_c) (Table 3). In comparison, the high N supply resulted in a higher C_c in ZY21 than low N treatment (Table 3), which offsets the increase in Rubisco enzyme content.

Conclusion

The present study demonstrated that the decrease in the allocation ratio of N into photosynthetic apparatus and the insufficient supply of CO_2 at chloroplast carboxylation sites are the main reasons leading to the decline in PNUE under high N supply in both genotypes. Besides, under high N application, the canola genotype with higher N content (QZ) allocated more N to the storage N and showed lower PNUE, which is not conducive to high-yield cultivation and can not meet the production demand. Hence, optimizing the N partitioning and enhancing g_m in plant leaves is expected to increase canola's net photosynthetic rate. These findings could have practical implications in developing strategies for enhancing canola productivity and sustainability.

Data availability statement

The original contributions presented in the study are included in the article/Supplementary Material. Further inquiries can be directed to the corresponding authors.

Author contributions

JL and LH planned and designed the research. JL and KZ performed the experiments. JL analysed the data. JL, KZ, JB, XY, LL, and LH wrote and revised the manuscript. All authors contributed to the article and approved the submitted version.

Funding

Breeding and Green Production Technology of New Varieties of high quality extra early maturing Water-saving and drought-resistant Rice (2021) No. 1-4. National Modern Rapeseed Industry Technology System (NYCYTC-00510) and Hubei Agricultural Science and Technology Innovation project (2016 6200 0000 1045).

Acknowledgments

The authors are very grateful to Prof. Dongliang Xiong for his valuable advice on the revision of this manuscript. Furthermore, useful suggestions given by expert reviewers are also acknowledged.

Conflict of interest

The authors declare that the research was conducted in the absence of any commercial or financial relationships that could be construed as a potential conflict of interest.

Publisher's note

All claims expressed in this article are solely those of the authors and do not necessarily represent those of their affiliated organizations, or those of the publisher, the editors and the reviewers. Any product that may be evaluated in this article, or claim that may be made by its manufacturer, is not guaranteed or endorsed by the publisher.

Supplementary material

The Supplementary Material for this article can be found online at: https://www.frontiersin.org/articles/10.3389/fpls.2023.1171331/full#supplementary-material

References

Ali, A. A., Xu, C., Rogers, A., Fisher, R. A., Wullschleger, S. D., Massoud, E. C., et al. (2016). A global scale mechanistic model of photosynthetic capacity (LUNA V1.0). *Geoscientific Model. Dev.* 9, 587–606. doi: 10.5194/gmd-9-587-2016

Bouchet, A.-S., Laperche, A., Bissuel-Belaygue, C., Snowdon, R., Nesi, N., and Stahl, A. (2016). Nitrogen use efficiency in rapeseed. a review. *Agron. Sustain. Dev.* 36, 1–20. doi: 10.1007/s13593-016-0371-0

Cheng, L., and Fuchigami, L. H. (2000). Rubisco activation state decreases with increasing nitrogen content in apple leaves. *J. Exp. Bot.* 51, 1687–1694. doi: 10.1093/jexbot/51.351.1687

Duursma, R. A. (2015). Plantecophys-an r package for analysing and modelling leaf gas exchange data. *PloS One* 10, e0143346. doi: 10.1371/journal.pone.0143346

Evans, J. R. (1989). Photosynthesis and nitrogen relationships in leaves of C_3 plants. *Oecologia* 78, 9–19. doi: 10.1007/BF00377192

Evans, J. R., and Clarke, V. C. (2019). The nitrogen cost of photosynthesis. *J. Exp. Bot.* 70, 7–15. doi: 10.1093/jxb/ery366

Evans, J. R., Kaldenhoff, R., Genty, B., and Terashima, I. (2009). Resistances along the CO_2 diffusion pathway inside leaves. *J. Exp. Bot.* 60, 2235–2248. doi: 10.1093/jxb/erp117

Farquhar, G. D., Von Caemmerer, S. V., and Berry, J. A. (1980). A biochemical model of photosynthetic CO_2 assimilation in leaves of C_3 species. *Planta* 149, 78–90. doi: 10.1007/BF00386231

Feng, Y.-L., Fu, G.-L., and Zheng, Y.-L. (2008). Specific leaf area relates to the differences in leaf construction cost, photosynthesis, nitrogen allocation, and use efficiencies between invasive and noninvasive alien congeners. *Planta* 228, 383–390. doi: 10.1007/s00425-008-0732-2

Feng, Y.-L., Lei, Y.-B., Wang, R.-F., Callaway, R. M., Valiente-Banuet, A., Inderjit,, et al. (2009). Evolutionary tradeoffs for nitrogen allocation to photosynthesis versus cell walls in an invasive plant. *Proc. Natl. Acad. Sci.* 106, 1853–1856. doi: 10.1073/pnas.0808434106

Funk, J. L., Glenwinkel, L. A., and Sack, L. (2013). Differential allocation to photosynthetic and non-photosynthetic nitrogen fractions among native and invasive species. *PloS One* 8, e64502. doi: 10.1371/journal.pone.0064502

Gallaher, R., Weldon, C., and Boswell, F. (1976). A semiautomated procedure for total nitrogen in plant and soil samples. *Soil Sci. Soc. America J.* 40, 887–889. doi: 10.2136/sssaj1976.03615995004000060026x

Garnier, E., Gobin, O., and Poorter, H. (1995). Nitrogen productivity depends on photosynthetic nitrogen use efficiency and on nitrogen allocation within the plant. *Ann Bot*, 76 (6), 667–672. doi: 10.1006/anbo.1995.1145

Grassi, G., and Magnani, F. (2005). Stomatal, mesophyll conductance and biochemical limitations to photosynthesis as affected by drought and leaf ontogeny in ash and oak trees. *Plant Cell Environ.* 28, 834–849. doi: 10.1111/j.1365-3040.2005.01333.x

Guan, L.-L., and Wen, D.-Z. (2011). More nitrogen partition in structural proteins and decreased photosynthetic nitrogen-use efficiency of *Pinus massoniana* under *in situ* polluted stress. *J. Plant Res.* 124, 663–673. doi: 10.1007/s10265-011-0405-2

Harley, P. C., Loreto, F., Di Marco, G., and Sharkey, T. D. (1992). Theoretical considerations when estimating the mesophyll conductance to CO_2 flux by analysis of the response of photosynthesis to CO_2. *Plant Physiol.* 98, 1429–1436. doi: 10.1104/pp.98.4.1429

Harrison, M. T., Edwards, E. J., Farquhar, G. D., Nicotra, A. B., and Evans, J. R. (2009). Nitrogen in cell walls of sclerophyllous leaves accounts for little of the variation in photosynthetic nitrogen-use efficiency. *Plant Cell Environ.* 32, 259–270. doi: 10.1111/j.1365-3040.2008.01918.x

Hikosaka, K., and Shigeno, A. (2009). The role of rubisco and cell walls in the interspecific variation in photosynthetic capacity. *Oecologia* 160, 443–451. doi: 10.1007/s00442-009-1315-z

Hou, W., Tränkner, M., Lu, J., Yan, J., Huang, S., Ren, T., et al. (2019). Interactive effects of nitrogen and potassium on photosynthesis and photosynthetic nitrogen allocation of rice leaves. *BMC Plant Biol.* 19, 1–13. doi: 10.1186/s12870-019-1894-8

Hu, W., Ren, T., Meng, F., Cong, R., Li, X., White, P. J., et al. (2019). Leaf photosynthetic capacity is regulated by the interaction of nitrogen and potassium through coordination of CO_2 diffusion and carboxylation. *Physiologia Plantarum* 167, 418–432. doi: 10.1111/ppl.12919

Lassaletta, L., Billen, G., Grizzetti, B., Anglade, J., and Garnier, J. (2014). 50 year trends in nitrogen use efficiency of world cropping systems: the relationship between yield and nitrogen input to cropland. *Environ. Res. Lett.* 9, 105011. doi: 10.1088/1748-9326/9/10/105011

Lehmeier, C. A., Wild, M., and Schnyder, H. (2013). Nitrogen stress affects the turnover and size of nitrogen pools supplying leaf growth in a grass. *Plant Physiol.* 162, 2095–2105. doi: 10.1104/pp.113.219311

Li, Y., Gao, Y., Xu, X., Shen, Q., and Guo, S. (2009). Light-saturated photosynthetic rate in high-nitrogen rice *(Oryza sativa* l.) leaves is related to chloroplastic CO_2 concentration. *J. Exp. Bot.* 60, 2351–2360. doi: 10.1093/jxb/erp127

Li, Y., Ren, B., Ding, L., Shen, Q., Peng, S., and Guo, S. (2013). Does chloroplast size influence photosynthetic nitrogen use efficiency? *PloS One* 8, e62036. doi: 10.1371/journal.pone.0062036

Liu, T., Ren, T., White, P. J., Cong, R., and Lu, J. (2018). Storage nitrogen coordinates leaf expansion and photosynthetic capacity in winter oilseed rape. *J. Exp. Bot.* 69, 2995–3007. doi: 10.1093/jxb/ery134

Liu, J., Zhang, J., Estavillo, G. M., Luo, T., and Hu, L. (2021). Leaf n content regulates the speed of photosynthetic induction under fluctuating light among canola genotypes *(Brassica napus* l.). *Physiologia Plantarum* 172 (4), 1844–1852. doi: 10.1111/ppl.13390

Muir, C. D., Hangarter, R. P., Moyle, L. C., and Davis, P. A. (2014). Morphological and anatomical determinants of mesophyll conductance in wild relatives of tomato *(S olanum sect.* l *ycopersicon, sect.* l ycopersicoides; s olanaceae). *Plant Cell Environ.* 37, 1415–1426. doi: 10.1111/pce.12245

Niinemets, Ü., and Tenhunen, J. (1997). A model separating leaf structural and physiological effects on carbon gain along light gradients for the shade-tolerant species acer saccharum. *Plant Cell Environ.* 20, 845–866. doi: 10.1046/j.1365-3040.1997.d01-133.x

Onoda, Y., Hikosaka, K., and Hirose, T. (2004). Allocation of nitrogen to cell walls decreases photosynthetic nitrogen-use efficiency. *Funct. Ecol.*, 419–425. doi: 10.1111/j.0269-8463.2004.00847.x

Onoda, Y., Wright, I. J., Evans, J. R., Hikosaka, K., Kitajima, K., Niinemets, Ü., et al. (2017). Physiological and structural tradeoffs underlying the leaf economics spectrum. *New Phytol.* 214, 1447–1463. doi: 10.1111/nph.14496

Poorter, H., and Evans, J. R. (1998). Photosynthetic nitrogen-use efficiency of species that differ inherently in specific leaf area. *Oecologia* 116, 26–37. doi: 10.1007/s004420050560

R Core Team (2020). *R: a language and environment for statistical computing* (Vienna: R Foundation for Statistical Computing). Available at: https://www.Rproject.org/.

Sun, J., Feng, Z., Leakey, A. D., Zhu, X., Bernacchi, C. J., and Ort, D. R. (2014). Inconsistency of mesophyll conductance estimate causes the inconsistency for the estimates of maximum rate of rubisco carboxylation among the linear, rectangular and non-rectangular hyperbola biochemical models of leaf photosynthesis–a case study of

CO_2 enrichment and leaf aging effects in soybean. *Plant Sci.* 226, 49–60. doi: 10.1016/j.plantsci.2014.06.015

Takashima, T., Hikosaka, K., and Hirose, T. (2004). Photosynthesis or persistence: nitrogen allocation in leaves of evergreen and deciduous quercus species. *Plant Cell Environ.* 27, 1047–1054. doi: 10.1111/j.1365-3040.2004.01209.x

Terashima, I., Hanba, Y. T., Tholen, D., and Niinemets, Ü. (2011). Leaf functional anatomy in relation to photosynthesis. *Plant Physiol.* 155, 108–116. doi: 10.1104/pp.110.165472

Valentini, R., Epron, D., De Angelis, P., Matteucci, G., and Dreyer, E. (1995). *In situ* Estimation of net CO_2 assimilation, photosynthetic electron flow and photorespiration in Turkey oak *(Q. cerris* l.) leaves: diurnal cycles under different levels of water supply. *Plant Cell Environ.* 18, 631–640. doi: 10.1111/j.1365-3040.1995.tb00564.x

Veres, S., Malik, A. I., and Rengel, Z. (2017). Differential nitrogen supply causes large variability in photosynthetic traits in wheat germplasm. *Crop Pasture Sci.* 68, 703–712. doi: 10.1071/CP17126

von Caemmerer, S., and Evans, J. R. (2010). Enhancing C_3 photosynthesis. *Plant Physiol.* 154, 589–592. doi: 10.1104/pp.110.160952

Xiong, D., Chen, J., Yu, T., Gao, W., Ling, X., Li, Y., et al. (2015a). SPAD-based leaf nitrogen estimation is impacted by environmental factors and crop leaf characteristics. *Sci. Rep.* 5, 13389. doi: 10.1038/srep13389

Xiong, D., Liu, X., Liu, L., Douthe, C., Li, Y., Peng, S., et al. (2015b). Rapid responses of mesophyll conductance to changes of CO_2 concentration, temperature and irradiance are affected by n supplements in rice. *Plant Cell Environ.* 38, 2541–2550. doi: 10.1111/pce.12558

Xiong, D., Yu, T., Zhang, T., Li, Y., Peng, S., and Huang, J. (2015c). Leaf hydraulic conductance is coordinated with leaf morpho-anatomical traits and nitrogen status in the genus oryza. *J. Exp. Bot.* 66, 741–748. doi: 10.1093/jxb/eru434

Xu, C., Fisher, R., Wullschleger, S. D., Wilson, C. J., Cai, M., and Mcdowell, N. G. (2012). Toward a mechanistic modeling of nitrogen limitation on vegetation dynamics. *PloS One* 7, e37914. doi: 10.1371/journal.pone.0037914

Yamori, W., Nagai, T., and Makino, A. (2011). The rate-limiting step for CO_2 assimilation at different temperatures is influenced by the leaf nitrogen content in several C_3 crop species. *Plant Cell Environ.* 34, 764–777. doi: 10.1111/j.1365-3040.2011.02280.x

Yamori, W., Noguchi, K. O., and Terashima, I. (2005). Temperature acclimation of photosynthesis in spinach leaves: analyses of photosynthetic components and temperature dependencies of photosynthetic partial reactions. *Plant Cell Environ.* 28 (4), 536–547. doi: 10.1111/j.1365-3040.2004.01299.x

Zhang, Y., Wang, J., Gong, S., Xu, D., and Sui, J. (2017). Nitrogen fertigation effect on photosynthesis, grain yield and water use efficiency of winter wheat. *Agric. Water Manage.* 179, 277–287. doi: 10.1016/j.agwat.2016.08.007

Zhu, K., Wang, A., Wu, J., Yuan, F., Guan, D., Jin, C., et al. (2020). Effects of nitrogen additions on mesophyll and stomatal conductance in Manchurian ash and Mongolian oak. *Sci. Rep.* 10, 10038. doi: 10.1038/s41598-020-66886-x

frontiers | Frontiers in Plant Science

TYPE Original Research
PUBLISHED 12 May 2023
DOI 10.3389/fpls.2023.1153235

Check for updates

OPEN ACCESS

EDITED BY
Jianwei Lu,
Huazhong Agricultural University, China

REVIEWED BY
Narendra Kumar Lenka,
Indian Institute of Soil Science (ICAR), India
Raziel A. Ordonez,
The Pennsylvania State University (PSU),
United States

*CORRESPONDENCE
Yinghua Duan
duanyinghua@caas.cn
Wenju Zhang
zhangwenju01@caas.cn

[†]These authors have contributed equally to this work

RECEIVED 29 January 2023
ACCEPTED 20 April 2023
PUBLISHED 12 May 2023

CITATION
Ren K, Sun Y, Zou H, Li D, Lu C, Duan Y and Zhang W (2023) Effect of replacing synthetic nitrogen fertilizer with animal manure on grain yield and nitrogen use efficiency in China: a meta-analysis. *Front. Plant Sci.* 14:1153235. doi: 10.3389/fpls.2023.1153235

Effect of replacing synthetic nitrogen fertilizer with animal manure on grain yield and nitrogen use efficiency in China: a meta-analysis

Keyu Ren[†], Yue Sun[†], Hongqin Zou, Dejin Li, Changai Lu, Yinghua Duan* and Wenju Zhang*

State Key Laboratory of Efficient Utilization of Arid and Semi-arid Arable Land in Northern China, Institute of Agricultural Resources and Regional Planning, Chinese Academy of Agricultural Sciences, Beijing, China

To reduce reliance on synthetic nitrogen (N) fertilizer and sustain food production, replacing synthetic N fertilizer with animal manure as an effective method is widely used. However, the effects of replacing synthetic N fertilizer with animal manure on crop yield and nitrogen use efficiency (NUE) remain uncertain under varying fertilization management practices, climate conditions, and soil properties. Here, we performed a meta-analysis of wheat (*Triticum aestivum* L.), maize (*Zea mays* L.), and rice (*Oryza sativa* L.) based on 118 published studies conducted in China. Overall, the results indicated that substituting synthetic N fertilizer with manure increased yield by 3.3%–3.9% for the three grain crops and increased NUE by 6.3%–10.0%. Crop yields and NUE did not significantly increase at a low N application rate (≤120 kg ha^{-1}) or high substitution rate (>60%). Yields and NUE values had higher increases for upland crops (wheat and maize) in temperate monsoon climate/temperate continental climate regions with less average annual rainfall (AAR) and lower mean annual temperature (MAT), while rice had higher increases in subtropical monsoon climate regions with more AAR and higher MAT. The effect of manure substitution was better in soil with low organic matter and available phosphorus. Our study shows that the optimal substitution rate was 44% and the total N fertilizer input cannot be less than 161 kg ha^{-1} when substituting synthetic N fertilizer with manure. Moreover, site-specific conditions should also be considered.

KEYWORDS

manure fertilizer, synthetic N fertilizer, crop yield, nitrogen use efficiency, meta-analysis

1 Introduction

Synthetic nitrogen (N) fertilizer is essential to ensure crop yield and quality in intensive agriculture (Zhang et al., 2013; He et al., 2021). In China, synthetic N fertilizer has been heavily applied in agricultural systems for decades in order to achieve a higher yield per unit area to feed 18% of the global population with only 9% of the world's arable land (Ren K. et al., 2022). Even though crop yield has been greatly increased by applying synthetic fertilizer, there is growing evidence that overuse of synthetic N fertilizer has led to large N losses, low N use efficiency (NUE), and substantial environmental risks (e.g., freshwater eutrophication, greenhouse gas emission, and soil acidification) (Guo et al., 2010; Feng et al., 2022; Xu et al., 2022). An overall N surplus of 2.76 × 10^{-3} billion tons (226.9 kg N ha^{-1}) was reported in Chinese croplands (Gu et al., 2017), and crop NUE ranges from 25% to 36% (Ju et al., 2009), which is much lower than that in most developed countries (52%–68%) (Yan et al., 2022). Therefore, management practices to reduce the application of synthetic N fertilizer and alleviate agricultural pollution while ensuring efficient crop production are required.

China, as the largest livestock producer in the world, has abundant livestock manure resources (FAOSTAT, 2018). Zhang et al. (2020) reported that livestock manure N had reached 2.3 × 10^{-3} billion tons in 2010, which is approximately half of its fertilizer N consumption. Regrettably, only 40% of livestock manure N is recycled to cropland (Niu and Ju, 2017). Therefore, replacing synthetic N fertilizer with animal manure in agricultural ecosystems may be an effective management practice to reduce the application of synthetic N fertilizer while maintaining crop yields. Multiple studies have found that manure contains abundant nutrients that are readily absorbed by crops, reducing the reliance on synthetic fertilizer (Wang et al., 2017; Zhang et al., 2020; Hou et al., 2022). Replacing synthetic N fertilizer with manure can increase the input of organic carbon into the soil, which is conducive to stimulating mineral N immobilization, thus reducing N losses from croplands (Xia et al., 2017; Liu et al., 2021). Furthermore, synthetic N fertilizer combined with manure can regulate the synchronization of crop N demand with soil N supply to increase crop yield and NUE (Edmeades, 2003; Chen et al., 2014). However, the effects of manure application on crop yield and NUE can be influenced by management practices, soil properties, and climate conditions (Zavattaro et al., 2017; Du et al., 2020). Thus, the reported effect of substituting fertilizer with manure on crop production is inconsistent in many field studies.

An 8-year field experiment on purple soil in southwest China showed that substituting 50% synthetic N with manure increased maize yield by 13.5% and 12.5% compared with full substitution and only synthetic fertilizer, respectively (Xie et al., 2016). However, Liu H. et al. (2017) found that rice yield did not significantly increase (or even decreased) at different manure substitution rates when compared with synthetic fertilizer. Analogously, there are inconsistent results in the published papers about the effect of manure substitution on NUE (Zhou, 2012; Gao et al., 2015; Liu Y. et al., 2017). Thus, it is necessary to further understand the effect of replacing synthetic N fertilizer with manure on crop yield and NUE so that manure can be used more effectively. As a formal statistical technique, a meta-analysis can integrate independent findings focused on the same purpose and conduct a comprehensive quantitative evaluation (Ding et al., 2018). A recent meta-analysis found that applying manure fertilizer could effectively improve soil quality and crop yield compared with applying synthetic fertilizer alone, but the same total N input was not considered (Du et al., 2020). The work by Zhang et al. (2020) comprehensively evaluated the advantages and disadvantages of replacing synthetic N fertilizer with manure in upland and paddy fields but did not fully consider the impact of climate and soil factors. A global-scale meta-analysis regarding the effect of manure substitution on crop productivity and reactive N losses was conducted but did not consider crop types, N application rates, or soil properties (Xia et al., 2017). Up to now, reports on climate conditions or key soil properties are rare, and the major factors that influence the effect of replacing N fertilizer with manure on crop yield and NUE have not been identified in published analyses. Therefore, it is still unclear in which regions (climate, soil) or under which management conditions the effect of substituting N fertilizer with manure is better.

In this study, we performed a comprehensive meta-analysis to integrate published data (118 peer-reviewed papers) from field studies in China on the effect of replacing N fertilizer with manure on grain yield and NUE across three major staple crops (wheat, maize, and rice). The objectives of the study were to 1) determine the effects of substituting N fertilizer with manure on the yields and NUE of three crops, 2) quantitatively analyze the effects of various factors (fertilization management practices, climate conditions, and soil properties), and 3) identify major factors influencing the effect of substituting N fertilizer with manure and analyze the relationships between factors and effect size.

2 Materials and methods

2.1 Data collection

In this study, we used the database of Web of Science (https://www.webofscience.com/wos/alldb/basic-search), Science Direct (https://www.sciencedirect.com/), or China National Knowledge Infrastructure (http://www.cnki.net/) to search for peer-reviewed literature published until 2018. Some keywords were set to perform the search (i.e., manure, grain yield, crop N uptake, and NUE). Meanwhile, we used the following criteria to screen the literature:

i) Trials on wheat, maize, or rice were conducted in Chinese fields.

ii) The literature must include both a control using only synthetic N fertilizer (in which the application rates of P and K can meet crop growth, NPK) and a treatment using manure to completely or partially replace synthetic N fertilizer (NPKM). The total N input of the NPKM treatment must be consistent with that of the NPK treatment.

iii) Treatments needed to have no less than three replicates within an experimental design.

iv) Crop yield, total aboveground N uptake, or NUE had to be reported. The total aboveground N uptake was used to calculate NUE if it was not reported in the studies (Duan et al., 2014):

$$NUE = \frac{N_t - N_0}{F_t} \times 100\,\% \tag{1}$$

where N_t and N_0 are the total aboveground N uptake from treatments with N input and without N input, respectively. F_t is the total N input.

A total of 118 peer-reviewed studies were extracted, including 31 studies on wheat, 53 studies on maize, and 49 studies on rice (Figure 1). Some studies included two or more crops. In addition, information on geographical locations, climatic variables [climate type, average annual rainfall (AAR), mean annual temperature (MAT), annual sunshine duration (ASD), and frost-free period (FFP)] for each experiment site, soil properties from a depth of 0 to 20 cm of soil layer [soil organic matter (SOM), soil total nitrogen (TN), soil alkali nitrogen (AN), soil available phosphorus (AP), soil available potassium (AK), and soil pH] in the treatment plots, and the N application rate of manure and synthetic N fertilizer was collected and used for the subgroup analysis.

2.2 Evaluated variables and grouping

To evaluate the effects of manure substitution on yield and NUE under different factors, each variable was further divided into subgroups. The N application rates (NR) were grouped into four levels (Yu and Shi, 2015): low (≤120 kg ha^{-1}), moderate (120–240 kg ha^{-1}), high (240–360 kg ha^{-1}), and overuse (>360 kg ha^{-1}). There were three substitution rate (SR) groups (Zhang et al., 2020; Ren F. et al., 2022):<30%, 30%–60%, and >60%. Based on climatic conditions and cropping system, the study areas were divided into three climatic regions (Wang et al., 2013): temperate monsoon climate (NTM), temperate continental climate (NTC), and subtropical monsoon climate (STM). The AAR (Shang et al., 2001), MAT (Fang et al., 2016), ASD (Li et al., 2013), and FFP (Ning et al., 2015) were all grouped into low, moderate, and high levels. The soil nutrient indices were also divided into three levels referring to the "Soil Nutrient Classification Standards" developed by the National Soil Census Office (1998) for a second soil survey in China. Soil pH was categorized into four groups [strongly acidic soils (≤5.5); acidic soils (5.5–6.5); neutral soils (6.5–7.5); alkaline soils (>7.5)]. The specific groups of each variable are shown in Table 1.

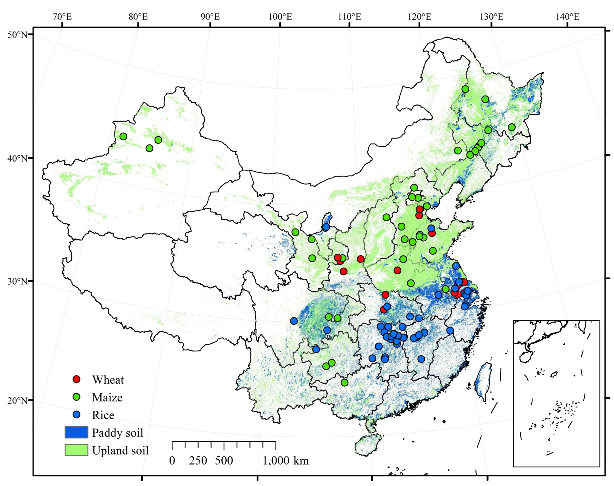

FIGURE 1
Location of the study sites included in this meta-analysis.

2.3 Data analysis

In this study, the effect size is used to quantitatively evaluate the effects of replacing synthetic N fertilizer with manure on crop yield and NUE, and it is calculated as the natural logarithm of the response ratio (RR) of NPK and NPKM treatments (Hedges and Curtis, 1999):

$$RR = \ln \frac{\bar{X}_{NPK}}{\bar{X}_{NPKM}} \tag{2}$$

where $\bar{X}_{NPK}$ and $\bar{X}_{NPKM}$ represent the mean yield (or NUE) of the NPK and NPKM treatments.

We used the equation $(e^{RR_{++}} - 1) \times 100\,\%$ to calculate the percentage of change in yield (or NUE) from the NPKM treatment compared with the NPK treatment (Ren F. et al., 2022), where RR_{++} is calculated as follows:

$$RR_{++} = \frac{\sum_{i=1}^{m}\sum_{j=1}^{ki} w_{ij}RR_{ij}}{\sum_{i=1}^{m}\sum_{j=1}^{ki} w_{ij}} \tag{3}$$

where m and ki represent the number of groups for a given variable (e.g., SR or AAR) and the number of comparisons between the NPKM treatment and the NPK treatment at the i-th group, respectively. RR_{ij} and W_{ij} represent the RR and weighted factor for the i-th group and the j-th pair, respectively. W_{ij} is calculated as:

$$w_{ij} = \frac{1}{v} \tag{4}$$

where v is a variance:

$$v = \frac{SD_{NPKM}^2}{n_{NPKM}\bar{X}_{NPKM}^2} + \frac{SD_{NPK}^2}{n_{NPK}\bar{X}_{NPK}^2} \tag{5}$$

where SD_{NPKM} and n_{NPKM} represent the standard deviation and the number of samples in the NPKM treatment, respectively, and SD_{NPK} and n_{NPK} represent the standard deviation and the number of samples in the NPK treatment, respectively.

The 95% confidence interval (CI) of RR_{++} is used to evaluate whether the effects of replacing synthetic N fertilizer with manure on crop yield (or NUE) are significant, and it was calculated as follows:

$$\mathrm{CI} = RR_{++} \pm 1.96S(RR_{++}) \tag{6}$$

$$S(RR_{++}) = \sqrt{\frac{1}{\sum_{i=1}^{m}\sum_{j=1}^{ki} w_{ij}}} \tag{7}$$

where $S(RR_{++})$ represents the standard error of RR_{++}.

TABLE 1 Grouping of each variable tested for significance as predictors in yield and NUE response in the meta-analysis.

Variables	Groups
Crop type	Wheat, maize, rice
N application rate (NR, kg N ha^{-1})	≤120, 120–240, 240–360, >360
Substitution rate (SR, %)	≤30, 30–60, >60
Climate type	Temperate monsoon climate (NTM), temperate continental climate (NTC), subtropical monsoon climate (STM)
Average annual rainfall (AAR, mm)	≤600, 600–1,200, >1,200
Mean annual temperature (MAT, °C)	≤12, 12–16, >16
Annual sunshine duration (ASD, h)	≤2,200, 2,200–2,600, >2,600
Frost-free period (FFP, days)	≤175, 175–250, >250
Soil organic matter (SOM, g kg^{-1})	≤20, 20–30, >30
Soil total nitrogen content (TN, g kg^{-1})	≤1, 1–1.5, >1.5
Soil alkali nitrogen content (AN, mg kg^{-1})	≤60, 60–120, >120
Soil available phosphorus content (AP, mg kg^{-1})	≤10, 10–20, >20
Soil available potassium content (AK, mg kg^{-1})	≤175, 175–250, >250
Soil pH	≤5.5, 5.5–6.5, 6.5–7.5, >7.5

In this study, if the 95% CI for yield (or NUE) overlaps with zero, we consider that manure substitution has no significant effect on yield (or NUE) compared with the NPK treatment (P > 0.05). Conversely, we consider that it has a significant effect (P< 0.05). The meta-analysis was performed by using the MetaWin 2.1 software (Rosenberg et al., 2000).

To explore the major factors affecting the effect of manure substitution, the random forest (RF) algorithm was used to investigate the importance of each variable to effect size. A higher mean squared error for percentage increase [MSE increase (%)] means a more important variable. The RF algorithm was run using the "RandomForest" package in R (version 3.3.3). In addition, we used linear and non-linear regression analyses (at P< 0.01) to assess the influence of the top three factors of MSE increase (%) on the effect sizes of yield and NUE (Hou et al., 2022). Microsoft Office Excel 2019 and ArcGIS 10.6 were used for data processing, and SPSS 21.0 was used for statistical analysis.

3 Results

3.1 Overall effects of substituting fertilizer with manure

Overall, the average yields were 5.21, 8.59, and 7.23 t ha^{-1} for wheat, maize, and rice, respectively, under the synthetic N fertilizer only (NPK) treatment, and the average NUE values were 33.6%, 34.5%, and 28.8% (Figures 2A, C, E). After the substitution of fertilizer N with manure (NPKM), the average respective yields were 5.38, 9.00, and 7.50 t ha^{-1} for wheat, maize, and rice, and the average NUE values were 35.6%, 36.9%, and 31.7% (Figures 2A, C, E). The meta-analysis results showed that the NPKM treatment significantly increased yields by 3.3%, 3.8%, and 3.9% for wheat, maize, and rice, respectively, compared with the NPK treatment and significantly increased NUE by 10.0% and 9.2% for maize and rice (Figures 2B, D, E). Although the NUE of wheat increased by 6.3%, there was no significant difference between NPK and NPKM.

3.2 Effects of fertilization management

Figure 3 depicts how field fertilization management influenced the effects of manure substitution on crop yield and NUE. At low N application rates (≤120 kg ha^{-1}), fertilizer substitution with manure did not significantly increase yields or NUE of the three crops. However, the yield significantly increased by 2.7%, 2.9%, and 4.3%, respectively, at moderate N application rates (120–240 kg ha^{-1}) for wheat, maize, and rice. The effect of manure on yield increased with increased N application rate (except for wheat with overuse of N fertilizer). The NUE of wheat did not significantly increase at different N application rates, but there were significant increases by 11.5% and 10.6% at moderate N application rates for maize and rice, respectively. For maize, fertilizer substitution with manure significantly increased NUE by 23.8% with the overuse of N fertilizer.

When the rates of substituting manure for fertilizer were less than 60% (SR ≤ 60%), the yield significantly increased by 3.3%–8.2% and 3.1%–5.2% for maize and rice, respectively, and NUE significantly increased by 13.9%–28.0% and 10.5%–11.6%, but there were no significant effects on wheat yield and NUE. However, at a high SR (>60%), the yield decreased by 3.2% and 5.3%, and NUE significantly decreased by 19.7% and 15.0% for wheat and maize, respectively, while there were no significant effects on rice yield and NUE.

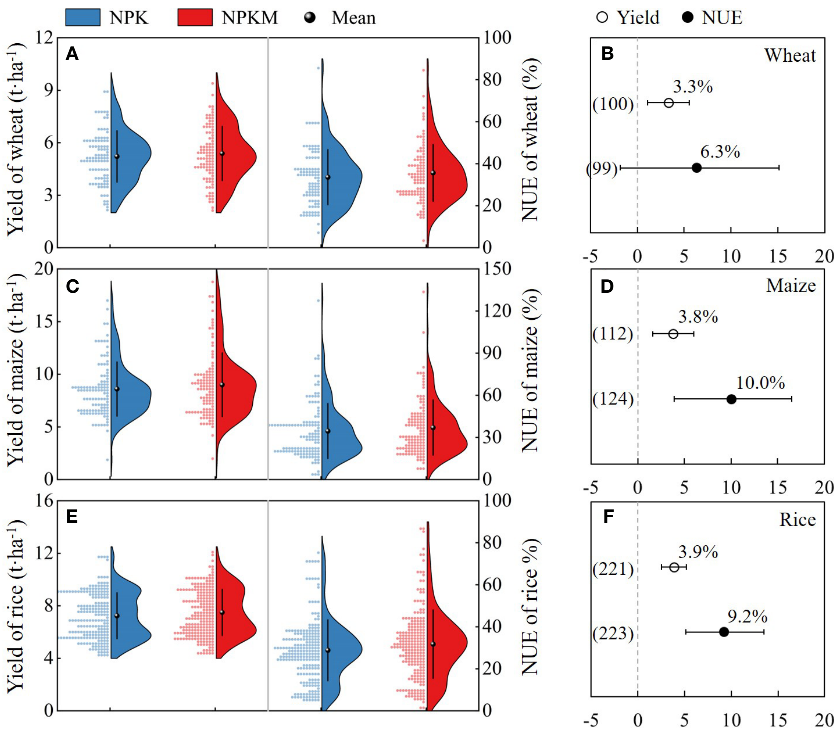

FIGURE 2
Yield and nitrogen use efficiency (NUE) of wheat **(A, B)**, maize **(C, D)**, and rice **(E, F)** in NPK and NPKM treatments. In **(A, C, E)**, curves are kernel-smoothed distributions fitted to frequency data; balls with error bars indicate mean and standard deviation. In **(B, D, F)**, dots with error bars indicate the overall mean response ratio and 95% CI, and numbers in parentheses represent the independent sample size.

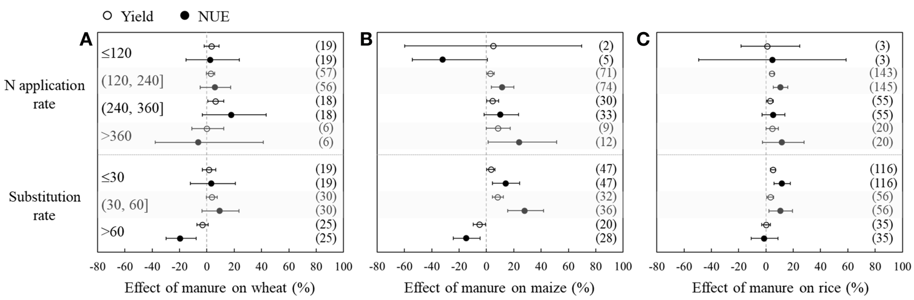

FIGURE 3
Changes in yield (hollow dots) and nitrogen use efficiency (NUE, black dots) after substitution of synthetic nitrogen fertilizer with manure as affected by fertilization management for wheat **(A)**, maize **(B)**, and rice **(C)**. Dots with error bars indicate the overall mean response ratio and 95% CI, and numbers in parentheses represent the independent sample size.

3.3 Effects of climate

The effects of replacing N fertilizer with manure on crop yields and NUE were different under different climate conditions (Figure 4). Yield and NUE significantly increased in the NTM region for wheat, in the NTC region for maize, and in the STM region for rice. Wheat yield and NUE increased by 7.5% and 10.0% by manure application in the regions with AAR ≤600 mm, respectively. In the regions with AAR ≤1,200 mm, maize yield and NUE significantly increased by 4.1%–6.9% and 8.0%–19.2%, respectively. Rice yield and NUE significantly increased in the regions with AAR >600 mm. The yield and NUE were significantly increased in the regions with MAT ≤12°C for wheat and MAT ≤16°C for maize, while rice yield and NUE were significantly increased in the regions with MAT >12°C. The response to manure substitution in wheat, maize, and rice varied in different ASD regions. Wheat yield and NUE significantly increased by 5.7% and 21.3% in the regions with 2200 h< ASD ≤ 2600 h, respectively. In contrast, maize yield and NUE significantly

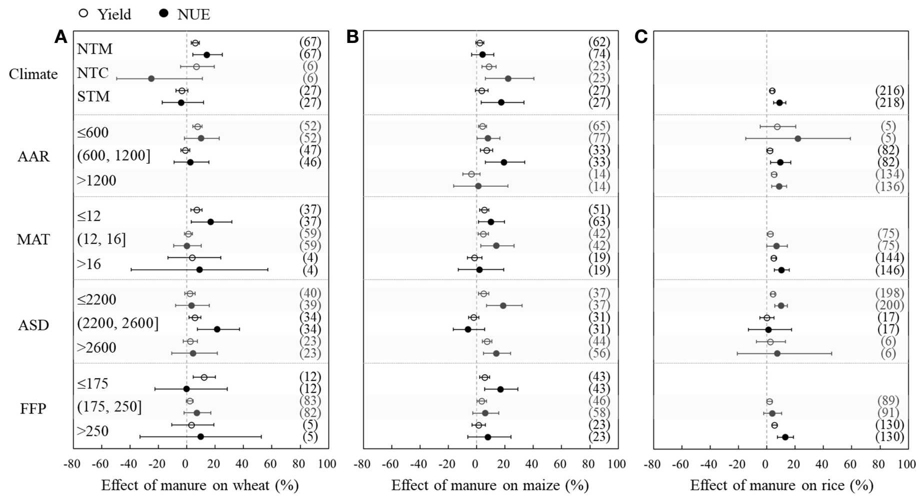

FIGURE 4
Changes in yield (hollow dots) and nitrogen use efficiency (NUE, black dots) after substitution of synthetic nitrogen fertilizer with manure as affected by climate conditions for wheat **(A)**, maize **(B)**, and rice **(C)**. Dots with error bars indicate the overall mean response ratio and 95% CI, and numbers in parentheses represent independent sample size. NTM, temperate monsoon climate; NTC, temperate continental climate; STM, subtropical monsoon climate; AAR, average annual rainfall; MAT, mean annual temperature; ASD, annual sunshine duration; FFP, frost-free period.

increased in the regions with ASD ≤ 2200 h and 2600 h< ASD. Rice yield and NUE significantly increased by 4.2% and 10.0% in the regions with ASD ≤2200 h. In different FFP regions, manure substitution led to an increase in wheat yield and maize NUE only in the regions with FFP ≤175 days, while the maize yield significantly increased in the regions with FFP ≤250 days. For rice, yield and NUE significantly increased in the regions with FFP >250 days.

3.4 Effects of soil properties

The responses of crop yields and NUE to manure substitution were affected by soil properties (Figure 5). At a low SOM (≤20 g kg^{-1}), wheat yield and NUE significantly increased by 3.5% and 10.8%, respectively. However, wheat NUE significantly decreased by 48.5% at SOM >30 g kg^{-1}. For maize, yield and NUE significantly

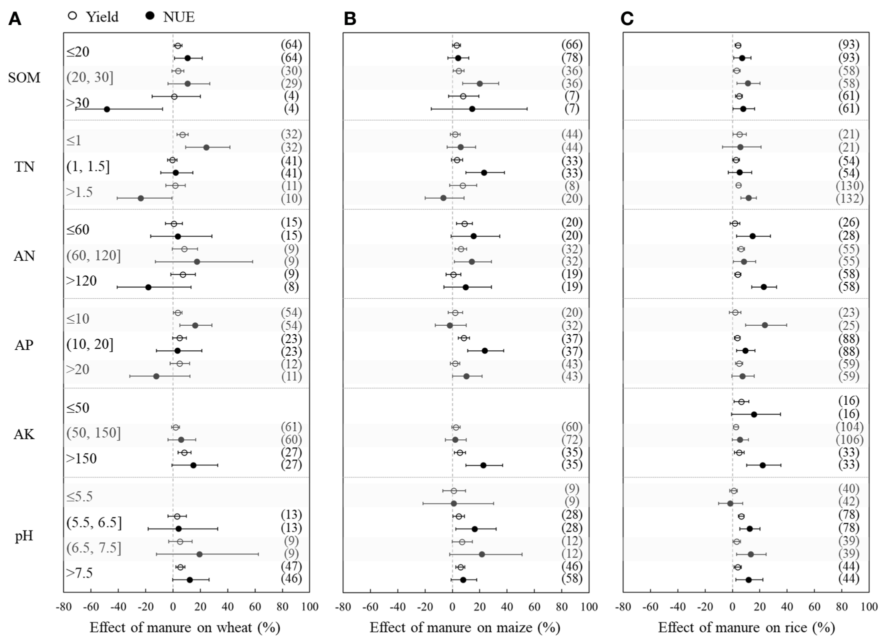

FIGURE 5
Changes in yield (hollow dots) and nitrogen use efficiency (NUE, black dots) after substitution of synthetic nitrogen fertilizer with manure as affected by soil properties for wheat **(A)**, maize **(B)**, and rice **(C)**. Dots with error bars indicate the overall mean response ratio and 95% CI, and numbers in parentheses represent the independent sample size. SOM, soil organic matter; TN, soil total nitrogen; AN, soil alkali nitrogen; AP, soil available phosphorus; AK, soil available potassium; pH, soil pH.

increased at 20 g kg^{-1}< SOM ≤ 30 g kg^{-1}. Rice yield (3.0%–4.8%) and NUE (7.1%–11.4%) significantly increased under different SOM contents. The responses of NUE for the three crops to the substitution of N fertilizer with manure varied for different TN contents. The NUE of wheat significantly increased at TN ≤1 g kg^{-1}, while it significantly decreased at TN >1.5 g kg^{-1}. The NUE of maize and rice significantly increased only at 1 g kg^{-1}< TN ≤ 1.5 g kg^{-1} and TN > 1.5 g kg^{-1}, respectively. The yield and NUE of wheat had no significant variations with different AN contents, whereas there were significant increases at 60 mg kg^{-1}< AN ≤ 120 mg kg^{-1} for maize and significant increases at AN >60 mg kg^{-1} for rice. At different AP content levels, the NUE values of wheat (16.1%) and rice (23.8%) had the highest increases at AP ≤10 mg kg^{-1}, while maize (23.7%) had the highest increase at 10 ≤ AP< 20 mg kg^{-1}. In contrast, the yield and NUE of all three crops significantly increased at high AK content (AK > 250 mg kg^{-1}). The substitution of fertilizer with manure had no significant influence on crop yields and NUE in strongly acidic soils (pH ≤ 5.5) (there were insufficient data on wheat) but significantly increased crop yields (wheat: 5.3%, maize: 5.8%, rice: 3.8%) in alkaline soils (pH > 7.5). Furthermore, maize yield (4.6%) and NUE (16.3%) significantly increased in acidic soils (5.5< pH ≤ 6.5). For rice, except in strongly acidic soils, substituting manure for fertilizer significantly increased yield and NUE by 3.1%–6.5% and 11.9%–13.3%, respectively.

3.5 Main factors influencing the effect of substituting N fertilizer with manure

Figure 6 depicts the importance of variables and correlations between the major factors and the effect size of substituting N fertilizer with manure on yield and NUE. Overall, SR, NR, and SOM were the most important factors for yield. When the substitution rate was 44%, yield had the highest increase (5.6%). The effect of manure on yield was positively correlated with NR but negatively correlated with SOM. The importance of variables on NUE was different from those on yield. NR, AN, and AP were the most important factors for NUE. When the NR >161 kg ha^{-1}, the manure substitution had a positive effect on NUE. Furthermore, the effect of manure on NUE increased with the increase of AN, while it decreased with the increase of AP.

4 Discussion

4.1 Responses of crop yield and NUE to N fertilizer substitution with manure

Overall, our meta-analysis indicates that replacing synthetic N fertilizer with manure increased crop yields and NUE by 3.3%–3.9% and 6.3%–9.2%, respectively (Figure 2). Xia et al. (2017) showed that manure substitution increased yields and NUE of grain crops by 5.2% and 10.4%, respectively, based on a global-scale meta-analysis. This suggests that the effect of manure substitution on crop production in China is basically consistent with that in other countries. The application of manure can increase the synchronization of nutrient supply, improve soil properties, and provide extra nutrients. First, the application of manure can increase the microbial immobilization for N owing to the organic carbon supply and then release more evenly throughout the crop growing season (Choi et al., 2001; Ren F. et al., 2019). Second, the input of manure fertilizer can improve soil aggregate structure, soil

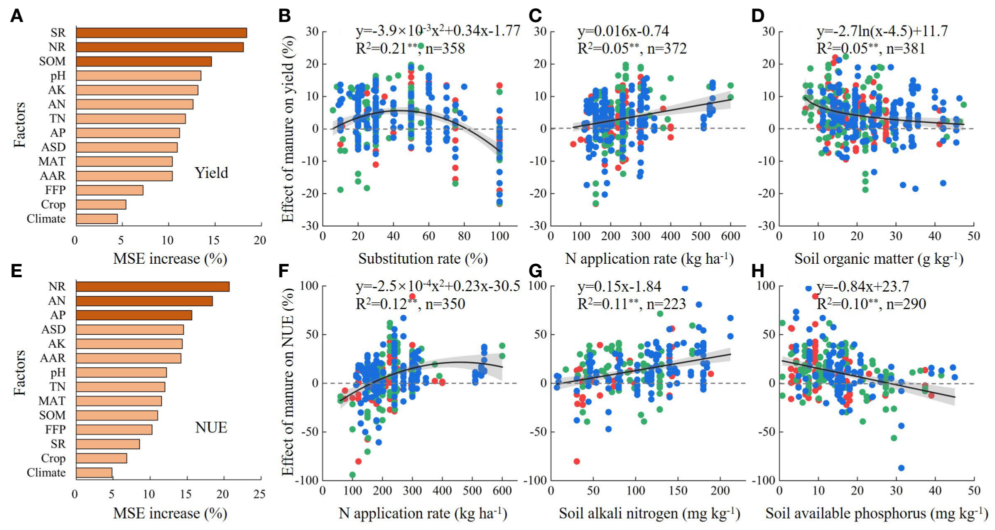

FIGURE 6
Major factors influencing the effect of substituting synthetic nitrogen fertilizer with manure on yields **(A–D)** and nitrogen use efficiency (NUE) **(E–H)**. The importance of each factor was determined based on mean squared error (MSE) for percentage increase by using random forest models **(A, E)**. Different crop types are indicated by different colors in **(B–D, F–H)**: red = wheat, green = maize, blue = rice. R^2, coefficient of determination; ** represents significance (*P*< 0.01); *n*, number of observations; NR, N application rate; SR, synthetic N fertilizer substitution rate; SOM, soil organic matter; TN, soil total nitrogen; AN, soil alkali nitrogen; AP, soil available phosphorus; AK, soil available potassium; pH, soil pH; AAR, average annual rainfall; MAT, mean annual temperature; ASD, annual sunshine duration; FFP, frost-free period.

water-holding capacity, and microbial activity, thus providing a more favorable soil environment for crop growth (Liu et al., 2010; Zhang et al., 2016). Third, manure fertilizer also provides additional essential micronutrients and nutrients (e.g., copper, zinc fatty acids, proteins, and polysaccharides), which also facilitate the improvement of crop yield and NUE (Hou et al., 2022).

However, crop yields and NUE decreased (or showed no significant effect for rice) when the substitution rate was more than 60% (Figure 3), and these results are consistent with recent studies (Xia et al., 2017; Zhang et al., 2020). This likely occurred because the high manure substitution rate does not provide sufficient N for early crop growth because manure N needs a longer time to mineralize than synthetic N fertilizer (Zhou et al., 2016). Similarly, crop yields and NUE did not significantly increase (and even decreased for maize NUE) at N application rates less than 120 kg ha^{-1} (Figure 3), which is also due to the insufficient and untimely supply of synthetic N for crop growth following substitution of synthetic N fertilizer with manure. Therefore, it is extremely important to ensure the optimal substitution rate by balancing the application rate of manure and synthetic N fertilizer.

4.2 Effects of climate and soil factors on manure substitution

This study also explored the impact of climate conditions and soil properties on the effects of manure substitution (Figures 4, 5). From the perspective of climate factors, relatively higher increases for wheat and maize were observed in the NTM/NTC climate regions with less AAR and lower MAT (Figures 4A, B). This is likely because manure was able to exert its heat preservation and water retention properties and stimulate the activity of microorganisms in the soil, to promote the absorption of nutrients by crops in these regions (Kallenbach and Grandy, 2011; Ma, 2018). In addition, the autotrophic nitrification rate is higher in arid climates, and organic N is more easily transformed into $NO_3^- - N$, which wheat and maize prefer to absorb (Zhang et al., 2011; Zhang et al., 2018). Previous studies also showed that organic fertilizer significantly improves wheat yield and NUE in drought years (Ma, 2018). However, a relatively higher increase for rice was observed in the STM climate regions with more AAR and higher MAT (Figure 4C). In these regions, synthetic N was lost more easily, while substituting synthetic N fertilizer with manure can slowly release nutrients required by rice (Wang et al., 2015). Moreover, organic N is more easily transformed into $NH_4^+ - N$, which rice prefers to absorb in humid climate conditions (Cheng et al., 2019).

In general, the positive effects of substituting synthetic N fertilizer with manure on yield and NUE were relatively high in low soil nutrient conditions (SOM, TN, and AP, Figure 5) because the crop yields and NUE were already high with only synthetic N fertilizer in high fertility soil, while the space for further improvement is lower. In contrast, the C source and other nutrients are provided by manure in a more timely and more effective way in low-fertility soil, which can improve soil fertility and promote nutrient absorption in crops (Du et al., 2020). However, yield and NUE did not significantly increase in low AN soil, which may have the same explanation as for the N fertilizer application rate (Zhou et al., 2016). Crop yield and NUE significantly increased in high AK soil, because manure application can alleviate the competitive effect of K^+ and NH_4^+ when crops absorb nutrients (Ren K. et al., 2019). Furthermore, the crop yields and NUE had no significant difference on the soil at pH ≤5.5 in this study, which may indicate that applying manure fertilizer on strongly acidic soil cannot completely improve crop production and that lime and other soil amendments are also needed (Guo et al., 2010).

4.3 Driving factors and recommendations for substituting N fertilizer with manure in grain crops

The results of the random forest model analysis showed that fertilization management (N application and substitution rate) and soil factors (SOM, AN, and AP) were the main factors influencing the effect of manure substitution (Figure 6), which is basically consistent with a recent study in paddy fields reported by Hou et al. (2022). Overall, our meta-analysis indicates that substituting synthetic N fertilizer with manure has great potential for improving crop production in China. However, manure substitution in field production needs site-specific strategies to effectively address the impacts of climate factors and soil properties on crop yield and NUE. The reasonable range of substitution rates was 6%–82% and the optimal substitution rate was 44%. The total N fertilizer input cannot be less than 161 kg ha^{-1} when substituting synthetic N fertilizer with manure. From the perspective of crop yields and NUE, the measures of substituting fertilizer with manure can achieve better effects in regions with low SOM and AP than in regions with high AN.

4.4 Limitations and uncertainties of the analysis

In this study, the effects of fertilization management practices (NR, SR), climate conditions, and soil properties on yield and NUE of three grain crops (wheat, maize, and rice) were analyzed independently. In fact, they might have interactions, but these were not analyzed due to the lack of data. The effect of manure substitution on yield and NUE is different under different experimental durations because continuous manure application will improve soil structure and fertility over time (Duan et al., 2014). However, experimental durations were not considered in our work, which may cause some uncertainties. In addition, the influencing factors of yield and NUE may be different between wheat, maize, and rice, and each crop needs to be evaluated separately.

5 Conclusion

In this study, we performed a meta-analysis to determine the effects of replacing synthetic N fertilizer with manure on crop yield and NUE in China. Substituting synthetic N fertilizer with manure significantly increased yield by 3.3%–3.9% for three grain crops and increased NUE by 6.3%–10.0%. The effect of manure substitution varied under different fertilization management practices, climate conditions, and soil properties. The optimal substitution rate was 44% in practice, and the total N fertilizer input cannot be less than 161 kg ha^{-1} when substituting synthetic N fertilizer with manure. In regions with low soil fertility, the strategy of substituting fertilizer with manure should be considered to improve crop production.

Data availability statement

The original contributions presented in the study are included in the article/supplementary material. Further inquiries can be directed to the corresponding authors.

Author contributions

YD designed the research. YS, HZ, and DL provided help with data collection. KR analyzed the data and wrote the manuscript. YD, WZ, and CL revised the manuscript. All authors contributed to the article and approved the submitted version.

Funding

This study was supported by the National Key Research and Development Program of China (2022YFD1500301, 2021YFD1900300) and the National Natural Science Foundation of China (42077098).

Conflict of interest

The authors declare that the research was conducted in the absence of any commercial or financial relationships that could be construed as a potential conflict of interest.

Publisher's note

All claims expressed in this article are solely those of the authors and do not necessarily represent those of their affiliated organizations, or those of the publisher, the editors and the reviewers. Any product that may be evaluated in this article, or claim that may be made by its manufacturer, is not guaranteed or endorsed by the publisher.

References

Chen, Z., Ding, W., Luo, Y., Yu, H., Xu, Y., Müller, C., et al. (2014). Nitrous oxide emissions from cultivated black soil: a case study in northeast China and global estimates using empirical model. *Global Biogeochem. Cycles* 28, 1311–1326. doi: 10.1002/2014GB004871

Cheng, Y., Zhang, J., and Cai, Z. (2019). Key role of matching of crop-specific n preference, soil n transformation and climate conditions in soil n nutrient management. *Acta Pedologica Sin.* 56, 507–515. doi: 10.11766/trxb201812030523

Choi, W., Jin, S., Lee, S., Ro, H., and Yoo, S. (2001). Corn uptake and microbial immobilization of ^{15}N-labeled urea-n in soil as affected by composted pig manure. *Plant Soil* 235, 1–9. doi: 10.1023/A:1011896912888

Ding, W., Xu, X., He, P., Ullah, S., Zhang, J., Cui, Z., et al. (2018). Improving yield and nitrogen use efficiency through alternative fertilization options for rice in China: a meta-analysis. *Field Crop Res.* 227, 11–18. doi: 10.1016/j.fcr.2018.08.001

Du, Y., Cui, B., Zhang, Q., Wang, Z., Sun, J., and Niu, W. (2020). Effects of manure fertilizer on crop yield and soil properties in China: a meta-analysis. *Catena* 193, 104617. doi: 10.1016/j.catena.2020.104617

Duan, Y., Xu, M., Gao, S., Yang, X., Huang, S., Liu, H., et al. (2014). Nitrogen use efficiency in a wheat-corn cropping system from 15 years of manure and fertilizer applications. *Field Crops Res.* 157, 47–56. doi: 10.1016/j.fcr.2013.12.012

Edmeades, D. C. (2003). The long-term effects of manures and fertilisers on soil productivity and quality: a review. *Nutr. Cycling Agroecosyst.* 66, 165–180. doi: 10.1023/A:1023999816690

Fang, X., Cai, B., and Zheng, S. (2016). Research progress and prospect of annual mean temperature and winter mean temperature in China. *J. Anhui Agric. Sci.* 12, 153–154. doi: 10.13989/j.cnki.0517-6611.2016.12.050

FAOSTAT (2018). *FAOSTAT database collections* (Rome: Food and Agriculture Organization of the United Nations). Available at: http://faostat.fao.org/.

Feng, S., Xu, W., Cheng, M., Ma, Y., Wu, L., Kang, J., et al. (2022). Overlooked nonagricultural and wintertime agricultural NH_3 emissions in quzhou county, north China plain: evidence from ^{15}N-stable isotopes. *Environ. Sci. Technol. Lett.* 9, 127–133. doi: 10.1021/acs.estlett.1c00935

Gao, H., Zhu, P., Peng, C., Zhang, X., Li, Q., and Zhang, W. (2015). Effects of partially replacement of inorganic n with organic materials on nitrogen efficiency of spring maize and soil inorganic nitrogen content under the same n input. *Plant Nutr. Fer. Sci.* 21, 318–325. doi: 10.11674/zwyf.2015.0205

Gu, B., Ju, X., Chang, S., Ge, Y., and Chang, J. (2017). Nitrogen use efficiencies in Chinese agricultural systems and implications for food security and environmental protection. *Reg. Environ. Change* 17, 1217–1227. doi: 10.1007/s10113-016-1101-5

Guo, J., Liu, X., Zhang, Y., Shen, J., Han, W., Zhang, W., et al. (2010). Significant acidification in major Chinese croplands. *Science* 327, 1008–1010. doi: 10.1126/science.1182570

He, G., Liu, X., and Cui, Z. (2021). Achieving global food security by focusing on nitrogen efficiency potentials and local production. *Glob. Food Secur.* 29, 100536. doi: 10.1016/j.gfs.2021.100536

Hedges, L. V., and Curtis, G. P. S. (1999). The meta-analysis of response ratios in experimental ecology. *Ecology* 80, 1150–1156. doi: 10.1890/0012-9658(1999)080[1150:TMAORR]2.0.CO;2

Hou, Q., Ni, Y., Huang, S., Zuo, T., Wang, J., and Ni, W. (2022). Effects substituting chemical fertilizers with manure on rice yield and soil labile nitrogen in paddy fields of China: a meta-analysis. *Pedosphere* 33, 172–184. doi: 10.1016/j.pedsph.2022.09.003

Ju, X., Xing, G., Chen, X., Zhang, S., Zhang, L., Liu, X., et al. (2009). Reducing environmental risk by improving n management in intensive Chinese agricultural systems. *Proc. Natl. Acad. Sci. USA* 106, 3041–3046. doi: 10.1073/pnas.0813417106

Kallenbach, C., and Grandy, A. S. (2011). Controls over soil microbial biomass responses to carbon amendments in agricultural systems: a meta-analysis. *Agr. Ecosyst. Environ.* 144, 241–252. doi: 10.1016/j.agee.2011.08.020

Li, H., Fu, Z., Wen, X., and Huang, J. (2013). Characteristic analysis of sunshine duration change in China during the last 50 years. *Climatic Environ. Res.* 18, 203–209. doi: 10.3878/j.issn.1006-9585.2012.11052

Liu, H., Jiang, H., Sun, G., Shen, M., Chen, L., and Zheng, J. (2017). Effect of different organic-inorganic fertilizers combination ratio on nitrogen use efficiency of rice. *China Soils Fert.* 5, 61–66. doi: 10.11838/sfsc.20170511

Liu, Y., Li, Y., Zhang, Y., Zhang, W., and Jiang, T. (2017). The dynamic of crop yield and nitrogen use efficiency under different long-term fertilization patterns in paddy soil from yellow earth in southwest China. *China Soils Fert.* 3, 20–27. doi: 10.11838/sfsc.20170305

Liu, B., Wang, X., Ma, L., Chadwick, D., and Chen, X. (2021). Combined applications of organic and synthetic nitrogen fertilizers for improving crop yield and reducing reactive nitrogen losses from china's vegetable systems: a meta-analysis. *Environ. pollut.* 269, 116143. doi: 10.1016/j.envpol.2020.116143

Liu, E., Yan, C., Mei, X., He, W., Bing, S., Ding, L., et al. (2010). Long-term effect of chemical fertilizer, straw, and manure on soil chemical and biological properties in northwest China. *Geoderma* 158, 173–180. doi: 10.1016/j.geoderma.2010.04.029

Ma, C. (2018). *Effects of combined application of inorganic fertilizer and organic manure on nitrogen fertilization rate wheat grain yield and soil environment on the loess plateau dryland* (Yangling: Northwest Agricultural and Forestry University). Available at: https://kns.cnki.net/kcms/detail/detail.aspx?dbcode=CMFD&dbname=CMFD201802&filename=1018955608.nh&uniplatform=NZKPT&v=PQLa_R2wKcsJo9D39RzkUiOHPTJyROar2Xn9mxQxK-KM5Dhv5HxRyaUSlSxKLB0O.

National Soil Census Office (1998). *China Soil* (Beijing: China Agriculture Press).

Ning, X., Zhang, L., Yang, Q., and Qin, Y. (2015). Trends in the frost-free period in China from 1951 to 2012. *Acta Geogr. Sin.* 70, 1811–1822. doi: 10.11821/dlxb201511010

Niu, X., and Ju, X. (2017). Organic fertilizer resources and utilization in China. *J. Plant Nutr. Fer.* 23, 1462–1479. doi: 10.11674/zwyf.17430

Ren, K., Duan, Y., Xu, M., and Zhang, X. (2019). Effect of manure application on nitrogen use efficiency of crops in China: a meta-analysis. *Sci. Agric. Sin.* 52, 2983–2996. doi: 10.3864/j.issn.0578-1752.2019.17.007

Ren, F., Sun, N., Misselbrook, T., Wu, L., Xu, M., Zhang, F., et al. (2022). Responses of crop productivity and reactive nitrogen losses to the application of animal manure to china's main crops: a meta-analysis. *Sci. Total Environ.* 850, 158064. doi: 10.1016/j.scitotenv.2022.158064

Ren, F., Sun, N., Xu, M., Zhang, X., Wu, L., and Xu, M. (2019). Changes in soil microbial biomass with manure application in cropping systems: a meta-analysis. *Soil Tillage Res.* 194, 104291. doi: 10.1016/j.still.2019.06.008

Ren, K., Xu, M., Li, R., Zheng, L., Liu, S., Reis, S., et al. (2022). Optimizing nitrogen fertilizer use for more grain and less pollution. *J. Clean. Prod.* 360, 132180. doi: 10.1016/j.jclepro.2022.132180

Rosenberg, M. S., Adams, D. C., and Curevitch, J. (2000). *MetaWin: statistical software for meta-analysis* (Sunderland, MA, USA: Sinauer Associates).

Shang, Z., Gao, Q., and Yang, D. (2001). Spatial pattern analysis of annual precipitation with climate information system of China. *Acta Ecol. Sin.* 21, 689–693.

Wang, Y., Hu, N., Ge, T. D., Kuzyakov, Y., Wang, Z., Li, Z., et al. (2017). Soil aggregation regulates distributions of carbon, microbial community and enzyme activities after 23-year manure amendment. *Appl. Soil Ecol.* 111, 65–72. doi: 10.1016/j.apsoil.2016.11.015

Wang, G., Luo, Z., Wang, E., and Huang, Y. (2013). Contrasting effects of agricultural management on soil organic carbon balance in different agricultural regions of China. *Pedosphere* 23, 717–728. doi: 10.1016/S1002-0160(13)60064-8

Wang, J., Zhu, B., Zhang, J., Müller, C., and Cai, Z. (2015). Mechanisms of soil n dynamics following long-term application of organic fertilizers to subtropical rain-fed purple soil in China. *Soil Biol. Biochem.* 91, 222–231. doi: 10.1016/j.soilbio.2015.08.039

Xia, L., Lam, S. K., Yan, X., and Chen, D. (2017). How does recycling of livestock manure in agroecosystems affect crop productivity, reactive nitrogen losses, and soil carbon balance? *Environ. Sci. Technol.* 51, 7450–7457. doi: 10.1021/acs.est.6b06470

Xie, J., Zhao, Y., Chen, X., Li, D., Xu, C., Wang, K., et al. (2016). Nitrogen of organic manure replacing chemical nitrogenous fertilizer improve maize yield and nitrogen uptake and utilization efficiency. *Sci. Agric. Sin.* 49, 3934–3943. doi: 10.3864/j.issn.0578-1752.2016.20.008

Xu, W., Zhao, Y., Wen, Z., Chang, Y., Pan, Y., Sun, Y., et al. (2022). Increasing importance of ammonia emission abatement in PM2.5 pollution control. *Sci. Bull.* 67, 1745–1749. doi: 10.1016/j.scib.2022.07.021

Yan, X., Xia, L., and Ti, c. (2022). Temporal and spatial variations in nitrogen use efficiency of crop production in China. *Environ. pollut.* 293, 118496. doi: 10.1016/j.envpol.2021.118496

Yu, F., and Shi, W. (2015). Nitrogen use efficiencies of major grain crops in China in recent 10 years. *Acta Pedol. Sin.* 52, 1311–1324. doi: 10.11766/trxb201501270058

Zavattaro, L., Bechini, L., Grignani, C., Van Evert, F. K., Mallast, J., Spiegel, H., et al. (2017). Agronomic effects of bovine manure: a review of long-term European field experiments. *Eur. J. Agron.* 90, 127–138. doi: 10.1016/j.eja.2017.07.010

Zhang, J., Cai, Z., and Müller, C. (2018). Terrestrial n cycling associated with climate and plant-specific n preferences: a review. *Eur. J. Soil Sci.* 69, 488–501. doi: 10.1111/ejss.12533

Zhang, W., Dou, Z., He, P., Ju, X., Powlson, D., Chadwick, D., et al. (2013). New technologies reduce greenhouse gas emissions from nitrogenous fertilizer in China. *Proc. Natl. Acad. Sci. U.S.A.* 110, 8375–8380. doi: 10.1073/pnas.1210447110

Zhang, X., Fang, Q., Zhang, T., Ma, W., Velthof, G. L., Hou, Y., et al. (2020). Benefits and trade-offs of replacing synthetic fertilizers by animal manures in crop production in China: a meta-analysis. *Glob. Change Biol.* 26, 888–900. doi: 10.1111/gcb.14826

Zhang, Y., Li, C., Wang, Y., Hu, Y., Christie, P., Zhang, J., et al. (2016). Maize yield and soil fertility with combined use of compost and inorganic fertilizers on a calcareous soil on the north China plain. *Soil Tillage Res.* 155(8), 5–94. doi: 10.1016/j.still.2015.08.006

Zhang, J., Zhu, T., Cai, Z., and Müller, C. (2011). Nitrogen cycling in forest soils across climate gradients in Eastern China. *Plant Soil* 342, 419–432. doi: 10.1007/s11104-010-0706-6

Zhou, J. (2012). Effect of combined application of organic and mineral fertilizers on yield, quality and nitrogen uptake of rice. *Plant Nutr. Fer. Sci.* 18, 234–240. doi: 10.11674/zwyf.2012.11186

Zhou, M., Zhu, B., Brüggemann, N., Dannenmann, M., Wang, Y., and Butterbach-Bahl, K. (2016). Sustaining crop productivity while reducing environmental nitrogen losses in the subtropical wheat-maize cropping systems: a comprehensive case study of nitrogen cycling and balance. *Agric. Ecosyst. Environ.* 231, 1–14. doi: 10.1016/j.agee.2016.06.0221

TYPE Original Research
PUBLISHED 20 June 2023
DOI 10.3389/fpls.2023.1179183

OPEN ACCESS

EDITED BY
Li Wang,
Shandong Academy of Agricultural Sciences, China

REVIEWED BY
Mariola Staniak,
Institute of Soil Science and Plant Cultivation, Poland
Saeid Hazrati,
Azarbaijan Shahid Madani University, Iran

*CORRESPONDENCE
Ramesh Chauhan
ramesh@ihbt.res.in

RECEIVED 03 March 2023
ACCEPTED 01 June 2023
PUBLISHED 20 June 2023

CITATION
Vishvamitera S, Dhiman D, Baghla S, Singh S, Kumar M, Kumar A, Kumar D, Singh S and Chauhan R (2023) Sustainable production of *Saussurea costus* under different levels of nitrogen, phosphorus and potassium fertilizers in cold desert region of Western Himalaya.
Front. Plant Sci. 14:1179183.
doi: 10.3389/fpls.2023.1179183

Sustainable production of *Saussurea costus* under different levels of nitrogen, phosphorus and potassium fertilizers in cold desert region of Western Himalaya

Sakshi Vishvamitera[1], Diksha Dhiman[1], Sidharth Baghla[1], Satbeer Singh[1], Manish Kumar[2], Ashok Kumar[1], Dinesh Kumar[2], Sanatsujat Singh[1] and Ramesh Chauhan[1*]

[1]Agrotechnology Division, Council of Scientific and Industrial Research - Institute of Himalayan Bioresource Technology, Palampur, India, [2]Chemical Technology Division, Council of Scientific and Industrial Research - Institute of Himalayan Bioresource Technology, Palampur, India

Introduction: *Saussurea costus*, an important critically endangered medicinal herb native to the Himalayan region, is commonly used in various ailments, *viz*. asthma, ulcer, inflammation, and stomach problems. In the international market, the dry roots and essential oil of *S. costus* has become an important drug. The lack of appropriate fertilizer dose recommendations is one of the limiting factors for its *ex-situ* conservation and large-scale cultivation, as plant nutrition is vital in determining crop growth and productivity. The study aimed to understand the comparative impact of different levels of fertilizer nutrients on growth, dry root and essential oil yield, and essential oil profile of *S. costus*.

Methods: A field experiment was conducted in Himachal Pradesh, India's cold desert region (Lahaul valley), during 2020-21. The experiment comprised three levels of nitrogen (60, 90, and 120 kg ha^{-1}), three levels of phosphorus (20, 40, 60 kg ha^{-1}), and two levels of potassium (20 and 40 kg ha^{-1}) in a factorial randomized block design.

Results: The fertilizer application had an immense effect on growth attributes, root yield attributes, dry root yield, and essential oil yield over control. The treatment combination N120, P60, and K_{40} had the largest effect on the plant height, number of leaves per plant, leaf length and width, root length and diameter, dry matter per plant, dry root yield, and essential oil yield. However, the results were at par with the treatment comprising N_{90}, P_{40}, and K_{20}. Dry root yield increased by 108.9%, and essential oil yield increased by 210.3% with fertilizer applications over unfertilized plots. The regression curve shows an increasing trend in dry root yield till N_{90}, P_{40}, and K_{20}; after that, it nearly stabilized. The heat map showed that applying fertilizer significantly affected the chemical constituents of *S. costus* essential oil. Similarly, the plots fertilized with the highest level of NPK recorded the utmost value of available N, P, and K, as compared to unfertilized plots.

Discussion: The results emphasize that for sustainable cultivation of *S. costus*, the application of N_{90}, P_{40}, and K_{20} combinations is the most suitable one.

KEYWORDS

chemical compound, critically endangered, dry root yield, essential oil, plant nutrition

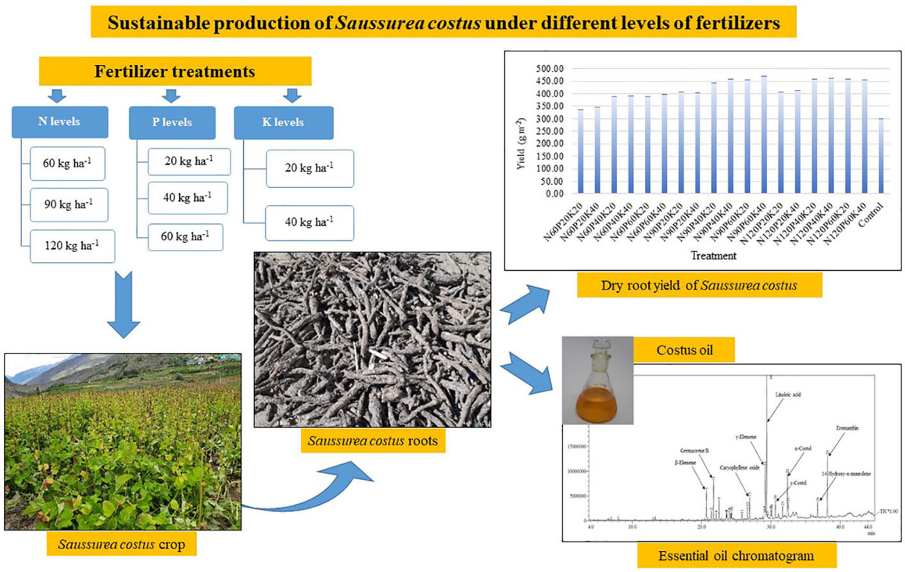

GRAPHICAL ABSTRACT

1 Introduction

Herbal drugs have recently received enormous popularity owing to their traditional and cultural causes among consumers. Approximately three-fourths of the global population relies heavily on plant species for curing health problems leading to pervasive growth in herbal-based pharmaceutical industries. Nearly 90% of the medicinal species are collected from wild sources, majorly (about 70%) through destructive harvesting (Sen and Chakraborty, 2017). The global estimated market for herbal medicines is nearly $2438.15 US, out of which India accounts for roughly 1% ($24.38 US) (Dhar and Dey, 2019). According to World Health Organization statistics, the global market worth of herbal products is anticipated to reach USD 5 trillion by 2050 (Shirolkar et al., 2015; Tahir et al., 2022) The Indian Himalayan region is a hotspot for herbal biodiversity and harbors more than 1748 plant species with known medicinal importance. One such genus of the family Asteraceae, with therapeutic benefits, is *Saussurea*, found in the wild at an elevation range of 2000-3500 meters above mean sea level (msl) in sub-alpine areas of the North-western Himalayas. Among all the species of *Saussurea*, *Saussurea costus* (Falc.) Lipsch. (Syn. *Saussurea lappa* C.B. Clarke), traditionally known as "Kuth" or "Kusth," is the utmost economically viable species. Its therapeutic properties are exquisitely catalogued in Ayurvedic, Tibetan, and Chinese medicine systems. It is one of the essential constituents in about 175 herbal preparations documented in "The Handbook of Traditional Tibetan Drugs (Butola and Samant, 2010). Musky scented roots are the most valuable portion of the plant and are renowned for their medicinal properties with antifungal, anthelmintic, antidiabetic, antimicrobial, immuno-stimulant, antiulcer, anti-inflammatory and antihepatotoxic characteristics that make it one of the fascinating herbs on the planet (Shah, 2019). The essential oil (also known as costus oil) obtained from kuth roots is light yellow to brownish, resembling oriss oil to some extent. It is an important and costly drug in the International market. *S. costus* oil is used in high-grade perfume preparations, hair oil, insect repellent, and incense, owing to its blending capability with rose, sandalwood, patchouli, violet, vetiver, etc. (Rathore et al., 2020). The phytochemical investigation revealed that *S. costus* roots contain several bioactive components such as flavonoids, steroids, monoterpenes, lignans, sesquiterpenoids, flavonoids, glycosides, triterpenes, etc. (Benedetto et al., 2019). In addition, *S. costus* oil also possesses sesquiterpene lactones *viz.*, costunolide and dehydrocostus lactone, which exhibit anti-cancerous activities (Zahara et al., 2014). Fluctuations in environmental conditions, chemotype, phenophase and ecotype impart significant variations in essential oil composition of *S. costus*.

S. costus is classified as a critically endangered herbal plant and is nearly on the brink of extinction, the reason being its overexploitation from the wild (more than 90% from natural habitats) (Sen and Chakraborty, 2017). It is one of 24 herbal plant species that the National Medical Plants Board (NMPB) and Planning Commission, Government of India, have prioritized for research and development for *in-situ* as well as *ex-situ* conservation to achieve the intended goal of the medicinal plant sector (Kala et al., 2006). To bring it out from the "critically endangered status," considering its therapeutic and commercial utility, farmers can play a pivotal role in conserving the herbal plant species through captive cultivation. Some innovative farmers of Lahaul valley, a cold desert region of Himachal Pradesh, started its cultivation on a large scale during the early 1900s but later replaced it with other cash crops like pea and potato owing to its long cultivation cycle and lower yield resulting in meager profits (Rawat et al., 2004; Ali and Venkatesalu, 2022). Despite government efforts to encourage the farmers for its cultivation, the response has not been very positive due to a lack of appropriate agro-technologies to attain higher yields with high marker compound content. The yield, quality, and composition of the secondary metabolites in medicinal plants depend on various biotic and abiotic factors. Among abiotic factors, soil fertility plays a significant role in developing quality medicinal plants (Verma and Shukla, 2015; Soltanbeigi, 2020). The quality and yield of herbal plants can be increased effectively by fertilization as amino acids and enzymes involved in the biosynthesis of numerous essential oil compounds are, in turn, synthesized by the plant using nitrogen (N), phosphorus (P), and potassium (K) primarily (Nurzynska-Wierdak, 2013).

The *S. Costus* plant has evidenced massive interest from several researchers in the recent past; still, there is a dearth of information on soil fertilization's effect on its growth, yield, and marker compound content. Thus, it is imperative to establish standardized fertilizer practices to promote *S. costus* as an economically-attractive crop competitive with food crops and to improve the essential oil yield and marker compound content for its sustainable use in the herbal industry. This prompted us to comprehensively analyze the differences in growth, yield, and marker compounds of *S. costus* grown under varying dosages of N, P, and K to standardize the best fertilizer dosages for its large-scale cultivation.

2 Material and methods

2.1 Experimental site, agro-meteorological conditions, and soil properties

A field experiment was carried out to standardize the fertilizer dose for *S. costus* in Lahaul valley to attain higher root and essential oil yield in the growing season of 2020 and 2021. The experimental field is situated in the cold desert region of western Himalaya at Lote, Distt. Lahaul & Spiti, Himachal Pradesh, India (32035'42" N; 76056'36" E; 1393 m above msl). The study of the research site with respect to cropping pattern revealed that cauliflower was grown from May to August, then left fallow over the winter (only one crop season due to heavy snowfall during winter). Average meteorological data of two experimental years (2020 and 2021) is shown in Figure 1. The experimental location is characterized by heavy snowfall (733.90 mm) from November to May and scanty rainfall (332.40 mm) from June to October. The minimum and maximum temperature were -10°C and 29°C, respectively, with an average annual temperature of 10°C during both years. Before the experiment's commencement, the research site's soil sample was collected from 0-0.15 m depth to analyse the initial physico-

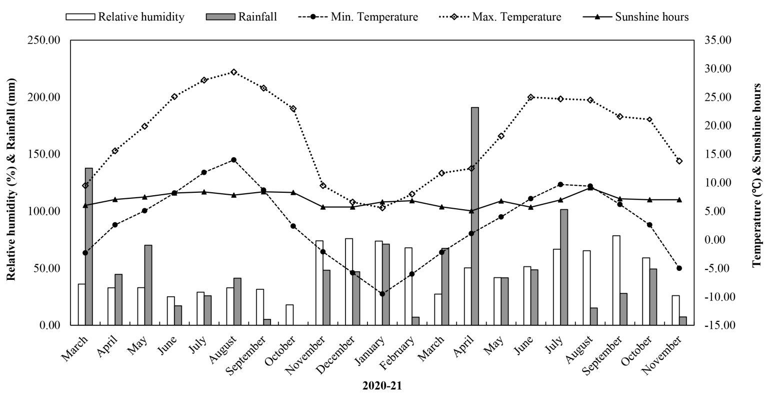

FIGURE 1
Average monthly meteorological data (relative humidity (%), rainfall (mm), mean maximum and minimum temperature (°C), and sunshine hours) during the cropping seasons of 2020 and 2021 at Lote, Distt. Lahaul & Spiti, Himachal Pradesh, India.

chemical properties. The soil texture was sandy clay loam with pH 6.15. The soil available nutrient content was 382.40, 39.20, and 142.15 kg ha^{-1} of available N, P, and K, respectively. The organic carbon (OC) content in the soil of the research site was 0.67%.

2.2 Planting material and experimental specifications

One-year-old healthy seedlings of *S. costus* with 4-5 cm root length were obtained from the Plant Breeding section of Agrotechnology Division, CSIR- Institute of Himalayan Bioresource Technology, Palampur and transplanted in the field on 15^{th} May 2020. The experiment was laid out using a factorial randomized block design (FRBD) with three factors arrangement *i.e.*, three levels of N (60, 90, and 120 kg ha^{-1}), three levels of P (20, 40, and 60 kg ha^{-1}), two levels of K (20 and 40 kg ha^{-1}) and control (where no fertilizer additions were made). The total treatment combinations (18) and one control were replicated thrice. The size of the experimental plots was 5 m^2 (2.5 × 2.0 m) and seedlings were transplanted in square shape planting geometry with a spacing of 0.25 × 0.25 m. At the time of transplanting, one-third dose of N and the full dose of P and K were mixed thoroughly in soil, while the remaining two-third dose of N was supplied into two equal splits *i.e.*,30 and 60 DAT (days after transplanting). In the second growing season, P and K were mixed in the soil with the help of a hand hoe in May, while N was applied as per the preceding year. The nutrient fertilizer source was urea (46% N) for N, single super phosphate (16% P_2O_5) for P, and muriate of potash (60% K_2O) for K. Weeding, irrigation, and other intercultural operations were performed as per the requirement of crop.

2.3 Sampling, measurements and methods

The impact of fertilizers treatment on plant growth and yield attributes was assessed by measuring the plant height, number of leaves per plant, leaf length & width, dry matter per plant, root length & diameter, and dry root yield. Ten plants were selected randomly from each plot to record all the growth parameters. Plant height at the harvesting stage was gauged from the ground level to the plant tip, whereas the number of leaves per plant was counted at the peak flowering period. The leaf length and width were determined by using the fresh leaves of selected plants with the help of a ruler and the mean value was calculated. For dry matter accumulation, the aerial part of selected plants was cut from the ground level using a sickle, and oven dried at 70 ± 2°C until a constant weight was achieved and averaged to analyze dry matter per plant. The root length was calculated by using intact roots of selected plants from each plot that were gently washed with running water to remove the soil, and then, root length was directly measured using a ruler, whereas root diameter was measured using a vernier calliper. For dry root yield estimation, ten plants' scale and soil-free roots were dried under shade until a constant weight was obtained, and then the yield of ten plants was converted into yield per m^2. After harvesting *S. costus*, the soil samples were collected from the top 0.15 m layer from each plot. The soil pH was calculated using pH meter (soil: water suspension, 1:2 w/v), whereas, Walkley and Black (1934) method was used to determine OC. Soil available N, P, and K were measured as per the method given by Subbiah and Asija (1956); Bray and Kurtz (1945), and Mehlich (1984), respectively.

2.4 Essential oil extraction

The essential oil was extracted from the dry roots of *S. costus* in three replicates as per treatment through hydrodistillation in a Clevenger apparatus. For that, 1 kg sample was placed in the distillation apparatus with 2 litres of water (1:2 ratio) and hydro-distilled for 6 hours. The obtained essential oil was dried by anhydrous sodium sulphate (Na_2SO_4) and kept separated in a sealed vial at 4°C for further examination under GC-MS and GC for identifying and quantifying the volatile compounds, respectively. The extracted essential oil content was computed as the weight of essential oil per weight of the sample (g per kg) on a dry weight basis, and essential oil yield was calculated by multiplying the dry root yield with essential oil content and expressed in kg per ha.

2.5 Gas chromatography analysis

The essential oil was analyzed with Shimadzu GC 2010 gas chromatograph with a flame ionization detector (FID). The SH-RX-5Si/MS capillary column, Shimadzu Asia pacific (USA) having dimensions of 30 m × 0.25 mm × 0.25 µm, was accoutred with gas chromatography. The auto-injection mode was run with a volume of 2 µL from 4 µL oil in 1.5 ml of CH_2Cl_2. Nitrogen was the carrier gas having a consistent velocity (1.05 ml min^{-1}). The oven temperature was set to 70°C for 3 min., and then to 220°C for 5 min. at a constant rate (4°C per min). The detector and injector temperatures were 250 and 220°C, respectively. The initial pressure was nearly about 65.3 kPa, and the approximate linear velocity was 37.6 cm s^{-1}.

2.6 Gas chromatography-mass spectrometry analysis

The concentrated essential oil samples were analyzed using Schimadzu GCMS-QP2010 (Shimadzu Corporation, Japan) system. An SH-RX-5Si/MS (30 m × 0.25 mm × 0.25 µm film thickness) column, fused with silica capillary was used, with nitrogen as a carrier gas at a flow rate of 1mL min^{-1}. The injector temperature was set to 250°C, and the sample volume injected was 2µL. The oven temperature was programmed for 3.0 min. to hold at 70°C and then increased from 4°C to 220°C for 5.0 min, respectively. The ion source and interface temperature was 200°C, and 250°C, respectively, while, electron energy was 0.85eV. Retention indices (RI) of the compounds relative to a mixture of n-Alkanes (C_9-C_{24}) were determined.

2.7 Statistical analysis

The data collected on growth, yield parameters and chemical compound of *S. costus* were analyzed by the standard statistical analysis of variance (ANOVA) technique for FRBD. Fisher's least significant difference (LSD) post-hoc test was performed to assess the differences among the treatments at 5% probability level (P=0.05). The multivariate principal component analysis (PCA), using the PAST 3 software, was used to understand the influence of treatments on growth, yield attributes and components of essential oil. The heat map was generated to assess the effect of treatments on composition of *S. costus* essential oil, and correlation studies were carried out to explore the relationship between different agronomic traits and essential oil compounds using R software. A first-degree regression model was established between fertilizer levels of N, P, and K and the dry root yield of *S. costus*.

3 Results and discussion

3.1 ANOVA due to different treatments

ANOVA showed that levels of N, P and K significantly affected the number of leaves per plant, dry matter per plant and root diameter of *S. costus* (Table 1). The leaf length, leaf width and root length were found significant only for N and P, while the plant height was significant for N and K. For dry root yield, the individual effect of N, P and K was found significant; however, their interaction effect was non-significant. None of the treatments (N, P and K) and their interaction (N×P, N×K, P×K and N×P×K) was found significant in case of essential oil content, while the sole effect of N, P and K was found significant for essential oil yield. The interaction effect of N and P (N×P) was found significant for plant height, number of leaves per plant, leaf width, dry matter per plant, root length and diameter; however, other interactions were found non-significant for all the growth and yield attributes, dry root and essential oil yield and essential oil content. When compared with control, all the treatments (N, P and K) were found significant for all the growth and yield attributes, dry root and essential oil yield, and essential oil content.

3.2 Growth attributes

The analyzed data presented in Table 2 revealed that different growth parameters, *viz.*, plant height at harvest, number of leaves per plant, leaf length & width, were significantly affected by varying levels of N. The highest level of N, *i.e.*, N_{120}, produced the tallest plants of *S. costus* (181.39 cm), which is significantly (P<0.05) different from N_{60} and N_{90}, however, the percent increase in plant height from N_{60} to N_{90} was higher, almost two times, compared from N_{90} to N_{120}. On comparing different P levels, higher plant height (173.75 cm) was observed with P_{40}; however, no significant differences were observed among varying P levels. Under different K levels, the tallest plants (174.55 cm) were registered with the highest level of K, *i.e.*, K_{40}, which was significantly different from K_{20}. In comparison, the control plots without adding NPK recorded the shortest plants (146.52 cm). An increase in N levels significantly augmented the height of plant that could be resulted from the beneficial effect of N in stimulating the meristematic activity rapidly for developing more tissues and organs as well as its essential role in protein synthesis, in addition to its vital role in several biochemical processes related to plant height. This corroborates the results of Eleiwa et al. (2012) in wheat (*Triticum aestivum*). The other two macronutrients (P and K) play an essential role in increasing the length and number of internodes leading to a progressive increment in plant growth with their increasing levels. The findings are in accordance with the results of Kwon et al. (2019) in bellflower

TABLE 1 Analysis of variance for the effects of N, P, and K levels on no. of leaves per plant, leaf length & width, dry matter per plant, root length & diameter, dry root yield, essential oil content, and essential oil yield of *S. costus*.

Source of variation	Degree of freedom	Plant height	No. of leaves plant^{-1}	Leaf length	Leaf width	Dry matter plant^{-1}	Root length	Root diameter	Dry root yield	Essential oil content	Essential oil yield
Treatment	18	366.57*	1.72*	4.55*	6.25*	4.35*	36.78*	94.78*	6931.35*	0.083*	6.13*
N	2	1738.69*	6.01*	15.89*	25.29*	17.95*	170.19*	380.04*	26123.74*	0.013	14.92*
P	2	40.86	2.54*	5.26*	11.04*	7.70*	70.11*	152.46*	15622.19*	0.006	8.42*
K	1	189.48*	0.44*	2.50	0.33	0.88*	2.34	4.92*	471.93*	0.008	0.69*
N×P	4	121.99*	0.95*	0.24	1.61*	1.54*	11.60*	3.93*	88.64	0.004	0.09
N×K	2	98.94	0.06	0.79	0.90	0.01	0.17	0.27	73.61	0.003	0.17
P×K	2	4.81	0.15	1.25	0.29	0.13	0.55	0.15	4.04	0.004	0.10
N×P×K	4	52.52	0.09	0.79	0.04	0.22	1.58	0.21	132.66	0.005	0.15
Control vs others	1	1944.06*	8.83*	29.00*	30.57*	18.89*	124.96*	618.67*	39760.02*	1.393*	61.52*
Error	36	35.02	0.10	0.74	0.38	1.56	1.87	1.01	107.96	0.006	0.14

Values represent the mean sum of squares.
*Significant at 0.05 levels of probability.

TABLE 2 Effect of N, P, and K levels on plant height, no. of leaves per plant, leaf length & width, dry matter per plant, root length & diameter, dry root yield, essential oil content, and essential oil yield of *S. costus*.

Treatments	Plant height (cm)	No. of leaves plant^{-1}	Leaf length (cm)	Leaf width (cm)	Dry matter plant^{-1} (g)	Root length (cm)	Root diameter (mm)	Dry root yield (g m^{-2})	Essential oil content (%)	Essential oil yield (kg ha^{-1})
Nitrogen Level (kg ha^{-1})										
N_{60}	162.03^{c}	6.31^{b}	15.85^{c}	12.98^{b}	7.81^{b}	20.44^{c}	37.69^{b}	375.31^{b}	2.12	7.95^{b}
N_{90}	174.61^{b}	7.20^{a}	17.03^{b}	14.80^{a}	9.43^{a}	25.20^{b}	45.32^{a}	440.19^{a}	2.14	9.44^{a}
N_{120}	181.39^{a}	7.39^{a}	17.71^{a}	15.21^{a}	9.64^{a}	26.19^{a}	45.94^{a}	442.34^{a}	2.17	9.61^{a}
SEm(±)	1.39	0.08	0.20	0.15	0.10	0.32	0.24	2.45	0.02	0.09
LSD (P = 0.05)	4.00	0.22	0.58	0.42	0.30	0.92	0.68	7.02	NS	0.26
Phosphorus Level (kg ha^{-1})										
P_{20}	170.95	6.54^{b}	16.31^{b}	13.50^{c}	8.21^{b}	21.73^{c}	39.65^{c}	385.35^{b}	2.13	8.22^{b}
P_{40}	173.75	7.16^{a}	16.89^{ab}	14.43^{b}	9.31^{a}	24.58^{b}	44.26^{b}	434.09^{a}	2.14	9.28^{a}
P_{60}	173.33	7.21^{a}	17.39^{a}	15.06^{a}	9.37^{a}	25.52^{a}	45.04^{a}	438.39^{a}	2.17	9.50^{a}
SEm(±)	1.39	0.08	0.20	0.15	0.10	0.32	0.24	2.45	0.02	0.09
LSD (P = 0.05)	NS	0.22	0.58	0.42	0.30	0.92	0.68	7.02	NS	0.26
Potassium Level (kg ha^{-1})										
K_{20}	170.80^{b}	6.88^{b}	16.65	14.25	8.83^{b}	23.73	42.68^{b}	416.32^{b}	2.13	8.89^{b}
K_{40}	174.55^{a}	7.06^{a}	17.08	14.41	9.09^{a}	24.15	43.29^{a}	422.23^{a}	2.16	9.11^{a}
SEm(±)	1.14	0.06	0.17	0.12	0.08	0.26	0.19	2.00	0.01	0.07
LSD (P = 0.05)	3.27	0.18	NS	NS	0.24	NS	0.55	5.74	NS	0.21
Control	146.52^{b}	5.21^{b}	13.67^{b}	11.05^{b}	6.38^{b}	17.31^{b}	28.23^{b}	301.00^{b}	1.44^{b}	4.35^{b}
Others	259.02^{a}	10.45^{a}	25.30^{a}	21.49^{a}	13.44^{a}	35.91^{a}	64.48^{a}	628.92^{a}	3.22^{a}	13.50^{a}
SEm(±)	2.48	0.14	0.36	0.26	0.18	0.57	0.42	4.36	0.03	0.16
LSD (P = 0.05)	7.12	0.39	1.04	0.74	0.53	1.65	1.21	12.50	0.09	0.46

SEm indicates Standard Error of Mean; LSD indicates Least Significant Difference; NS indicates not significant at P = 0.05.
The meaning of lowercase letter is N60, N90, N120, represents N levels @ 60, 90, and, 120 kg ha-1, respectively; P20, P40 and P60, represents P levels @ 20, 40 and 60 kg ha-1, respectively; and K20 and K40 indicates K levels @ 20 and 40 kg ha-1, respectively.

(*Platycodon grandiflorum*), an important medicinal plant, and Arab et al. (2015) in marigold (*Calendula officinalis*).

Applying different levels of N significantly influenced the number of leaves per plant. The highest value *i.e.* 7.39 was found in the plots fertilized with the highest N level (N_{120}), which was statistically at par (7.20) with N_{90}; however, both N_{90} and N_{120} levels were significantly different from N_{60}. Different levels of P and K also significantly affected the number of leaves per plant. The effect of P_{40} and P_{60} was significantly higher compared with P_{20}; however, these two levels were at par with each other, and the highest number of leaves per plant (7.21) was registered with the highest level of P, *i.e.*, P_{60}. A similar pattern was noticed in the case of K, where the highest level of K (K_{40}) resulted in a higher number of leaves per plant (7.06); however, it did not produce any significant differences with K_{20}. Moreover, absolute control without fertilizer addition registered the lowermost number of leaves per plant. Higher NPK fertilizer doses might result in maintaining optimal cytokinin-auxin ratio by promoting more activity of cytokinin in roots, which leads to activate the dormant axillary buds into branches, thereby, resulting in higher number of leaves per plant. Furthermore, plant height was significantly affected by higher doses of N, P, and K, which might contribute to a higher number of leaves per plant with augmented levels of macroelements. The results are in agreement with the findings of Kawatani et al. (1980); Aladakatti et al. (2012) and Mahajan et al. (2021) in *Stevia rebaudiana*.

The performance of *S. costus* plant in terms of leaf length and width was recorded as superior (17.71 cm and 15.21 cm, respectively) with N_{120}; however, in the case of leaf width, N_{120} was found statistically at par with N_{90}. When different P levels were compared, the highest leaf length (17.39 cm) and width (15.06 cm) were registered in P_{60}, which produced non-significant (*P*<0.05) differences with P_{40} (16.89 cm and 14.43 cm, respectively). Nevertheless, the increasing scale from P_{20} to P_{40} was higher than from P_{40} to P_{60}. Among different K levels, K applied @ 40 kg ha^{-1} (K_{40}) recorded the highest leaf length (17.08 cm) and width (14.41 cm); though changes among levels of K were found non-significant. The positive impact of higher levels of N on leaf growth could be attributed to its essential role in chlorophyll, enzymes, and protein synthesis, which tends to increase the length and width of the leaves. In the current study, applying higher doses of P leads to considerably higher leaf length and width that might be attributed that P is a vital constituent of several essential molecules such as phospholipids, ATP, and nucleic acids for energy transfer, protein synthesis, carbohydrate, and lipid metabolism (Rhykerd and Overdahl, 1972). The results conform to the findings of Medda and Hore (2003); Mohan et al. (2004) and Verma et al. (2019) in *Curcuma longa*. The application of fertilizers causing a significant increase in all the growth attributes over control could be resulted from the adequate provision of essential nutrients to the plants.

3.3 Dry matter per plant

The analyzed data (Table 2) revealed that the dry matter per plant was superior with N_{120} (9.64 $_{g}$); however, it produced non-significant differences with N_{90} (9.43 $_{g}$). Irrespective of P and K treatments, N_{120} significantly (*P*<0.05) increased the dry matter per plant by about 23% compared with N_{60}. Different levels of P also significantly affected the dry matter per plant, and the plants fertilized with P_{60} produced the highest dry matter per plant (9.37 g), though it remained statistically at par (9.31 g) with P_{40}. Despite that, the increase in dry matter per plant from P_{20} to P_{40} was higher than from P_{40} to P_{60}. The consequences of applied K on dry matter per plant were found to be significant, and the utmost value (9.09 g) was attained with K_{40}. In addition, the lowest dry matter per plant was recorded under control (6.38 g).

A positive effect of higher levels of nutrients on the number of leaves per plant, leaf length & width due to taller plants might have resulted in increased dry matter per plant with increasing levels of nutrient fertilizers. The results of Chalapathi et al. (1999) and Aladakatti et al. (2012) in *Stevia rebaudiana*, supported the findings of the present study.

3.4 Root yield attributes and dry root yield

The data given in Table 2 described that the root length and diameter were significantly (*P*<0.05) influenced by varying levels of N. The maximum root length (26.19 cm) was recorded with N_{120}; however, the increase from N_{60} to N_{90} was higher than N_{90} to N_{120}. Root length was also significantly affected by levels of P and K, and the highest root length, *i.e.*, 25.52 cm and 24.15 cm was recorded with P_{60} and K_{40}, respectively, though, the differences in root length with different levels of K were found non-significant.

Root diameter showed significant variations with different levels of N and the highest root diameter (45.94 mm) was registered with N_{120}, which was at par (45.32 mm) with N_{90}. Nevertheless, the percent increase in root diameter from N_{60} to N_{90} was about 21.9%, and from N_{90} to N_{120}, it was 1.4%. Root diameter in response to P showed the utmost value (45.04 mm) with P_{60}, which showed significant variations with P_{20} and P_{40}. Irrespective of applying N and P, the root diameter of *S. costus* was significantly affected by varying levels of K, and the highest root diameter was found to be 43.29 mm with K_{40}. In addition, the lowest root diameter (28.23 mm) was found in the control, where no fertilizer was applied.

In the present study, root length and diameter were significantly higher with higher doses of N, which could be attributed that N stimulates lateral root elongation and development through the production of auxin and cytokinin, respectively in response to a systematic N-signalling (Takei et al., 2001; Krouk et al., 2010). The positive impact of higher doses of P and K on root growth parameters might be due to the vital role of P in root morphology *via* affecting the carbon budget of the whole plant (Mollier and Pellerin, 1999), and furthermore, K has a pivotal role in the photosynthates' translocation from source (leaves) to sink (roots) that led to increased root growth. Kwon et al. (2019) in their study on a medicinally important plant, *Platycodon grandiflorum,* also reported similar results.

The dry root yield in response to N was significant, and the highest dry root yield (442.34 g m^{-2}) was recorded with N_{120}, that showed significant variations with N_{60}. The effect of N_{120} and N_{90} on dry root yield was significantly higher than that of N_{60}; however, both treatments were statistically at par. The dry root yield of *S. costus* was also significantly affected by P and K, and the highest dry root yield *i.e.*, 438.39 and 422.23 g m^{-2} was registered with P_{60} and K_{40}, respectively. In contrast, the lowest dry root yield was recorded under control. The rise in dry root yield with higher levels of fertilizers might be attributed to favorable impact of utmost levels of N, P, and K on root yield attributes like root length and diameter. The findings of the present study corroborate the earlier results of Singh and Negi (2003) in *S. costus.*

3.5 Essential oil content and essential oil yield

The analyzed data revealed that essential oil content was not considerably influenced by varying levels of N, P, and K fertilizers; however, it increased slightly with increased doses (Table 2). Nevertheless, the effect of fertilizer application on essential oil content was significantly ($P \leq 0.05$) higher when compared to the control. Averaged across P and K levels, essential oil yield showed significant variations with different levels of N, and highest essential oil yield (9.61 kg ha^{-1}) was registered with N_{120}, which was found at par (9.44 kg ha^{-1}) with N_{90}. However, the percent increase in essential oil yield from N_{60} to N_{90} was about 19%, and from N_{90} to N_{120}, it was only 2%. The essential oil yield of *S. costus* in response to P was found to be significant, and the highest essential oil yield (9.50 kg ha^{-1}) was found in P_{60}, which showed non-significant variations with P_{40} (9.28 kg ha^{-1}). Irrespective of applying N and P, varying levels of K fertilizer also significantly influenced the essential oil yield, and the maximum essential oil yield (9.11 kg ha^{-1}) was recorded with K_{40}, which showed significant variations with K_{20}. In addition, overall fertilizer application (13.5 kg ha^{-1}) recorded significantly higher essential oil yield over control (4.35 kg ha^{-1}) where no NPK was applied.

The positive impact of higher NPK doses on essential oil yield might be attributed to their direct or indirect involvement in the production of primary or secondary metabolites, in addition to the favorable effect of macro-elements on root growth parameters and root yield. The results are in accordance with the earlier findings of Bhuvaneshwari et al. (2002) in *Pimpinella anisum*; Abbaszadeh and Haghighi (2013) in *Thymus vulgaris*.

3.6 Essential oil composition

In the present study, a total of 25 compounds in the essential oil of *S. costus* were identified. Only 17 major compounds, which contributed about 57.66-78.63% were analyzed in the heat map that depicts the variations in the chemical profile of volatile constituent of essential oil owing to the interaction of varying levels of N, P, and K (Figure 2). Heat map analysis indicated that accumulation pattern of the chemical compound was not constant over the treatment combination. The clustering showed that $N_{90}P_{20}K_{20}$ recorded a higher concentration of 14-hydroxy-α-muurolene, spathulenol and dihydro-α-ionone. However, the concentration of ar-curcumene and γ-costol were higher under $N_{90}P_{60}K_{20}$. Similarly, application of $N_{120}P_{20}K_{40}$ resulted in higher concentration of α-selinene, β-elemene and α-costol while, linoleic acid was recorded higher under $N_{120}P_{40}K_{40}$.

To understand the individual effect of N, P, and K levels on chemical compositions, their mean data is presented in Table 3. Means given in Table 2 revealed that except β-elemene, all other chemical compounds were significantly affected by different levels of N, P and K, however the pattern of concentration was not uniform between the levels. The higher amount of N levels *i.e.* N_{120} resulted in significantly highest concentration of (E)-β-ionone, α-selinene, linoleic acid and eremanthin over N_{90} and N_{60}, while α-trans-bergamotene was at par with N_{60}. However, N_{90} recorded highest values for dihydro-α-ionone, germacrene B, geranyl acetone, ar-curcumene, α-costol and 14-hydroxy-α-muurolene. The other compounds *viz.* spathulenol, caryophyllene oxide, (Z)-α-trans-bergamotol acetate and valerenol were highest under N_{60}; and γ-costol was at par with N_{90}. Among P levels, P_{60} resulted in significantly highest concentration of (E)-β- ionone, ar-curcumene, linoleic acid, γ-costol, valerenol, α-costol and eremanthin. Similarly, P_{40} recorded maximum values for (Z)-α-trans-bergamotol acetate and 14-hydroxy-α-muurolene while caryophyllene oxide was at par with P_{60}. The lowest level of P *i.e.* P_{20} resulted in highest concentration of dihydro-α-ionone, germacrene B, α-trans-bergamotene, geranyl acetone, α-selinene and spathulenol. Under K levels, K_{40} recorded highest concentration for germacrene B, linoleic acid, γ-costol, α-costol and eremanthin over K_{20}. While the

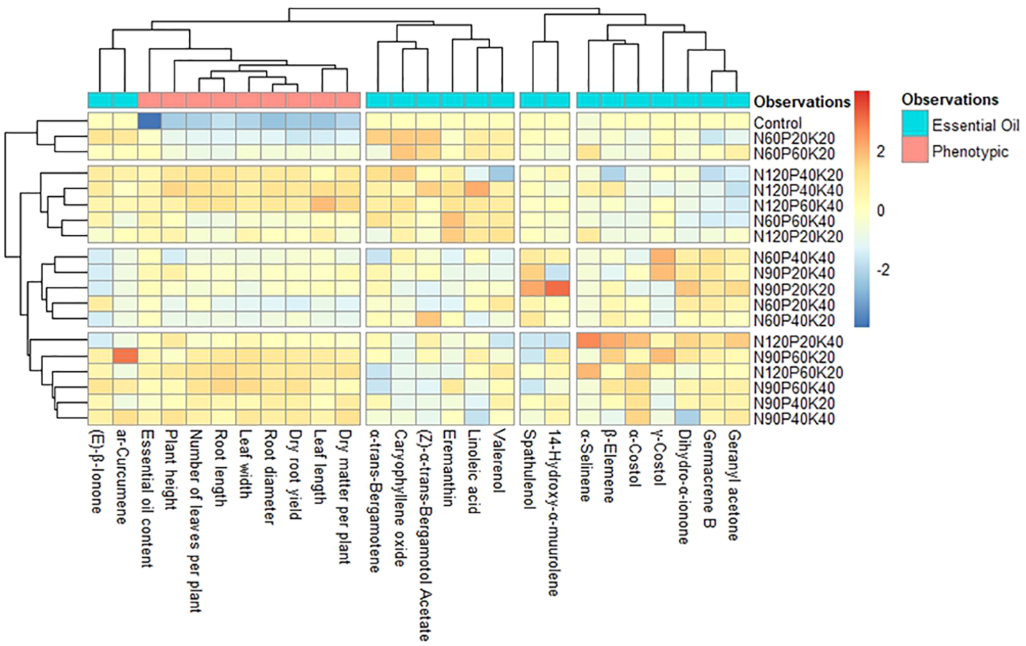

FIGURE 2
Heat map depicting the variation of chemical compounds identified in the costus oil in response to different NPK treatment combinations. N_{60}, N_{90} and N_{120}: N applied @ 60, 90 and 120 kg ha^{-1}, respectively; P_{20}, P_{40} and P_{60}: P applied @ 20, 40 and 60 kg ha^{-1}, respectively; K_{20} and K_{40}: K applied @ 20 and 40 kg ha^{-1}, respectively.

TABLE 3 Variation in essential oil composition of *S. costus* due to N, P, and K levels.

Treatments	β-Elemene	Dihydro-α-ionone	Germacrene B	α-trans-Bergamotene	Geranyl acetone	(E)-β-Ionone	α-Selinene	ar-Curcumene	Spathulenol	Caryophyllene oxide	Linoleic acid	(Z)-α-trans-Bergamotol Acetate	γ-Costol	Valerenol	α-Costol	14-Hydroxy-α-muurolene	Eremanthin
RT	20.7	21.4	21.7	22.1	22.5	23.6	24.2	23.7	26.6	26.9	29.4	30.2	31.7	32.4	32.5	36.8	38.2
RI	1392	1413	1420	1433	1445	1477	1495	1479	1576	1585	1668	1700	1747	1772	1775	1934	1990
Nitrogen Level (kg ha^{-1})																	
N_{60}	2.57	1.80^{b}	4.14^{b}	2.34^{a}	2.33^{b}	1.48^{b}	0.42^{b}	0.47^{c}	1.60^{a}	4.62^{a}	17.17^{b}	6.17^{a}	3.88^{a}	8.68^{a}	2.13^{c}	3.01^{b}	6.47^{b}
N_{90}	2.70	2.05^{a}	5.89^{a}	2.07^{b}	2.92^{a}	1.54^{b}	0.22^{c}	1.26^{a}	1.33^{b}	0.51^{c}	14.42^{c}	2.12^{c}	3.87^{a}	7.2^{4c}	6.62^{a}	4.00^{a}	5.87^{c}
N_{120}	2.64	1.62^{c}	3.30^{c}	2.39^{a}	2.08^{c}	1.71^{a}	1.10^{a}	0.70^{b}	1.06^{c}	3.84^{b}	17.74^{a}	5.02^{b}	3.18^{b}	7.62^{b}	4.48^{b}	2.63^{c}	8.96^{a}
SEm(±)	0.05	0.04	0.04	0.03	0.04	0.02	0.02	0.01	0.05	0.03	0.13	0.04	0.07	0.09	0.06	0.07	0.13
LSD	NS	0.10	0.13	0.09	0.11	0.06	0.06	0.03	0.15	0.08	0.36	0.13	0.20	0.26	0.18	0.20	0.37
Phosphorus Level (kg ha^{-1})																	
P_{20}	2.68	2.17^{a}	5.02^{a}	2.63^{a}	2.73^{a}	1.07^{c}	0.80^{a}	0.47^{c}	1.69^{a}	2.58^{b}	16.74^{b}	4.16^{b}	3.67^{b}	7.88^{b}	3.83^{c}	2.98^{c}	5.79^{c}
P_{40}	2.54	1.63^{b}	4.30^{b}	2.34^{b}	2.29^{b}	1.53^{b}	0.30^{c}	0.70^{b}	1.51^{b}	3.20^{a}	14.91^{c}	5.12^{a}	2.55^{c}	6.16^{c}	4.55^{b}	3.56^{a}	7.18^{b}
P_{60}	2.70	1.68^{b}	4.01^{c}	1.83^{c}	2.32^{b}	2.14^{a}	0.65^{b}	1.26^{a}	0.79^{c}	3.19^{a}	17.67^{a}	4.04b	4.71^{a}	9.49^{a}	4.85^{a}	3.09^{b}	8.33^{a}
SEm(±)	0.05	0.04	0.04	0.03	0.04	0.02	0.02	0.01	0.05	0.03	0.13	0.04	0.07	0.09	0.06	0.07	0.13
LSD	NS	0.10	0.13	0.09	0.11	0.06	0.06	0.03	0.15	0.08	0.36	0.13	0.20	0.26	0.18	0.20	0.37
Potassium Level (kg ha^{-1})																	
K_{20}	2.61	1.86	4.10^{b}	2.37^{a}	2.45	1.58	0.60	0.99^{a}	1.41^{a}	3.35^{a}	16.27^{b}	5.10^{a}	3.22^{b}	7.99^{a}	3.95^{b}	4.02^{a}	6.72^{b}
K_{40}	2.67	1.79	4.78^{a}	2.16^{b}	2.44	1.57	0.57	0.62^{b}	1.25^{b}	2.62^{b}	16.61^{a}	3.78^{b}	4.06^{a}	7.70^{b}	4.87^{a}	2.40^{b}	7.48^{a}
SEm(±)	0.04	0.03	0.04	0.02	0.03	0.02	0.02	0.01	0.04	0.02	0.10	0.04	0.06	0.08	0.05	0.06	0.10
LSD	NS	NS	0.11	0.07	NS	NS	NS	0.03	0.12	0.07	0.29	0.10	0.16	0.22	0.14	0.17	0.30
Control	2.64	1.83	4.44	2.27	2.44	1.58	0.07^{b}	0.81	1.33	2.99	16.44	4.44	3.86	7.85	4.41	3.21	7.10
Others	3.96	2.74	6.66	3.40	3.67	2.37	0.87^{a}	1.21	1.99	4.48	24.66	6.66	5.46	11.77	6.61	4.82	10.65
SEm(±)	0.09	0.06	0.08	0.05	0.07	0.04	0.04	0.02	0.09	0.05	0.22	0.08	0.12	0.16	0.11	0.13	0.23
LSD	NS	NS	NS	NS	NS	NS	0.11	NS	NS	NS	NS	NS	NS	NS	NS	NS	NS

RT-Retention time; RI-Retention indices.
N60, N90, N120, represents N levels @ 60, 90, and, 120 kg ha-1, respectively; P20, P40 and P60, represents P levels @ 20, 40 and 60 kg ha-1, respectively; and K20 and K40 indicates K levels @ 20 and 40 kg ha-1, respectively. NS indicates "not significant at P = 0.05".

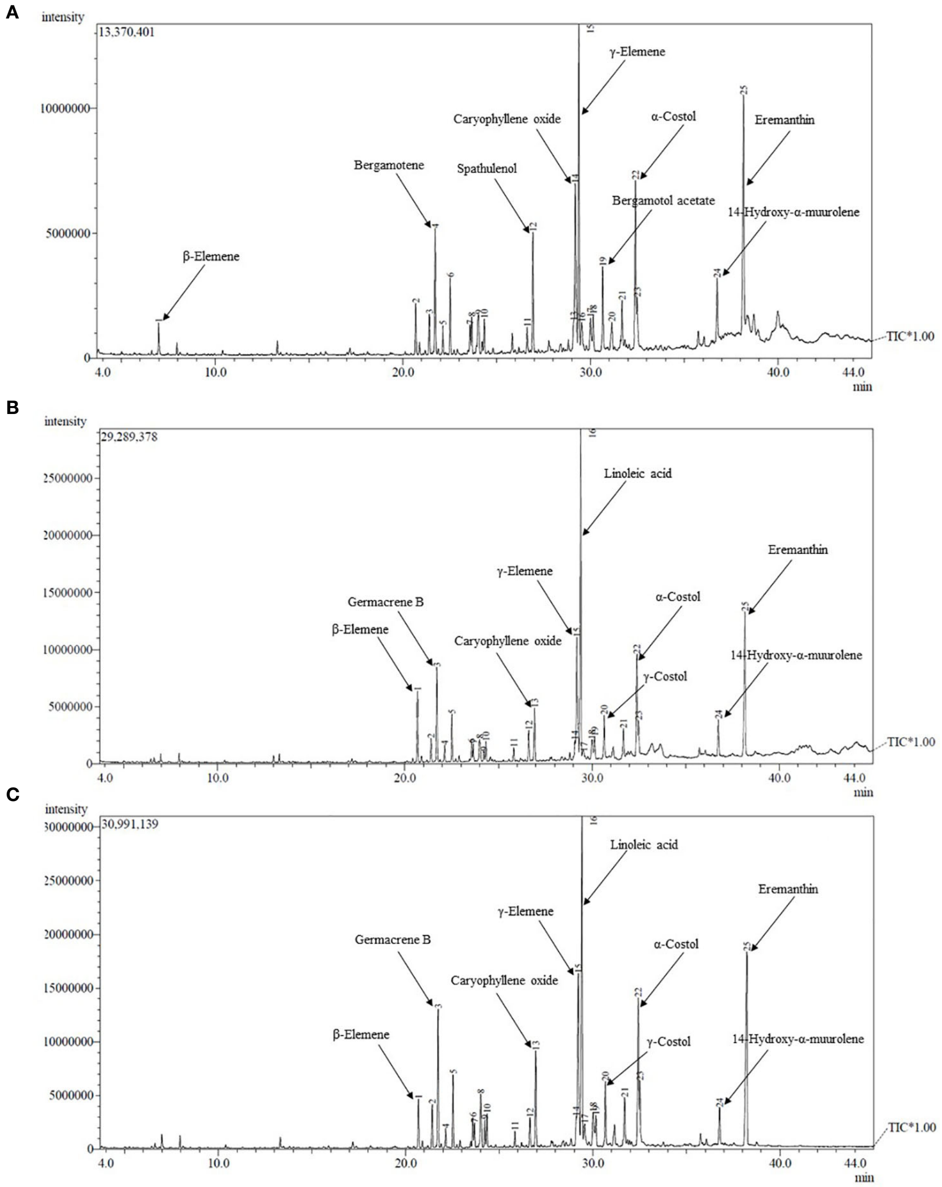

FIGURE 3
GC-MS Chromatogram of essential oil of *S. costus* in response to different treatment combinations; **(A)** Control, **(B)** $N_{90}P_{40}K_{20}$ and **(C)** $N_{120}P_{60}K_{40}$.

other chemical compounds *viz.* α-trans-bergamotene, ar-curcumene, spathulenol, caryophyllene oxide, (Z)-α-trans-bergamotol acetate, valerenol and 14-hydroxy-α-muurolene were recorded higher under K_{20}. The increase in essential oil constituents with application of fertilizers might be resulted from improved availability of essential nutrients that consequently led to improved photosynthetic rate which affects the formation of precursor compounds of fatty acids that determines the oil quality, in addition to their role in development of glandular trichomes, secretory ducts and oil channels (Salehi et al., 2019; Chiyaneh et al., 2022). Further, several researchers also reported that the application of fertilizer nutrients alters the composition of essential oil in many medicinal and aromatic plants like *Artemisia dracunculus* (Heidari et al., 2014), *Rosa damascena* (Pal & Mahajan, 2017) and *Cymbopogon flexuosus* (Zheljazkov et al., 2011). The representative GC-MS chromatogram of *S. costus* essential oil in response to different treatment combinations are given in Figure 3.

3.7 PCA

The PCA was carried out using 17 chemical compounds of essential oil isolated from dried roots of *S. costus*. The PCA analyzed data showed that component 1 and 2 (PC_1 and PC_2) jointly accounted for 59.12% of the total variations in biochemical traits (Figures 4A, B). The eigenvalues of PC_1 and PC_2, (the relevant and informative principal components), was 36.5 and 20.6, respectively. Component 1 (explained about 37.80% of the total variations), was found positively correlated with linoleic acid, caryophyllene oxide, (Z)-α-trans-bergamotol acetate, α-trans-bergamotene, ar-

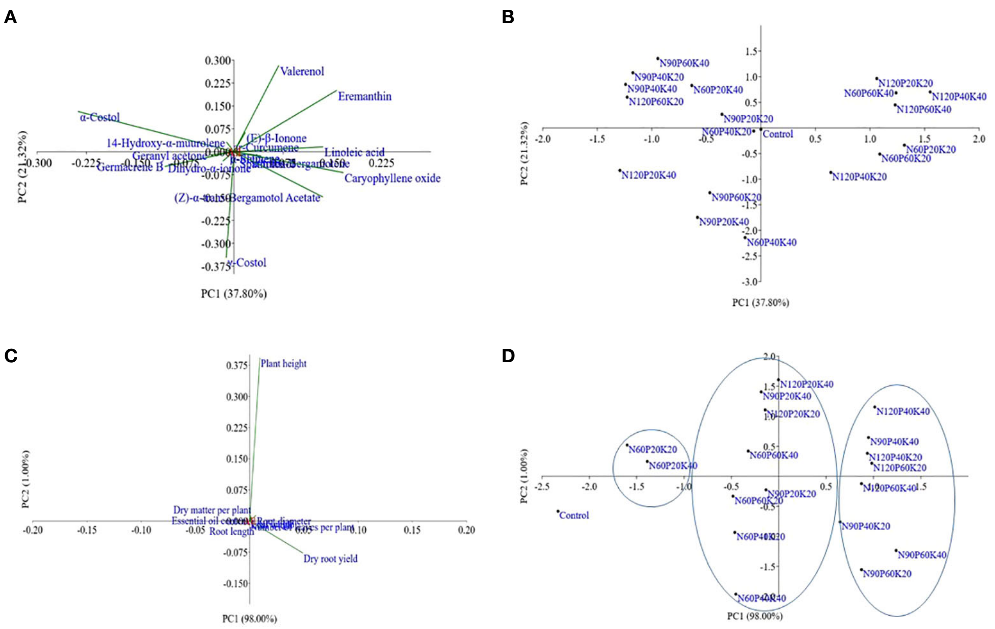

FIGURE 4
Scatter plots of principal components analysis **(A)** bi-plot of biochemical constituents **(B)** treatments' distribution based on biochemical constituents, **(C)** bi-plot of agronomic traits, and **(D)** treatments distribution based on agronomic traits. In the bi-plots, N60, N90, N120, represents N levels @ 60, 90, and, 120 kg ha-1, respectively, P20, P40 and P60, represents P levels @ 20, 40 and 60 kg ha-1, respectively, and K20 and K40 indicates K levels @ 20 and 40 kg ha-1, respectively.

curcumene, eremanthin and spathulenol with loading values of 0.33, 0.41, 0.33, 0.10, 0.02, 0.38 and 0.02, respectively, and negatively correlated with rest of the compounds. In addition, the compound valerenol related more positively to PC_2 having loading value of 0.52. The γ-costol was separated from the other compounds by PC_1 and PC_2 and situated in the negative coordinate. The PCA bi-plot did not show any specific trend for the treatment effects on major compounds of essential oil (Figure 4B).

PCA was also performed to study the interaction of different levels of N, P, and K on *S. costus'* agronomic traits (Figures 4C, D). The findings of the PCA indicated that the first component solely contributed to 98.0% of the total variations in agronomic traits. Among all the agronomic traits, dry root yield contributed the maximum towards the total variation with a loading value of 0.99. The PCA bi-plot (Figure 4D) categorized the treatment combinations into three distinct clusters, and all the treatment combinations comprising N_{60} were positioned in the negative end of PC_1. In addition, all the N_{120} consisting treatments were located in the positive end of PC_1, except $N_{120}P_{20}K_{20}$. PC_1 also separated all the treatment combinations comprising P_{20}, irrespective of N and K levels, and put them in the negative coordinate.

3.8 Correlation and regression analysis

The correlation matrix among agronomic traits (plant height, number of leaves per plant, leaf length & width, root length & diameter, dry matter per plant, dry root yield), and essential oil components of *S. costus* is depicted in Figure 5. The figure showed that all the agronomic traits exhibited a strongly positive correlation with each other with r values >0.77 ($p<0.001$). The robust relationship between dry root yield, and root diameter compared to root length (r=0.99 and 0.95, $p<0.001$) suggested that root diameter might be a more substantial yield attribute for determining the total dry root yield of *S. costus*.

Although 25 chemical compounds were found in the essential oil, the correlation matrix has been constructed amongst the 17 major constituents. The analyzed data revealed that caryophyllene oxide and eremanthin showed a strong and negative correlation with geranyl acetone (r=-0.65, $p<0.01$), germacrene B (r=-0.76 and r=-0.71, respectively, $p<0.001$) and dihydro-α-ionone (r=-0.47, $p<0.05$ and r=-0.61, $p<0.01$, respectively); however, former one also showed a negative correlation with α-costol (r=-0.72, $p<0.001$) and β-elemene (r=-0.59, $p<0.01$). The results illustrated that germacrene B was strongly and positively correlated with geranyl acetone with r value=0.90 ($p<0.001$). In addition, (E)-β- ionone exhibited a positive correlation with ar-curcumene (r= 0.54, $p<0.05$) and negative correlation with spathulenol (r= -0.5, $p<0.05$), dihydro-α-ionone (r= -0.53, $p<0.05$), germacrene B (r= -0.56, $p<0.05$) and geranyl acetone (r= -0.51, $p<0.05$).

Regression equations among N, P and K levels (independent variables), and dry root yield (dependent variables), were also studied (Figure 6). Among N, P, and K levels, dry root yield enhanced till 90 kg N ha^{-1}, 40 kg P ha^{-1} and 20 kg K ha^{-1}, respectively, with a constant value thereafter. A strong relationship of fertilizer levels, *i.e.*, N, P, and K with dry root yield, was observed by using linear equations $y=12.69x + 3040.4$ ($r^2 = 0.947$), $y=23.04x + 3205.7$ ($r^2 = 0.868$) and $y=30.30x + 3192.4$ ($r^2 = 0.786$), respectively.

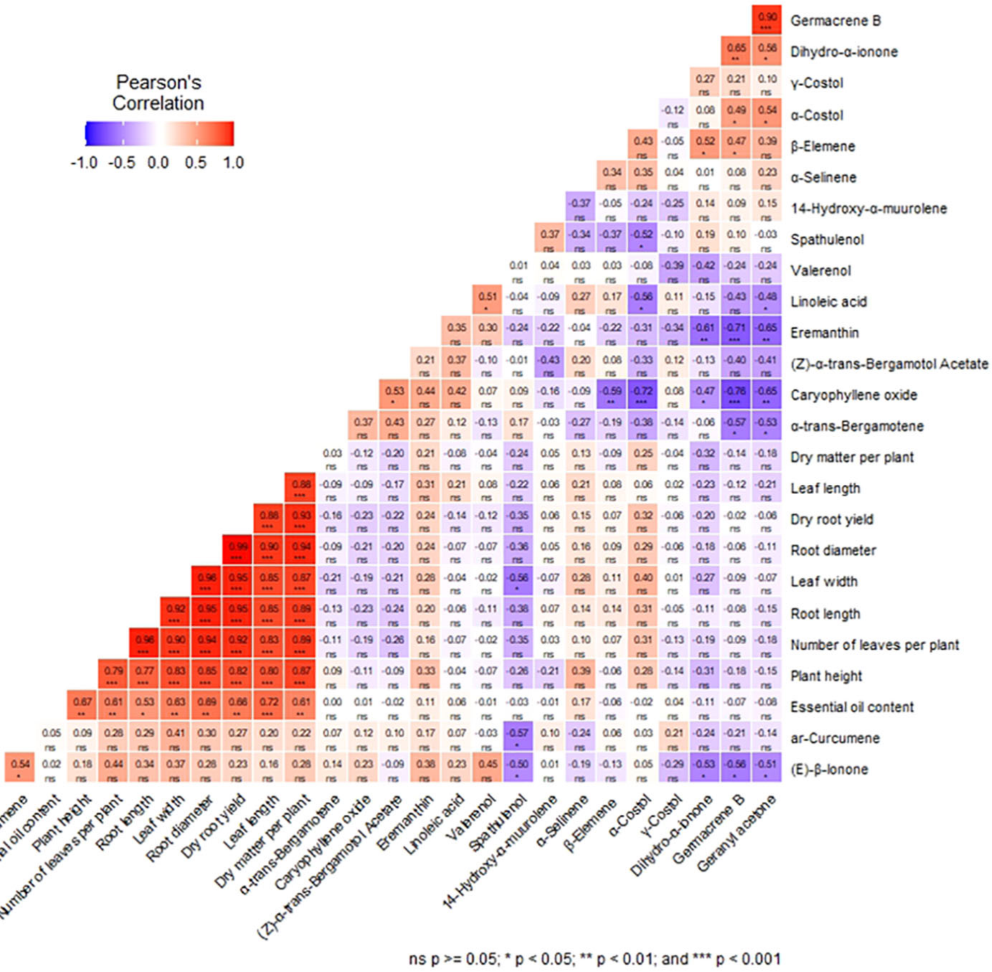

FIGURE 5
Correlation matrix among the agronomic traits, and 17 major compounds of costus oil. *, **, *** indicates significant at P = 0.05, P = 0.01 and P = 0.001, respectively'ns' indicates not significant at P = 0.05.

3.9 Soil nutrient status after crop harvest

The analyzed data showed a non-significant effect of different levels of N, P, and K on soil pH and OC, however; a significant impact of fertilizer application on pH was observed over control. Besides this, N level had a significant impact on OC content. The results align with the previous outcomes of Begum et al. (2021), who reported increased OC content with higher levels of N fertilization.

After the harvest of *S. costus* roots, a significant effect of fertilizer application over control on major soil nutrients was observed (Table 4). Available N and P content increased with the rise in the dose of N and P. The highest available N (391.23 and 382.42 kg ha^{-1}) and P (38.37 and 37.93 kg ha^{-1}) were registered with N_{120} and P_{60} among levels of N and P, respectively. In contrast, levels of K didn't show any significant variation in available N and P. However, available K was significantly affected by varying levels of nutrients and, the highest value was recorded with N_{120} (175.86 kg ha^{-1}), P_{60} (174.62 kg ha^{-1}), and K_{40} (176.54 kg ha^{-1}) among their respective levels. In addition, the fertilizer additions recorded significantly higher available N (569.89 kg ha^{-1}), P (55.69 kg ha^{-1}), and K (251.42 kg ha^{-1}) content after crop harvest over control (357.06 kg N ha^{-1}, 33.16 kg P ha^{-1} and 129.33 kg K ha^{-1}). The results corroborate the conclusions of Dong et al. (2012), who reported a notable influence of fertilizer applications on available nutrients in paddy soils.

4 Conclusions

Fertilizer applications of N, P, and K modulated the crop growth, dry root and essential oil yield, and chemical profile of *S. costus* essential oil. Among different levels of N, P, and K, the highest level of N (N_{120}), P (P_{60}), and K (K_{40}) produced the tallest plant, the maximum number of leaves per plant, increased dry matter per plant, higher leaf length & width, and root length & diameter, followed by N_{90}, P_{40}, and K_{20}. Similarly, the highest dry root yield was obtained by applying N_{120}, P_{60}, and K_{40} (4423.41, 4383.91, and 4222.34 kg ha^{-1}, respectively), which produced at par results with N_{90}, P_{40}, and K_{20} (4401.87, 4340.92 and 4163.22 kg ha^{-1}, respectively). The overall fertilizers applications increased the dry root yield and essential oil yield by 108.9% and 210.3%, respectively,

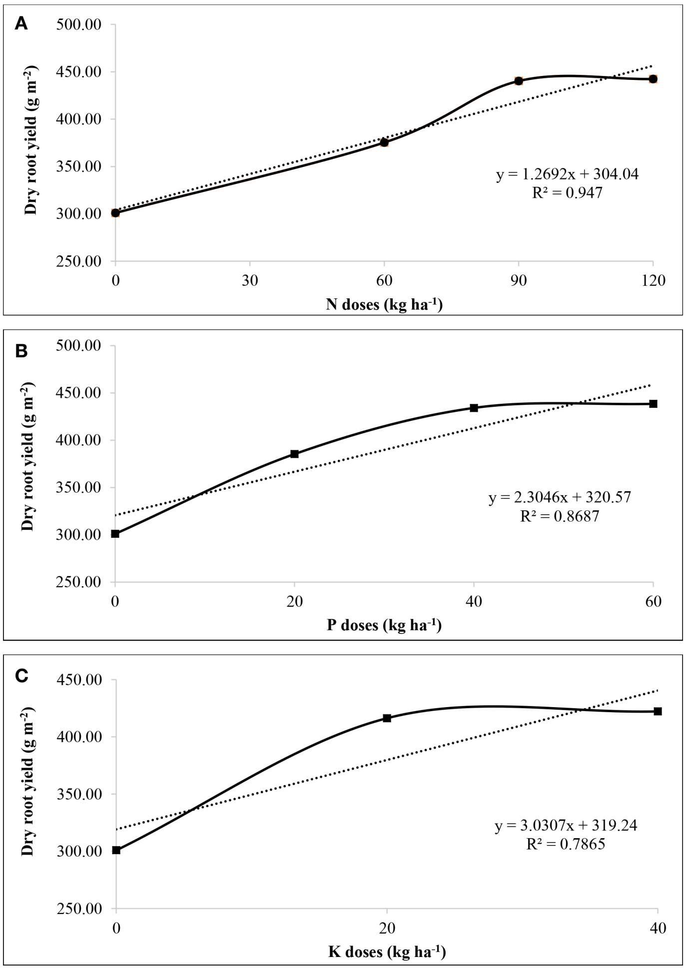

FIGURE 6
Regression equation developed between dry root yield, and N levels **(A)**, P levels **(B)**, and K levels **(C)**. The X-axis displays N, P and K levels in their respective graphs, and Y-axis represents the dry root yield in all three graphs.

TABLE 4 Effect of N, P, and K doses on soil pH, OC (%), available N, P and K (kg ha^{-1}) after harvest of *S. costus*.

Treatments	pH	OC (%)	Available N (kg ha^{-1})	Available P (kg ha^{-1})	Available K (kg ha^{-1})
Nitrogen Level (kg ha^{-1})					
N_{60}	6.64	0.67^{b}	370.20^{c}	36.15^{c}	158.02^{c}
N_{90}	6.64	0.78^{a}	378.34^{b}	36.87^{b}	168.96^{b}
N_{120}	6.62	0.81^{a}	391.23^{a}	38.37^{a}	175.86^{a}
SEm (±)	0.02	0.02	1.35	0.20	1.47
LSD (*P*=0.05)	NS	0.05	3.87	0.57	4.21
Phosphorus Level (kg ha^{-1})					
P_{20}	6.66	0.72	377.44^{b}	36.42^{c}	161.44^{c}
P_{40}	6.64	0.76	379.92^{b}	37.03^{b}	166.78^{b}
P_{60}	6.61	0.77	382.42^{a}	37.93^{a}	174.62^{a}

(Continued)

TABLE 4 Continued

Treatments	pH	OC (%)	Available N (kg ha^{-1})	Available P (kg ha^{-1})	Available K (kg ha^{-1})
SEm(±)	0.02	0.02	1.35	0.20	1.47
LSD (P=0.05)	NS	NS	3.87	0.57	4.21
Potassium Level (kg ha^{-1})					
K_{20}	6.64	0.74	379.15	37.03	158.68^a
K_{40}	6.63	0.75	380.69	37.23	176.54^b
SEm(±)	0.01	0.01	1.10	0.16	1.20
LSD (P=0.05)	NS	NS	NS	NS	3.44
Control	6.87^b	0.66	357.06^b	33.16^b	129.33^b
Others	9.95^a	1.12	569.89^a	55.69^a	251.42^a
SEm(±)	0.03	0.03	2.40	0.35	2.61
LSD (P=0.05)	0.09	NS	6.88	1.02	7.50

SEm indicates standard error of mean; LSD indicates Least Significant Difference; NS indicates not significant at P = 0.05.
N60, N90, N120, represents N levels @ 60, 90, and, 120 kg ha-1, respectively; P20, P40 and P60, represents P levels @ 20, 40 and 60 kg ha-1, respectively; and K20 and K40 indicates K levels @ 20 and 40 kg ha-1, respectively.

over control. The fertilizer application caused significant variations in the chemical makeup of the root essential oil. The regression curve showed that dry root yield increased till the application of N_{90}, P_{40}, and K_{20} among varying levels of N, P, and K, after that, increased marginally. Hence, from the present study, we concluded that economically sustainable cultivation and *ex-situ* conservation of *S. costus* could be achieved by applying N_{90}, P_{40}, and K_{20} doses of fertilizer. Further studies are desired to understand the influence of other factors, especially micronutrients, on crop growth, productivity, and *S. costus* essential oil composition.

Data availability statement

The raw data supporting the conclusions of this article will be made available by the authors, without undue reservation.

Author contributions

SV: Manuscript writing. DD: Data collection. SB: Data collection. SatS: Statistical analysis. MK: Chemical profiling. AK: Manuscript editing. DK: Chemical profiling. SanS: Planting material. RC: Conceptualisation, monitoring, statistical analysis, review and editing. All authors contributed to the article and approved the submitted version.

Acknowledgments

The authors are grateful to the Director of CSIR-IHBT, Palampur, India, for his unwavering support and providing necessary facilities required for this work. The authors acknowledge the Council of Scientific and Industrial Research (CSIR), Government of India, for financial support. This research work has been undertaken under the CSIR network project MLP-0172. The CSIR-IHBT communication number of this paper is 5210.

Conflict of interest

The authors declare that the research was conducted in the absence of any commercial or financial relationships that could be construed as a potential conflict of interest.

Publisher's note

All claims expressed in this article are solely those of the authors and do not necessarily represent those of their affiliated organizations, or those of the publisher, the editors and the reviewers. Any product that may be evaluated in this article, or claim that may be made by its manufacturer, is not guaranteed or endorsed by the publisher.

References

Abbaszadeh, B., and Haghighi, M. L. (2013). Effect of nutrition and harvest time on growth and essential oil content of *Thymus vulgaris* l. *J. Med. Plants By-products* 2, 143–151.

Aladakatti, Y. R., Palled, Y. B., Chetti, M. B., Halikatti, S. I., Alagundagi, S. C., Patil, P. L., et al. (2012). Effect of nitrogen, phosphorus and potassium levels on growth and yield of stevia (*Stevia rebaudiana* bertoni.). *Karn. J. Agric. Sci.* 25 (1), 25–29.

Ali, S. I., and Venkatesalu, V. (2022). Botany, traditional uses, phytochemistry and pharmacological properties of *Saussurea costus*-an endangered plant from himalaya- a review. *Phytochem. Lett.* 47, 140–155. doi: 10.1016/j.phytol.2021.12.008

Arab, A., Zamani, G. R., Sayyari, M. H., and Asili, J. (2015). Effects of chemical and biological fertilizers on morpho-physiological traits of marigold (*Calendula officinalis* l.). *Eur. J. Med. Plants* 8 (1), 60–68. doi: 10.9734/EJMP/2015/16697

Begum, R., Jahangir, M. M. R., Jahiruddin, M., Islam, M. R., Rahman, M. T., Rahman, M. L., et al. (2021). Nitrogen fertilization impact on soil carbon pools and their stratification and lability in subtropical wheat-mungbean-rice agroecosystems. *PloS One* 16 (10), e0256397. doi: 10.1371/journal.pone.0256397

Benedetto, C., D'Auria, M., Mecca, M., Prasad, P., Singh, P., Singh, S., et al. (2019). Chemical and biological evaluation of essential oil from *Saussurea costus* (Falc.) lipsch. from garhwal himalaya collected at different harvesting periods. *Nat. Prod. Res.* 33 (16), 2355–2358. doi: 10.1080/14786419.2018.1440219

Bhuvaneshwari,, Farooqi, A. A., Sreeramu, B. S., and Srinivasappa, K. N. (2002). Influence of nitrogen, phosphorus and potassium levels on growth, seed yield and essential oil content in anise (*Pimpinella anisum* l.). *J. Spices Aromat. Crops* 11 (2), 112–117.

Bray, R. H., and Kurtz, L. T. (1945). Determination of total, organic and available forms of phosphorus in soils. *Soil Sci.* 59, 39–45. doi: 10.1097/00010694-194501000-00006

Butola, J. S., and Samant, S. S. (2010). *Saussurea* species in Indian Himalayan region: diversity, distribution and indigenous uses. *Int. J. Plant Biol.* 1 (1), e9. doi: 10.4081/pb.2010.e9

Chalapathi, M. V., Kumar, N. D., Rao, G. G. E., and Jayaramaiah, R. (1999). Comparative performance of plant and ratoon crops of stevia. *Indian Agril.* 43, 211–212.

Chiyaneh, S. F., Rezaei-Chiyaneh, E., Amirnia, R., Afshar, R. K., and Siddique, K. H. M. (2022). Changes in the essential oil, fixed oil constituents, and phenolic compounds of ajowan and fenugreek in intercropping with pea affected by fertilizer sources. *Ind. Crops Prod.* 178, 114587. doi: 10.1016/j.indcrop.2022.114587

Dhar, P., and Dey, S. (2019). A study on the consumer behaviour for ayurvedic products with special reference to consumers in kolkata. *Int. J. Rec. Tren. Bus. Tour.* 3 (1), 76–84.

Dong, W., Zhang, X., Wang, H., Dai, X., Sun, X., Qiu, W., et al. (2012). Effect of different fertilizer application on the soil fertility of paddy soils in red soil region of southern China. *PloS One* 7 (9), e44504. doi: 10.1371/journal.pone.0044504

Eleiwa, M. E., Hamed, E. R., and Shehata, H. S. (2012). Biofertilizers and/or some micronutrients role on wheat plants grown on newly reclaimed soil. *Afr. J. Ecol.* 50 (4), 464–475. doi: 10.1111/j.1365-2028.2012.01342.x

Heidari, S., Azizi, F., Soltani, F., and Hadian, J. (2014). Foliar application of $Ca(NO_3)_2$ and KNO_3 affects growth, essential oil content, and oil composition of French tarragon. *Ind. Crops Prod.* 62, 526–532. doi: 10.1016/j.indcrop.2014.09.026

Kala, C. P., Dhyani, P. P., and Sajwan, B. S. (2006). Developing the medicinal plants sector in northern India: challenges and opportunities. *J. Ethnobio. Ethnomed.* 2 (1), 32–46. doi: 10.1186/1746-4269-2-32

Kawatani, T., Kaneki, Y., Tanabe, T., and Takahashi, T. (1980). On the cultivation of kaa he-e (*Stevia rebaudiana* bertoni) VI. response of kaa he-e to potassium fertilization rates and to the three major elements of fertilizer. *Japan. J. Trop. Agric.* 24 (3), 105–112. doi: 10.11248/jsta1957.24.105

Krouk, G., Lacombe, B., Bielach, A., Perrine-Walker, F., Malinska, K., Mounier, E., et al. (2010). Nitrate-regulated auxin transport by NRT1.1 defines a mechanism for nutrient sensing in plants. *Dev. Cell* 18 (6), 927–937. doi: 10.1016/j.devcel.2010.05.008

Kwon, S. J., Kim, H. R., Roy, S. K., Kim, H. J., Boo, H. O., Woo, S. H., et al. (2019). Effects of nitrogen, phosphorus and potassium fertilizers on growth characteristics of two species of bellflower (*Platycodon grandiflorum*). *J. Crop Sci. Biotech.* 22 (5), 481–487. doi: 10.1007/s12892-019-0277-0

Mahajan, M., Thakur, B. K., and Pal, P. K. (2021). Moisture stress and nitrogen availability modulate the secondary metabolite profiles, enzymatic activity, and physiological and agronomic traits of *Stevia rebaudiana*. *Plant Physiol. Biochem.* 162, 56–68. doi: 10.1016/j.plaphy.2021.02.018

Medda, P. S., and Hore, J. K. (2003). Effect of n and K on the growth and yield of turmeric in alluvial plains of West Bengal. *Indian J. Hortic.* 60 (1), 84–88.

Mehlich, A. (1984). Mehlich-3 soil test extractant: a modification of mehlich-2 extractant. *Commun. Soil Sci. Plant Anal.* 15 (12), 1409–1416. doi: 10.1080/00103628409367568

Mohan, E., Guruprasad, T. R., Herle, P. S., Seetharamu, G. K., and Murthy, M. K. K. (2004). Studies on biomass production, harvest index, concentration and uptake of NPK in different turmeric cultivars. *Indian J. Arecanut Spices Med. Plant* 6 (4), 122126.

Mollier, A., and Pellerin, S. (1999). Maize root system growth and development as influenced by phosphorus deficiency. *J. Exp. Bot.* 50 (333), 487–497. doi: 10.1093/jxb/50.333.487

Nurzynska-Wierdak, R. (2013). Does mineral fertilization modify essential oil content and chemical composition in medicinal plants? *Acta Sci. Pol. Hortorum. Cultus.* 12 (5), 3–16.

Pal, P. K., and Mahajan, M. (2017). Pruning system and foliar application of $MgSO_4$ alter yield and secondary metabolite profile of *Rosa damascena* under rainfed acidic conditions. *Front. Plant Sci.* 8. doi: 10.3389/fpls.2017.00507

Rathore, S., Debnath, P., and Kumar, R. (2020). Kuth {*Saussurea costus* (Falc.) lipsch.}: a critically endangered medicinal plant from himalaya. *J. Appl. Res. Med. Aromat. Plants* 20, 100277. doi: 10.1016/j.jarmap.2020.100277

Rawat, Y. S., Oinam, S. S., Vishvakarma, S. C. R., and Kuniyal, J. C. (2004). *Saussurea costus* (Falc.) lipsch.: a promising medicinal crop under cold desert agroecosystem in north western himalaya. *Indian J. Forest.* 27 (3), 297–303.

Rhykerd, C. L., and Overdahl, C. J. (1972). Nutrition and fertilizer use. In: C. H. Hanson (Eds.), Alfalfa Science and Technology. *Agronomy* 15, 437–465. doi: 10.2134/agronmonogr15.c20

Salehi, A., Fallah, S., Zitterl-Eglseer, K., Kaul, H. P., Surki, A. A., and Mehdi, B. (2019). Effect of organic fertilizers on antioxidant activity and bioactive compounds of fenugreek seeds in intercropped systems with buckwheat. *Agronomy* 9 (7), 367. doi: 10.3390/agronomy9070367

Sen, S., and Chakraborty, R. (2017). Revival, modernization and integration of Indian traditional herbal medicine in clinical practice: importance, challenges and future. *J. Tradit. Complement Med.* 7 (2), 234–244. doi: 10.1016/j.jtcme.2016.05.006

Shah, N. C. (2019). Kustha, *Saussurea costus* (*Saussurea lappa*): its unexplored history from the atharvaveda. *Indian J. Hist. Sci.* 54 (4), 420–434. doi: 10.16943/ijhs/2019/v54i4/49769

Shirolkar, S., Tripathi, R. K., and Potey, A. V. (2015). Evaluation of package inserts of ayurveda drug formulations from Mumbai city. *Ayu* 36 (4), 370–374. doi: 10.4103/0974-8520.190694

Singh, R. V., and Negi, S. C. (2003). Response of kuth (*Saussurea lappa* l.) to seed rates and nitrogen fertilizer. *Agric. Sci. Digest* 23, 155–156.

Soltanbeigi, A. (2020). Qualitative variations of lavandin essential oil under various storage conditions. *J. Essent. Oil Bear. Plants* 23 (6), 1237–1252. doi: 10.1080/0972060X.2020.1871076

Subbiah, B. V., and Asija, G. L. (1956). A rapid procedure for the determination of available nitrogen in soils. *Curr. Sci.* 25, 259–260.

Tahir, A. H., Hussain, Z., Yousuf, H., Fazal, F., Tahir, M. A., and Kashif, M. (2022). Traditional herbal medicine and its clinical relevance: a need to preserve the past for the future. *J. Biosci. Med.* 10 (7), 64–75. doi: 10.4236/jbm.2022.107005

Takei, K., Sakakibara, H., Taniguchi, M., and Sugiyama, T. (2001). Nitrogen-dependent accumulation of cytokinins in root and the translocation to leaf: implication of cytokinin species that induces gene expression of maize response regulator. *Plant Cell Physiol.* 42 (1), 85–93. doi: 10.1093/pcp/pce009

Verma, P. P. S., Padalia, R. C., Singh, V. R., Kumar, A., and Agri, B. K. (2019). Effect of nitrogen, phosphorus and potassium levels on growth and yield of turmeric (*Curcuma longa* l.) under the katyur valley of Western Himalayan region of uttarakhand. *J. Med. Plants Stud.* 7 (2), 117–122.

Verma, N., and Shukla, S. (2015). Impact of various factors responsible for fluctuation in plant secondary metabolites. *J. Appl. Res. Med. Aromat. Plants* 2 (4), 105–113. doi: 10.1016/j.jarmap.2015.09.002

Walkley, A., and Black, I. A. (1934). An examination of degtjareff method for determining soil organic matter and a proposed modification of the chromic acid titration method. *Soil Sci.* 37, 29–37. doi: 10.1097/00010694-193401000-00003

Zahara, K., Tabassum, S., Sabir, S., Arshad, M., Qureshi, R., Amjad, M. S., et al. (2014). A review of therapeutic potential of *Saussurea lappa*-an endangered plant from himalaya. *Asian Pac. J. Trop. Med.* 7, S60–S69. doi: 10.1016/S1995-7645(14)60204-2

Zheljazkov, V. D., Cantrell, C. L., Astatkie, T., and Cannon, J. B. (2011). Lemongrass productivity, oil content, and composition as a function of nitrogen, sulfur, and harvest time. *Agron. J.* 103 (3), 805–812. doi: 10.2134/agronj2010.0446

frontiers | Frontiers in Plant Science

TYPE Original Research
PUBLISHED 20 June 2023
DOI 10.3389/fpls.2023.1186890

Check for updates

OPEN ACCESS

EDITED BY
Jianwei Lu,
Huazhong Agricultural University, China

REVIEWED BY
Krishan K. Verma,
Guangxi Academy of Agricultural Sciences, China
Akbar Hossain,
Bangladesh Wheat and Maize Research Institute, Bangladesh
Milan Skalicky,
Czech University of Life Sciences Prague, Czechia

*CORRESPONDENCE
Cheng Xue
xuecheng@hebau.edu.cn

†These authors have contributed equally to this work

RECEIVED 15 March 2023
ACCEPTED 26 May 2023
PUBLISHED 20 June 2023

CITATION
Pan Y, Han X, Xu H, Wu W, Liu X, Li Y and Xue C (2023) Elevated atmospheric CO_2 delays the key timing for split N applications to improve wheat (*Triticum aestivum* L.) protein composition.
Front. Plant Sci. 14:1186890.
doi: 10.3389/fpls.2023.1186890

Elevated atmospheric CO_2 delays the key timing for split N applications to improve wheat (*Triticum aestivum* L.) protein composition

Yue Pan[1†], Xue Han[2†], Huasen Xu[1], Wei Wu[1], Xiaoming Liu[1], Yingchun Li[2] and Cheng Xue[1*]

[1]State Key Laboratory of North China Crop Improvement and Regulation/Key Laboratory for Farmland Eco-Environment of Hebei/College of Resources and Environmental Science, Hebei Agricultural University, Baoding, China, [2]Key Laboratory of Agro-environment and Climate Change of Agriculture Ministry, Institute of Environment and Sustainable Development in Agriculture, Chinese Academy of Agricultural Sciences, Beijing, China

Late stage nitrogen (N) applications following basic fertilization are commonly used to ensure grain yield and increase grain protein content in wheat. Split N applications at the late growth stage of wheat are an effective measure to improve N absorption and transport and thus increase grain protein content. However, whether split N applications can alleviate the decrease in grain protein content induced by elevated atmospheric CO_2 concentrations (e[CO_2]) remains unclear. In the present study, a free-air CO_2 enrichment system was used to investigate the effects of split N applications (at booting or anthesis) on grain yield, N utilization, protein content, and the composition of wheat under atmospheric (ACO_2; 400 ± 15 ppm) and elevated CO_2 concentrations (ECO_2; 600 ± 15 ppm). The results showed that wheat grain yield and grain N uptake increased by 5.0% (being grains per ear by 3.0%, 1000-grain weight by 2.0%, and harvest index by 1.6%) and 4.3%, respectively, whereas grain protein content decreased by 2.3% under ECO_2 conditions. Although the negative effect of e [CO_2] on grain protein content was not alleviated by split N applications, gluten protein content was enhanced due to the alteration of N distribution in different protein fractions (albumins, globulins, gliadins, and glutenins). Compared to that without split N applications, the gluten content of wheat grains increased by 4.2% and 4.5% when late stage N was applied at the booting stage under ACO_2 and anthesis under ECO_2 conditions, respectively. The results indicate that rational handling of N fertilizers may be a promising approach to coordinating grain yield and quality under the effects of future climate change. However, compared to ACO_2 conditions, the key timing for improving grain quality by split N applications should be postponed from the booting stage to anthesis under e [CO_2] conditions.

KEYWORDS

wheat, free-air CO_2 enrichment (FACE), split N application, grain yield, protein

1 Introduction

Elevated atmospheric CO_2 concentrations (e[CO_2]) are an important factor affecting global climate change. Atmospheric CO_2 concentrations have increased by nearly 50% since the Industrial Revolution, owing to the massive combustion of fossil fuels and excessive deforestation (IPCC, 2022). It is estimated that atmospheric CO_2 concentrations will increase from slightly over 410 ppm to 550 ppm by the mid-21st century and will further increase to 1000 ppm by the end of the 21st century if no effective restrictive measures are taken (Naidoo, 2022). As a substrate for photosynthesis, e[CO_2] has an important effect on crop yield and quality.

As the second most stable crop in the world, wheat (*Triticum aestivum* L.) supplies approximately 20% and 20–40% of human nutritional protein and minerals, respectively, and occupies approximately 25% of the global cereal production area (Punia et al., 2017; FAO, 2019). Changes in atmospheric CO_2 concentrations can affect the yield and quality of wheat by regulating its physiological and metabolic activities, thus influencing the development of roots, stems, leaves, and other organs (Wang et al., 2013; Dubey et al., 2015; Gojon et al., 2023). e[CO_2] can increase wheat grain yield by promoting photosynthesis; however, the mechanism of the increase in yield components is inconsistent (Han et al., 2015; Jing et al., 2017). Some studies have found that e[CO_2] increases wheat grain yield mainly by enhancing the ear number per unit area (Jing et al., 2017; Wang et al., 2023). However, other studies have indicated that an increase in the number of grains per spike is the main reason for the yield increase under e[CO_2] (Kimball et al., 2010; Han et al., 2015). Nitrogen (N), an essential nutrient for plants, is mainly stored in wheat grains in the form of proteins, which can be further sequentially fractionated into albumin, globulin, gliadin, and glutenin proteins based on their solubility in different solvents (Rossmann et al., 2019; Peng et al., 2022). Gliadins and glutenins together form gluten proteins, which play a crucial role in influencing the processing quality of wheat flour. The processing quality of wheat flour is positively correlated with grain protein content (GPC) and gluten protein content (accounting for 50–80% of GPC) within a certain range (Xue et al., 2019). Unfortunately, the increase in grain yield affected by e[CO_2] is often accompanied by a decrease in GPC, leading to a reduction in the processing quality of wheat flour (Bloom and Plant, 2021). Therefore, maintaining the increase in grain yield without reducing the processing quality is an urgent problem that requires investigation to ensure both grain yield and quality of wheat under future climate change conditions with respect to e[CO_2].

Rational management of N fertilization is an effective measure to ensure both high yield and quality of wheat (Zörb et al., 2018). Many studies have been conducted on the influence of N fertilizer management on grain yield and quality of wheat under e[CO_2] conditions (Dubey et al., 2015; Han et al., 2015; Dier et al., 2018; Pleijel et al., 2019; Bloom and Plant, 2021; Li et al., 2021). Unfortunately, the negative effect of e[CO_2] on wheat GPC cannot be eliminated by simply increasing the N application rate (Pleijel et al., 2019). In addition, excessive N application leads to reduced N uptake and use efficiency due to N losses, thus increasing the risk of environmental pollution (Dier et al., 2019; Bloom and Plant, 2021). In addition to the N fertilization rate, the timing of N application also significantly affects wheat grain yield and quality (Blandino et al., 2015; Wu et al., 2022). The N source for protein synthesis in wheat grains is partly derived from the N stored in the vegetative organs before anthesis and then transported to the grains (accounting for approximately 60–95%) and partly from the N absorbed after anthesis and transported directly to the grains (accounting for approximately 5–40%); the latter is more conducive to grain protein synthesis (Blandino et al., 2015). Gluten proteins (gliadins and glutenins) are mainly synthesized and accumulated from approximately 7 (for gliadins) and 10 (for glutenins) days after anthesis until maturity (Gupta et al., 1996; Panozzo et al., 2001). Therefore, the application of N fertilizer during the late growth stages of wheat (e.g., at booting, anthesis, or even post-anthesis) is considered an effective way to achieve the desired GPC and thus improve the processing quality of wheat (Barneix, 2007). Besides, the interaction between various plant N statuses and hormones plays an important role in regulating the senescence of wheat leaves and the source-sink relationship of carbon and N (Abid et al., 2018). If a relatively high level of plant hormones (such as cytokinin and auxin) is maintained in wheat during the post-anthesis period due to a sufficient N supply, a higher storage capacity and filling capacity can be obtained, leading to increased wheat yield and N use efficiency (Zhang et al., 2021). Previous studies from our group have shown that the booting stage is the key timing for split N applications in late wheat to improve both grain yield and quality by altering N partitioning into different fractions of gluten proteins and their subunits in the wheat grain (Xue et al., 2016a; Xue et al., 2016b; Xue et al., 2019; Wu et al., 2022). e[CO_2] could enhance the photosynthetic carbon assimilation of wheat, resulting in high N demand and promoting N uptake during vegetative growth and N translocation or distribution after wheat anthesis (Dier et al., 2019). However, no studies have reported whether the effects and mechanisms of late stage split N applications on the protein and quality of wheat still exist under e[CO_2]. Therefore, further studies are needed to elucidate whether late stage split N applications could coordinate the correlation between grain yield and quality of wheat by alleviating the reduction in GPC as a result of the enhancement of grain yield under e[CO_2]. In addition, the key timing for split N applications under e[CO_2] could be later than that under atmospheric CO_2 concentration conditions to increase GPC because the N absorbed post-anthesis is considered more conducive to grain protein synthesis (Blandino et al., 2015; Zörb et al., 2018).

Currently, the free-air CO_2 enrichment (FACE) system is recognized as an ideal research method for studying the response of plants to e[CO_2] conditions (Han et al., 2015; Li et al., 2021). This system is preferred over controllable chambers, open-top chambers, and other similar closed systems. In this study, the FACE system was used to investigate the responses of grain yield, protein and its

Abbreviations: e[CO_2], elevated atmospheric CO_2 concentrations; FACE, free-air CO_2 enrichment; GPC, grain protein content.

composition, and N uptake and utilization of wheat, as affected by split N applications at different timings under e[CO_2] conditions. The main objectives of this study were: (i) to determine whether split N applications at late growth stages of wheat could coordinate grain yield and quality of wheat under e[CO_2]; (ii) to verify whether the key timing for split N applications should be postponed under e [CO_2] compared with that under atmospheric CO_2 concentration conditions; and (iii) to reveal the mechanism of split N applications on grain yield and quality of wheat from the perspective of N absorption, utilization, and distribution in wheat plants and grain protein fractions under e[CO_2] conditions.

2 Materials and methods

2.1 Location

The experiment was conducted using the mini-FACE system of the Institute of Environment and Sustainable Development in Agriculture, Chinese Academy of Agricultural Sciences, from October 2020 to June 2022. The experimental site was located in Changping, Beijing (40°13′N, 116°14′E), China.

2.2 Agro-climatic conditions

The region has a continental monsoon climate, with an average annual precipitation of 267 mm and an average annual temperature of 9.6°C. The average monthly precipitation and temperature for the test years 2010–2019 are summarized in Figure 1. The soil type (0–0.2 m) was a clay loam with a pH of 8.4, an organic matter content of 29.4 g·kg^{-1}, total N content of 1.60 g·kg^{-1}, available phosphorus content of 39.4 mg·kg^{-1}, and available potassium content of 157.1 mg·kg^{-1}.

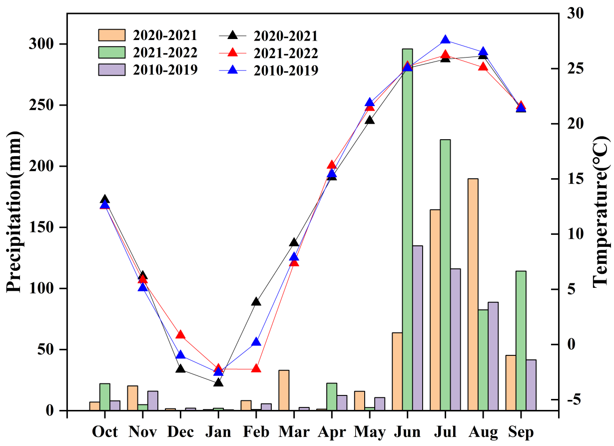

FIGURE 1
Monthly precipitation (bar) and temperature (line) during the experimental years in the growing period of wheat and mean values from 2010 to 2019 at the experimental site.

2.3 Experimental procedures

Three FACE circles and three control circles were used for the experiment. Each FACE circle comprised eight CO_2 gas release pipes with regular octagonal shapes, and the diameter of each circle was 4 m. The control circle was not installed with FACE pipes, and the other environmental conditions were consistent with the natural environmental conditions. The distance between each FACE and the control circle was greater than 14 m to eliminate interference from the CO_2 concentrations. The increase in CO_2 concentrations started at the beginning of March and ended in the middle of June of each year. The CO_2 ventilation time was 6:30–18:30 every day.

2.4 Experimental design

This experiment used a split-plot design with two factors: CO_2 concentrations and split N application timing. CO_2 concentrations were the main treatment, with control and elevated CO_2 concentrations. Control atmospheric CO_2 (ACO_2) was 400 ± 15 ppm, and elevated CO_2 (ECO_2) was 600 ± 15 ppm. The timing of the split N applications was a by-treatment, including no late stage N application (N_E), split N application at the booting stage (N_B), and split N application at the anthesis stage (N_F). Six treatments were set up in the experiment, with three replicates (Table 1). Treatment 1 (AN_E) and Treatment 4 (EN_E) had 69 kg N hm^{-2} applied at the jointing stage, without split N applications at the late stage; Treatment 2 (AN_B) and Treatment 5 (EN_B) had 29 kg N hm^{-2} applied at the jointing stage and 40 kg N hm^{-2} at the booting stage; Treatment 3 (AN_F) and Treatment 6 (EN_F) had 29 kg N hm^{-2} applied at the jointing stage and 40 kg N hm^{-2} at the anthesis stage. The total N fertilizer application rate for each treatment was 212 kg N hm^{-2}. Phosphate fertilizer (P_2O_5) and potassium fertilizer (K_2O) were applied as basal fertilizers at 136 kg·hm^{-2} and 43 kg·hm^{-2}, respectively. The base fertilizer was a mixed fertilizer, and the N fertilizer was urea (N ≥ 46%) in the late stage. Each experimental plot was 0.16 m^2 (0.4 m × 0.4 m).

Zhongmai 1062 winter wheat variety with high gluten content was used in this study. Wheat for the 2020–2021 season was sown on 6 October 2020, with a seeding rate of 187.5 kg·hm^{-2} and a row spacing of 0.2 m, and harvested on 19 June 2021. The 2021–2022 wheat season was sown on 21 October 2021, with a seeding rate of 225 kg·hm^{-2} and a row spacing of 0.2 m, and harvested on 17 June 2022. Other field management practices were conducted according to local standards.

2.5 Sample collection

At maturity, aboveground plant samples were collected, and 40 representative plants were selected to measure the grain yield and yield components. The remaining plants were separated into flag leaves, grains, glumes, cobs, remaining straws, and leaves. The fresh weight of samples was weighed and dried at 70°C to a constant weight.

TABLE 1 Overview of CO_2 level, N application rate, and timing in each treatment.

CO_2 levels	Treatment	N application rate (kg N hm^{-2})			
		Before sowing	Stem elongation	Booting	Anthesis
ACO_2	AN_E	143	69		
	AN_B	143	29	40	
	AN_F	143	29		40
ECO_2	EN_E	143	69		
	EN_B	143	29	40	
	EN_F	143	29		40

2.6 Measurements

2.6.1 Grain yield and yield components

A total of 40 plant samples were individually examined, and the number of ears and grains per plant was recorded and weighed. After drying, two groups of 500 grains each were randomly selected and weighed (accuracy set to 0.01 g). The 1000-grain weight was determined as follows: if the quotient of the difference between the two groups divided by the average value of the two groups did not exceed 5%, the sum of the weights of the two groups was used for the weight of 1000 grains; if the value was more than 5%, a third group was counted, and the two groups with the most similar weights were added to obtain the weight of 1000 grains.

2.6.2 Nitrogen content, absorption, and utilization in aboveground wheat organs

The aboveground wheat organs were milled into powder using a universal high-speed grinding machine (FW100, Tianjin Taenite Instrument Co. Ltd., Tianjin, China), and the total N content of each organ was determined using the H_2SO_4-H_2O_2 digestion Kjeldahl method (Zhang et al., 2019). The values were then calculated using the following equations:

$$\text{N uptake of aboveground organs } (g \cdot m^{-2}) = \text{organ biomass}(g \cdot m^{-2}) \times \text{total N content of each organ } (\%)$$

$$\text{Total aboveground N uptake} = \text{sum of organ N uptake}$$

$$\text{Harvest index } (\%) = \text{grain yield } (g \cdot m^{-2}) / \text{aboveground plant dry biomass } (g \cdot m^{-2}) \times 100$$

$$\text{N fertilizer partial factor productivity } (g \cdot g^{-1}) = \text{grain yield } (g \cdot m^{-2}) / \text{N fertilizer application rate } (g \cdot m^{-2})$$

$$\text{N harvest index } (\%) = \text{grain N uptake at maturity } (g \cdot m^{-2}) / \text{aboveground plant N uptake } (g \cdot m^{-2}) \times 100$$

$$\text{N absorption efficiency } (\%) = \text{plant N uptake } (g \cdot m^{-2}) / \text{N fertilizer application rate } (g \cdot m^{-2}) \times 100$$

$$\text{N use efficiency } (g \cdot g^{-1}) = \text{grain yield } (g \cdot m^{-2}) / \text{aboveground plant N uptake } (g \cdot m^{-2})$$

2.6.3 Protein composition and content

Wheat grains were milled using a Laboratory Mill 120 (Perten, Sweden) to obtain whole wheat flour. Albumin, globulin, gliadin, and glutenin in the grains were sequentially extracted using a continuous extraction method as previously described (Zhang et al., 2019). The protein content was determined using the Kjeldahl method and calculated by multiplying the N content by 5.7 (Liu et al., 2005; Zhang et al., 2019).

2.7 Statistical analyses

The experiment was designed as a split-plot; the CO_2 levels (atmospheric or elevated CO_2) were the whole-plot treatment, and the split N application timing levels (jointing, booting, and anthesis stages) were the split-plot treatment. The ANOVAs were used to examine the effects of CO_2 levels and split N application timing levels on yield performance (grain yield, ear number per unit area, grain number per ear, 1000-grain weight, and harvest index), quality traits (protein, albumin, globulin, gliadin, glutenin, and gluten), and N use traits (grain and aboveground N uptake, N uptake efficiency, partial factor productivity of N fertilizer, and N harvest index) using the statistical software R 4.2.3. The LSD was performed at the 5% probability level in ANOVAs. The general linear mixed model was performed to determine the effect of the year. A normal distribution test was performed for each model. The CO_2 level and split N application timing level were considered fixed factors, and the year, CO_2 concentrations, and block were considered random factors (Mitchell, 2003) when comparing the differences in yield performance, quality traits, and N use traits among different treatments in different years. If they did not follow a normal distribution, the data were converted to meet a normal distribution using different methods (Zuur et al., 2009). Origin Pro 2023 was used as the graphing software.

3 Results

3.1 Grain yield and components

Elevated atmospheric CO_2 concentrations were beneficial in increasing wheat grain yield, but there were significant differences between the years (Figure 2). Wheat grain yields in 2020–2021 and 2021–2022 amounted to 821.0–887.2 $g{\cdot}m^{-2}$ and 626.3–694.9 $g{\cdot}m^{-2}$, respectively. Compared to ACO_2, ECO_2 increased wheat yield by an average of 5.0% in both seasons. Wheat grain yield was not influenced by split N applications under ACO_2 and ECO_2 conditions.

According to the analysis of yield components and harvest index of wheat in both seasons (Table 2), CO_2 concentrations and split N applications at the late growth stage had no significant effect on the number of ears per unit area of wheat. However, ECO_2 significantly increased the number of grains per spike, 1000-grain weight, and harvest index of wheat by 3.03, 1.98, and 1.58%, respectively, compared to ACO_2. The split N application at the late growth stages significantly affected the 1000-grain weight and harvest index of wheat. Compared to no split N application (EN_E), the split N application under ECO_2 conditions increased the 1000-grain weight by 1.12% at the booting stage (EN_B) and decreased it by 1.12% at anthesis (EN_F). No significant effects were observed under the ACO_2 conditions. In addition, under ACO_2 and ECO_2 conditions, the wheat harvest index with split N application at the booting stage was the highest and increased by 2.52% and 1.56%, respectively, compared to that without split N application. However, this effect was not observed in split N applications at anthesis.

3.2 Grain protein concentration and protein composition

Elevated atmospheric CO_2 concentrations were generally detrimental to wheat grain protein content, but there were significant differences between the years (Figure 3). The grain protein content of wheat in 2020–2021 and 2021–2022 was 10.9–11.5% and 12.2–12.4%, respectively. On average, the grain protein content of wheat under ECO_2 conditions was reduced by 2.32% compared to that under ACO_2 conditions. There were no significant effects of the different late stage split N applications on wheat grain protein content under both ACO_2 and ECO_2 conditions.

From the two-year average value, CO_2 concentrations had no significant effect on the grain protein composition (albumin, globulin, gliadin, and glutenin contents) of wheat (Figure 4). The wheat grain contained 2.16–2.33% albumin, 0.95–1.03% globulin, 3.25–3.48% gliadin, and 3.90–4.18% glutenin. The gliadin content of wheat grains was significantly affected by late stage split N application; under ACO_2 conditions, split N application at the booting stage (AN_B) increased gliadin content by 6.43% compared to that without split N application (AN_E) (Figure 4C).

Although the effects on the content of gliadin and glutenin in wheat grains were inconsistent, different split N applications at the late stages had significant effects on the content of gluten (gliadin and glutenin) in wheat grains (Figure 5). Under ACO_2 and ECO_2 conditions, late stage split N application increased gluten protein content by 3.12% and 4.06%, respectively, compared to that without split N application. Under ACO_2 conditions, AN_B was more effective than AN_E in increasing grain gluten protein by 4.24%. In contrast, under ECO_2 conditions, EN_F was more effective than EN_E in increasing grain gluten protein by 4.52%. The results showed that the key timing of split N application for improving grain gluten protein was delayed under ECO_2 conditions compared to that under ACO_2 conditions.

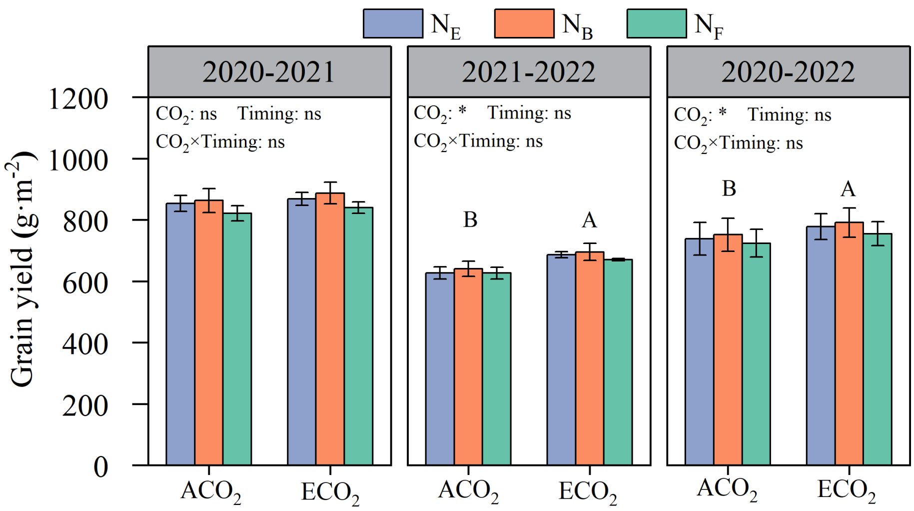

FIGURE 2
Effects of e[CO_2] and split N application on wheat grain yield. Error bars represent the standard error. Multiple comparisons were performed within the same year: lowercase letters indicate significant differences between treatments at different N application periods at the same CO_2 concentrations in the same year (p< 0.05); uppercase letters indicate significant differences between treatments at different CO_2 concentrations in the same year (p < 0.05). ns, not significant; *p< 0. 05.

TABLE 2 Effects of elevated atmospheric CO_2 concentrations and N topdressing timing on wheat yield components and harvest index.

Year	CO_2 levels	Treatment	Number of ears per unit area (m^{-2})	Grains per ear	1000-grain weight (g)	Harvest index (%)
2020-2021	ACO_2	N_E	595.8 ± 20.5 aA	29.8 ± 0.3 aA	47.4 ± 0.1 aA	42.3 ± 0.3 bA
		N_B	602.1 ± 17.1 aA	28.2 ± 0.8 aA	47.8 ± 0.1 aA	43.8 ± 0.2 aA
		N_F	597.9 ± 18.5 aA	28.8 ± 0.8 aA	47.4 ± 0.4 aA	42.1 ± 0.3 bA
	ECO_2	N_E	580.8 ± 18.4 aA	29.4 ± 0.9 aA	47.7 ± 0.3 abA	42.8 ± 0.5 aA
		N_B	600.0 ± 18.8 aA	29.2 ± 0.5 aA	48.5 ± 0.2 aA	43.8 ± 0.3 aA
		N_F	573.8 ± 14.2 aA	30.0 ± 0.2 aA	47.3 ± 0.2 bA	42.2 ± 0.5 aA
2021-2022	ACO_2	N_E	500.0 ± 9.5 aA	27.6 ± 0.6 aA	40.4 ± 0.3 aB	45.4 ± 0.2 bB
		N_B	494.2 ± 16.9 aA	28.9 ± 0.6 aA	39.9 ± 0.2 aB	46.2 ± 0.2 aA
		N_F	497.9 ± 18.2 aA	28.3 ± 0.9 aA	39.9 ± 0.1 aB	45.3 ± 0.2 bB
	ECO_2	N_E	555.0 ± 16.8 aA	30.0 ± 0.6 aA	41.8 ± 0.2 aA	46.8 ± 0.3 aA
		N_B	541.7 ± 24.0 aA	29.3 ± 0.7 aA	41.9 ± 0.1 aA	47.2 ± 0.5 aA
		N_F	535.4 ± 11.0 aA	28.9 ± 0.7 aA	41.2 ± 0.1 bA	46.7 ± 0.2 aA
2020-2022	ACO_2	N_E	547.9 ± 23.7 aA	28.7 ± 0.6 aA	43.9 ± 1.6 aB	43.9 ± 0.7 bB
		N_B	548.1 ± 26.4 aA	28.5 ± 0.5 aA	43.9 ± 1.8 aB	45.0 ± 0.6 aA
		N_F	547.9 ± 25.2 aA	28.6 ± 0.6 aA	43.7 ± 1.7 aA	43.7 ± 0.8 bA
	ECO_2	N_E	567.9 ± 12.6 aA	29.7 ± 0.5 aA	44.7 ± 1.3 bA	44.8 ± 1.0 bA
		N_B	570.8 ± 18.9 aA	29.3 ± 0.4 aA	45.2 ± 1.5 aA	45.5 ± 0.8 aA
		N_F	554.6 ± 11.8 aA	29.4 ± 0.4 aA	44.2 ± 1.4 cA	44.4 ± 1.0 bA
ANOVA results	Year		***	ns	***	***
	CO_2		ns	*	***	***
	Timing		ns	ns	**	***
	Year×CO_2		**	ns	***	*
	Year×Timing		ns	ns	*	ns
	CO_2×Timing		ns	ns	ns	ns
	Year×CO_2×Timing		ns	ns	ns	ns

Error bars represent the standard error. Multiple comparisons were performed within the same year: lowercase letters indicate significant differences between treatments at different N application rates at the same CO_2 concentrations in the same year ($p< 0.05$); uppercase letters indicate significant differences between treatments at different CO_2 concentrations in the same year ($p< 0.05$). ns, not significant; *p< 0.05; **p< 0.01; ***p< 0.001.

3.3 N uptake and utilization

The elevated atmospheric CO_2 concentrations significantly increased the aboveground N uptake of wheat, but there were significant differences between years (Figure 6A). The aboveground N uptake of wheat in 2020–2021 and 2021–2022 amounted to 18.42–19.78 g·m^{-2} and 16.91–18.70 g·m^{-2}, respectively. The aboveground N uptake of wheat in both seasons increased by 3.21% under ECO_2 conditions compared to that under ACO_2 conditions. The aboveground N uptake of wheat was significantly affected by the split N application at the late growth stage. AN_B increased by 4.55% compared to AN_E under ACO_2 conditions, whereas there was no such effect with split N applications at anthesis (AN_F). Under ECO_2 conditions, there was no difference between EN_B and EN_E, while EN_F reduced aboveground N uptake of wheat by 4.82% compared to EN_E.

From the two-year average value, the grain N uptake for each treatment was analyzed with the same significance as that of the aboveground N uptake (Figures 6A, B). The grain N uptake of wheat in 2020–2021 and 2021–2022 amounted to 15.66–16.95 g·m^{-2} and 13.67–15.86 g·m^{-2}, respectively. The N uptake of wheat grains significantly increased by 4.34% under ECO_2 conditions compared to that under ACO_2 conditions. In addition, the N uptake of wheat grains was significantly affected by late stage split N applications (Table 3). Under ACO_2 and ECO_2 conditions, the N uptake of wheat grains with split N applications at the booting stage was the highest, increasing by 5.98% and 0.98%, respectively, compared to that without split N application, whereas there was no such effect

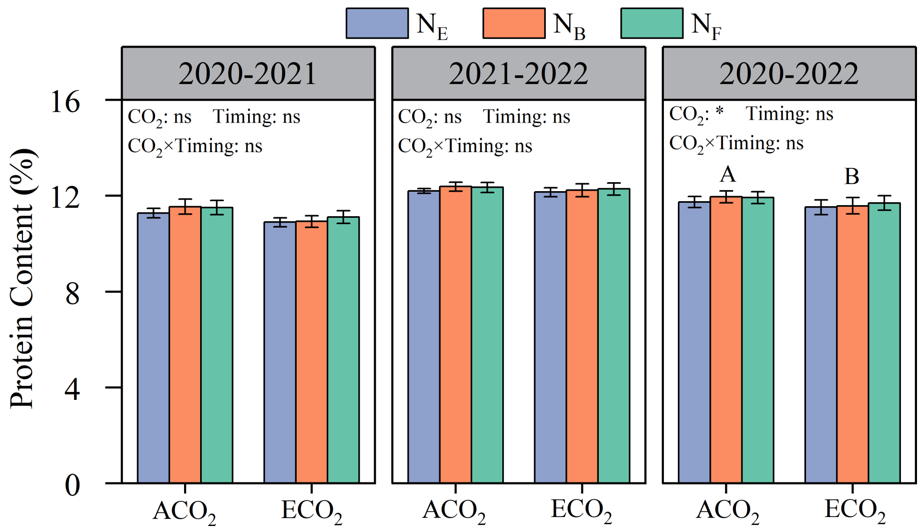

FIGURE 3
Effects of e[CO_2] and split N application on grain protein concentration in wheat grain. Error bars represent the standard error. Multiple comparisons were performed within the same year: lowercase letters indicate significant differences between treatments at different N application rates at the same CO_2 concentrations in the same year ($p < 0.05$); uppercase letters indicate significant differences between treatments at different CO_2 concentrations in the same year ($p < 0.05$). ns, not significant; *$p < 0.05$.

with split N applications at anthesis. The results showed that split N applications at the booting stage promoted the uptake and accumulation of N in wheat and grains.

The elevated atmospheric CO_2 concentrations were beneficial for increasing the partial factor productivity of N fertilizers and the N harvest index, but there were significant differences between the years (Figures 6C, D). Under ECO_2, the partial factor productivity of N fertilizers and harvest index increased by 4.96% and 1.15%, respectively, compared to those under ACO_2. Under ACO_2 and ECO_2 conditions, there was no significant effect of split N application on the partial factor productivity of N fertilizers or the N harvest index. Although there was a significant effect of ECO_2 and split N application on the N uptake efficiency of wheat (Figure 6E), there was no significant interaction effect on the N use efficiency of wheat (Figure 6F). The results showed that elevated atmospheric CO_2 concentrations increased grain yield and promoted N uptake in wheat. The N use efficiency of wheat grain in 2020–2021 and 2021–2022 was 43.46–45.65% and 36.03–37.79%, respectively. Overall, grain N uptake was not affected by CO_2 concentrations.

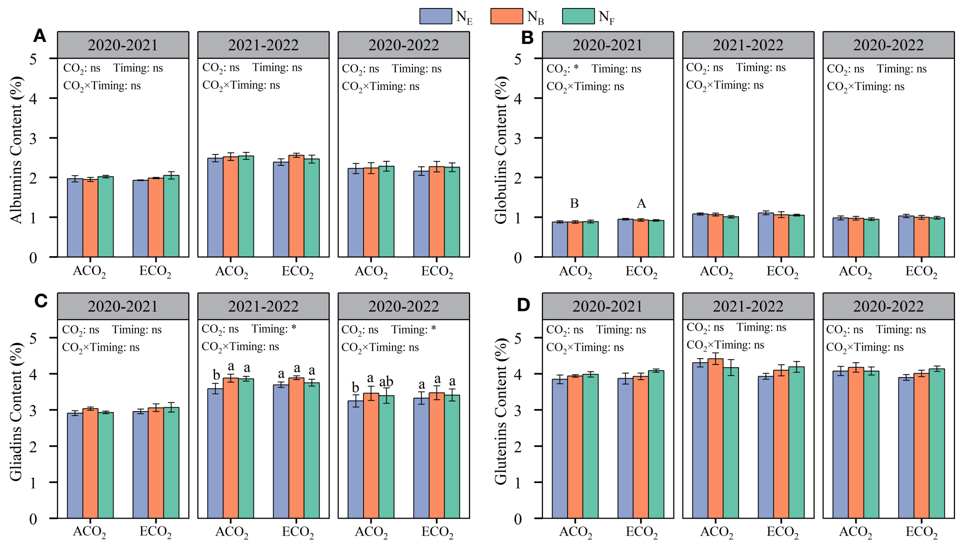

FIGURE 4
Effects of e[CO2] and split N application on albumins content **(A)**, globulims content **(B)**, gliadims content **(C)**, and glutenins content **(D)** in wheat grain. Error bars represent the standard error. Multiple comparisons were performed within the same year: lowercase letters indicate significant differences between treatments at different N application rates at the same CO2 concentrations in the same year ($p < 0.05$); uppercase letters indicate significant differences between treatments at different CO2 concentrations in the same year ($p < 0.05$). ns, not significant; *$p < 0.05$.

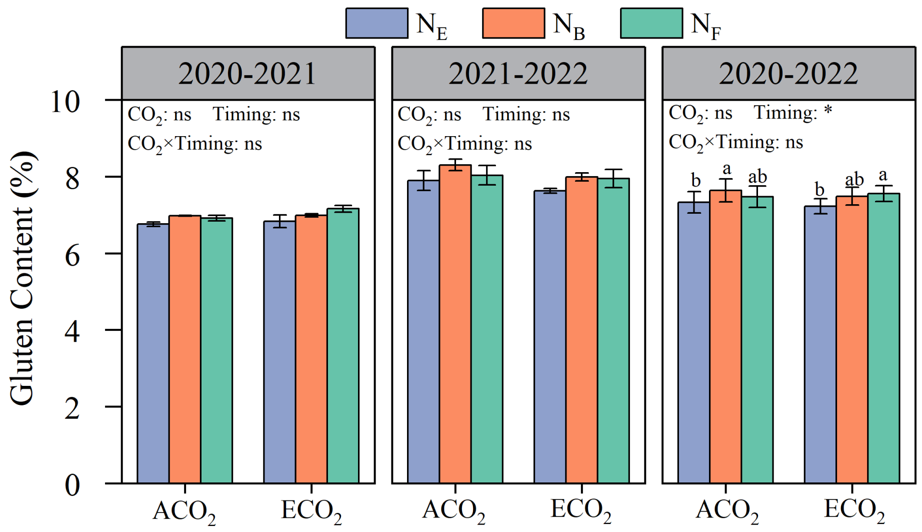

FIGURE 5
Effects of e[CO_2] and split N application on the gluten protein content of wheat grain. Error bars represent the standard error. Multiple comparisons were performed within the same year: lowercase letters indicate significant differences between treatments at different N application rates at the same CO_2 concentrations in the same year ($p< 0.05$); uppercase letters indicate significant differences between treatments at different CO_2 concentrations in the same year ($p< 0.05$). ns, not significant; *p< 0.05.

4 Discussion

4.1 Yield components influenced by e[CO_2] and split N application in wheat

High variations in wheat grain yield were achieved between seasons; yield ranged from 821.0 to 887.2 g·m^{-2} in 2020–2021 and from 626.3 to 694.9 g·m^{-2} in 2021–2022. The relatively low grain yield in the 2021–2022 season may have resulted from high precipitation in the wheat grain-filling period, which impacted the growth of wheat grain, leading to a much lower kernel weight than that in 2020–2021 (Figure 1 and Table 2). Wheat grain yield was increased (5.0%) by ECO_2 compared to that by ACO_2 in this study (Figure 2), which is consistent with several studies reporting that e [CO_2] can improve wheat grain yield (Wang et al., 2013; Han et al., 2015; Dier et al., 2018; Dier et al., 2019). e[CO_2] improves the net photosynthetic rate of wheat leaves by promoting the carboxylation reaction of RuBisCO to improve the carboxylation rate and reducing photorespiration by inhibiting the oxidative competition of RuBisCO enzymes, thus enhancing the net photosynthetic efficiency. An increase in photosynthetic efficiency is conducive to photosynthetic carbon assimilation, thereby increasing carbohydrate accumulation (Hasan et al., 2021; Hamani et al., 2023). Although the highest grain yield was obtained when late N applications were split at the booting stage, no significant effects of split N application on grain yield were observed in either the ACO_2 or ECO_2 treatments. One possible reason is that the N supply from fertilizer and soil was sufficient to meet the N demand of wheat, which ensured the tillering and growth of wheat because the total N and organic matter contents in the soil were at medium to high levels (Navarro et al., 2020). On the other hand, the N loss from the soil decreased due to inhibition in the nitrifying and denitrifying communities, which ensured N availability for wheat (Liu et al., 2023). Further analysis of the yield components and harvest index showed that the number of kernels per ear, 1000-grain weight, and harvest index of wheat increased under e[CO_2] conditions. Moreover, split N applications significantly influenced the 1000-kernel weight and harvest index of wheat (Table 2). These results indicate that e[CO_2] during grain filling limits the carbon sink but enriches the N sink capacity, as demonstrated by other studies, thus increasing the N demand of wheat (Martínez-Peña et al., 2022; Martínez-Peña et al., 2023). Split N applications at the late growth stages (booting or anthesis) met the elevated N demand of wheat during grain filling due to e[CO_2], which prolonged the grain-filling period (Kong et al., 2016) and promoted dry matter accumulation and transport to the grains, leading to an improved grain weight and harvest index of wheat.

4.2 Grain protein composition influenced by e[CO_2] and split N applications in wheat

Consistent with most studies (Högy et al., 2013; Walker et al., 2017; Rezvi et al., 2023), the results of the present study clearly show that e[CO_2] decreased GPC (Figure 3) because of the higher rate of increase in grain yield (5.0%, Figure 2) compared to that of grain N uptake (3.2%, Figure 6), resulting in a dilution effect in GPC. In addition, other mechanisms such as lowered transpiration (reduced nutrient acquisition in the roots due to reduced mass flow in the soil and diminished nutrient translocation *via* the xylem sap in the shoots), disruption of N assimilation (reduced photorespiration leads to reduced NO_3^- assimilation and N content in the shoots due to the insufficient NADH in the cytosol to drive the NO_3^- reduction reaction), and regulation of root N uptake and signaling

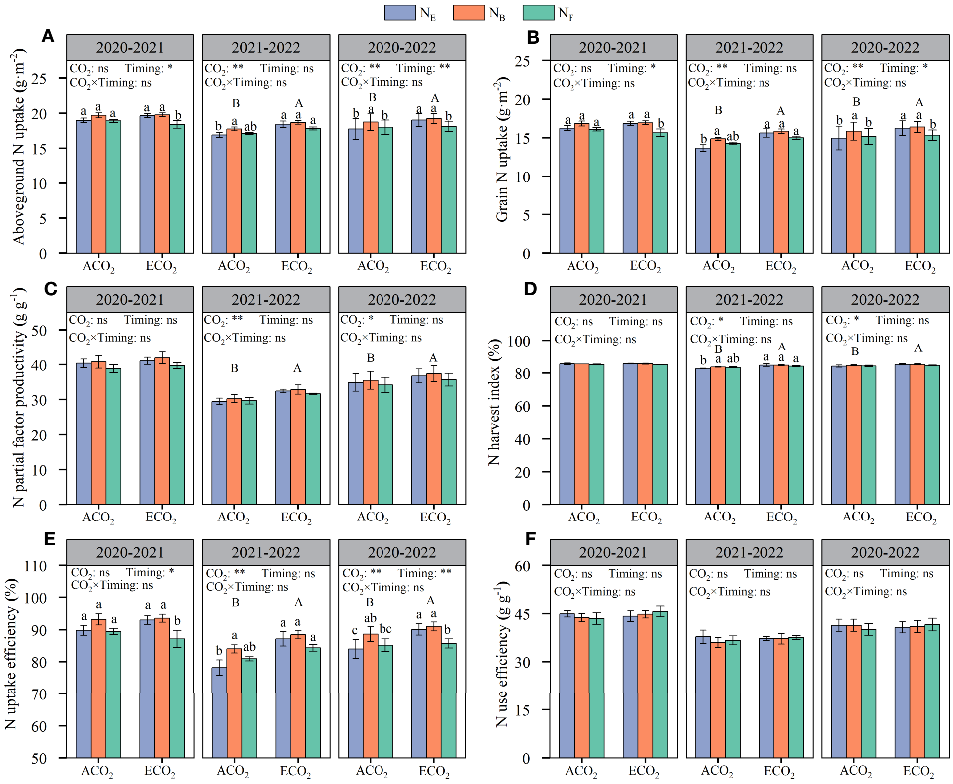

FIGURE 6
Effects of e[CO2] and split N application on aboveground N uptake **(A)**, grain N uptake **(B)**, N partial factor productivity **(C)**, N harvest index **(D)**, N uptake efficiency **(E)**, and N use efficiency **(F)** in wheat. Error bars represent the standard error. Multiple comparisons were performed within the same year: lowercase letters indicate significant differences between treatments at different N application rates at the same CO2 concentrations in the same year ($p < 0.05$); uppercase letters indicate significant differences between treatments at different CO2 concentrations in the same year ($p < 0.05$). ns, not significant; *$p < 0.05$; **$p < 0.01$.

(deregulated NO_3^- uptake systems in the root leading to a lower rate of NO_3^- acquisition) may also exert a great contribution to the decrease in GPC under e[CO_2] conditions (Gojon et al., 2023). e[CO_2] increased carbon sources, and limited storage capacity led to excessive accumulation of soluble sugars, such as sucrose and starch, in photosynthetic organs, resulting in an imbalance in the source-sink relationship of carbon and N in wheat (Hasan et al., 2021). Furthermore, although the GPC was reduced, the grain protein composition (albumins, globulins, gliadins, and glutenins) was not altered by e[CO_2] (Figures 4 and 5). This is inconsistent with Wieser et al. (2008), who reported that gliadin and glutenin content decreased by 20% and 15%, respectively, under e[CO_2] conditions. Besides, Soba et al. (2019) found that e[CO_2] increased gluten content by 32% and gliadin content by 79.6%, while glutenin content decreased by 4.3%. It is concluded that e[CO_2] altered the N metabolism and the kinetics of protein accumulation, suggesting a critical impact on amino acid synthesis, N remobilization, and redistribution (Singh et al., 2020). However, the grain protein composition was altered by split N applications. Gluten protein content (gliadins and glutenins) was increased by split N applications at booting and anthesis under the ACO_2 and ECO_2 treatments, respectively, compared to that without split N applications (Figure 5). Changes in gliadin content were more sensitive to split N applications than those in glutenin content, which may be closely related to the synthesis of grain protein fractions (Rossmann et al., 2019; Xue et al., 2019). Structural proteins (mainly albumins and globulins) begin to accumulate in the early stages of wheat grain development, are synthesized and accumulated from anthesis to approximately 20 days post-anthesis, and are mainly regulated by sinks (Martre et al., 2003). However, gluten proteins (mainly gliadins and glutenins, accounting for approximately 80% of grain protein) are mainly considered source-regulated and begin to synthesize and accumulate from around 7 to 10 days post-anthesis until the end of grain filling, with gliadins being synthesized slightly earlier than glutenins (Barneix, 2007). Therefore, since N absorbed post-anthesis contributes more directly to grain N accumulation (Blandino et al., 2015), split N applications at late growth stages of wheat may induce the reprogramming of various biosynthetic pathways, such as hormone signal transduction and photosynthesis, by regulating leaf senescence and N reabsorption to provide more available N for grains, thus promoting gluten (especially gliadin) synthesis based on meeting N demand for structural protein synthesis (Zhong et al., 2023). In addition, the key timing of split N applications for optimizing grain protein composition differed under atmospheric CO_2 and e[CO_2] conditions. Compared to that without split N applications, the gluten protein content of wheat grains improved when late N was applied at booting (AN_B) and

TABLE 3 Results of the ANOVA analysis.

		Grain yield ($g{\cdot}m^{-2}$)	Protein Content (%)	Albumins Content (%)	Globulins Content (%)	Gliadins Content (%)	Glutenins Content (%)	Gluten Content (%)	Grain N uptake ($g{\cdot}m^{-2}$)	Aboveground N uptake ($g{\cdot}m^{-2}$)	N harvest index (%)	N uptake efficiency (%)	N use efficiency ($g{\cdot}g^{-1}$)	N partial factor productivity ($g{\cdot}g^{-1}$)
ANOVA results	Year	**	**	**	**	**	*	**	**	**	**	**	**	**
	CO_2	*	*	ns	ns	ns	ns	ns	**	**	*	**	ns	*
	Timing	ns	ns	ns	ns	*	ns	*	*	**	ns	ns	ns	ns
	Year×CO_2	ns	ns	ns	ns	ns	ns	ns	**	*	*	*	ns	ns
	Year×Timing	ns	ns	ns	ns	ns	ns	ns	ns	ns	ns	ns	ns	ns
	CO_2×Timing	ns	ns	ns	ns	ns	ns	ns	ns	ns	ns	*	ns	ns
	Year×CO_2×Timing	ns	ns	ns	ns	ns	ns	ns	ns	ns	ns	ns	ns	ns

Error bars represent the standard error. ns, not significant; *$p < 0.05$; **$p < 0.01$; ***$p < 0.001$.

anthesis (EN_F) under atmospheric CO_2 (ACO_2) and e[CO_2] (ECO_2) conditions, respectively (Figure 5). One possible reason for this is that e[CO_2] promotes dry matter and N accumulation in wheat (Figure 6) and increases N translocation and its contribution to grain N accumulation compared to atmospheric CO_2 concentration conditions (Högy et al., 2009; Dier et al., 2019). Therefore, split N applications at a relatively later stage (at anthesis compared to the booting stage) provided a more effective N source for gluten synthesis and accumulation and altered N distribution in grain protein fractions (Hellemans et al., 2018; Rossmann et al., 2019; Ar et al., 2020).

In conclusion, e[CO_2] increased the grain yield while reducing GPC in wheat. Although split N applications at the late growth stages of wheat could not eliminate the negative effect of e[CO_2] on GPC, grain protein composition was improved owing to the optimized distribution of N into different grain protein fractions, leading to an increase in gluten protein content, which was beneficial for wheat quality improvement. In addition, the key timing for split N applications in coordinating the yield and quality of wheat by improving grain protein composition was postponed from the booting stage to around anthesis under e[CO_2] conditions compared to that under atmospheric CO_2 concentration conditions. Therefore, it is possible to achieve both high wheat yield and quality without increasing the input of N fertilizer through the rational application of N fertilizer at the critical growth stage of wheat under elevated atmospheric CO_2 concentrations.

5 Conclusion

e[CO_2] can increase the grain yield but reduce the protein content of wheat. The application of N fertilizer (split from the N applied at the jointing stage) at the late growth stage of wheat did not alleviate the negative effects of e[CO_2]. However, it can alter the distribution of N in the grain protein fractions to increase the gluten protein content, which is conducive to improving the processing quality of wheat. The key timing for split N applications in coordinating wheat yield and quality by improving grain protein composition should be moved from the booting stage to around anthesis under e[CO_2] conditions. Results from the present study indicate that rational handling of N fertilizer applications at the critical growth stage may be a promising approach to coordinate grain yield and quality of wheat under future climate change conditions. This offers the potential to maintain or even reduce N fertilizer inputs when N fertilizers are rationally distributed during wheat growth at the optimal time for wheat production under elevated atmospheric CO_2 concentrations in the future.

Data availability statement

The original contributions presented in the study are included in the article/supplementary material. Further inquiries can be directed to the corresponding author.

Author contributions

YP conducted the experiments under the supervision of CX. YP and XH performed the statistical analysis and wrote the manuscript. CX revised the manuscript. XH, HX, WW, XL, and YL finalized the experiments and the manuscript. All authors contributed to the article and approved the submitted version.

Funding

This work was supported by the National Key Research & Development project (No. 2019YFA0607403), the National Natural Science Foundation of China (No. 31801931), the Youth top-notch talent project of Hebei Provincial Department of Education (No. BJ2020026), and the State Key Laboratory of North China Crop Improvement and Regulation (No. NCCIR2021ZZ-8).

Conflict of interest

The authors declare that the research was conducted in the absence of any commercial or financial relationships that could be construed as a potential conflict of interest.

Publisher's note

All claims expressed in this article are solely those of the authors and do not necessarily represent those of their affiliated organizations, or those of the publisher, the editors and the reviewers. Any product that may be evaluated in this article, or claim that may be made by its manufacturer, is not guaranteed or endorsed by the publisher.

References

Abid, M., Tian, Z., Zahoor, R., Ata-Ul-Karim, S. T., Daryl, C., Snider, J. L., et al. (2018). Pre-drought priming: a key drought tolerance engine in support of grain development in wheat. *Adv. Agron.* 152, 51–85. doi: 10.1016/bs.agron.2018.06.001

Ar, A., Kas, B., Gr, C., Jmg, C., and Khm, A. (2020). Effects of a late n fertiliser dose on storage protein composition and bread volume of two wheat varieties differing in quality. *J. Cereal Sci.* 93, 102944. doi: 10.1016/j.jcs.2020.102944

Barneix, A. J. (2007). Physiology and biochemistry of source-regulated protein accumulation in the wheat grain. *J. Plant Physiol.* 164, 581–590. doi: 10.1016/j.jplph.2006.03.009

Blandino, M., Vaccino, P., and Reyneri, A. (2015). Late-season nitrogen increases improver common and durum wheat quality. *Agron. J.* 107, 680–690. doi: 10.2134/agronj14.0405

Bloom, A. J., and Plant, R. E. (2021). Wheat grain yield decreased over the past 35 years, but protein content did not change. *J. Exp. Bot.* 72, 6811–6821. doi: 10.1093/jxb/erab343

Dier, M., Meinen, R., Erbs, M., Kollhorst, L., Baillie, C. K., Kaufholdt, D., et al. (2018). Effects of free air carbon dioxide enrichment (FACE) on nitrogen assimilation and growth of winter wheat under nitrate and ammonium fertilization. *Glob. Change Biol.* 24, 40–54. doi: 10.1111/gcb.13819

Dier, M., Sickora, J., Erbs, M., Weigel, H. J., Zörb, C., and Manderscheid, R. (2019). Positive effects of free air CO_2 enrichment on n remobilization and post-anthesis n uptake in winter wheat. *Field Crops Res.* 234, 107–118. doi: 10.1016/j.fcr.2019.02.013

Dubey, S. K., Tripathi, S. K., and Pranuthi, G. (2015). Effect of elevated CO_2 on wheat crop: mechanism and impact. *Crit. Rev. Env. Sci. Tec.* 45, 2283–2304. doi: 10.1080/10643389.2014.1000749

FAO (2019). Food and agriculture organization of the united nations for a world without hunger fisheries and aquaculture department cultured aquatic species information programme siganus spp. doi: 10.1016/B978-0-12-386454-3.00988-X

Gojon, A., Cassan, O., Bach, L., Lejay, L., and Martin, A. (2023). The decline of plant mineral nutrition under rising CO_2: physiological and molecular aspects of a bad deal. *Trends Plant Sci.* 28, 185–198. doi: 10.1016/j.tplants.2022.09.002

Gupta, R. B., Masci, S., Lafiandra, D., Bariana, H. S., and Macritchie, F. (1996). Accumulation of protein subunits and their polymers in developing grains of hexaploid wheats. *J. Exp. Bot.* 47, 1377–1385. doi: 10.1093/jxb/47.9.1377

Hamani, A. K. M., Abubakar, S. A., Wang, G. S., Kama, R., Kurihara, T., Liu, K., et al. (2023). Optimized application of combined nitrogen and microbial decomposing inoculants increases wheat (*Triticum aestivum* l.) physiological growth and mitigates global warming potential under different water regimes. *Environ. Exp. Bot.* 206, 105170. doi: 10.1016/j.envexpbot.2022.105170

Han, X., Hao, X. Y., Lam, S. K., Wang, H. R., Li, Y. C., Wheeler, T., et al. (2015). Yield and nitrogen accumulation and partitioning in winter wheat under elevated CO_2: a 3-year free-air CO_2 enrichment experiment. *Agr. Ecosyst. Environ.* 209, 132–137. doi: 10.1016/j.agee.2015.04.007

Hasan, M. M., Rahman, M. A., Skalicky, M., Alabdallah, N. M., Waseem, M., Jahan, M. S., et al. (2021). Ozone induced stomatal regulations, MAPK and phytohormone signaling in plants. *Int. J. Mol. Sci.* 22 (12), 6304. doi: 10.3390/ijms22126304

Hellemans, T., Landschoot, S., Dewitte, K., Van Bockstaele, F., Vermeir, P., Eeckhout, M., et al. (2018). Impact of crop husbandry practices and environmental conditions on wheat composition and quality: a review. *J. Agric. Food Chem.* 66, 2491–2509. doi: 10.1021/acs.jafc.7b05450

Högy, P., Brunnbauer, M., Koehler, P., Schwadorf, K., Breuer, J., Franzaring, J., et al. (2013). Grain quality characteristics of spring wheat (*Triticum aestivum*) as affected by free-air CO_2 enrichment. *Environ. Exp. Bot.* 88, 11–18. doi: 10.1016/j.envexpbot.2011.12.007

Högy, P., Wieser, H., Kohler, P., Schwadorf, K., Breuer, J., Franzaring, J., et al. (2009). Effects of elevated CO_2 on grain yield and quality of wheat: results from a 3-year free-air CO_2 enrichment experiment. *Plant Biol.* 11, 60–69. doi: 10.1111/j.1438-8677.2009.00230.x

IPCC (2022). "Mitigation of climate change contribution of working group III to the sixth assessment report of the intergovernmental panel on climate change (chap. 3)," in *Climate change (2022)* (Cambridge University Press).

Jing, L., Zhao, X., Ning, Z., Qian, X., Wang, Y., Zhu, J., et al. (2017). Effect of increasing atmospheric CO_2 concentration on photosynthetic diurnal variation characteristics of hybrid rice: a FACE study. *Acta Ecologica Sinica.* 37, 2033–2044. doi: 10.5846/stxb201509261974

Kimball, B., Pinter, P. J., Garcia, R. L., Lamorte, R. L., Wall., G., Hunsaaker, D., et al. (2010). Productivity and water use of wheat under free-air CO_2 enrichment. *Glob. Change Biol.* 1, 429–442. doi: 10.1111/j.1365-2486.1995.tb00041.x

Kong, L., Xie, Y., Hu, L., Feng, B., Li, S., et al. (2016). Remobilization of vegetative nitrogen to developing grain in wheat (Triticum aestivumL.). *Field Crops Res.* 196, 134–144. doi: 10.1016/j.fcr.2016.06.015

Li, Y. T., Li, X., Li, Y. J., Zhuang, S., Feng, Y. X., Lin, E. D., et al. (2021). Does a large ear type wheat variety benefit more from elevated CO_2 than that from small multiple ear-type in the quantum efficiency of PSII photochemistry? *Front. Plant Sci.* 12. doi: 10.3389/fpls.2021.697823

Liu, Z. H., Cheng, F. M., Cheng, W. D., and Zhang, G. P. (2005). Positional variations in phytic acid and protein content within a panicle of japonica rice. *J. Cereal Sci.* 41, 297–303. doi: 10.1016/j.jcs.2004.09.010

Liu, Q., Liu, Y. J., Hao, X. Y., Song, C. X., Zong, Y. Z., Zhang, D. S., et al. (2023). Effects of controlled-release fertilizer on N_2O emissions in wheat under elevated CO_2 concentration and temperature. *Plant Soil.* doi: 10.1007/s11104-023-05972-1

Martínez-Peña, R., Schlereth, A., Höhne, M., Encke, B., Morcuende, R., Nieto-Taladriz, M. T., et al. (2022). Source-sink dynamics in field-grown durum wheat under contrasting nitrogen supplies: key role of non-foliar organs during grain filling. *Front. Plant Sci.* 13. doi: 10.3389/fpls.2022.869680

Martínez-Peña, R., Vergara-Díaz, O., Schlereth, A., Höhne, M., Morcuende, R., Nieto-Taladriz, M. T., et al. (2023). Analysis of durum wheat photosynthetic organs during grain filling reveals the ear as a water stress-tolerant organ and the peduncle as the largest pool of primary metabolites. *Planta* 257, 19. doi: 10.1007/s00425-023-04115-1

Martre, P., Porter, J. R., Jamieson, P. D., and Tribo, E. (2003). Modeling grain nitrogen accumulation and protein composition to understand the sink/source regulations of nitrogen remobilization for wheat. *Plant Physiol.* 133, 1959–1967. doi: 10.1104/pp.103.030585

Mitchell, L. (2003). Generalized, linear, and mixed models. *J. R. Stat. Soc* 52, 242–243. doi: 10.1111/1467-9884.00356

Naidoo, S. (2022). Commentary on the contribution of working group III to the sixth assessment report of the intergovernmental panel on climate change. *S. Afr. J. Sci.* 118, 9–10. doi: 10.17159/sajs.2022/14690

Navarro, E. C., Lam, S. K., and Trebicki, P. (2020). Elevated carbon dioxide and nitrogen impact wheat and its aphid pest. *Front. Plant Sci.* 11. doi: 10.3389/fpls.2020.605337

Panozzo, J. F., Eagles, H. A., and Wootton, M. (2001). Changes in protein composition during grain development in wheat. *Aust. J. Agr. Res.* 52, 485–493. doi: 10.1071/AR00101

Peng, Y. C., Zhao, Y., Yu, Z. T., Zeng, J. B., Xu, D. G., Dong, J., et al. (2022). Wheat quality formation and its regulatory mechanism. *Front. Plant Sci.* 13. doi: 10.3389/fpls.2022.834654

Pleijel, H., Broberg, M. C., Hgy, P., and Uddling, J. (2019). Nitrogen application is required to realize wheat yield stimulation by elevated CO_2 but will not remove the CO_2-induced reduction in grain protein concentration. *Glob. Change Biol.* 25, 1868–1876. doi: 10.1111/gcb.14586

Punia, S., Sandhu, K. S., and Siroha, A. K. (2017). Difference in protein content of wheat (*Triticum aestivum* l.): effect on functional, pasting, color and antioxidant properties. *J. Saudi Soc Agric. Sci.* 18, 378–384. doi: 10.1016/j.jssas.2017.12.005

Rezvi, H. U., Tahjib-Ul-Arif, M., Azim, M. A., Tumpa, T. A., Tipu, M. M. H., Najnine, F., et al. (2023). Rice and food security: climate change implications and the future prospects for nutritional security. *Food Energy Secur.* 12, 1. doi: 10.1002/fes3.430

Rossmann, A., Buchner, P., Savill, G. P., Powers, S. J., and Mühling, K. (2019). Foliar n application at anthesis stimulates gene expression of grain protein fractions and alters protein body distribution in winter wheat (*Triticum aestivum* l.). *J. Agric. Food Chem.* 67, 12709–12719. doi: 10.1021/acs.jafc.9b04634

Singh, P. K., Prasad, S., Verma, A. K., and Dwivedi, D. (2020). Screening for heat tolerant traits in wheat (*Triticum aestivum* l.) genotypes by physio-biochemical markers. *Int. J. Curr. Microbiol. Appl. Sci.* 9, 2335–2343. doi: 10.20546/ijcmas.2020.902.265

Soba, D., Ben Mariem, S., Fuertes-Mendizábal, T., Méndez-Espinoza, A. M., Gilard, F., González-Murua, C., et al. (2019). Metabolic effects of elevated CO_2 on wheat grain development and composition. *J. Agric. Food Chem.* 67, 8441–8451. doi: 10.1021/acs.jafc.9b01594

Walker, C., Armstrong, R., Panozzo, J., Partington, D., and Fitzgerald, G. (2017). Can nitrogen fertiliser maintain wheat (Triticum aestivum) grain protein concentration in an elevated CO_2 environment? *Soil Res.* 55, 518–523. doi: 10.1071/sr17049

Wang, L., Feng, Z. Z., and Schjoerring, J. K. (2013). Effects of elevated atmospheric CO_2 on physiology and yield of wheat (*Triticum aestivum* l.): a meta-analytic test of current hypotheses. *Agric. Ecosyst. Environ.* 178, 57–63. doi: 10.1016/j.agee.2013.06.013

Wang, J. Q., Li, L. Q., Lam, S. K., Shi, X. Z., and Pan, G. X. (2023). Changes in plant nutrient status following combined elevated CO_2 and canopy warming in winter wheat. *Front. Plant Sci.* 14. doi: 10.3389/fpls.2023.1132414

Wieser, H., Manderscheid, R., Erbs, M., and Weigel, H. J. (2008). Effects of elevated atmospheric CO_2 concentrations on the quantitative protein composition of wheat grain. *J. Agric. Food Chem.* 56, 6531–6535. doi: 10.1021/jf8008603

Wu, W., Wang, Y., Wang, L., Xu, H. S., Zörb, C., Geilfus, C. M., et al. (2022). Booting stage is the key timing for split nitrogen application in improving grain yield and quality of wheat - a global meta-analysis. *Field Crops Res.* 287, 108665. doi: 10.1016/j.fcr.2022.108665

Xue, C., Auf'm Erley, G. S., Rossmann, A., Schuster, R., Koehler, P., and Mühling, K. H. (2016a). Split nitrogen application improves wheat baking quality by influencing protein composition rather than concentration. *Front. Plant Sci.* 7. doi: 10.3389/fpls.2016.00738

Xue, C., Matros, A., Mock, H. P., and Mühling, K. H. (2019). Protein composition and baking quality of wheat flour as affected by split nitrogen application. *Front. Plant Sci.* 10. doi: 10.3389/fpls.2019.00642

Xue, C., Schulte Auf'm Erley, G., Rücker, S., Koehler, P., Obenauf, U., and Mühling, K. H. (2016b). Late nitrogen application increased protein concentration but not baking quality of wheat. *J. Plant Nutr. Soil Sci.* 179, 591–601. doi: 10.1002/jpln.201500569

Zhang, Y., Du, W., Zhang, Y., Wang, Z., and Kong, L. (2021). Metabolic analysis reveals temporal changes in C/N metabolites and senescence of flag leaf in wheat during grain filling. *Acta Physiol. Plant* 43, 104. doi: 10.1007/s11738-021-03272-8

Zhang, X., Shi, Z., Jiang, D., Hogy, P., and Fangmeier, A. (2019). Independent and combined effects of elevated CO_2 and post-anthesis heat stress on protein quantity and quality in spring wheat grains. *Food Chem.* 277, 524–530. doi: 10.1016/j.foodchem.2018.11.010

Zhong, C., Huang, J. W., Jiang, D., Zhong, Y. X., Wang, X., Cai, J., et al. (2023). Metabolomic analysis reveals patterns of whole wheat and pearling fraction flour quality response to nitrogen in two wheat lines with contrasting protein content. *J. Agric. Food Chem.* 71, 2290–2300. doi: 10.1021/acs.jafc.2c07413

Zörb, C., Ludewig, U., and Hawkesford, M. J. (2018). Perspective on wheat yield and quality with reduced nitrogen supply. *Trends Plant Sci.* 23, 1029–1037. doi: 10.1016/j.tplants.2018.08.012

Zuur, A. F., Ieno, E. N., Walker, N., Saveliev, A. A., and Smith, G. M. (2009). *Incorporating temporal correlation in seal abundance data with MCMC* Vol. 23 (Springer New York), 503–529. doi: 10.1007/978-0-387-87458-6-23

frontiers | Frontiers in Plant Science

TYPE Original Research
PUBLISHED 11 July 2023
DOI 10.3389/fpls.2023.1152817

Check for updates

OPEN ACCESS

EDITED BY
Li Wang,
Shandong Academy of Agricultural Sciences, China

REVIEWED BY
Lei Ding,
Université Catholique de Louvain, Belgium
Zhiguang Liu,
Shandong Agricultural University, China

*CORRESPONDENCE
Qian Wang
wangqian01@caas.cn
Haobao Liu
liuhaobao@caas.cn

†These authors have contributed equally to this work

RECEIVED 28 January 2023
ACCEPTED 19 May 2023
PUBLISHED 11 July 2023

CITATION
Li C, Aluko OO, Shi S, Mo Z, Nong T, Shi C, Li Z, Wang Q and Liu H (2023) Determination of optimal NH_4^+/K^+ concentration and corresponding ratio critical for growth of tobacco seedlings in a hydroponic system. *Front. Plant Sci.* 14:1152817.
doi: 10.3389/fpls.2023.1152817

Determination of optimal NH_4^+/K^+ concentration and corresponding ratio critical for growth of tobacco seedlings in a hydroponic system

Chuanzong Li[1†], Oluwaseun Olayemi Aluko[1,2†], Sujuan Shi[1,3], Zhijie Mo[1,4], Tongjia Nong[1], Chuhan Shi[1], Zhihao Li[1,4], Qian Wang[1*] and Haobao Liu[1*]

[1]Tobacco Research Institute, Chinese Academy of Agricultural Sciences, Qingdao, China, [2]State Key Laboratory of Plant Stress Biology, School of Life Sciences, Henan University, Kaifeng, China, [3]Technology Center, Shanghai Tobacco Company, Ltd, Beijing, China, [4]Yichang City Company, Hubei Tobacco Company, Yichang, China

Inherently, ammonium (NH_4^+) is critical for plant growth; however, its toxicity suppresses potassium (K^+) uptake and vice-versa. Hence, attaining a nutritional balance between these two ions (NH_4^+ and K^+) becomes imperative for the growth of tobacco seedlings. Therefore, we conducted a 15-day experimental study on tobacco seedlings exposed to different concentrations (47 treatments) of NH_4^+/K^+ at different corresponding 12 ratios simultaneously in a hydroponic system. Our study aimed at establishing the optimal NH_4^+-K^+ concentration and the corresponding ratio required for optimal growth of different tobacco plant organs during the seedling stage. The controls were the baseline for comparison in this study. Plants with low or excessive NH_4^+-K^+ concentration had leaf chlorosis or dark greenish colouration, stunted whole plant part biomass, and thin roots. We found that adequate K^+ supply is a pragmatic way to mitigate NH_4^+-induced toxicity in tobacco plants. The optimal growth for tobacco leaf and root was attained at NH_4^+-K^+ concentrations 2-2 mM (ratio 1:1), whereas stem growth was optimal at NH_4^+-K^+ 1-2 mM (1:2). The study provided an insight into the right combination of NH_4^+/K^+ that could mitigate or prevent NH_4^+ or K^+ stress in the tobacco seedlings.

KEYWORDS

NH_4^+ -K^+ concentrations, NH_4^+: K^+ ratios, tobacco seedling growth, NH_4^+ toxicity, tobacco plant organs (leaf, stem, and root)

Introduction

Ammonium (NH_4^+) is a predominant form of nitrogen (N) that supports plant growth, especially when furnished with an adequate amount of nitrate (NO_3^-) (Dubey et al., 2021; Vu et al., 2021; Zhu et al., 2021; Ninkuu et al., 2023). Compared to sole NO_3^- or NH_4^+, crop growth and yield peaks when NH_4^+ and NO_3^- are appropriately combined in growth medium (Liang et al., 2022; Saloner and Bernstein, 2022; Xiao et al., 2023). However, compelling evidence has shown that excessive or sole application of NH_4^+ could negate plant growth and yield potentials, causing leaf chlorosis, stunted growth, and other major crop physiological disorder (Britto and Kronzucker, 2002; Guo et al., 2019; Aluko et al., 2021; Katz et al., 2022). Over time, the mechanisms underlying NH_4^+ toxicity in plants have been debatable, with much speculations accrued to the displacement of cytosolic cations, including K^+ (Walch-Liu et al., 2000; Guo et al., 2019).

Given that, the interactive effects of K^+ and NH_4^+ on plant growth and development became a focus of research (Witold et al., 2017; Shi et al., 2020a; Nawarathna et al., 2021; Aluko et al., 2022; Xiao et al., 2023). Excessive NH_4^+ was found to limit growth and yield by reducing K^+ uptake and influx in wheat (Kong et al., 2014), *Arabidopsis* (Walch-Liu et al., 2000), rice (Szczerba et al., 2008) and tobacco (Lu et al., 2005). Research has shown the potency of potassium in alleviating NH_4^+ toxicity symptoms in these crops. (Chen et al., 2021; Fang et al., 2021). Recently, Guo et al. (2019) reported a marked increase in the growth, nutrient uptake, and yield (improved panicle biomass production) when K^+ concentration was supplied to high NH_4^+- induced wheat, demonstrating the positive impact of K^+ in offsetting NH_4^+ stress in plants. Moreover, excessive application of K^+ could hinder the uptake of NH_4^+, resulting to a competition in the uptake of both essential ions (K^+ and NH_4^+) (Balkos et al., 2010). Disruption in the uptake of either of these two cations limit plant growth potentials. Despite the promising results of K^+ ameliorative effects on NH_4^+, it is yet unknown the appropriate amount of NH_4^+ and K^+ required for optimal yield, knowledge of which is important given the increasing NH_4^+ toxicity symptoms in plants. Hence, an in-depth understanding of a nutritional balance between NH_4^+ and K^+ becomes expedient.

Tobacco plants require an adequate supply of K^+ for improved growth and quality (Borges et al., 2012). Similarly, supply of NH_4^+ further promote growth, but becomes toxic if excessive. However, the issue of nutritional imbalances between K^+ and NH_4^+ poses a great challenge to adopting a hydroponic system for tobacco cultivation. Hence, it becomes imperative to understand the appropriate NH_4^+/K^+ concentration and the corresponding ratio required for the growth of tobacco. Research-based information on the basic NH_4^+/K^+ concentration and corresponding ratio required for optimal growth of tobacco under a hydroponic system is still lacking. Moreover, little is known about the influence of increasing NH_4^+ and K^+ supplies on the physiological growth of tobacco plants. Hence, an in-depth understanding of tobacco's optimum NH_4^+- K^+ concentration range is required to furnish hydroponic farmers with reliable information on the best NH_4^+/K^+ combination to attain optimum growth output. This study aimed to investigate the effects of different levels of NH_4^+- K^+ concentration on the growth of tobacco seedlings, and also critically evaluate and determine the optimal NH_4^+ - K^+ concentration, and corresponding ratio that is required for the growth of different parts of tobacco seedlings.

Materials and methods

Plant materials and growth conditions

The experiment was conducted in a controlled plant growth culture room at Tobacco Research Institute, Chinese Academy of Agricultural Sciences (TR1,CAAS), Qingdao, China. All methods used in this study were performed in accordance with the relevant guidelines and regulations. The seed of *Nicotiana tabacum* used in the present study was Zhongyan 100 (ZY100). ZY100 developed in TR1CAAS passed the variety approval in 2002. Tobacco seeds were initially sown in a potting soil mixture (soil/perlite, 3:1 v/v) under controlled conditions (continuous light at 24°C). At the three-leaf stage, uniformly grown seedlings were transferred into hydroponic pots (48 cm x 22.5 cm x 3.5 cm) with 2 liters of nutrient solution (one-fifth-strength Hoagland solution, 1/5 HS) for 6 days. The 1/5 HS, which was supplemented with 1mM K^+ (K_2SO_4 is the K^+ source) had the following composition in mM: 0.35 $MgSO_4$, 0.2 NaH_2PO_4, 0.0125 H_3BO_3, 0.001 $MnSO_4$, 0.0005 $CuSO_4$, 0.001 $ZnSO_4$, 0.0001 Na_2MoO_4, 0.01 Fe-EDTA, 1.4 Ca $(NO_3)_2$, 0.15 $CaCl_2$. NH_4^+ was sourced from $(NH_4)_2SO_4$.

NH_4^+ and K^+ treatments

After six days, tobacco seedlings with the same growth potential were transferred into another hydroponic container (26 cm x 17.5 cm x 8 cm) of 1/5 HS. NH_4^+ and K^+ were supplied depending on the designated NH_4^+- K^+ concentration in each treatment group. Seedlings were held in place by the conventional tip and grown at 24°C. The experiment was sectioned into two NH_4^+/K^+ categories. The first category was fractioned into increasing NH_4^+ at constant K^+, comprising 7 ratio, while the other, constant $NH_4^{+/}$increasing K^+ had 5 ratios, giving 12 ratios in total. The 12 NH_4^+: K^+ ratios comprise 45 different NH_4^+-K^+ concentrations, and two additional controls (positive and negative control), bringing the total to 47 different NH_4^+-K^+ concentrations (for composition; refer to Table 1). While the nutrient solution of the negative control was neither supplied with K^+ nor NH_4^+, the medium with the positive control was supplemented with 1 mM K^+ but no NH_4^+ supply. Tobacco seedlings were exposed to varying concentrations (47 treatments) of NH_4^+/K^+ at different corresponding 12 ratios concurrently in a hydroponic system for 15 days. The nutrient solution was renewed every two days to ensure a steady nutritional state for tobacco

TABLE 1 NH_4^+/K^+ concentrations with their corresponding ratios.

Ratios NH_4^+: K^+	NH_4^+-K^+ treatments (mM)
1:1	0.1-0.1、0.5-0.5、1-1、2-2、5-5、10-10
2:1	0.2-0.1、1-0.5、2-1、10-5、20-10
5:1	0.5-0.1、1-0.2、5-1、10-2、50-10
10:1	1-0.1、5-0.5、10-1、20-2
20:1	2-0.1、10-0.5、20-1
50:1	5-0.1、10-0.2、50-1
100:1	10-0.1、20-0.2、50-0.5
1:2	0.1-0.2、0.5-1、1-2、5-10
1:5	0.1-0.5、0.2-1、1-5、2-10
1:10	0.1-1、0.2-2、0.5-5、1-10
1:20	0.1-2、0.5-10
1:50	0.1-5、0.2-10
Positive control Negative control	0-0.5 0-0

NH_4^+-K^+; millimolar: (mM)).

seedlings. The solution pH was maintained between 5.6 and 6.0. The placements of the hydroponic pots were interchanged to avoid edge effects.

We had a pre-experimental trial, with the plants exceeding 15 days of NH_4^+- K^+ treatments. when plants exceeded the 15th day, tobacco wilting and overall death were observed due to the excessive supply of NH_4^+ or K^+ to some of the treated samples. As such, some samples were not available for phenotype analysis. Therefore, we considered sampling the tobacco seedlings at 15 days after treatment for thorough evaluation of the physiological parameters.

. After 15 days of treatment, tobacco seedlings were harvested for leaf, stem, and root growth, NH_4^+ and K^+ content, and root activity analysis.

Plant biomass, leaf and root surface area, stem and root length

At harvest, uniformly grown seedlings from each treatment were fractioned into; (i) leaves, (ii) stems, and (iii) roots. Photos of different plant parts were taken with a camera. Subsequently, leaf and root surface area were determined using the ImageJ software (https://imagej.en.softonic.com/). Primary root length and stem length were measured with a scaling ruler. Plant root was carefully rinsed once with 10 mM $CaSO_4$ and twice in double-distilled water (Szczerba et al., 2008), and then fresh weights of leaves, stems, and roots of plants were measured. The dry weights of the measured samples were taken after oven-drying at 110°C for 30 min and then 80 °C to a constant weight. The dry samples were crushed into fine powders with the mortar and pestle for K^+ concentrations determination.

K^+ and NH_4^+ content measurements

To measure K^+ content, approximately 0.01 g of ground leaves, stems, and roots samples were weighed and digested in 8 ml 0.5 M HCl. The suspension was homogenized at 25°C, 100-150 rpm for 1hr and filtered into a new centrifuge tube. The aliquot of the filtrate was used for K^+ determination by flame photometry (6400A) (Shi et al., 2020a). The reading obtained was used to calculate K^+ concentrations in plant tissue as follows:

K^+ (mmol g^{-1} DW) = ((A/M) * V *Dilution multiples*0.001)/m

where A = calculated concentration according to the readings on the standard curve (μg·ml^{-1})

M = relative molecular mass of K^+

V = reading volume (ml)

m = dry weight (g)

For NH_4^+ content measurement, the freshly harvested plant was separated into different plant parts (leaves, stems, and roots). The root was washed with 10mM $CaSO_4$ to eliminate any extracellular NH_4^+ (Szczerba et al., 2008). Fresh plant tissues of ≤ 0.5 g were homogenized under liquid nitrogen, and 6 ml of 10 mM formic acid was added to extract NH_4^+. The suspension was allowed to sit for 5 minutes and then centrifuged at 4°C and 12000 rpm for 10 minutes. The supernatant was centrifuged repeatedly 3 times. The supernatant obtained from the last centrifugation step was diluted with 2.5 ml o-phthalaldehyde (OPA) solution as previously described (Shi et al., 2020a). The absorbance of the sample was measured at 410 nm using a spectrophotometer (UV-7502PC, AOE Instruments). The reading obtained was used to calculate NH_4^+ concentrations in plant tissue as follows:

NH_4^+ (μmol g^{-1} FW) = ((A/M) * V * Dilution multiples)/m

where A = calculated concentration according to the readings on the standard curve (μg ml^{-1})

M = relative molecular mass of NH_4^+;

V = reading volume (ml)

m = fresh weight (g).

Chlorophyll content measurement

After 15 days of NH_4^+/K^+ treatment, chlorophyll content was measured according to the previous method (Dong et al., 2015). The fourth leaf of each treatment was weighed (0.2 g) and incubated in 95% ethyl alcohol until the leaf strands became completely pale (approximately 48 hours). The absorbance of the extract was measured at 665 nm and 649 nm using a spectrophotometer.

Root activity assays

Root activity was measured as described previously (Liu et al., 2008) using triphenyl tetrazolium chloride (TTC) method. Approximately 0.5 grams of freshly weighed root was fully immersed into 5 ml 0.4% TTC and phosphate buffer (adjusted to pH 7.0) and incubated at 37 °C for 3 hours to accelerate the reduction of TTC to triphenyl formazan (TTF). The resulting chemical reaction was halted by adding 2 ml of 1 mol/L sulphuric acid into each tube. Subsequently, the roots were moved out of the tubes, gently patted with tissue paper, and then crushed with 3-4 ml ethyl acetate. The liquid portion was removed into a new tube and made up to 10 ml with ethyl acetate. The absorbance was measured at 485 nm wavelength using spectrometer UV-7502PC, AOE Instruments). The OD values were expressed as mg TTF/(g·h).

Statistical analysis

Data was analyzed using the IBM SPSS Statistics 23 software. Variations among treatments were examined by one-way ANOVA, and means were compared using Duncan's multiple range tests at P<0.05. All graphs were drawn using GraphPad Prism 6.0. The correlation analysis was performed using pearson correlation in R studio. ns: no significance difference; *p < 0.05; **p < 0.01; ***p < 0.001.

Results

Leaf growth of tobacco seedlings as affected by varying NH_4^+-K^+ concentrations and ratios

The observed results showed the influence of NH_4^+-K^+ concentrations on fresh leaf weight (Figure 1). There were variations within treatments in all NH_4^+: K^+ ratios. Within each of the increasing NH_4^+: constant K^+ ratios, fresh leaf weight increases with increasing NH_4^+ -increasing K^+ concentration until a point was reached where further increase led to a gradual reduction. NH_4^+-K^+ millimolar concentration 2-2 mM (within1:1), 2-1 mM (within 2:1) and 5-1 mM (within 5:1) had the highest weight, with 57.7%, 21.7% and 6.5% increase in fresh leaf weight, respectively, compared with the positive control (0.5 mM K^+, without NH_4^+). NH_4^+-K^+ concentrations 0.1-0.1 mM, 0.2-0.1 mM and 50-10 mM had the lowest leaf weight following the same ratio pattern above. The fresh leaf weight of 0.5-0.5 mM at ratio 1:1 was also significantly lower than the positive control (0 mM NH_4^+- 0.5 mM K^+) but higher than the negative control (no NH_4^+- K^+). The leaf weight of the positive control was substantially higher than all the NH_4^+-K^+ concentrations at ratios 2:1 and 5:1, with the exemption of 2-1 mM (2:1) and 5-1 mM (5:1). Compared with other concentrations within ratios 10:1, 20:1, 50:1, and 100:1, the positive control (0.5 mM K^+, without NH_4^+) had the highest leaf weight. In fact, 50-1 mM (50:1) and 50-0.5 mM (100:1) were either insignificant or 75.2% lower than the negative control (without NH_4^+ and K^+). When NH_4^+ was kept constant (at 1) at an increasing K^+ ratio, the leaf fresh weight of NH_4^+: K^+ ratios 1:2, 1:5, and 1:20 increased with increasing NH_4^+/K^+ millimolar concentration, albeit concentrations at ratios 1:10 and 1:50 were exceptions to this. Following the same ratio pattern, the leaf weight of NH_4^+-K^+ concentrations was substantially higher than both controls. Yet, the leaf weight of lower treatments such as 0.1-0.2 mM (1:2) and 0.1-0.5 mM (1:5) was drastically reduced by 47.1% and 15.2% compared with the positive control. With the exemption of 5-10 mM, all other treated concentrations under increasing K^+ ratios had considerably lower leaf weight values relative to 2-2 mM (1:1). NH_4^+-K^+ 5-10 mM (within a 1:2 ratio) had the highest leaf weight; however, when compared with 2-2 mM (within ratio 1:1; which was the highest under increasing NH_4^+/constant K (1)), 5-10 mM was higher, although at a small difference of 2.9%.

NH_4^+-K^+ concentrations at different ratios also significantly affected the leaf K^+ content (Figure 2). Within each of the increasing NH_4^+: constant K^+ ratios, leaf K^+ content increases with increasing NH_4^+- increasing K^+ concentration until a point is reached where further increase results in a gradual reduction. The leaf K^+ content of 2-2 mM, 2-1 mM,10-2 mM at ratios 1:1, 2:1 and 5:1, respectively, were increased by 69.7%, 31.7% and 19.6% respectively, when compared with the positive control. Also, the leaf K^+ contents were reduced at lower NH_4^+-K^+ concentration 0.1-0.1 mM (1:1), 0.2-0.1 mM and 1-0.5 mM (2:1) relative to the positive control. At ratios 5:1, the leaf K^+ content of the positive control was significantly higher than all other treated concentrations, except 5-1 mM. All other concentrations at ratios 10:1, 20:1, 50:1, and 100:1 exhibit reduced K^+ contents compared with the positive control. When K^+ was increased at constant NH_4^+ (1), K^+ content increased with increasing NH_4^+-K^+ millimolar concentration, irrespective of the controls (positive and negative). At such increasing K^+ ratios, only the leaf K^+ content of the lower concentration, 0.1-0.2 (1:2) and 0.1-0.5 (1:5), were reduced relative to the positive control; other NH_4^+-K^+ treatments within these ratios were higher. Comparing the highest at both ends (constant NH_4^+/increasing K^+ and increasing NH_4^+/constant K^+ ratios), 0.5-10 mM (1:20) had the highest, and the leaf K^+ content was approximately 1% higher than 2-2 mM (1:1; under increasing NH_4^+ and constant K^+).

Leaf NH_4^+ content was determined to evaluate the optimal NH_4^+-K^+ concentration required for the growth of tobacco seedlings. There were variations among concentrations at different ratios. At ratios 1:1, 2:1 and 5:1, leaf NH_4^+ content increases with increasing NH_4^+-K^+ millimolar concentration until a point was reached where a notable decrease in NH_4^+ content was observed (NH_4^+-K^+ 2-2Mm (ratio 1:1); 2-1mM (2:1); 1-0.2mM (5:1). A further increase in NH_4^+-K^+ millimolar concentration resulted in a surge in leaf NH_4^+ content. However, at ratios 10:1,20:1, 50:1 and 100:1, a steady rise in leaf NH_4^+ content was observed with increasing NH_4^+-K^+ concentration. The concentrations within these ratios were significantly lower than the positive control (0-0.5 mM) (Figure 3). Compared to the treated concentration at a constant NH_4^+/increasing K^+ ratio, treatments without NH_4^+ and K^+ (negative control) had the highest leaf NH_4^+ content. In all, the leaf NH_4^+ content was highest at NH_4^+-K^+ concentration 50-1 mM (72.7 μmol/g FW).

There were significant differences in the leaf area of tobacco seedlings exposed to varying NH_4^+-K^+ concentrations, as presented in Figure 4. Within each of the increasing NH_4^+/constant K^+ (1) ratios (irrespective of both controls), leaf area

10.3389/fpls.2023.1152817

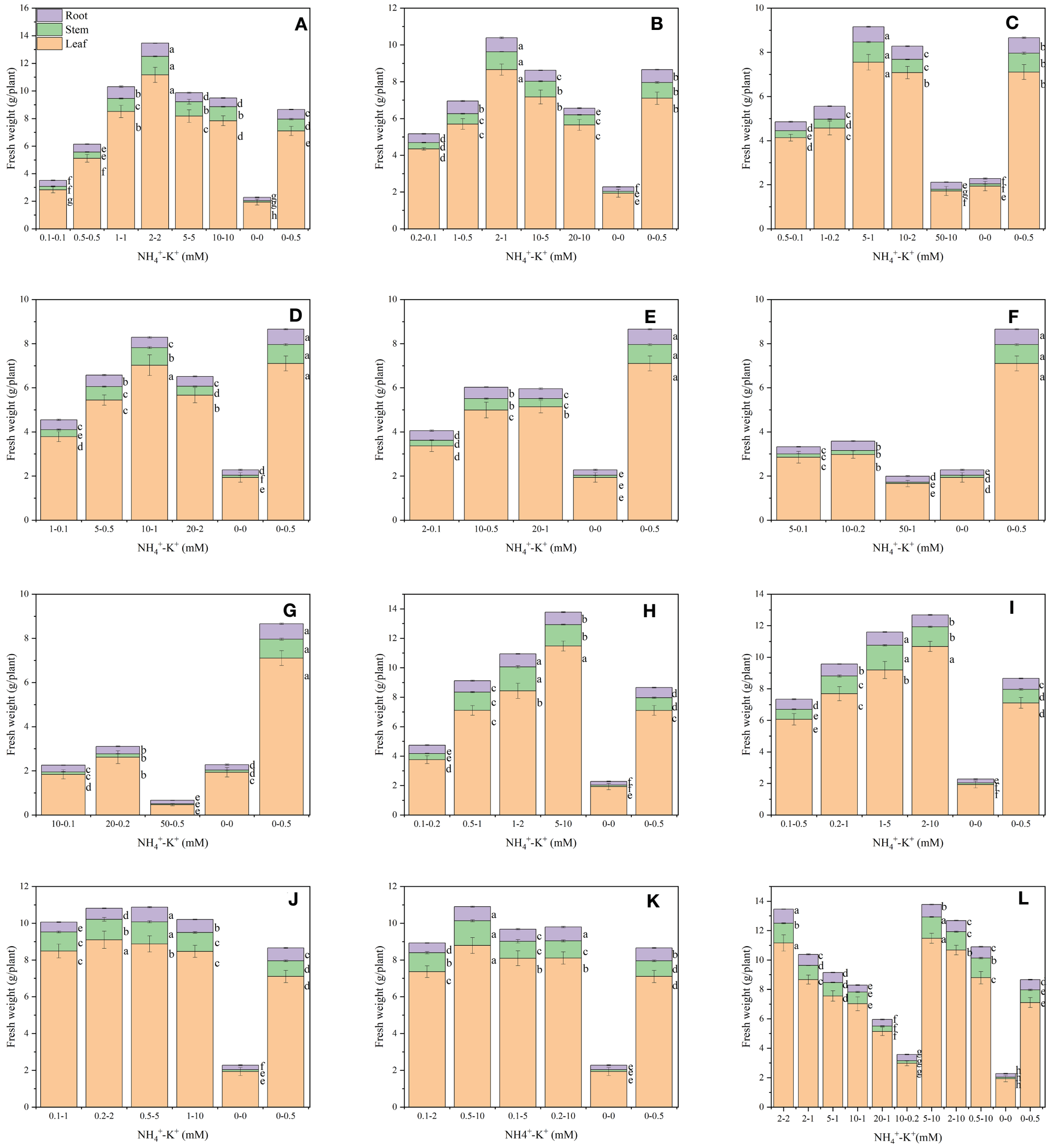

FIGURE 1
Fresh leaf weight (FLW), fresh stem weight (FSW), and fresh root weight (FRW) of tobacco plants as affected by different NH_4^+: K^+ ratios. Graphs **(A–G)** represent NH_4^+-K^+ concentrations at increasing NH_4^+/constant K^+ (at 1) ratios. **(A)** NH_4^+: K^+ ratio 1:1, **(B)** 2:1, **(C)** 5:1, **(D)** 10:1, **(E)** 20:1, **(F)** 50:1, and **(G)** 100:1. Graphs **(H-K)** indicate NH_4^+-K^+ concentrations at constant NH_4^+ (at 1)/increasing K^+ ratio. **(H)** NH_4^+: K^+ ratio 1:2, **(I)** 1:5, **(J)** 1:10, **(K)** 1:20 (0.1-2 mM and 0.5-10 mM) and 1:50 (0.1-5 mM and 0.2-10 mM), **(L)** comparison of NH_4^+-K^+ concentration within each ratio. All the NH_4^+-K^+ concentration within each ratio were compared with the positive (without NH_4^+, but with K^+).and negative control (without NH_4^+ and K^+). Fresh weights were determined 15 days after treatment. Letters represent the mean values ± SD (n=15 biological replicates). The bars without letters have extremely low mean values.

increases with increasing NH_4^+-K+ millimolar concentration until a point is reached where further increase led to a gradual reduction in leaf area. Following the same ratio pattern, leaf area peaks at concentration 2-2 mM (1:1), followed by 2-1 mM (2:1), 5-1 mM (5:1), and 10-1 mM (10:1), but was significantly reduced at ratios 20:1, 50:1 and 100:1 compared with the positive control (Figure 4). However, at constant NH_4^+/increasing K^+, a direct relationship was observed between the treated concentrations and leaf area; leaf area increases as NH_4^+/K^+ concentration increases. With the exemption of 0.1-0.2 mM (1:2), the leaf area of all other treated concentrations was significantly increased relative to the positive control. In all, leaf area of concentrations 5-10 mM (1:2) and 2-10 mM (1:5) were substantially increased by 10.5% and 6.1% relative to 2-2 mM (1:1; with the highest leaf area under increasing NH_4^+/constant K^+) while the negative control had the lowest leaf area.

As shown in (Figure 5), there were significant differences in the chlorophyll content of tobacco subjected to concentration at different NH_4^+: K^+ ratios. In each NH_4^+: K^+ ratio, the chlorophyll content increased with increasing NH_4^+ - K^+ concentration and was highest at 20-1 mM (20:1); a further increase in NH_4^+ ratio to 50:1 and 100:1 led to a gradual decrease in chlorophyll content.

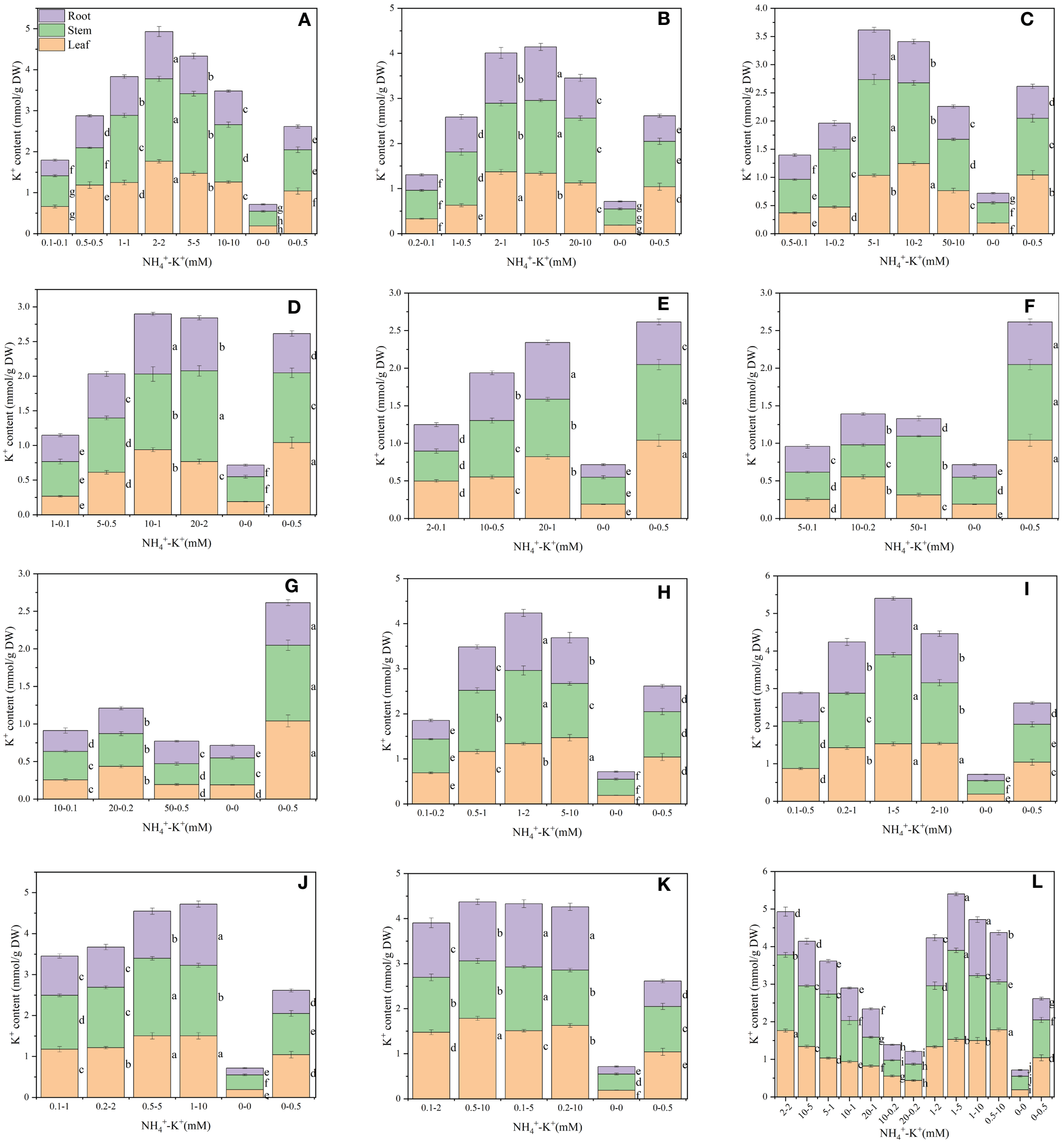

FIGURE 2
Potassium (K^+) contents in the leaf (LKC), stem (SKC) and root (RKC) of tobacco subjected to different NH_4^+: K^+ ratios. Graphs **(A-G)** represent NH_4^+- K^+ concentrations at increasing NH_4^+/constant K^+ (at 1) ratios. **(A)** NH_4^+: K^+ ratio 1:1, **(B)** 2:1, **(C)** 5:1, **(D)** 10:1, **(E)** 20:1, **(F)** 50:1, and **(G)** 100:1. Graphs **(H-K)** connote NH_4^+- K^+ concentrations at constant NH_4^+ (at 1)/increasing K^+ ratio. **(H)** NH_4^+: K^+ ratio 1:2, **(I)** 1:5, **(J)** 1:10, **(K)** 1:20 (0.1-2 mM and 0.5-10 mM) and 1:50 (0.1-5 mM and 0.2-10 mM) **(L)** comparison of NH_4^+-K^+ concentration within each ratio. All the NH_4^+- K^+ concentration within each ratio were compared with the positive (without NH_4^+, but with K^+).and negative control (without NH_4^+ and K^+). K^+ content was measured 15 days after treatment. Letters represent the mean values + SD (n= 12 biological replicates).

Compared with increasing NH_4^+/constant K^+, constant NH_4^+/increasing K^+- plants had lower chlorophyll content.

Stem growth of tobacco seedlings as affected by varying NH_4^+/K^+ concentration and ratios

Increasing NH_4^+ at constant K^+ exerts varying effects on the fresh stem weight (Figure 1). Fresh stem weight increases with a progressive increase in NH_4^+-K^+ concentration until a point was reached where further increase resulted in drastic stem reduction. Within this increasing NH_4^+/constant K^+ ratio pattern, NH_4^+-K^+ concentrations 2-2 mM (1:1) had the highest stem weight, followed by 2-1 mM (2:1) and 5-1 mM (5:1 mM), and their stem weight were increased by 56.4%, 13.2% and 7.1%, respectively, relative to the positive control. Positive control was considerably higher than all other treated concentrations at ratios 2:1 and 5:1, except at 2-1 mM (2:1) and 5-1 mM (5:1). Positive control had the highest stem weight at ratios 10:1, 20:1, 50:1, and 100:1. Indeed, stem weights of 50-1 mM (50:1) and 50-0.5 mM (100:1) were drastically reduced compared with the negative control. At constant NH_4^+/increasing K^+, stem weight of all the concentrations at different ratios was remarkably higher than the positive control, though stem weight reduction was observed at 0.1-0.2 mM (1:2) and 0.1-0.5 mM (1:5). Compared with 2-2 mM (1:1; highest at constant K^+ and increasing

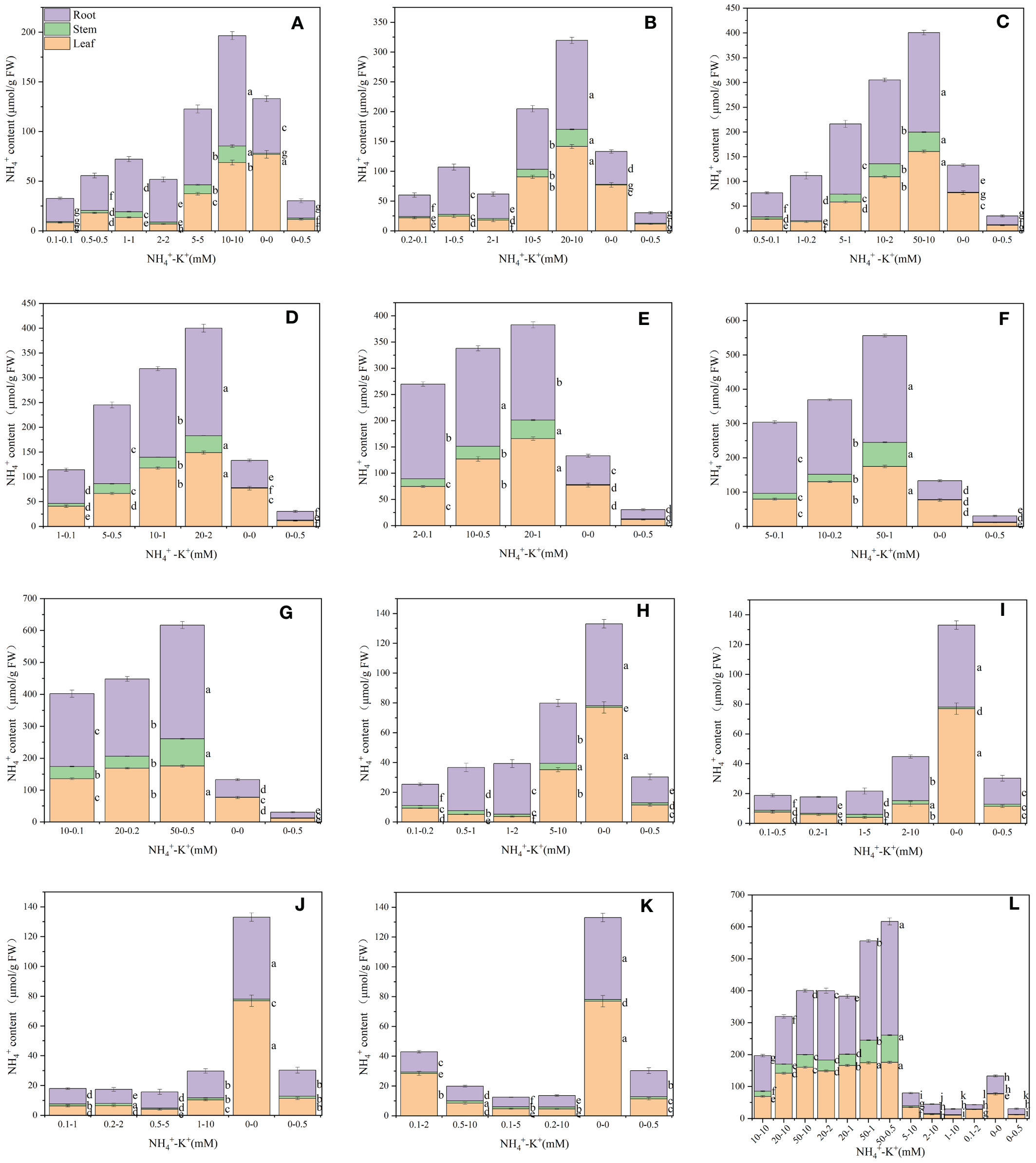

FIGURE 3
Ammonium (NH_4^+) contents in the leaf, stem and root of tobacco subjected to different NH_4^+: K^+ ratios. Graphs **(A-G)** represent increasing NH_4^+ at constant K^+ (at 1) ratios. **(A)** NH_4^+: K^+ ratio 1:1, **(B)** 2:1, **(C)** 5:1, **(D)** 10:1, **(E)** 20:1, **(F)** 50:1, and **(G)** 100:1. Graphs **(H–K)** connote constant NH_4^+ (at 1) at increasing K^+ ratio. **(H)** NH_4^+: K^+ ratio 1:2, **(I)** 1:5, **(J)** 1:10, **(K)** 1:20 (0.1-2 mM and 0.5-10 mM) and 1:50 (0.1-5 mM and 0.2-10 mM) **(L)** comparison of NH_4^+-K^+ concentration within each ratio. All the NH_4^+- K^+ concentration within each ratio were compared with the positive (without NH_4^+, but with K^+).and negative control (without NH_4^+ and K^+). NH_4^+ content was measured 15 days after treatment. Letters represent the mean values + SD (n= 9 biological replicates). The bars without letters have extremely low mean values.

NH_4^+ ratio), the stem weight of 1-2 mM (1:2) and 1-5 mM (1:5) (highest stem weight under constant NH_4^+/increasing K^+ ratio) increased by 21.4% and 17.4%, respectively.

Furthermore, there were significant differences in the stem K^+ content at various ratios (Figure 2). At increasing NH_4^+ and constant K^+, 2-2 mM (1:1) had the highest stem K^+ content, followed by 10-5 mM (2:1), 5-1 mM (5:1) and 20-2 mM (10:1), exhibiting approximately 99.8%, 60.5%, 69.0% and 30.2%, increase in K^+ content, respectively, relative to the positive control. However, compared with the positive control, stem K^+ contents were significantly lower in concentration at ratios 20:1, 50:1, and 100:1. A 15.4% reduction in stem K+ content was observed in 50-0.5 mM (100:1) medium compared with negative control. Within each of the constant NH_4^+/increasing K^+ ratios (except for ratio 1:20), increasing NH_4^+-K^+ concentration led to gradual improvement in the stem K^+ content until a peak was reached where further increase led to reduction. Generally, stem K^+ content was highest at 1-5 mM (1:5), and was 1.2% higher than 2-2 mM (1:1).

Stem NH_4^+ contents were affected by various NH_4^+-K^+ concentrations at different ratios (Figure 3). Under increasing NH_4^+/constant K^+ ratios 1:1, 2:1, and 5:1, the NH_4^+ content of stem was much lower compared to 10:1, 20:1, 50:1, and 100:1 as

10.3389/fpls.2023.1152817

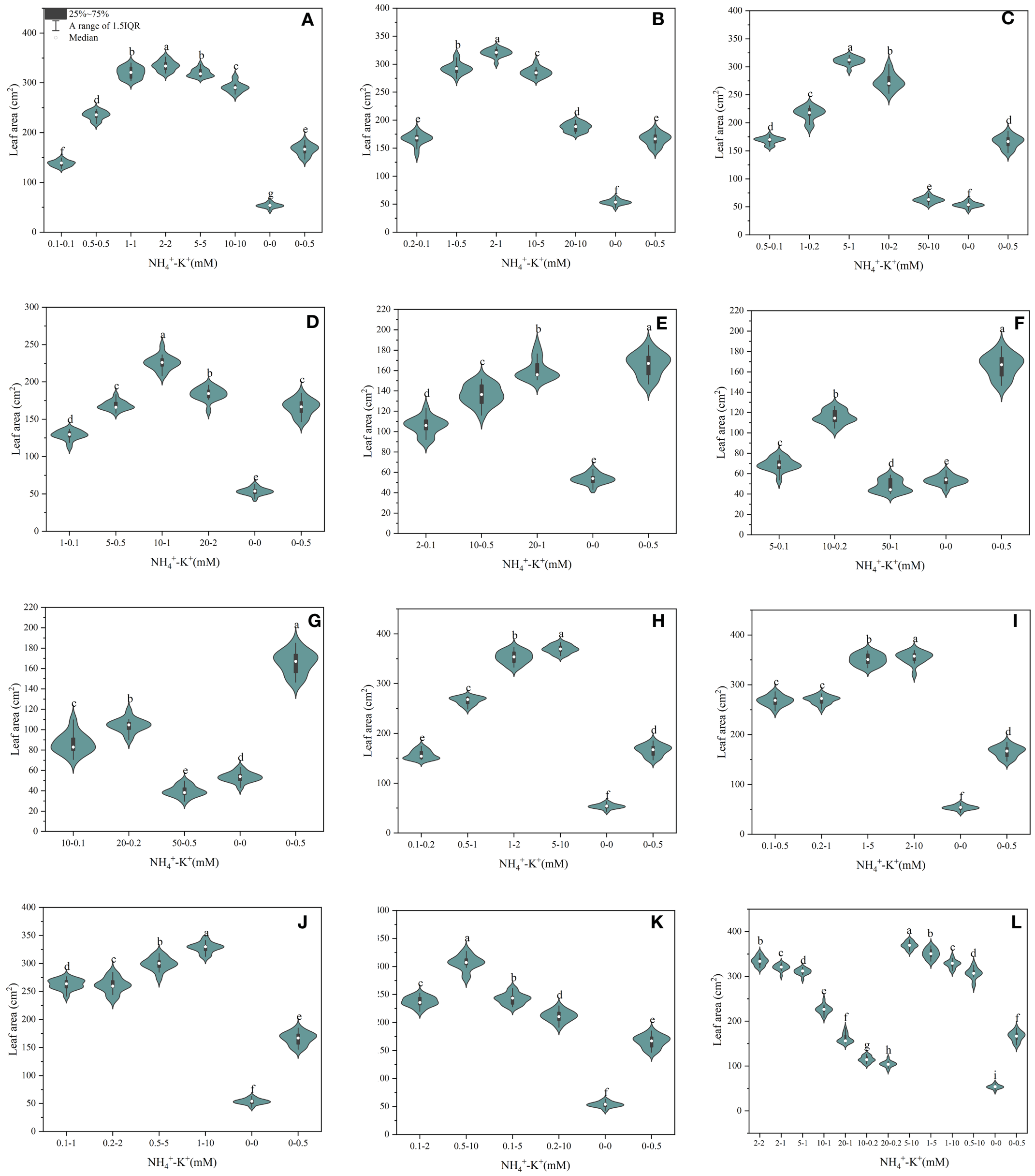

FIGURE 4
Leaf area of tobacco as affected by different NH_4^+: K^+ ratios. Graphs **(A–G)** represent increasing NH_4^+ at constant K^+ (at 1) ratios. **(A)** NH_4^+/K^+ ratio 1:1, **(B)** 2:1, **(C)** 5:1, **(D)** 10:1, **(E)** 20:1, **(F)** 50:1, and **(G)** 100:1. Graphs **(H–K)** connote constant NH_4^+ (at 1) at increasing K^+ ratio. **(H)** NH_4^+/K^+ ratio 1:2, **(I)** 1:5, **(J)** 1:10, **(K)** 1:20 (0.1-2 mM and 0.5-10 mM) and 1:50 (0.1-5 mM and 0.2-10 mM) **(L)** comparison of NH_4^+-K^+ concentration within each ratio. All the NH_4^+/K^+ concentration within each ratio were compared with the positive (without NH_4^+, but with K^+) and negative control (without NH_4^+ and K^+). The above growth parameters were measured 15 days after treatment. Significant means were separated using standard deviation ± SD (n= 12 biological replicates).

visually represented in the graphs; however, a marked increase in stem NH_4^+content was observed when these treatments were compared with controls. Following this same increasing NH_4^+/K^+ ratio pattern, stem NH_4^+ content peaks at the highest NH_4^+- K^+ concentration. With the exemption of ratios 1:10 (0.2-2 mM), a similar increase in the stem NH_4^+ content was observed at highest NH_4^+-K^+ concentration grown under constant NH_4^+/increasing K^+ ratios. Interestingly, stem NH_4^+ content of such increasing K^+ concentrations were drastically lower than most of the increasing NH_4^+/constant K^+ treated medium (NH_4^+: K^+ 20:1, 50:1, and 100:1).

To further evaluate stem growth, stem diameter, which is one of the most important stem growth variables, was measured. At increasing NH_4^+/constant K^+, stem diameter increases as the NH_4^+/K^+ concentration increases; however, a point was reached where further increase led to a drop in stem diameter (Figure 6). There were significant reductions in the stem diameters of NH_4^+-K^+ 50-10 mM (5:1), 50-1 mM (50:1), and 50-0.5 mM (100:1) compared with the negative control. In all the treated concentrations subjected to increasing NH_4^+ ratio, only 2-2 mM at ratio 1:1 had the largest stem diameter. Despite the increasing K^+ at ratio 1:2, positive control still had the largest stem diameter. In case of further

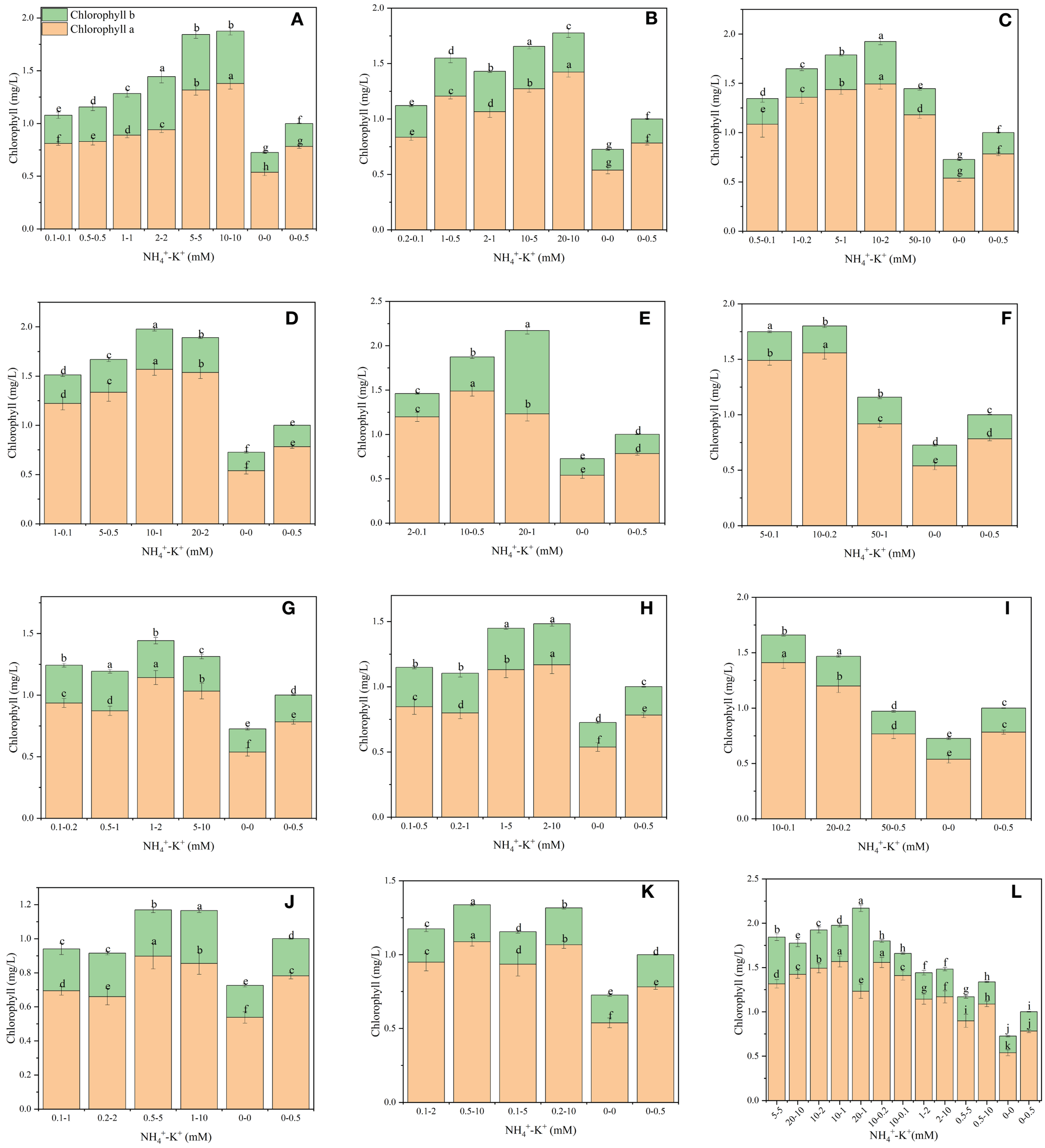

FIGURE 5
Chlorophyll contents of tobacco subjected to different NH_4^+: K^+ ratios. Graphs **(A–G)** represent increasing NH_4^+ at constant K^+ (at 1) ratios. **(A)** NH_4^+/K^+ ratio 1:1, **(B)** 2:1, **(C)** 5:1, **(D)** 10:1, **(E)** 20:1, **(F)** 50:1, and **(G)** 100:1. Graphs **(H–K)** connote constant NH_4^+ (at 1) at increasing K^+ ratio. **(H)** NH_4^+/K^+ ratio 1:2, **(I)** 1:5, **(J)** 1:10, **(K)** 1:20 (0.1-2 mM and 0.5-10 mM) and 1:50 (0.1-5 mM and 0.2-10 mM) **(L)** comparison of NH_4^+-K^+ concentration within each ratio. All the NH_4^+/K^+ concentration within each ratio were compared with the positive (without NH_4^+, but with K^+). And negative control (without NH_4^+ and K^+). Chlorophyll content was measured 15 days after treatment. Significant means were separated using standard deviation + SD (n= 12 biological replicates).

increase in K^+ to 5 (1:5) and 10 (1:10), only 2-10 mM (1:5) and 0.5-5 mM (1:10) had larger stem diameter compared with positive control. The stem diameter of concentrations at ratios 1:20 and 1:50 was negligible since both had similar or smaller stem diameters compared with the positive control. In the overall treatments, 2-2 mM at ratio 1:1 had the largest stem diameter.

Stem length was measured to fully understand the optimal NH_4^+-K^+ concentration required for stem growth. At increasing NH_4^+/constant K^+, an increase in NH_4^+/K^+ concentration led to a rapid surge in stem length, but further increase led to a decline (Figure 7). Compared with the positive control, stem length was markedly increased in all concentrations at ratios 1:1 and 2:1, except at concentration 20-10 mM (2:1), which had a 30.9% reduction. The stem length of the positive control was significantly higher than all other treatments under increasing NH_4^+ ratios (5:1, 10:1, 20:1, 50:1, and 100:1). Following the same ratio pattern, 50-1 mM and 20-0.2 mM (50:1) and 50-0.5 mM (100:1) were lower than the negative control. Regardless of both controls, stem length increases as NH_4^+/K^+ concentration increases at ratios 1:2 and 1:5. Conversely, at ratios 1:10, 1:20, and 1:50, a drastic reduction in the stem length was observed when the concentration was increased. Taken together, stem length peaks at 2-2 mM (1:1), and was 35.1% higher than 5-10 mM (1:2) (which was the highest under constant NH_4^+/increasing K^+ ratio).

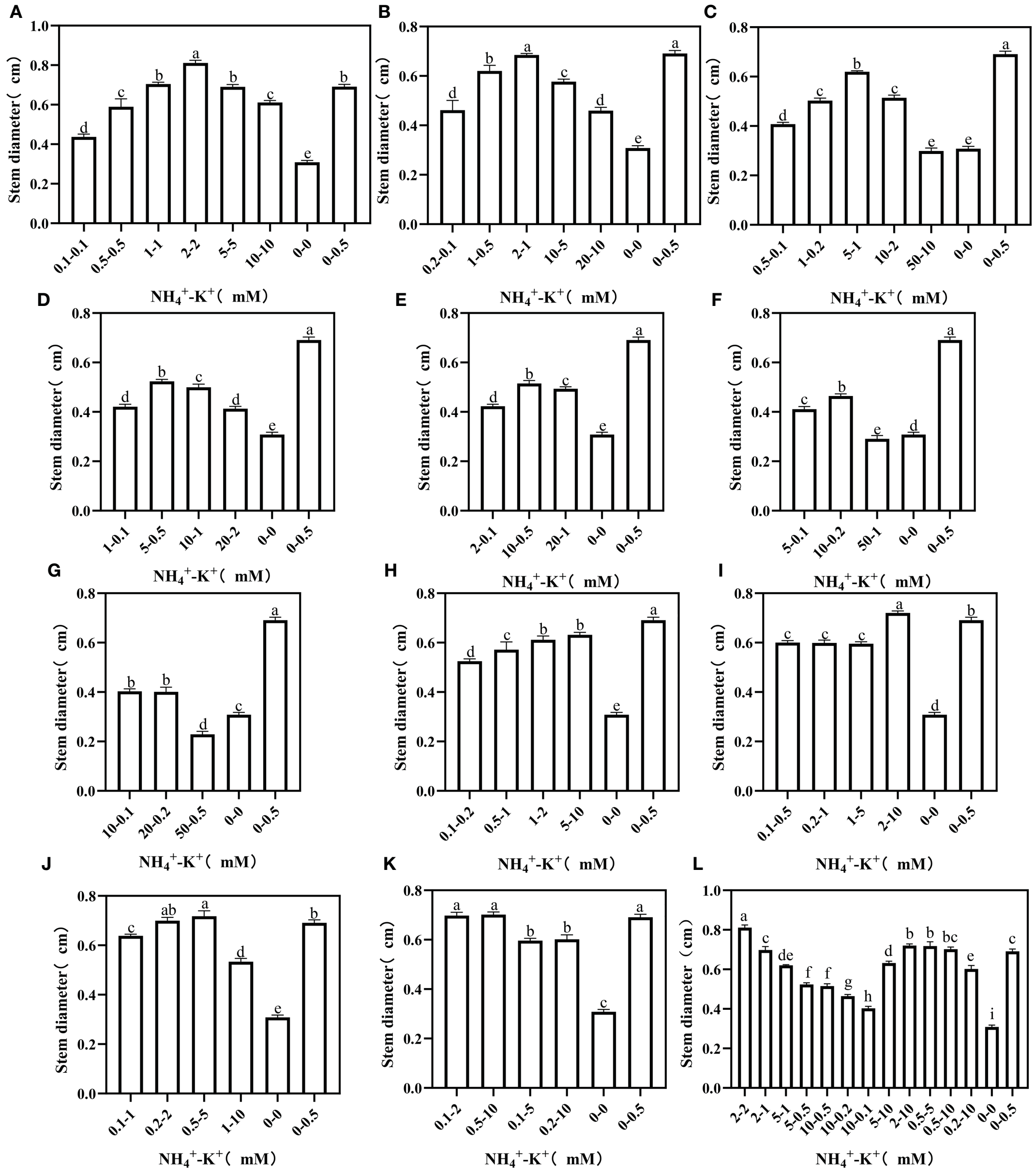

FIGURE 6
Stem diameter of tobacco as affected by different NH_4^+: K^+ ratios. Graphs **(A-G)** represent increasing NH_4^+ at constant K^+ (at 1) ratios. **(A)** NH_4^+/K^+ ratio 1:1, **(B)** 2:1, **(C)** 5:1, **(D)** 10:1, **(E)** 20:1, **(F)** 50:1, and **(G)** 100:1. Graphs **(H–K)** connote constant NH_4^+ (at 1) at increasing K^+ ratio. **(H)** NH_4^+/K^+ ratio 1:2, **(I)** 1:5, **(J)** 1:10, **(K)** 1:20 (0.1-2 mM and 0.5-10 mM) and 1:50 (0.1-5 mM and 0.2-10 mM) **(L)** comparison of NH_4^+-K^+ concentration within each ratio. All the NH_4^+/K^+ concentration within each ratio were compared with the positive (without NH_4^+, but with K^+).and negative control (without NH_4^+ and K^+). The above growth parameters were measured 15 days after treatment. Significant means were separated using standard deviation ± SD (n= 3 biological replicates).

Root growth of tobacco seedlings as affected by varying NH_4^+/K^+ concentration and ratios

Root weight differs within the treated concentrations at different ratios (Figure 1). Within each of the increasing NH_4^+: constant K^+ ratios, fresh root weight increases with increasing NH_4^+ -increasing K^+ concentration until a point was reached where further increase led to a gradual decrease. Compared with the positive control (1 mM K^+ supply in the absence of NH_4^+), the fresh root weight of NH_4^+-K^+ millimolar concentration 2-2 mM at ratios 1:1 was the highest, followed by 2-1 mM (2:1), with 37.1% and 8.2% increase, respectively. At ratios 5:1, 10:1, 20:1, 50:1, and 100:1, positive control had the highest root weight, but when compared with the negative control, which seems lower than all observed treatments, root weight of 50-0.5 mM at ratio 100:1 decreased by 36%. Except at lower NH_4^+ - K^+ concentrations of constant NH_4^+/increasing K^+ ratios, all other treated concentrations had increased root weight compared with the positive control. In all the concentrations examined, root weight peaks at 2-2 mM (1:1).

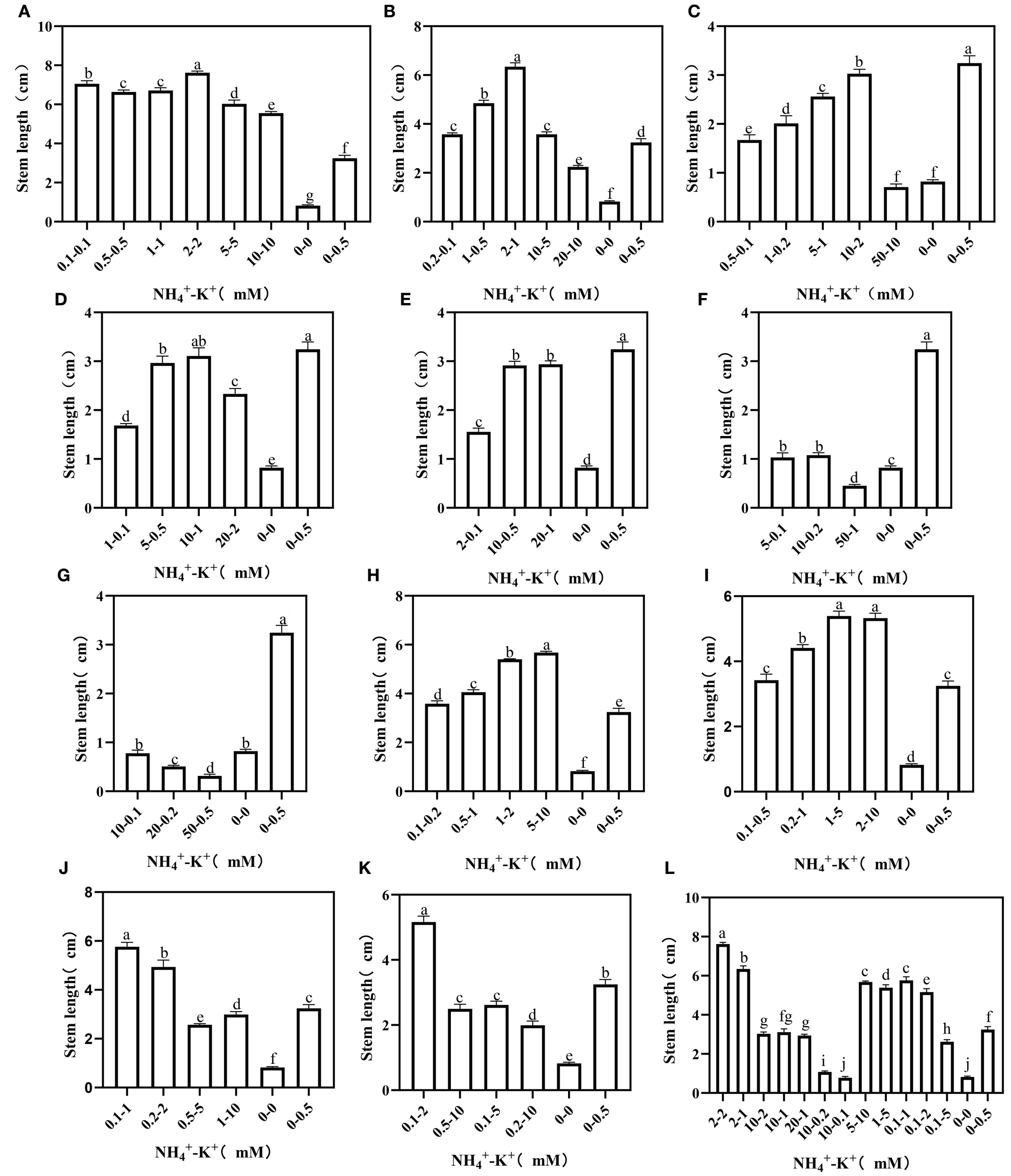

FIGURE 7
Stem length of tobacco as affected by different NH_4^+: K^+ ratios. Graphs **(A-G)** represent increasing NH_4^+ at constant K^+ (at 1) ratios. **(A)** NH_4^+/K^+ ratio 1:1, **(B)** 2:1, **(C)** 5:1, **(D)** 10:1, **(E)** 20:1, **(F)** 50:1, and **(G)** 100:1. Graphs **(H–K)** connote constant NH_4^+ (at 1) at increasing K^+ ratio. **(H)** NH_4^+/K^+ ratio 1:2, **(I)** 1:5, **(J)** 1:10, **(K)** 1:20 (0.1-2 mM and 0.5-10 mM) and 1:50 (0.1-5 mM and 0.2-10 mM) **(L)** comparison of NH_4^+-K^+ concentration within each ratio. All the NH_4^+/K^+ concentration within each ratio were compared with the positive (without NH_4^+, but with K^+).and negative control (without NH_4^+ and K^+). The above growth parameters were measured 15 days after treatment. Significant means were separated using standard deviation ± SD (n= 3 biological replicates).

There were significant differences in the K^+ content of roots under varying NH_4^+-K^+ concentration, and are presented in Figure 2. A progressive increase in NH_4^+- K^+ concentrations at increasing NH_4^+/constant K^+ ratios resulted in a marked increase in the root K^+ content, however, a point was reached where further increase led to a marked reduction. Except at lower NH_4^+-K^+ concentrations (for example 0.1-0.1 mM, 0.2-0.1mM, 0.5-0.1mM, 1-0.2mM, 1-0.1mM and 2-0.1mM), the root K^+ content of all other concentrations at NH_4^+: K^+ ratios 1:1, 2:1, 5:1, 10:1, and 20:1 was significantly higher than the positive control. Root K^+ content was highest at 10-5 mM (2:1), followed by 2-2 mM (1:1), 2-1 mM (2:1), 5-1 mM (5:1), 10-1 mM (10:1) and 20-1 mM (20:1). However, all concentrations at ratios 50:1 and 100:1 exhibit reduced K^+ content relative to the positive control. Compared with the positive control, all observed concentrations under constant NH_4^+/increasing K^+ ratios, had marked increment in their root K^+ content, except 0.1-

0.2 mM (1:2). At such NH_4^+/K^+ ratio, root K^+ content peaks at 1-5 mM (1:5), and increased by 26.4% relative to 10-5 mM (2:1), which was highest under increasing NH_4^+/constant K^+ ratio.

There were significant differences in the NH_4^+ content of root under varying NH_4^+-K^+ concentration, and are presented in Figure 3. At ratios 1:1, 2:1, 5:1, and 10:1 root NH_4^+ content increases with increasing NH_4^+- K^+ millimolar concentration until a point was reached where a notable reduction in NH_4^+ content was observed (NH_4^+-K^+ 2-2 mM (ratio 1:1); 2-1mM (2:1); 10-2mM (5:1); 10-1 mM (10:1); 10-0.2 mM (50:1)). A further increase in NH_4^+-K^+ millimolar concentration resulted in a marked increase in leaf NH_4^+ content. However, at ratios 20:1 and 100:1, leaf NH_4^+ content increases with increasing NH_4^+-K^+ concentration. Following same increasing NH_4^+ ratio pattern, positive control had the lowest root NH_4^+ content. Regardless of both controls, at constant NH_4^+/increasing K^+ ratios, a direct relationship was observed between the root NH_4^+ content and NH_4^+/K^+ concentration, except 1-20 mM (1:20). Under the same ratio pattern, treatment with no K^+ and NH_4^+ (negative control) had the highest root NH_4^+ content.

As shown in Figure 8, root activity was affected by NH_4^+/K^+ concentration at different ratios. At ratios 1:1, 2:1, and 5:1, root activity was enhanced as NH_4^+/K^+ concentrations increased; however, a point was reached where further increase resulted in a decrease in root activity. Conversely, at NH_4^+/K^+ ratios 10:1, 20:1, 50:1 and 100:1, root activity decreases with increasing NH_4^+/K^+ concentrations. Concentrations 2-2 mM and 1-1 mM at ratios 1:1 had the strongest root activity. However, relative to the positive control, the root activity of other increasing NH_4^+ ratios (10:1, 20:1, 50:1, and 100:1) was either insignificant or decreased. At constant NH_4^+/increasing K^+ ratio, root activity was strongest at concentrations 1-2 mM (1:2) and 0.2-1 mM (1:5), whereas, at NH_4^+/K^+ ratios 1:10, 1:20 and 1:50, positive control had the highest root activity. Of all the treated concentration, root activity peaks at concentrations NH_4^+ - K^+ 2-2 mM (1:1).

The effects of variations in NH_4^+-K^+ concentration at different ratios were further evaluated in root length. The root length of the negative control was significantly higher than all other treated concentrations at an increasing NH_4^+/constant K^+ ratio; only the root length of 2-2 mM at ratio 1:1 increased by 6.8% relative to the negative control (Figure 9). Similarly, at constant NH_4^+/increasing K^+ ratios, only concentration 0.2-1 mM (1:5) had markedly increased (13.16 cm) root length compared with the negative control (12.29 cm), all other observed concentrations had a pronounced reduction in root length.

Under increasing NH_4^+/constant K^+, root area was highest at 2-2 mM (1:1), 2-1 mM (2:1), 1-0.2 mM (5:1), 5-0.5 mM (10:1) and 20-1 mM (20:1), but when compared with the positive control, all concentrations at ratios 50:1 and 100:1 had significantly lower root area (Figure 10). At constant NH_4^+/ increasing K^+ ratio, only 0.2-2 mM at ratio 1:10 had a lower root area relative to the positive control; all other observed concentrations under such increasing K^+ ratio pattern was significantly higher. In all the treated concentrations, the root area peaks at 0.5-10 mM (1:20).

Correlation among the growth parameters

We performed correlation analysis to establish the relationship between different growth parameters and their contributions to tobacco performance under different NH_4^+/K^+ concentrations (Figure 11). Most of the growth traits are either positively or negatively correlated, very few are not significantly correlated. The strongest negative correlations ($p < 0.001$) are obtained between NH_4^+ content (leaves, stems and roots) and the other growth indicator such as dry root weight (DRW), fresh root weight (FRW), stem girth (diameter), root area, dry leaf weight (DLW), fresh leaf weight (FLW), dry stem weight (DSW), fresh stem weight (FSW), leaf area, stem K^+ content (SK), leaf K^+ content (LK), root K^+ content (RK), root length, root activity, and stem length. This implies that value increase of NH_4^+ content in the leaves, stems, and roots leads to a decrease in each of the listed growth variables. However, nearly all other growth variables are positively correlated with each other. For example, increase in SK led to an increase in leaf area ($p < 0.001$), fresh weights ($p < 0.001$), among others. The relationship further supported the notion that excessive NH_4^+ supply leads to plant growth retardation.

Discussion

The influence of K^+ and nitrogen forms (NH_4^+ and NO_3^-) on plant growth and development has been a focus of research (Wang et al., 2003; Szczerba et al., 2008; Zhang et al., 2010; Witold et al., 2017). However, no such research has addressed the appropriate quantity of K^+ and NH_4^+ required to enhance plant growth. To fully understand the effects of varying NH_4^+/K^+ concentration on growth, and the appropriate amount required for optimal growth of tobacco seedlings, the 15-day- NH_4^+/K^+ treated samples were evaluated on a leaf, stem and root basis. Our study revealed that NH_4^+- K^+ concentration had a profound effect on the growth of tobacco seedlings while pinpointing the right combination needed for the optimum seedling growth.

Leaf parameter

It has been shown that potassium (K^+) and nitrogen (N) (ammonium (NH_4^+) as a major form of inorganic nitrogen) is the most limiting nutrient during plant growth (Szczerba et al., 2008; El Gendy et al., 2015). Thus, symptoms ensued from their excessive supply/deficiency are notable on fresh leaf weight (Figure 1), dry leaf weight (Figure S1) leaf NH_4^+ and K^+ content (Figures 2, 3), leaf area (Figure 4), leaf color (Figure S2) and chlorophyll content (Figure 5). The supply of NH_4^+ and K^+ concentrations to tobacco plants during the seedling stage exerted varying effects on leaf weight. Under increasing NH_4^+ at constant K^+ ratios, the tolerance of tobacco leaf to increasing NH_4^+/K^+ nutrition was optimal at ratios 1:1 (2-2mM, which had the highest fresh leaf weight; 11.2 g/ plant), 2:1(2-1 mM; 8.6 g/plant) and 5:1 (5-1 mM; 7.6 g/plant), and beyond these ratios, the tolerance capacity decreased drastically

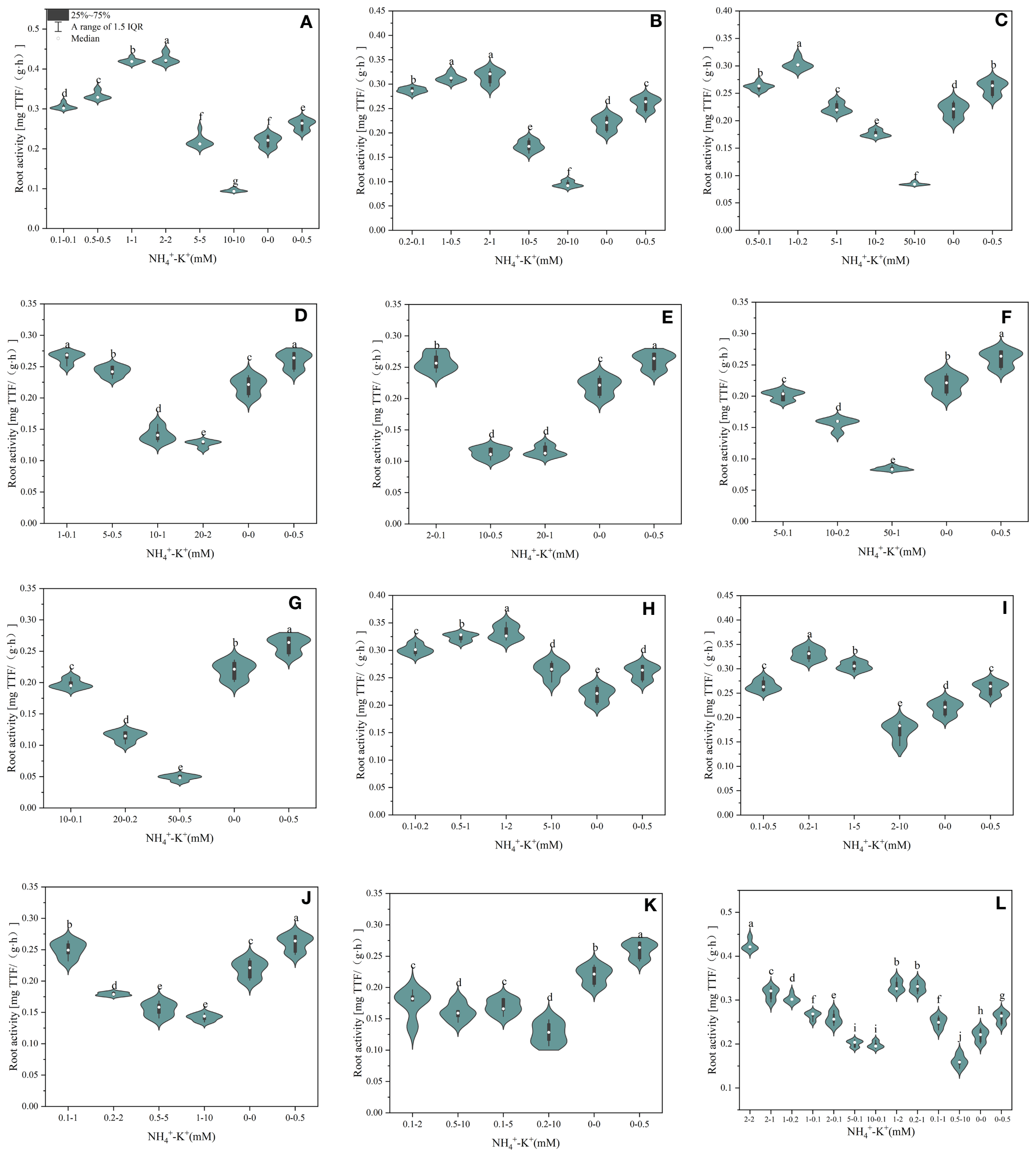

FIGURE 8
Root activity of tobacco as affected by different NH_4^+: K^+ ratios. Graphs **(A–G)** represent increasing NH_4^+ at constant K^+ (at 1) ratios. **(A)** NH_4^+/K^+ ratio 1:1, **(B)** 2:1, **(C)** 5:1, **(D)** 10:1, **(E)** 20:1, **(F)** 50:1, and **(G)** 100:1. Graphs **(H–K)** connote constant NH_4^+ (at 1) at increasing K^+ ratio. **(H)** NH_4^+/K^+ ratio 1:2, **(I)** 1:5, **(J)** 1:10, **(K)** 1:20 (0.1-2 mM and 0.5-10 mM) and 1:50 (0.1-5 mM and 0.2-10 mM) **(L)** comparison of NH_4^+-K^+ concentration within each ratio. All the NH_4^+/K^+ concentration within each ratio were compared with the positive (without NH_4^+, but with K^+).and negative control (without NH_4^+ and K^+). The above growth parameters were measured 15 days after treatment. Significant means were separated using standard deviation ± SD (n= 9 biological replicates).

(Figure 1). However, the study by Balkos et al. (2010) revealed optimum leaf growth in rice plants with NH_4^+- K^+ concentration 10-5 mM (ratio 2:1), suggesting strong tolerance of rice to high NH_4^+ nutrition, indicating that plant tolerance to high NH_4^+ is plant species dependent. Here, NH_4^+: K^+ ratios beyond 5:1 impaired leaf growth, leading to stunted leaf weight and shrank leaves with deep greenish or yellowish colouration (leaf chlorosis). These symptoms, as presented in Figure S2, are typical of NH_4^+ toxicity. Also, at NH_4^+: K^+ ratios 10:1, 20:1, 50:1 and 100:1, NH_4^+ toxicity repressed leaf growth, and reduced leaf K^+ content (Figure 2). Following the same ratio pattern (increasing NH_4^+/constant K^+), for example, NH_4^+/K^+ millimolar concentration 2-2 mM at ratio 1:1 had improved leaf weight (11.2 g/plant) and K^+ content (1.76 mmolg/DW), whereas, a drastic leaf weight (3.37 g) and K^+ content (0.49 mmolg/DW) reduction was observed in NH_4^+: K^+ ratio 20:1 (2-0.1 mM) (Figures 1, 2). This result indicates that leaf growth and K^+ content are optimum at equal NH_4^+/K^+ ratios 1:1, but are suppressed beyond ratios 5:1 during the seedling stage (Figures 1, 2). This is supported by previous studies, which reported that excessive supply of NH_4^+ nutrient represses leaf growth and K^+ uptake (Szczerba et al., 2006; Shi et al., 2020a; Aluko et al., 2022). It is worth noting that the reduced K^+ content in the leaf could be

10.3389/fpls.2023.1152817

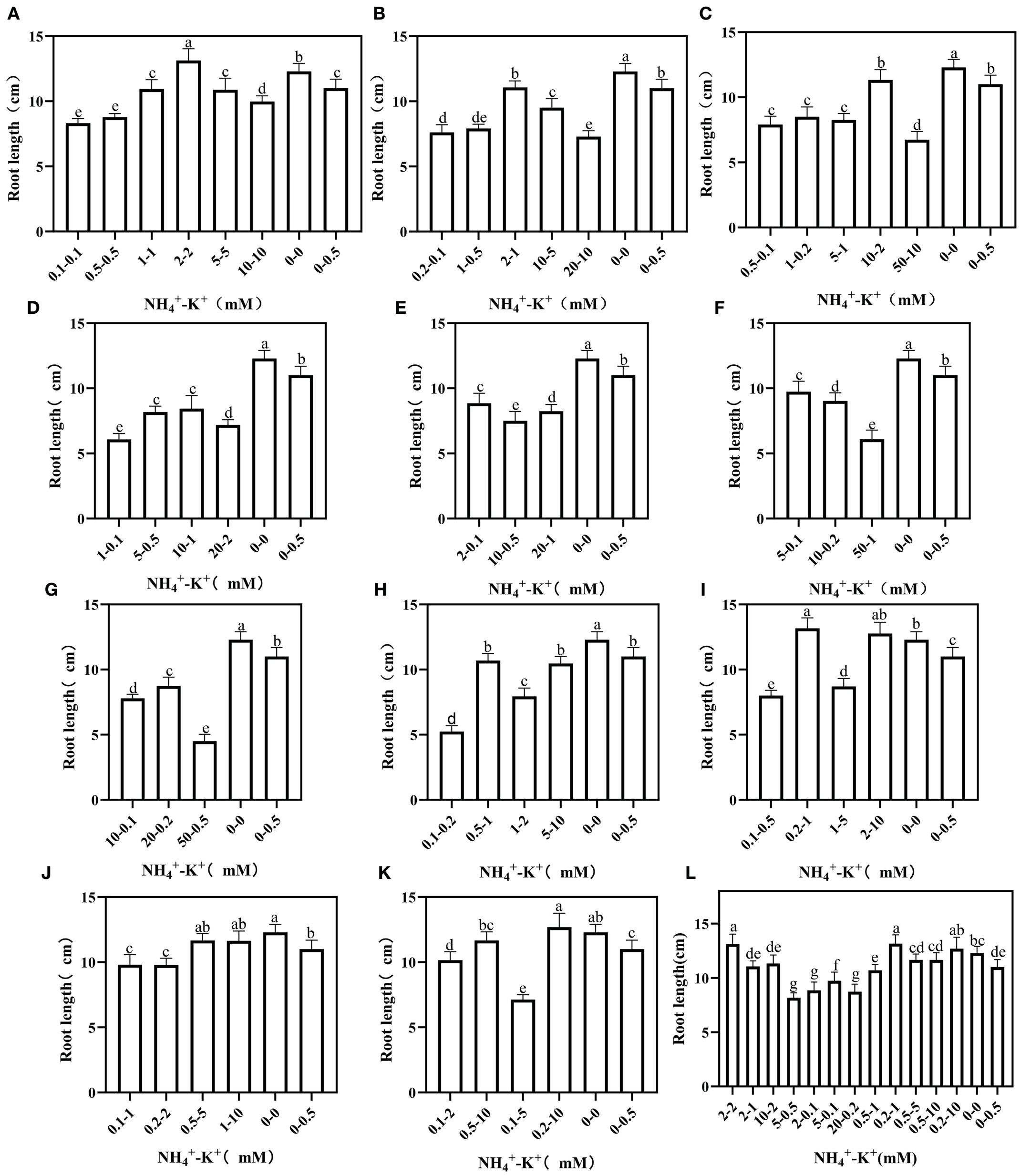

FIGURE 9
Root length of tobacco as affected by different NH_4^+: K^+ ratios. Graphs **(A-G)** represent increasing NH_4^+ at constant K^+ (at 1) ratios. **(A)** NH_4^+/K^+ ratio 1:1, **(B)** 2:1, **(C)** 5:1, **(D)** 10:1, **(E)** 20:1, **(F)** 50:1, and **(G)** 100:1. Graphs **(H–K)** connote constant NH_4^+ (at 1) at increasing K^+ ratio. **(H)** NH_4^+/K^+ ratio 1:2, **(I)** 1:5, **(J)** 1:10, **(K)** 1:20 (0.1-2 mM and 0.5-10 mM) and 1:50 (0.1-5 mM and 0.2-10 mM) **(L)** comparison of NH_4^+-K^+ concentration within each ratio. All the NH_4^+/K^+ concentration within each ratio were compared with the positive (without NH_4^+, but with K^+).and negative control (without NH_4^+ and K^+). The above growth parameters were measured 15 days after treatment. Significant means were separated using standard deviation ± SD (n= 3 biological replicates).

linked to NH_4^+ toxicity. Samples with high NH_4^+ tends to have higher leaf NH_4^+ content and lower leaf K+ content (Figure 11), an indication that an appropriate amount of these two nutrients is required for growth. Perhaps, the strong negative correlation between NH_4^+ toxicity and reduced K^+ content in plant tissue altered in the balance between these two cations (NH_4^+ and K^+) (Shi et al., 2020a).

Interestingly, beyond the optimal NH_4^+ - K^+ concentrations (at increasing concentrations of both nutrients (NH_4^+ and K^+), leaf weight decreases. Using ratio 1:1 as a good example, tobacco leaf weight at NH_4^+- K^+ concentrations 5-5 mM and 10-10 mM, decreases by 37.5% and 43.5%, respectively, relative to the NH_4^+-K^+ 2-2 mM (where optimal leaf weight was attained) (Figure 1). It appears that excessive supply of NH_4^+ and K^+ beyond the optimal triggers leaf weight reduction, and in line with Shi et al., 2020a, who reported the same for *Arabidopsis*. The reductions in leaf growth under such high K^+ and NH_4^+ conditions may partly be due to the energetic drain on root cells catalyzing substantial futile cycling of both cations (K^+ and NH_4^+) when nutrient supply is high (Britto and Kronzucker, 2001; Britto and Kronzucker, 2002; Szczerba et al.,

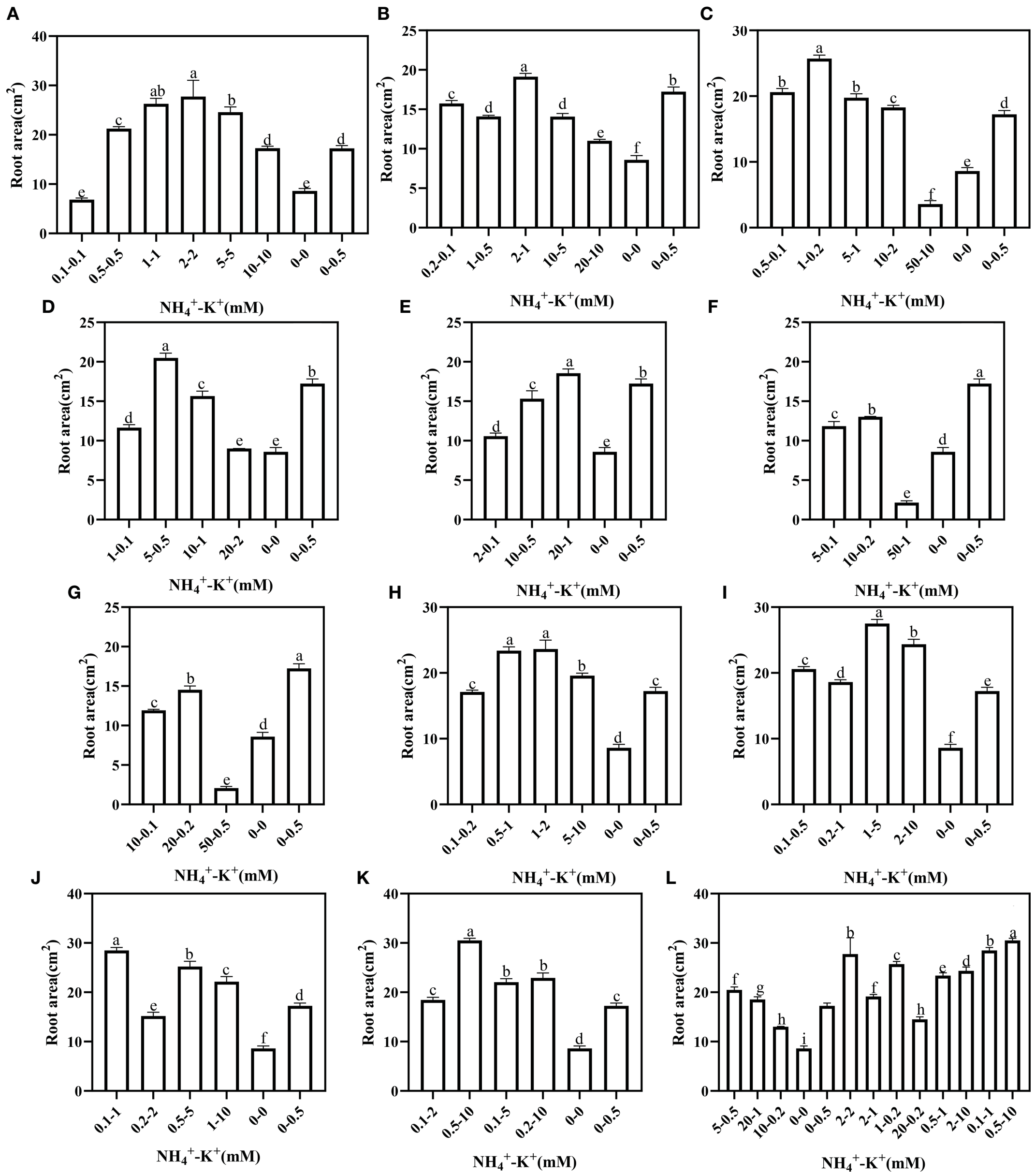

FIGURE 10
Root area of tobacco as affected by different NH_4^+: K^+ ratios. Graphs **(A-G)** represent increasing NH_4^+ at constant K^+ (at 1) ratios. **(A)** NH_4^+/K^+ ratio 1:1, **(B)** 2:1, **(C)** 5:1, **(D)** 10:1, **(E)** 20:1, **(F)** 50:1, and **(G)** 100:1. Graphs **(H-K)** connote constant NH_4^+ (at 1) at increasing K^+ ratio. **(H)** NH_4^+/K^+ ratio 1:2, **(I)** 1:5, **(J)** 1:10, **(K)** 1:20 (0.1-2 mM and 0.5-10 mM) and 1:50 (0.1-5 mM and 0.2-10 mM) **(L)** comparison of NH_4^+-K^+ concentration within each ratio. All the NH_4^+/K^+ concentration within each ratio were compared with the positive (without NH_4^+, but with K^+).and negative control (without NH_4^+ and K^+). The above growth parameters were measured 15 days after treatment. Significant means were separated using standard deviation ± SD (n= 3 biological replicates).

2006). Also, low concentrations of NH_4^+ and K^+ may adversely affect leaf growth. In the present study, low NH_4^+- K^+ concentrations (0.1-0.1 mM, 0.1-0.2 mM) had significantly reduced fresh leaf weight (Figures 1, 11). This result demonstrated that K^+ and NH_4^+ deficiency also impair leaf growth (Shi et al., 2020a; Li et al., 2021; Liu et al., 2022), and as such, maintaining an optimal nutritional balance between these two cations becomes expedient.

NH_4^+ toxicity was mitigated with an additional K^+ supply to wheat plants (Guo et al., 2019). Similarly, Kong et al. (2014) revealed that an extra supply of K^+ mitigated the detrimental effects of excessive supply of NH_4^+, thus increasing the culm mechanical strength and N remobilization efficiency of wheat by 23% and 35%, respectively. Our findings showed that maintaining NH_4^+ and K^+ at appropriate concentrations rather than an excessive supply of NH_4^+, could reduce the incidence of stunted leaf weight and leaf chlorosis. Given that leaf weight and leaf K^+ content peaks at NH_4^+- K^+ concentration 2-2 mM (at ratio 1:1), increased leaf weight at this concentration is strongly associated with the leaf K^+ content (Figure 11) (Santos et al., 2021). However, at increasing K^+ concentrations, the highest leaf weight (11.5 g) was attained at 5-10 mM and was comparable to that observed under 2-2mM (11.2 g)

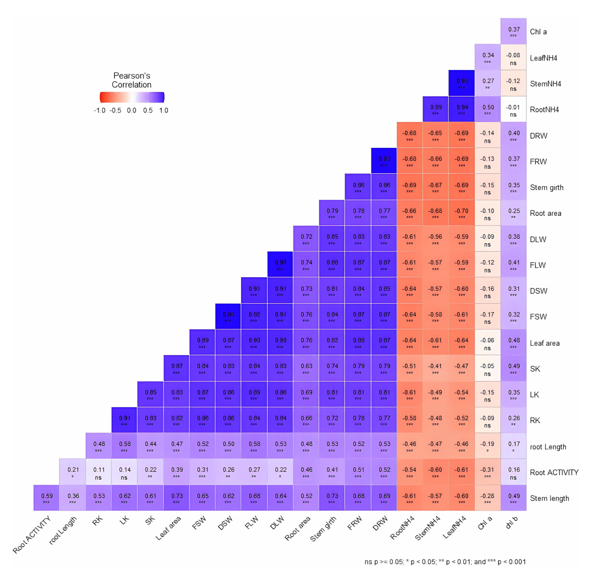

FIGURE 11
Relationship between growth variables in tobacco leaves, stems, and roots. The correlation analysis was performed using pearson correlation in R studio. ns: no significance difference; *p < 0.05; **p < 0.01; ***p < 0.001. The growth variables is represented by the acronyms in the figure, which include, dry root weight (DRW), fresh root weight (FRW), stem girth (diameter), root area, dry leaf weight (DLW), fresh leaf weight (FLW), dry stem weight (DSW), fresh stem weight (FSW), leaf area, stem K^+ content (SK), leaf K^+ content (LK), root K^+ content (RK), chlorophyll a (Chl a), chlorophyll b (Chl b), leaf NH_4^+ content (LeafNH4), stem NH_4^+ content (stem NH4), root NH_4^+ content (root NH4), root length, root activity, and stem length.

NH_4^+ - K^+ concentration (Figure 1L), demonstrating the putative role of K^+ in leaf development. In addition, NH_4^+: K^+ at equal ratios (1:1) enhances the fresh leaf weight of tobacco seedlings. A similar trend was reported in *Arabidopsis*, with optimal shoot weight attained at NH_4^+: K^+ ratio 1:1 (0.5-0.5 mM) (Shi et al., 2020a).

Leaf surface area is a crucial parameter that determines the capacity of a crop to intercept photosynthetic light, thus, affecting leaf growth and productivity (Weraduwage et al., 2015). Reduction in leaf area was more severe under a high NH_4^+: constant K^+ ratio (Figure 4), thus limiting leaf growth under such conditions. Similar findings have been reported in tobacco (Weraduwage et al., 2015), wheat (Guo et al., 2019), and sugar beet (Raab and Terry, 1994). This finding showed that there is a strong correlation between reduced leaf area and leaf growth; hence the inhibition of tobacco leaf growth could be attributed to a reduction in leaf area (Figure 11). However, at increasing K^+ concentration, increased leaf area suggests the crucial role of K^+ in leaf expansion (Figures 4, 11) (Hu et al., 2020).

Based on the visual evaluation, leaf chlorophyll content is often assessed in terms of leaf colour. In the present study, we observed that the leaf colour of high NH_4^+-fed seedlings was dark green (Figure S2), and consequently, higher chlorophyll content was observed in such plants (Figures 5 , 11). This is in line with the study of Bojović and Marković (2009), which revealed that plants exposed to high N have leaves with dark green colour. The dark green leaf colour and enhanced chlorophyll content are associated with N being a structural component of chlorophyll, thereby influencing chloroplast formation in plants. Thus, leaf colour is strongly associated with the N content of the leaf. Nonetheless, under high NH_4^+ and constant K^+ ratios 50:1 and 100:1, a drastic decline in the chlorophyll content was observed, reflecting leaf chlorosis (Figures S2, 5). Light green colouration was observed in the leaves of constant NH_4^{+}/increasing K^+ - fed plants (Figure S2; Bojović and Marković (2009) reported that cultivars with low N content had reduced chlorophyll content in their leaves. Hence, reductions in the intensity of leaf green colour could be due to the reduced N content and, consequently low chlorophyll content.

We deduced that optimal growth for tobacco leaf during the seedling stage could be achieved with NH_4^+ and K^+ at concentrations of 2-2 mM (ratio 1:1) (Figure 1L). This is because at such concentration, all leaf growth variables were significantly improved compared to positive control. Thus, any further increase or decrease beyond such concentration might not be crucial for tobacco leaf growth at the seedling stage. From our findings, the severity of K^+ and NH_4^+ symptoms due to excessive supply or deficiency was apparent on the leaf growth parameters, which is in line with previous studies (Shi et al., 2020a; Li et al., 2021; Poucet et al., 2021; Saloner and Bernstein, 2022).

Stem parameter

Stem growth often depends on the availability of nutrients such as N and K^+ (Souza and Tavares, 2021; Xie et al., 2021; Aluko et al., 2022; Marschner and Rengel, 2023). Therefore, stem growth must be ensured to facilitate photosynthates and uptake of nutrient through the root, hence, the need for optimal supply of NH_4^+ - K^+ at the right concentration and ratio.

Various NH_4^+ - K^+ concentrations at different ratios influence stem growth. Our findings showed that thin stems were evident under high NH_4^+/constant K^+, especially at ratios beyond 5:1 (Figures 1, S2), which suggests that the stem biomass was significantly suppressed due to NH_4^+ toxicity. In addition, stem weight was optimal at 1-2 mM (1:2), demonstrating the preference of stem for K^+ over NH_4^+. This result indicates that tobacco stems are more susceptible to an excessive supply of NH_4^+, unlike the leaf weight, which was optimal at 2-2 mM (Figure 1).

Moreover, stem K^+ content and stem growth were reduced when plants were exposed to NH_4^+/K^+ ratios above 10:1, while NH_4^+ stem content was increased (Figures 2, 11). This observation was not unexpected as an excessive supply of NH_4^+ inhibits K^+ uptake. Our research findings are in accordance with earlier studies in rice (Szczerba et al., 2008), barley (Walch-Liu et al., 2000), and wheat (Guo et al., 2019), that high NH_4^+ nutrition reduces K^+ uptake and content. The effects of NH_4^+ toxicity was obviated with the supply of K^+ at an increased concentration over NH_4^+. However, at high NH_4^+ - K^+ concentrations [e.g., 20-2 mM and 10-1 mM (at ratio 10:1)] of both nutrients, K^+ content was higher than the positive control (without NH_4^+) (Figure 2), probably because the K^+ concentration was sufficient to counteract the effect of excessive NH_4^+. Furthermore, our results showed that at concentrations beyond 5-1 mM (at ratio 5:1), a decrease in stem growth was observed, but the K^+ content was still high at ratio 10:1 (e.g. 20-2 mM and 10-1 mM) (Figures 1, 2), which indicates that tobacco stem can tolerate excess K^+ up to ratios 10:1. The reason for such findings could partly be that under high nutrient supply, there is diversion of energy needed for growth to recycle excessive K^+ and NH_4^+ which culminates in poor nutrient utilization due to energy drain and negative feedback mechanism (Britto et al., 2001; Britto and Kronzucker, 2002; Britto and Kronzucker, 2006). Unexpectedly, at constant NH_4^+/increasing K^+ concentration, a drop in K^+ content was notable at; 1-2 mM, 1-5 mM and 0.5-5 mM (Figure 1). A similar reduction was observed when external K^+ supply was raised from 1.5 mM to 40 mM in rice seedlings (Szczerba et al., 2008). This interesting phenomenon may suggest the crucial need for a nutritional balance between these ions (NH_4^+ and K^+) for plant growth and development.

We investigated the effect of NH_4^+ and K^+ treatments on stem length and diameters, which are crucial indicators for stem growth. Our results showed that stem diameter was suppressed at ratios exceeding NH_4^+: K^+ ratios 1:1 (Figure 6), while stem length was reduced at NH_4^+: K^+ ratios beyond 2:1 (Figure 7). Also, stem length and stem diameter were increased at an elevated K^+ concentration of 5 (NH_4^+: K^+ ratio 1:5) but decreased when K^+ exceeded such limit. These findings further demonstrated that stem growth could be enhanced when there is a balance between these ions (NH_4^+: K^+). Zaman et al. (2015) mitigated the negative impact of excessive N application by supplementing with external K^+ to improve stem strength and yield. Following the obtained result from stem weight and other growth variables, stem growth appears optimal at NH_4^+ - K^+ concentrations 1-2 mM or 2-2 mM.

Root parameter

The root is the major plant organ responsible for the uptake of water and other mineral nutrients, including K^+ and NH_4^+; hence, it becomes imperative to understand the optimal NH_4^+ - K^+ concentrations required for the proper functioning of the root. The present study evaluated the root growth of tobacco plants at the seedling stage based on their exposure to NH_4^+ and K^+ nutrients at various concentrations. Reductions in root growth evident in thin root and reduced K^+ content was observed in increasing NH_4^+ - constant K^+ concentrations beyond 5-1 mM (5:1), suggesting visible symptoms of NH_4^+ toxicity (Figures 1, S2). In support of this claim, Banuelos et al. (2002) reported reduced K^+ uptake in detached rice roots exposed to high NH_4^+ concentration. The negative effect observed with high NH_4^+ nutrition was obviated when external K^+ was increased (Figure S2), suggesting that NH_4^+ supply in plants depend on the optimal supply of K^+ (Shi et al., 2020a).

Also, root growth variables, including root activity, root length, and root area, were improved with increasing K^+ ratios (Figures 8-10). Although increasing K^+ exerts a positive effect on root growth, optimal root growth was attained at equal concentrations of NH_4^+- K^+ 2-2 mM (1:1). The response of various parts of tobacco plants organs (leaf, stem, and root) are influenced by both NH_4^+ - K^+ millimolar concentration and ratio at which the nutrient was supplied. This is the first study that examined such influence, regarding NH_4^+: K^+ ratios and concentration to ascertain optimum growth. This justifies why nutrient supply cannot be based only on either concentration or ratio, but on a combination of both provides an in-depth understanding of the optimal growth of tobacco seedlings.

Conclusion

Our study showed that various parts of the tobacco plant (leaf, stem, and root) respond differently to varying concentrations of NH_4^+/K^+ as well as ratios. Optimum growth of tobacco leaf and root were observed with equal concentrations of NH_4^+/K^+ (2-2 mM) at ratio 1:1, whereas stem growth was attained with concentration of 1 mM NH_4^+ and 2 mM K^+ at ratio (1:2). Interestingly, our results explained the degree of tolerance of different organs of tobacco plant to ammonium despite its natural low tolerance for ammonium. This novelty was not explained in previous research on other crops which have low tolerance for ammonium like tobacco, rather the investigations was concentrated on the physiological response of NH_4^+ to plant yield. The study provided an insight into the right combination of NH_4^+/K^+ that could mitigate or prevent NH_4^+ or K^+ stress in the tobacco seedlings. In the same lieu, the large sample size (47 treatments) at 12 NH_4^+/K^+ ratios lends an evidence for determination of optimal concentration of NH_4^+/K^+ required for growth of tobacco seedling in a hydroponic system. Although, this present study found that NH_4^+/K^+ concentrations stated above would be required for optimal growth of different organs of tobacco plant at seedling stage, further research would be required to validate the optimal NH_4^+ - K^+ concentration, and at what ratio, required for growth at a later developmental stage of tobacco plant.

Data availability statement

The original contributions presented in the study are included in the article Supplementary Material. Further inquiries can be directed to the corresponding authors.

Author contributions

CL and OA, designed the experiment, carried out most experiments, data analysis, and wrote the manuscript. SS participated in the design and provided useful advice. ZM, TN, CS, and ZL participated in the sample collection and parameter measurements. QW and HL conceived of the study and participated in its design and coordination. All authors contributed to the article and approved the submitted version.

Funding

This work was funded by the National Natural Science Foundation of China (32170387); the Agricultural Science and Technology Innovation Program (ASTIP-TRIC02); the International Foundation of Tobacco Research Institute of Chinese Academy of Agricultural Sciences (IFT202102); the Fundamental Research Funds for China Agricultural Academy of Sciences (1610232021002); the Key Funding of CNTC (No. 110202101035(JY-12)) and YNTI (No. 2022JY03).

Acknowledgments

We would like to thank Guang Yuan, Jiaping Yuan, Jingjing Mao from Tobacco Research Institute for valuable suggestions in tobacco breeding, Prof. Yuhe Sun, Prof. Yongfeng Guo, Prof. Aiguo Yang and Mengmeng Cui from Tobacco Research Institute for the support during the experiments, and G.A. Adegbite for helping out with the correlation analysis.

Conflict of interest

SS was employed by Shanghai Tobacco Company, Ltd. ZM and ZL were was employed by Yichang City Company, Hubei Tobacco Company.

The remaining authors declare that the research was conducted in the absence of any commercial or financial relationships that could be constructed as a potential conflict of interest.

Publisher's note

Supplementary material

The Supplementary Material for this article can be found online at: https://www.frontiersin.org/articles/10.3389/fpls.2023.1152817/full#supplementary-material

SUPPLEMENTARY FIGURE 1

Dry weight of leaf (FLW), stem (FSW), and root (FRW) of tobacco plants as affected by different NH_4^+/K^+ ratios. Graphs **(A-G)** represent increasing NH_4^+ at constant K^+ (at 1) ratios. **(A)** NH_4^+/K^+ ratio 1:1, **(B)** 2:1, **(C)** 5:1, **(D)** 10:1, **(E)** 20:1, **(F)** 50:1, and **(G)** 100:1. Graphs **(H-K)** connote constant NH_4^+ (at 1) at increasing K^+ ratio. **(H)** NH_4^+/K^+ ratio 1:2, **(I)** 1:5, **(J)** 1:10, **(K)** 1:20 (0.1-2 mM and 0.5-10 mM) and 1:50 (0.1-5 mM and 0.2-10 mM). **(L)** comparison of NH_4^+-K^+ concentration within each ratio. All the NH_4^+/K^+ concentration within each ratio were compared with the positive (without NH_4^+, but with K^+).and negative control (without NH_4^+ and K^+). Dry weight was determined 15 days after treatment. Letters represent the mean values ± SD (n= 15 biological replicates). The bars without letters have extremely low mean values.

SUPPLEMENTARY FIGURE 2

Tobacco seedlings subjected to various NH_4^{+}/K^+ concentrations at different ratios. Plants were grown in a hydroponic system with all nutrients, including 1.4 mM NO_3^- as N source but without NH_4^+ or K^+ for 6 days and subsequently treated with different NH_4^+ and K^+ for 15 days as indicated.

References

Aluko, O. O., Li, C., Wang, Q., and Liu, H. (2021). Sucrose utilization for improved crop yields: a review article. *Int. J. Mol. Sci.* 22, 4704. doi: 10.3390/ijms22094704

Aluko, O. O., Li, C., Yuan, G., Nong, T., Xiang, H., Wang, Q., et al. (2022). Differential effects of ammonium (NH4+) and potassium (K+) nutrition on photoassimilate partitioning and growth of tobacco seedlings. *Plants* 11, 3295. doi: 10.3390/plants11233295

Balkos, K. D., Britto, D. T., and Kronzucker, H. J. (2010). Optimization of ammonium acquisition and metabolism by potassium in rice (Oryza sativa l. cv. IR-72). *Plant Cell Environ.* 33 (1), 23–34. doi: 10.1111/j.1365-3040.2009.02046.x

Banuelos, M. A., Garciadeblas, B., Cubero, B., and Rodrıguez-Navarro, A. (2002). Inventory and functional characterization of the HAK potassium transporters of rice. *Plant Physiol.* 130, 784–795. doi: 10.1104/pp.007781

Bojović, B., and Marković, A. (2009). Correlation between nitrogen and chlorophyll content in wheat (Triticum aestivum L.). *Kragujevac J. Sci.* 31, 69–74.

Borges, A., Morejón, R., Izquierdo, A., Ortega, E., and Rodes, R. (2012). Nitrogen fertilization for optimizing the quality and yield of shade grown Cuban cigar tobacco: required nitrogen amounts, application schedules, adequate leaf nitrogen levels, and early season diagnostic tests. *Contributions to Tobacco Nicotine Res.* 25, 336–349. doi: 10.2478/cttr-2013-0913

Britto, D. T., and Kronzucker, H. J. (2001). Can unidirectional influx be measured in higher plants? a mathematical approach using parameters from efflux analysis. *New Phytol.* 150, 37–47. doi: 10.1046/j.1469-8137.2001.00080.x

Britto, D. T., and Kronzucker, H. J. (2002). NH4+ toxicity in higher plants: a critical review. *J. Plant Physiol.* 159, 567–584. doi: 10.1078/0176-1617-0774

Britto, D. T., and Kronzucker, H. J. (2006). Futile cycling at the plasma membrane: a hallmark of low-affinity nutrient transport. *Trends Plant Sci.* 11, 529–534. doi: 10.1016/j.tplants.2006.09.011

Britto, D. T., Siddiqi, M. Y., Glass, A. D., and Kronzucker, H. J. (2001). Futile transmembrane NH4+ cycling: a cellular hypothesis to explain ammonium toxicity in plants. *Proc. Natl. Acad. Sci.* 98, 4255–4258. doi: 10.1073/pnas.061034698

Chen, H., Zhang, Q., Wang, X., Zhang, J., Ismail, A. M., and Zhang, Z. (2021). Nitrogen form-mediated ethylene signal regulates root-to-shoot k+ translocation *via* NRT1. 5. *Plant Cell Environ.* 44, 3806–3818. doi: 10.1111/pce.14182

Dong, L., Wang, Q., Manik, S. N., Song, Y., Shi, S., Su, Y., et al. (2015). Nicotiana sylvestris calcineurin b-like protein NsylCBL10 enhances salt tolerance in transgenic arabidopsis. *Plant Cell Rep.* 34, 2053–2063. doi: 10.1007/s00299-015-1851-4

Dubey, R. S., Srivastava, R. K., and Pessarakli, M. (2021). "Physiological mechanisms of nitrogen absorption and assimilation in plants under stressful conditions," in *Handbook of plant and crop physiology* (New York: CRC Press), 579–616. doi: 10.1201/9781003093640

El Gendy, A., El Gohary, A., Omer, E., Hendawy, S., Hussein, M., Petrova, V., et al. (2015). Effect of nitrogen and potassium fertilizer on herbage and oil yield of chervil plant (Anthriscus cerefolium l.). *Ind. Crops Products* 69, 167–174. doi: 10.1016/j.indcrop.2015.02.023

Fang, G., Yang, J., Sun, T., Wang, X., and Li, Y. (2021). Evidence that synergism between potassium and nitrate enhances the alleviation of ammonium toxicity in rice seedling roots. *PloS One* 16, e0248796. doi: 10.1371/journal.pone.0248796

Guo, J., Jia, Y., Chen, H., Zhang, L., Yang, J., Zhang, J., et al. (2019). Growth, photosynthesis, and nutrient uptake in wheat are affected by differences in nitrogen levels and forms and potassium supply. *Sci. Rep.* 9, 1248. doi: 10.1038/s41598-018-37838-3

Hu, W., Lu, Z., Meng, F., Li, X., Cong, R., Ren, T., et al. (2020). The reduction in leaf area precedes that in photosynthesis under potassium deficiency: the importance of leaf anatomy. *New Phytol.* 227, 1749–1763. doi: 10.1111/nph.16644

Katz, E., Knapp, A., Lensink, M., Keller, C. K., Stefani, J., Li, J.-J., et al. (2022). Genetic variation underlying differential ammonium and nitrate responses in arabidopsis thaliana. *Plant Cell* 34, 4696–4713. doi: 10.1093/plcell/koac279

Kong, L., Sun, M., Wang, F., Liu, J., Feng, B., Si, J., et al. (2014). Effects of high NH+ 4 on k+ uptake, culm mechanical strength and grain filling in wheat. *Front. Plant Sci.* 5, 703. doi: 10.3389/fpls.2014.00703

Li, J., Hu, W., Lu, Z., Meng, F., Cong, R., Li, X., et al. (2021). Imbalance between nitrogen and potassium fertilization influences potassium deficiency symptoms in winter oilseed rape (Brassica napus L.) leaves. *Crop J.* 10 (2), 565–576. doi: 10.1016/j.cj.2021.06.001

Liang, H., Wang, L., Wang, Y., Quan, X., Li, X., Xiao, Y., et al. (2022). Root development in cunninghamia lanceolata and schima superba seedlings expresses contrasting preferences to nitrogen forms. *Forests* 13, 2085. doi: 10.3390/f13122085

Liu, J., Xia, H., Gao, Y., Pan, D., Sun, J., Liu, M., et al. (2022). Potassium deficiency causes more nitrate nitrogen to be stored in leaves for low-K sensitive sweet potato genotypes. *Front. Plant Sci.* 13, 4688. doi: 10.3389/fpls.2022.1069181

Liu, R.-X., Zhou, Z.-G., Guo, W.-Q., Chen, B.-L., and Oosterhuis, D. M. (2008). Effects of n fertilization on root development and activity of water-stressed cotton (Gossypium hirsutum l.) plants. *Agric. Water Manage.* 95, 1261–1270. doi: 10.1016/j.agwat.2008.05.002

Lu, Y. X., Li, C. J., and Zhang, F. (2005). Transpiration, potassium uptake and flow in tobacco as affected by nitrogen forms and nutrient levels. *Ann. Bot.* 95, 991–998. doi: 10.1093/aob/mci104

Marschner, P., and Rengel, Z. (2023). “Chapter 12 - Nutrient availability in soils,” in Z. Rengel, I. Cakmak and P. J. White Eds. *Marschner's Mineral Nutrition of Plants (Fourth Edition)* (Academic Press), 499–522. doi: 10.1016/B978-0-12-819773-8.00003-4

Nawarathna, K., Dandeniya, W., Dharmakeerthi, R., and Weerasinghe, P. (2021). Vegetable crops prefer different ratios of ammonium-n and nitrate-n in the growth media. *Trop. Agric. Res.* 32, 95–104. doi: 10.4038/tar.v32i1.8445

Ninkuu, V., Liu, Z., and Sun, X. (2023). Genetic regulation of nitrogen use efficiency in gossypium spp. *Plant Cell Environ.* 46 (6), 1749–1773. doi: 10.1111/pce.14586

Poucet, T., González-Moro, M. B., Cabasson, C., Beauvoit, B., Gibon, Y., Dieuaide-Noubhani, M., et al. (2021). Ammonium supply induces differential metabolic adaptive responses in tomato according to leaf phenological stage. *J. Exp. Bot.* 72, 3185–3199. doi: 10.1093/jxb/erab057

Raab, T. K., and Terry, N. (1994). Nitrogen source regulation of growth and photosynthesis in beta vulgaris l. *Plant Physiol.* 105, 1159–1166. doi: 10.1104/pp.105.4.1159

Saloner, A., and Bernstein, N. (2022). Nitrogen source matters: high NH4/NO3 ratio reduces cannabinoids, terpenoids, and yield in medical cannabis. *Front. Plant Sci.* 1209. doi: 10.3389/fpls.2022.830224

Santos, E. F., Mateus, N. S., Rosario, M. O., Garcez, T. B., Mazzafera, P., and Lavres, J. (2021). Enhancing potassium content in leaves and stems improves drought tolerance of eucalyptus clones. *Physiol. Plant* 172, 552–563. doi: 10.1111/ppl.13228

Shi, S., Xu, F., Ge, Y., Mao, J., An, L., Deng, S., et al. (2020a). NH4+ toxicity, which is mainly determined by the high NH4+/K+ ratio, is alleviated by CIPK23 in arabidopsis. *Plants* 9, 501. doi: 10.3390/plants9040501

Souza, L. A., and Tavares, R. (2021). Nitrogen and stem development: a puzzle still to be solved. *Front. Plant Sci.* 12, 630587. doi: 10.3389/fpls.2021.630587

Szczerba, M. W., Britto, D. T., Ali, S. A., Balkos, K. D., and Kronzucker, H. J. (2008). NH4+-stimulated and-inhibited components of k+ transport in rice (Oryza sativa l.). *J. Exp. Bot.* 59, 3415–3423. doi: 10.1093/jxb/ern190

Szczerba, M. W., Britto, D. T., and Kronzucker, H. J. (2006). Rapid, futile k+ cycling and pool-size dynamics define low-affinity potassium transport in barley. *Plant Physiol.* 141, 1494–1507. doi: 10.1104/pp.106.082701

Vu, D. H., Stuerz, S., Pieters, A., and Asch, F. (2021). Leaf gas exchange of lowland rice in response to nitrogen source and vapor pressure deficit. *J. Plant Nutr. Soil Sci.* 184, 448–460. doi: 10.1002/jpln.202100032

Walch-Liu, P., Neumann, G., Bangerth, F., and Engels, C. (2000). Rapid effects of nitrogen form on leaf morphogenesis in tobacco. *J. Exp. Bot.* 51, 227–237. doi: 10.1093/jexbot/51.343.227

Wang, G., Li, C., and Zhang, F. (2003). Effects of different nitrogen forms and combination with foliar spraying with 6-benzylaminopurine on growth, transpiration, and water and potassium uptake and flow in tobacco. *Plant Soil* 256, 169–178. doi: 10.1023/A:1026268722353

Weraduwage, S. M., Chen, J., Anozie, F. C., Morales, A., Weise, S. E., and Sharkey, T. D. (2015). The relationship between leaf area growth and biomass accumulation in arabidopsis thaliana. *Front. Plant Sci.* 6, 167. doi: 10.3389/fpls.2015.00167

Witold, G., Pavel, Č., Evan, R., Witold, S., Jarosław, P., and György, F. (2017). Potassium impact on nitrogen use efficiency in potato–a case study from the central-East Europe. *Plant Soil Environ.* 63, 422–427. doi: 10.17221/344/2017-PSE

Xiao, C., Fang, Y., Wang, S., and He, K. (2023). The alleviation of ammonium toxicity in plants. *J. Integr. Plant Biol.* 10.1111/jipb.13467. Advance online publication. doi: 10.1111/jipb.13467

Xie, K., Cakmak, I., Wang, S., Zhang, F., and Guo, S. (2021). Synergistic and antagonistic interactions between potassium and magnesium in higher plants. *Crop J.* 9, 249–256. doi: 10.1016/j.cj.2020.10.005

Zaman, U., Ahmad, Z., Farooq, M., Saeed, S., Ahmad, M., and Wakeel, A. (2015). Potassium fertilization may improve stem strength and yield of basmati rice grown on nitrogen-fertilized soils. *Pakistan J. Agric. Sci.* 52, 439–445.

Zhang, F., Niu, J., Zhang, W., Chen, X., Li, C., Yuan, L., et al. (2010). Potassium nutrition of crops under varied regimes of nitrogen supply. *Plant Soil* 335, 21–34. doi: 10.1007/s11104-010-0323-4

Zhu, Y., Qi, B., Hao, Y., Liu, H., Sun, G., Chen, R., et al. (2021). Appropriate NH4+/NO3–ratio triggers plant growth and nutrient uptake of flowering Chinese cabbage by optimizing the pH value of nutrient solution. *Front. Plant Sci.* 12, 656144. doi: 10.3389/fpls.2021.656144

frontiers | Frontiers in Plant Science

TYPE Original Research
PUBLISHED 14 November 2023
DOI 10.3389/fpls.2023.1274943

OPEN ACCESS

EDITED BY
S. Qiu,
Chinese Academy of Agricultural Sciences, China

REVIEWED BY
Wenfeng Hou,
Jilin Agriculture University, China
Zhanjun Liu,
Northwest A&F University, China
Wu Xueping,
Chinese Academy of Agricultural Sciences, China

*CORRESPONDENCE
Zhaohui Liu
liuzhaohui6666@sina.com
Deshui Tan
tandeshui@163.com

RECEIVED 09 August 2023
ACCEPTED 23 October 2023
PUBLISHED 14 November 2023

CITATION
Wang L, Ma L, Li Y, Geilfus C-M, Wei J, Zheng F, Liu Z and Tan D (2023) Managing nitrogen for sustainable crop production with reduced hydrological nitrogen losses under a winter wheat–summer maize rotation system: an eight-season field study.
Front. Plant Sci. 14:1274943.
doi: 10.3389/fpls.2023.1274943

Managing nitrogen for sustainable crop production with reduced hydrological nitrogen losses under a winter wheat–summer maize rotation system: an eight-season field study

Li Wang[1,2,3], Lei Ma[1], Yan Li[1], Christoph-Martin Geilfus[4], Jianlin Wei[1], Fuli Zheng[1], Zhaohui Liu[1*] and Deshui Tan[1*]

[1]State Key Laboratory of Nutrient Use and Management, Institute of Agricultural Resources and Environment, Shandong Academy of Agricultural Sciences, Jinan, China, [2]Institute of Modern Agriculture on Yellow River Delta, Shandong Academy of Agricultural Sciences, Jinan, China, [3]State Key Laboratory of North China Crop Improvement and Regulation, Hebei Agricultural University, Baoding, China, [4]Department of Soil Science and Plant Nutrition, Hochschule Geisenheim University, Geisenheim, Germany

Excessive nitrogen (N) application in wheat–maize cropping systems was adjusted towards more sustainable practices to reduce hydrological N losses while maintaining crop yield. In comprehensive quantification of N management effects on crop yield, N use efficiency (NUE), hydrological N losses, and soil nitrate residual across eight seasons, we have added to growing evidence of strategies beneficial for sustainable crop production with lower hydrological N losses. The results show that adjusted N practices enhanced crop yield and NUE, as compared to farmer's practices, but benefits varied with N rates and types. Optimized N treatment (OPT, 180 kg N ha^{-1} in both maize and wheat seasons) with or without straw returning produced the most crop yield. They increased maize yield by 5.5% and 7.3% and wheat yield by 6.2% and 3.2% on average, as compared to farmer's practice with huge N application (FP, 345 kg N ha^{-1} and 240 kg N ha^{-1} in maize and wheat). Regulation of N release through amendment with controlled release urea at a rate of 144 kg N ha^{-1} crop^{-1} (CRU treatment) obtained 4.4% greater maize yield than FP, and sustained a similar wheat yield with less N input, resulting in the highest crop NUE. Additionally, CRU was most effective in mitigating hydrological N loss, with 39.5% and 45.5% less leachate N and 31.9% and 35.9% less runoff N loss than FP in maize and wheat seasons. Synthetic N input correlated significantly and positively with runoff and leachate N losses, indicating it was one of the dominant factors driving hydrological N losses. Moreover, compared to OPT, additional straw returning (STR) or substituting 20% of the nutrients by duck manure (DMS) further reduced runoff N discharges due to the fact that organic matter incorporation increased resilience to rainfall. N over-application in FP caused considerable nitrate accumulation in the 0–90-cm soil profile, while the adjusted N practices, i.e., OPT, STR, CRU, and DMS treatments effectively controlled it to a range of 79.6–92.9 kg N ha^{-1}. This study suggests that efforts using optimized N treatment integrated with CRU or straw returning should be encouraged for sustainable crop production in this region.

KEYWORDS

nitrogen management, nitrogen leaching, nitrogen runoff, nitrogen use efficiency, wheat-maize rotation system

Introduction

Crop production must increase dramatically to meet the growing demand for food and biofuels projected for 2050 (Zhang et al., 2015). Over the past several decades, the improvement in global crop production has been associated with the increased use of nitrogen (N) fertilizer (Bodirsky et al., 2014; Kanakidou, 2019). However, on average, less than 50% of the nitrogen added to croplands globally is harvested as crop products (Ju et al., 2009). Inefficient use of N fertilizer by crops will result in substantial agricultural N losses, posing threats to human and ecosystem health. To boost crop yield with a lowered environmental cost, not only the use of high-potential crop cultivars but also efficient N management practices are required (Meng et al., 2016; Wang et al., 2019; Wang et al., 2020). Winter wheat–summer maize rotation is the most dominant cropping system in the North China Plain, one of China's largest regions of agricultural importance (Sun et al., 2007; Zhang et al., 2018). Due to knowledge constraints and old habitats, N over-application and imbalanced use of P and K are common in farmers' conventional practices. According to on-farm investigations, the N rates for maize and wheat production were as high as ca. 257 kg ha^{-1} and 325 kg ha^{-1} on average, while the estimated maize and wheat N uptake was only ca. 132 kg ha^{-1} and 160 kg ha^{-1}, respectively (Cui et al., 2010; Chen et al., 2011), resulting in a high N surplus in the rotation system (Meng et al., 2016). To meet the dual challenges of increasing crop yield while mitigating adverse environmental impacts, many management strategies have been suggested to improve N use efficiency (NUE) (Qiu et al., 2012; Peng et al., 2017; Wang et al., 2019; Wang et al., 2020; Ren et al., 2023). However, the technological opportunity and socio-economic situation for NUE promotion differ regionally (Zhang et al., 2015). Suitable management practices have to be carefully adapted and adopted, taking advantage of local resources (Tan et al., 2013).

The Nansi Lake watershed is a part of the south-to-north water transfer scheme (Liu and Zheng, 2002), serving as an important water source in Shandong province, China. Excessive N fertilization in agricultural practices and abundant and concentrated precipitation have posed great risks to the water quality in this region. It was reported that ca. 40% of the total N entering the lake came from agricultural N loss through runoff and leachates (Tan et al., 2013). Following the government-guided shifts in agricultural management, local N management was converted towards more sustainable practices. Adjusting fertilizer amounts and types, such as balanced fertilization based on soil testing and the use of controlled-release urea (CRU), have been introduced, as these were believed to enhance crop NUE and minimize environmental pollution (He et al., 2009; He et al., 2013; Wang et al., 2018; Zheng et al., 2020). Moreover, huge amounts of crop straw and manure have been produced each year in this region, providing rich sources of organic N fertilizer that can be combined with synthetic N applications. Plenty of research has demonstrated improved cereal yield and NUE by the use of CRU (Li et al., 2018; Wang et al., 2018; Zheng et al., 2020) or co-application of organic and synthetic N fertilizers (Wei et al., 2016; Tang et al., 2019), because the N release synchronized better with plant N uptake. However, the effects of these management practices may vary with soil and weather conditions, cultivation regimes, CRU, and organic fertilizer types (Chivenge et al., 2010; Liu et al., 2021). A quantitative understanding of the practice effects on crop yield, NUE, and N losses is lacking in the Nansi Lake watershed.

To fill the knowledge gaps, an on-farm investigation was conducted over eight consecutive seasons to examine the effects of N management practices on mitigating hydrological N loss and sustaining crop yield under winter wheat–summer maize rotation. The specific objectives were to (1) quantify the crop yield and NUE as influenced by different N management practices and (2) explore the characteristics of runoff and leachate N losses to screen optimal N management practices.

Materials and methods

Study area

The experimental site is located in the Nansi Lake watershed (34°46′58″ N, 117°08′56″ E), Shandong province, North China, which has a temperate monsoon climate with an average annual precipitation of 550–720 mm and an average annual temperature of 14.4°C. The rainfall from June 2009 to June 2013 is shown in Supplementary Figure S1. The seasonal rainfall for maize was 359.1 mm, 524.6 mm, 479.9 mm, and 436.3 mm during the four growing seasons. In contrast, less rainfall occurred in wheat seasons, which were 260.1 mm, 72.7 mm, 222.3 mm, and 344.5 mm, respectively.

The soil in the experimental site is fluvo-aquic soil in an alluvial clay loam texture. The initial properties of the topsoil (0–20 cm) in

2009 were measured using standard chemical methods described by Sparks et al. (1996). They were as follows: pH 8.3, 8.87 g kg^{-1} organic carbon, 9.3 mg kg^{-1} available P, 140.8 mg kg^{-1} available K, 2.06 mg kg^{-1} nitrate-N (NO_3^--N), and 1.69 mg kg^{-1} ammonium-N (NH_4^+-N). The dominant crop system in this region is winter wheat rotated with summer maize.

Experimental design and management

A field experiment was carried out from June 2009 to June 2013. The experiment consisted of six treatments with three replicates that were arranged in a randomized complete block design. In total, 60-cm concrete levees bordered each plot with a size of 45 m^2 to avoid water and fertilizer penetration. The treatments were (1) PK, with only P and K but no N fertilization; (2) farmers' practice (FP) based on a survey of 15 households near the experimental sites; (3) optimized NPK treatment (OPT), designed by local experts based on soil nutrient analysis and crop nutrient demand; (4) CRU treatment, with the same P and K rates as in OPT, but N applied using resin-coated urea (42% N, Jinzhengda Ecological Engineering Co. Ltd., Shandong, China) at a reduced N rate by 20%; (5) duck manure supplement treatment (DMS), 20% of the total nutrients of the OPT replaced by the inputs from duck manure; and (6) straw returning treatment (STR), with the same fertilization rate as OPT plus straw returning. The detailed application rates of fertilizers for wheat and maize seasons are shown in Table 1.

The basal fertilizers, including all P (triple superphosphate, 44% P_2O_5), K (potassium chloride, 60% K_2O), CRU, duck manure, and 50% of normal N fertilizer (urea, 46% N), were broadcasted before soil plowing and leveling. The rest of N was top-dressed at the F3 and VT stages for wheat and maize. The N top-dressing was done by row application except in the FP treatment where N was broadcasted. In the STR treatment, wheat and maize straw at 6,000 and 7,500 kg ha^{-1} was spread evenly over the ground surface after harvest. Maize (cv. Zhongyu 9) was planted on 15 June and harvested on 7 October each year. Wheat (cv. Jimai 22) was planted on 12 October and harvested on 12 June the next year.

Sampling and measurement

Leachate was sampled using an *in situ* collection plate (40 cm × 50 cm) inserted at a depth of 90 cm (Li et al., 2008). Soil surface runoff was collected by the runoff tank collection method (Supplementary Figure S2). Leachate and runoff samples were collected at V1, VT, R1, R3, and R6 stages for maize, and F2, F3, F4, F10, and F11 stages for wheat. Thereafter, leachate and runoff samples were transported immediately to the laboratory and stored below 0°C until analysis. Leachate and runoff volumes were recorded and the NO_3^--N and NH_4^+-N concentrations were measured using an automatic flow analyzer. At harvest, all crops within each plot were manually harvested and threshed to determine the total yield after grains were air-dried. Maize and wheat samples were separated into grain and straw parts, and the N concentrations were measured after being digested with H_2SO_4-H_2O_2.

Calculations

N uptake by maize and wheat plants was calculated by multiplying the biomass of grain and straw by the corresponding N concentrations.

The apparent fertilizer NUE was computed using the following equation:

$$NUE = (T_N - T_0)/F_N \times 100\,\% \tag{1}$$

Where T_N was the plant N uptake in the plots receiving N fertilization; T_0 was the plant N uptake in the treatment without N application (i.e., the PK treatment in the present study); F_N was the fertilizer N amount.

To evaluate the sensibility of surface runoff to rainfall under different N management practices, the relationship between rainfall and runoff was analyzed with the linear regression model:

$$y = a + bx \tag{2}$$

Where rainfall and runoff were used as the independent variable x and dependent variable y, respectively; the corresponding runoff sensibility to rainfall was defined as the first-order derivative of variable y, i.e., b.

TABLE 1 Fertilization rates (kg ha^{-1}) for maize and wheat under different N management practices.

Treatment	Maize				Wheat			
	N	P_2O_5	K_2O	Organic material	N	P_2O_5	K_2O	Organic material
FP	345	0	0	0	240	172.5	0	0
PK	0	66	99	0	0	90	60	0
OPT	180	66	99	0	180	90	60	0
CRU	144	66	99	0	144	90	60	0
DMS	144	52.8	79.2	1,200	144	72	48	1,148
STR	180	66	99	6,000	180	90	60	7,500

FP, farmers' fertilization practice; PK, P and K fertilizers only; OPT, optimized NPK fertilization; CRU, control-release N fertilization; DMS, optimized NPK fertilization with 20% of the total nutrients replaced by inputs from duck manure; STR, optimized NPK fertilization plus straw covering.

The residual soil nitrate (RSN) in each soil layer was calculated according to Dai et al. (2016):

$$RSN = T_i \times D_i \times C_i/10 \quad (3)$$

Where T_i, D_i, and C_i are the thickness, bulk density, and nitrate-N concentration of the corresponding soil layers.

Statistical analyses

The effects of N management treatment, crop season, year, and their interactions on the measured parameters were tested via analysis of variance, with N management treatment, season as fixed factors, and year as a random factor. The means of different N management practices were separated by the least significant difference (LSD) test at the $p< 0.05$ probability level. The relationships between synthetic N input, runoff, and leachate N losses and between rainfall and runoff amount were analyzed with one-way regression analysis. Data were checked using the Shapiro–Wilk test for normal distribution before statistical analyses. All statistical tests were conducted with SPSS 20. Figures were plotted with SigmaPlot 12.0.

Results

Runoff and leachate amount

The high rainfall during maize seasons produced runoff and leachate at almost every stage of maize growth, with the exception of the V1 and R1 stages in 2012 (Supplementary Figures S3, S4). In contrast, runoff and leachate occurred less frequently in wheat seasons. For instance, only the F3 stage had runoff produced during the 2010–2011 wheat season.

N management practices resulted in considerable variation in the runoff amount (Table 2). In general, PK treatment was the highest in runoff, while STR was the lowest. The second-lowest runoff occurred in DMS. This treatment had on average 6.5%, 13.6%, and 9.2% less surface runoff than FP in maize, wheat seasons, and the whole rotations ($p< 0.05$), respectively. OPT and CRU did not vary with FP in runoff amounts in both maize and wheat seasons.

Moreover, the runoff amount increased linearly with rainfall, as shown in Table 3. In line with its highest runoff amounts, the PK treatment showed significantly higher b values than other treatments in both the maize and wheat seasons, indicating a greater runoff sensibility to rainfall. STR and DMS significantly reduced the runoff sensibility to rainfall, as compared to FP treatment.

The leachate amount was considerably higher in the maize season than in the wheat season, and it differed significantly among N management practices (Table 2). PK treatment had the lowest leachate amounts in both the maize and wheat seasons. Compared to FP, STR enhanced soil water infiltration most, followed by DMS treatment. However, OPT and CRU showed limited effects on leachate reduction. CRU treatment had a slightly lower leachate amount than FP only at the beginning of the rotation.

Runoff and leachate N

The seasonal runoff N concentration dynamics are shown in Figure 1. The runoff NO_3^--N concentration was generally higher

TABLE 2 Runoff and leachate amount during maize, wheat season, and the whole rotation under different N management practices.

Treatment	2009–2010			2010–2011			2011–2012			2012–2013		
	Maize	Wheat	Total	Maize	Wheat	Total	Maize	Wheat	Total	Maize	Wheat	Total
Runoff amount (mm)												
FP	48.9a	26.0b	74.9b	72.6b	12.3ab	84.9b	88.2b	45.0b	133.2b	67.7b	46.2b	113.9b
PK	49.8a	28.9a	78.6a	86.4a	13.1a	99.5a	99.2a	50.2a	149.4a	82.7a	51.3a	134.0a
OPT	49.1a	26.2b	75.2b	70.2b	12.1ab	82.3b	87.7b	44.4b	132.1b	65.8b	45.1b	110.9b
CRU	49.7a	26.9b	76.6b	74.5b	12.0ab	86.4b	89.8b	44.6b	134.5b	67.8b	48.0b	115.8b
DMS	47.7b	24.2c	71.9c	63.7c	11.3b	75.0c	83.9c	33.9c	117.8c	63.4c	39.5c	102.9c
STR	46.2c	19.8d	66.0d	56.6d	10.7c	67.2d	79.1d	28.8d	107.8d	58.9d	35.0d	93.9d
Leachate amount (mm)												
FP	103.6c	49.2c	149.8c	123.5c	25.7b	148.7c	143.8c	51.4c	195.2c	145.0c	71.3c	216.3c
PK	95.3d	45.4d	140.7d	111.2d	23.5c	134.7d	128.3d	46.5d	174.8d	136.3d	67.8d	204.1d
OPT	104.5c	48.5c	153.0c	121.5c	26.9b	147.9c	142.8c	49.5c	192.3c	140.6c	73.1c	213.7c
CRU	96.2d	46.3d	142.5d	122.9c	23.6c	146.5c	145.4c	48.2c	193.6c	142.1c	69.5cd	211.6c
DMS	109.7b	55.6b	165.3b	129.6a	27.5b	157.1a	153.9b	55.5b	209.4b	153.4b	80.9b	234.3b
STR	118.8a	61.7a	180.5a	132.7a	30.0a	162.7a	159.3a	59.5a	218.8a	157.5a	86.7a	244.2a

FP, farmers' fertilization practice; PK, P and K fertilizers only; OPT, optimized NPK fertilization; CRU, control-release N fertilization; DMS, optimized NPK fertilization with 20% of the total nutrients replaced by inputs from duck manure; STR, optimized NPK fertilization plus straw covering. Means within a column followed by the same letter are not significantly different at $p< 0.05$ level, LSD.

TABLE 3 Regression analysis ($y = a + bx$) showing the sensibility of runoff (y) to rainfall (x) during maize and wheat seasons under different N management practices.

Treatment	Crop season	a	b	R^2	p-value
FP	Maize	2.752 ± 2.485a	0.133 ± 0.025b	0.604	< 0.001
PK		2.469 ± 2.793a	0.160 ± 0.028a	0.638	< 0.001
OPT		2.621 ± 2.291a	0.131 ± 0.023b	0.638	< 0.001
CRU		2.641 ± 2.155a	0.137 ± 0.022b	0.683	< 0.001
DMS		2.061 ± 1.952a	0.130 ± 0.020b	0.703	< 0.001
STR		1.832 ± 1.912a	0.122 ± 0.019c	0.685	< 0.001
FP	Wheat	0.558 ± 1.697a	0.131 ± 0.026b	0.585	< 0.001
PK		0.535 ± 1.849a	0.147 ± 0.028a	0.599	< 0.001
OPT		0.655 ± 1.647a	0.127 ± 0.025b	0.584	< 0.001
CRU		0.606 ± 1.698a	0.132 ± 0.026b	0.589	< 0.001
DMS		0.574 ± 1.196a	0.108 ± 0.018c	0.658	< 0.001
STR		0.423 ± 1.128a	0.095 ± 0.017d	0.627	< 0.001

Means within a column followed by the same letter are not significantly different at p< 0.05 level.

than NH_4^+-N. Averaged across eight seasons, PK treatment was the lowest in runoff NO_3^--N and NH_4^+-N concentrations (1.37 mg N L^{-1} and 0.09 mg N L^{-1}, respectively, Figures 1B, D). The second-lowest runoff N concentration was observed in CRU treatment, with average NO_3^--N and NH_4^+-N concentrations of 2.97 mg N L^{-1} and 0.27 mg N L^{-1}, respectively. FP, OPT, DMS, and SRT did not vary in runoff N concentrations, but they were higher than PK and CRU treatments (p< 0.05).

N omission in PK treatment led to the lowest runoff N losses compared to other treatments receiving N (p< 0.05). FP resulted in the highest runoff N losses, which were on average 3.11 kg N ha^{-1} and 2.17 kg N ha^{-1} in maize and wheat seasons (Figures 2A, C). CRU treatment was most effective in reducing runoff N loss, and it had 39.2% and 45.7% less N loss than FP in maize and wheat seasons (p< 0.05). DMS and STR treatments had similar effects, and they had on average 28.7% and 27.7% less runoff N loss in maize season and 32.7% and 34.6% less in wheat season, as compared to FP. Moreover, to a lesser magnitude, OPT treatment also decreased runoff N losses compared to FP (by 17.2% and 14.2% in maize and wheat seasons, respectively). The regression analysis demonstrates linear increases in runoff N losses with increasing synthetic N inputs for both maize (Figure 2B, p< 0.0001) and wheat seasons (Figure 2D, p< 0.01).

The dynamics of leachate N concentrations are shown in Figure 3. The NO_3^--N concentration in leachate was slightly higher than that of NH_4^+-N. N management practices significantly affected leachate N concentrations. Averaged across eight seasons monitored, the lowest leachate NO_3^--N and NH_4^+-N concentrations were recorded in PK, while the greatest was in FP treatment. CRU was the most effective measure to lower leachate N concentration, with average declines of 33.0% and 32.4% in NO_3^--N and NH_4^+-N, as compared to FP. DMS was the second most effective, and it reduced NO_3^--N and NH_4^+-N concentrations by 26.7% and 24.9%, respectively. Moreover, the leachate NO_3^--N concentrations in OPT and STR were 15.0% and 20.8% lower, and NH_4^+-N concentrations were 16.1% and 21.1% lower relative to FP treatment.

More leachate N loss occurred in maize than in wheat seasons (Figure 4). The leachate N was lost mainly as NO_3^--N in maize seasons, but the leachate loads of NH_4^+-N and NO_3^--N were comparable in wheat seasons. In both maize and wheat seasons, the lowest and highest leachate N losses were consistently observed in PK and FP treatments, respectively. Compared to FP, adjusted N management practices significantly mitigated leachate N losses. CRU treatment was the most effective, and it reduced leachate N losses by 34.2% and 36.3% in maize and wheat seasons, respectively. OPT and DMS treatments showed similar effects, and they decreased average leachate N losses by 18.1% and 25.3% in maize and 14.3% and 15.8% in wheat seasons, as compared to FP. STR was less effective and declined average leachate N loss only in maize seasons (10.2%, p< 0.05).

Soil nitrate residual

N management practices resulted in significant variations in soil nitrate residuals in the 0–90-cm layer after the wheat harvest in 2013 (Figure 5), and the difference decreased with increasing soil depth. PK treatment had the lowest nitrate residual in each soil layer, while FP treatment was constantly the highest (Figure 5A). The nitrate accumulation in the 0–90-cm layer was 50.8 kg N ha^{-1} in the PK treatment and increased significantly up to 153.5 kg N ha^{-1} in FP treatment. The adjusted N practices did not vary in nitrate accumulation in the 0–90-cm soil layer (ranging from 79.6 to 92.9 N ha^{-1}) but were 41.2%, 44.4%, 48.2%, and 39.5% lower than that in FP treatment (p< 0.05).

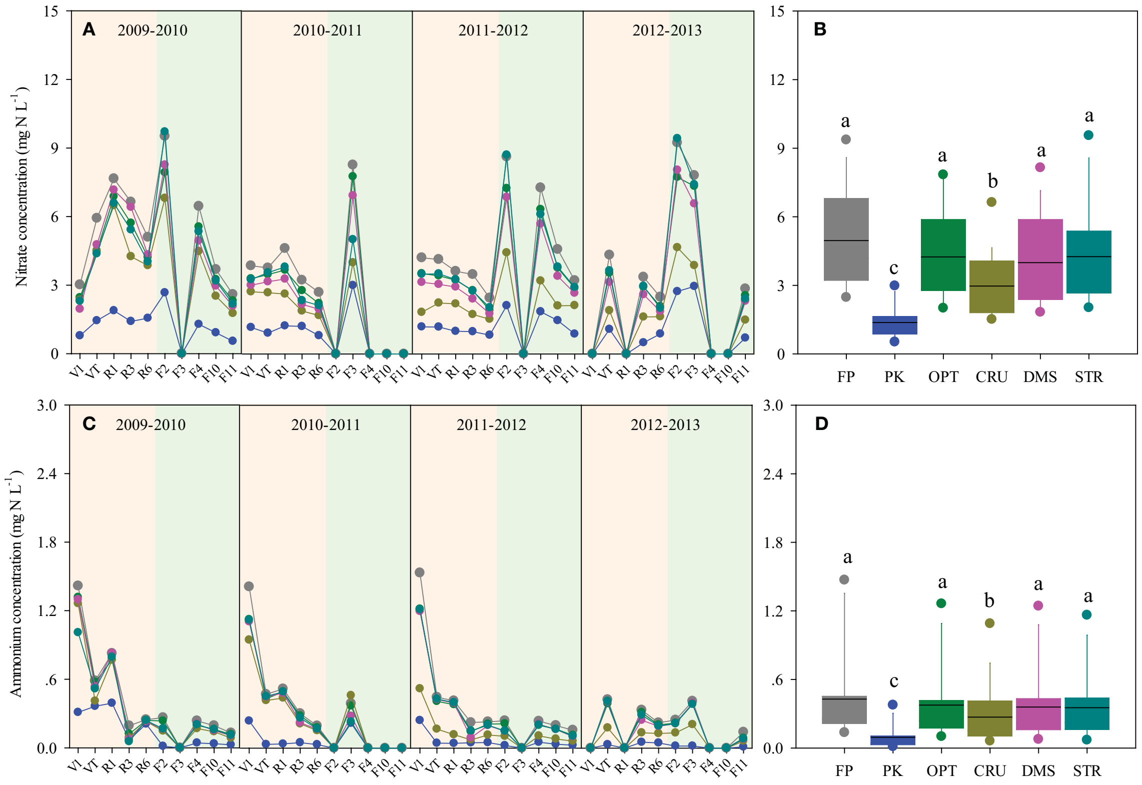

FIGURE 1
Dynamics of NO_3^--N **(A)** and NH_4^+-N **(C)** concentrations in runoff during maize (in the yellow-pink background) and wheat seasons (in the yellow-green background) and the seasonal averages **(B, D)** under different N management practices. Box-whisker showed the average, 25th, 50th, and 75th percentiles. Boxes with the same letter indicated that the averages were not significantly different at the $p < 0.05$ level.

Crop yield and NUE

N management practices significantly influenced maize and wheat grain yields (Table 4). N omission in PK treatment reduced grain yields, with average declines of 34.8% in maize and 80.1% in wheat as compared to FP treatment. STR treatment produced on average 7.3% more maize yield than FP. OPT and CRU showed significantly higher maize yield than FP in the last two seasons, and the average increments were 5.5% and 4.4% over four seasons. DMS treatment, in general, did not vary with FP in maize yield, except for a slight increase in 2011. Moreover, OPT, STR, and DMS increased wheat yields in the last two seasons. Averaged over four seasons, they produced 6.2%, 3.2%, and 2.7% greater wheat yields than FP. CRU treatment did not differ from FP in wheat grain yield, although it had a reduced N input.

N management practices led to significant variations in crop NUE (Table 4). N overapplication in FP treatment led to the lowest NUE, i.e., only 17.1% and 24.0% in maize and wheat, respectively. In contrast, adjusted N management practices greatly enhanced crop NUE. CRU treatment resulted in the most efficient N use, showing an average NUE of 43.4% and 53.9% for maize and wheat, followed by STR and OPT, while, to a lesser magnitude, DMS also achieved higher NUE than FP treatment.

Discussion

Runoff and leachate N losses

Agricultural practices greatly impact soil nutrient losses, which may vary as a result of fertilization regimes, tillage, and weather conditions (Dai et al., 2016; Wei et al., 2021). High soil N accumulation was prone to being lost through hydrological pathways when there was rainfall or irrigation (Wang et al., 2010; Liu et al., 2017; Zhang et al., 2021a). In the present study, runoff and leachate amounts were regulated by N management practices that differed in soil disturbance, as these tended to change the sensibility of surface runoff to rainfall. The runoff in PK treatment was the most sensitive to rainfall due to poor plant growth and a lack of soil surface disturbance (e.g., no topdressing) that retained the soil compacted with low impedance to surface water flow. STR and DMS significantly reduced runoff and its sensibility to rainfall but increased leachate. This could be explained by the fact that straw covering and organic matter incorporation increased the resistance to surface water flow and promoted water retention and infiltration due to increased soil porosity and reduced bulk density (Liu et al., 2012; Wang et al., 2019).

Many studies focused on identifying the optimal N fertilizer rates for high crop yield with reduced runoff and leaching N losses

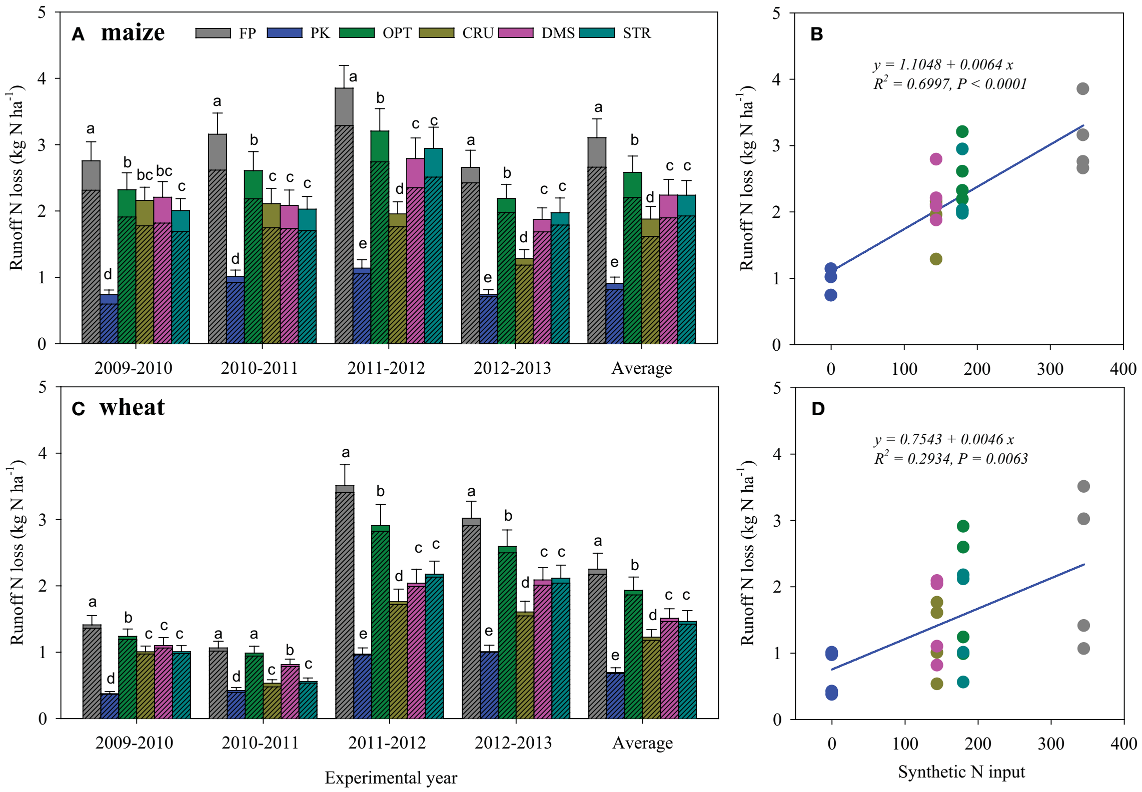

FIGURE 2
Runoff N losses during maize **(A)** and wheat seasons **(C)** under different N management practices and their relations with synthetic N inputs **(B**, **D)**. Bars in the same season, followed by the same letter, indicated the means were not significantly different at the p< 0.05 level. Bars with and without slashes were NO_3^--N and NH_4^+-N losses, respectively.

(Yang et al., 2017; Zhang et al., 2021a; Zhang et al., 2021b). Our results demonstrated that runoff and leachate N losses were significantly and positively correlated with synthetic N input (Figures 2, 4), indicating it was one of the dominant factors affecting hydrological N losses. FP practice resulted in the greatest N losses via hydrological pathways (Figures 2, 4). The continuous over-application of N fertilizer in FP treatment would drive the soil into an N-saturated condition, resulting in poor N retention (Ju, 2014). By contrast, the reduced N and balanced P and K use in OPT facilitated crop N uptake and considerably decreased runoff and leaching N losses in both maize and wheat seasons.

Hydrological N losses were also regulated by N types and management practices. In comparison to OPT, STR and DMS treatments further reduced runoff N discharges (Figure 2), but they sustained or slightly increased N leaching. These results were probably associated with modified soil physical properties (e.g., improved soil porosity and decreased bulk density) following organic matter incorporation, which reduced surface flow but increased water infiltration (Liu et al., 2012; Wang et al., 2019). Moreover, CRU was proven to be the most effective in alleviating hydrological N losses. Regulation of N release through amendment with CRU enhanced crop N uptake (Table 4), leaving less soil N to be lost with rainfall.

The magnitude of hydrologic N losses in this study was attributed more to the N concentration than the amount of discharge, as evidenced by the much higher variations in the former (Table 2; Figures 1, 3). In line with previous findings (Zhang et al., 2021b), NO_3^--N was obviously dominant over NH_4^+-N in inorganic N losses via runoff in the present study (Figure 1). Moreover, 70% of the inorganic N discharged in leachate was in the form of NO_3^--N in maize seasons, but there were similar fractions of NO_3^--N and NH_4^+-N loads lost to leachate in wheat seasons. This might be due to the low soil temperature limiting the nitrification process (Rodríguez et al., 2005), leading to an increased NH_4^+-N concentration in percolation water during the early stages of wheat growth (Figure 3C).

Soil nitrate residual

Excessive N application has resulted in high soil nitrate residuals in cereal and vegetable cropping systems (Cui et al., 2010; Zhang et al., 2021a), leading to an increased risk of N loss and lack of yield response to applied N (Liu et al., 2017; Zhang et al., 2021a). In the current study, FP treatment resulted in a huge soil nitrate accumulation of 153.5 kg N ha^{-1} in the 0–90-cm profile after the last wheat season (Figure 5). It was much higher than the acceptable soil nitrate-N level of 90 kg N ha^{-1}, as suggested for winter wheat–summer maize rotation fields of North China Plain (Cui et al., 2008a; Cui et al., 2008b). These results indicated the high N rate in FP must be reasonably reduced with the large indigenous

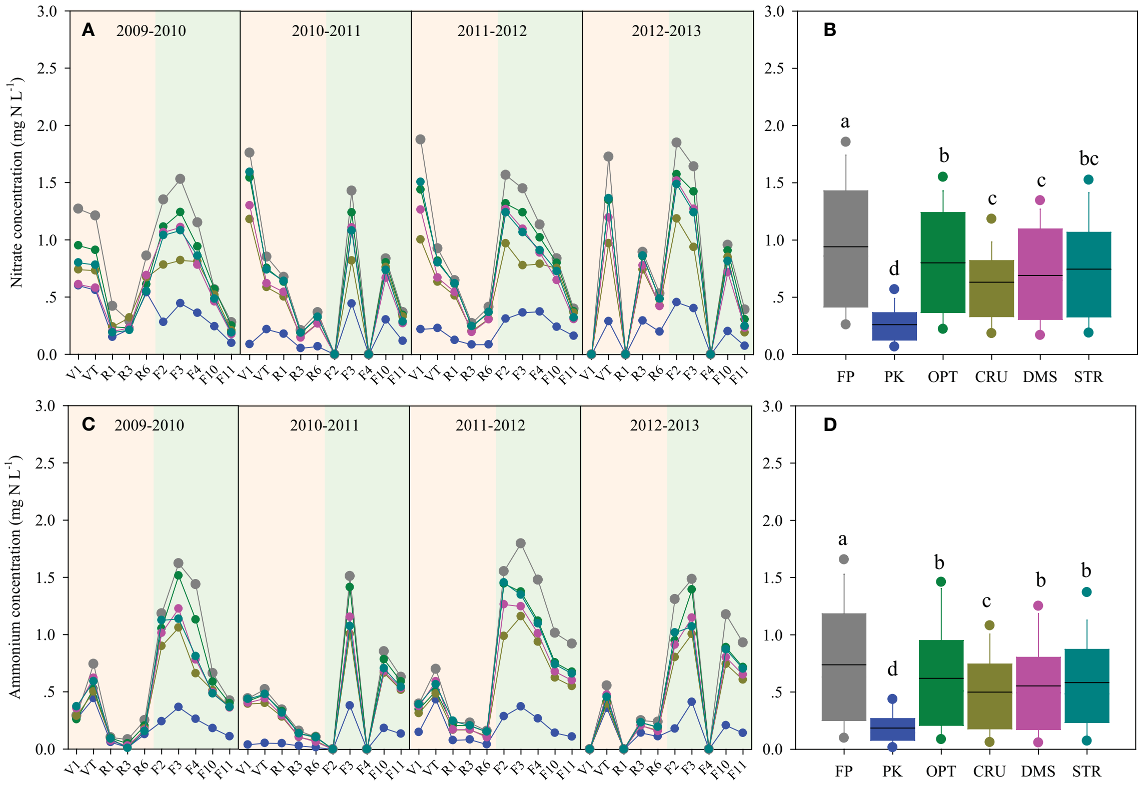

FIGURE 3
Dynamics of NO_3^--N **(A)** and NH_4^+-N **(C)** concentrations in leachate during maize (in the yellow-pink background) and wheat seasons (in the yellow-green background) and the seasonal averages **(B, D)** under different N management practices. Box-whisker showed the average, 25th, 50th, and 75th percentiles. Boxes with the same letter indicated that the averages were not significantly different at the p< 0.05 level.

soil N being carefully considered. In contrast, adjusted N management practices significantly decreased soil nitrate accumulation to 79.6–92.9 N ha^{-1}, suggesting that these practices were generally effective in controlling soil nitrate residual.

Crop yield and NUE

Improving crop yield and NUE simultaneously is vital to sustainable agricultural production. N fertilization practices have to be managed to match crop N demand in terms of N rate, source, timing, and space (Cui et al., 2010). In the present study, N over-application in FP treatment did not benefit crop yield. Rather, it led to the lowest NUE (averaged 17.1% and 24.0% in maize and wheat, respectively, Table 4) at the cost of potential P and K limitations. By contrast, OPT and STR treatments with a reduced N rate of 180 kg N ha^{-1} $crop^{-1}$ and balanced use of P and K facilitated crop N uptake and enhanced crop yield and NUE. Moreover, the positive effects of STR may also result from the more favorable soil conditions created with straw covering, e.g., improved soil temperature status and reduced water loss by evaporation (Chen et al., 2015; Liu et al., 2017). Corroborating our results, a regionwide optimal N rate of 150–180 kg N ha^{-1} $crop^{-1}$ has been recommended for the maize–wheat rotation systems in North China (Cui et al., 2008b; Zhang et al., 2011). These results suggest that a reduced N rate of 180 kg N ha^{-1} $crop^{-1}$ is sufficient, and the combination with straw covering is one measure suitable for the studied region in terms of crop yield and NUE improvement.

Several studies indicated improved cereal yield and NUE by co-applicating organic and synthetic N fertilizers relative to synthetic N alone (Das and Adhya, 2014; Wei et al., 2021), as the mineral N matched better with crop N demand. In the present study, however, DMS treatment appeared to be less effective than OPT in boosting crop yield and NUE. The discrepancy in results might be associated with differences in organic fertilizers and cropping systems. In our study, the organic matter incorporation with manure may have induced N immobilization and reduced the size of available N pools, particularly in the maize season with relatively high soil moisture and short growth duration (Devevre and Horwath, 2000; Said-Pullicino et al., 2014). Regulation of N release through amendment with CRU greatly improved crop NUE. Meanwhile, it increased maize yield and sustained a similar wheat yield to FP with reduced N input. Overall, our results suggest that CRU could be used as a feasible and effective approach to improve crop NUE and grain yield under maize-wheat rotation, provided that it is applied in the right type and rate according to crop N demand.

Implication and perspectives

During the past decades, the intensification of agricultural production has played a crucial role in nourishing the livelihood of the growing population (Li et al., 2017). However, excessive input of

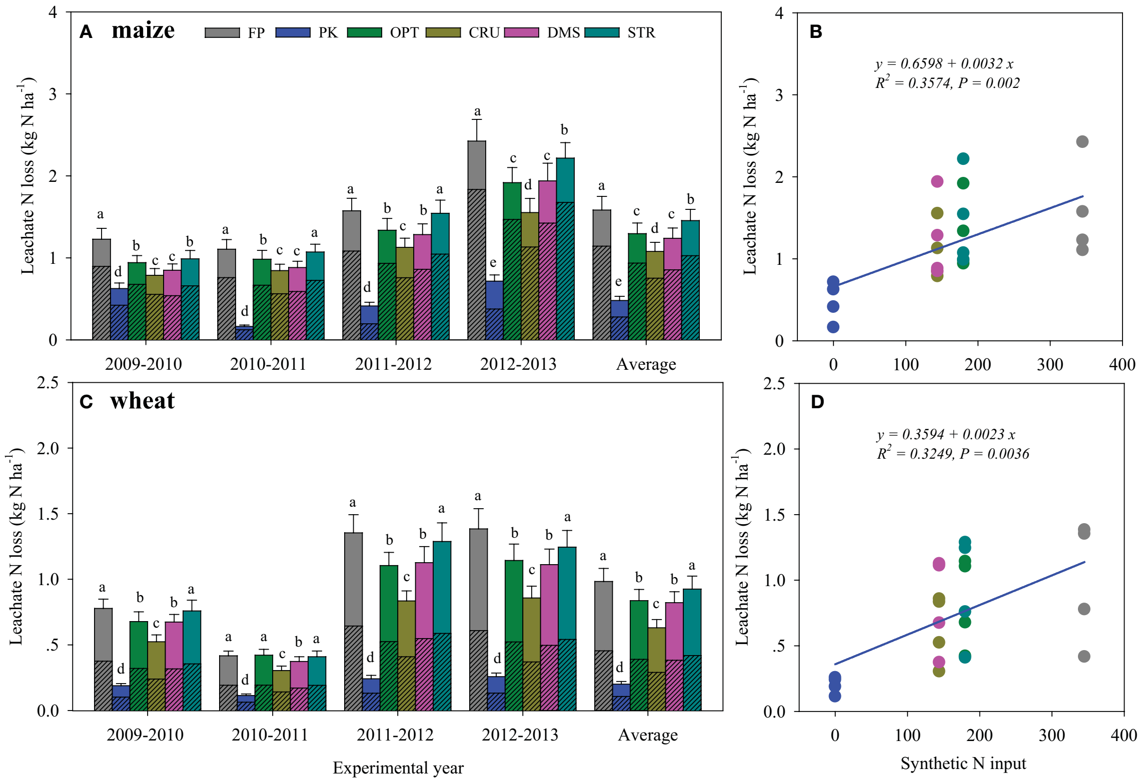

FIGURE 4
Leachate N losses during maize **(A)** and wheat seasons **(C)** under different N management practices and their relations with synthetic N inputs **(B, D)**. Bars in the same season, followed by the same letter, indicated the means were not significantly different at the *p*< 0.05 level. Bars with and without slashes were NO_3^--N and NH_4^+-N losses, respectively.

synthetic N also brought great challenges to agricultural sustainability (Zhang et al., 2015). A package of rational N management practices needs to be integrated to achieve the dual goals of ensuring food security and mitigating environmental costs (Chen et al., 2014). The present study illustrated that the adjusted N management practices significantly promoted crop NUE, increased or at least sustained crop yield, and reduced hydrological N losses and soil nitrate N residual, which is essential for agricultural sustainability. While we are encouraged by the great potential of these approaches, we need to know the limitations of this study. The field investigations were conducted in a lakeshore agricultural area, and the main concerns were the hydrological N losses. The other N pathways, such as gas N emissions, should be explored. More experiments and model-based studies are warranted to achieve a more comprehensive understanding of the interactions of soil C, N, and water processes and balances in the agriculture system.

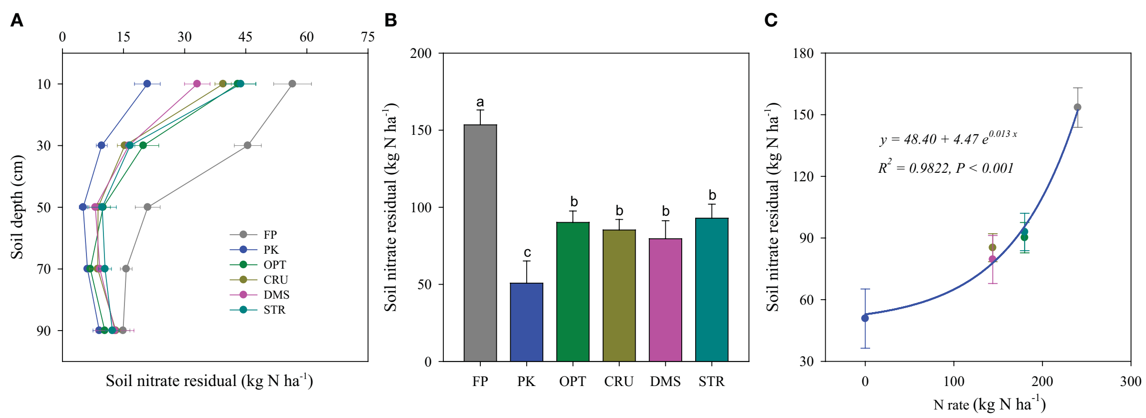

FIGURE 5
Soil nitrate residual distribution **(A)** and accumulation **(B)** in the 0–90-cm profile under different N management practices and their relation to the N rate **(C)**. Bars, followed by the same letter, indicated the means were not significantly different at the *p*< 0.05 level.

TABLE 4 Crop yield and NUE during maize and wheat seasons under different N management practices.

Treatment	2009–2010	2010–2011	2011–2012	2012–2013	Average yield	2009–2010	2010–2011	2011–2012	2012–2013	Average NUE
	Maize grain yield (kg ha^{-1})					NUE in maize (%)				
FP	8,734a	10,643b	6,366c	8,720b	8,616c	18.6c	30.0c	8.5c	11.2d	17.1d
PK	6,085b	4,895c	4,736d	6,765c	5,620d					
OPT	9,403a	10,267b	7,247a	9,441a	9,090b	34.7b	53.7b	25.1a	26.8b	35.1b
CRU	9,249a	10,192b	6,916ab	9,623a	8,995b	44.5a	66.2a	27.3a	35.7a	43.4a
DMS	9,048a	9,803b	6,763b	8,570b	8,546c	34.4b	49.1b	20.3b	18.1c	30.4c
STR	8,865a	11,234a	7,542a	9,334a	9,244a	31.6b	63.4a	28.1a	25.7b	37.2b
	Wheat grain yield (kg ha^{-1})					NUE in wheat (%)				
FP	7,140a	6,384b	5,488b	3,610c	5,656b	30.8c	27.4d	23.2b	14.5c	24.0c
PK	1,233c	1,421c	1,036c	823d	1,128c	–	–	–	–	–
OPT	6,317b	6,740a	6,454a	4,510a	6,005a	50.8b	50.2b	54.2a	36.9b	48.8b
CRU	6,230b	6,360b	5,706b	4,074b	5,593b	62.5a	59.2a	53.1a	40.6a	53.9a
DMS	6,167b	6,307b	6,250a	4,500a	5,806a	49.3b	44.7b	52.1a	36.8b	45.7b
STR	6,264b	6,192b	6,364a	4,525a	5,836a	50.3b	45.7b	53.3a	37.0b	46.6b

FP, farmers' fertilization practice; PK, P and K fertilizers only; OPT, optimized NPK fertilization; CRU, control-release N fertilization; DMS, optimized NPK fertilization with 20% of the total nutrients replaced by inputs from duck manure; STR, optimized NPK fertilization plus straw covering. Means within a column followed by the same letter are not significantly different at $p< 0.05$ level, LSD.

Conclusion

Adjusted N management practices significantly enhanced crop NUE and improved grain yield, but the magnitude of these benefits varied with N rates and types used. The optimized N rate with or without straw returning achieved the highest crop yield. Regulation of N release through amendment with CRU was the most effective in fertilizer N use and mitigation of hydrological N loss. Moreover, organic matter incorporation in STR and DMS treatments further reduced runoff N discharges than OPT, but they sustained or slightly increased N leaching. Excessive N application in FP resulted in considerable nitrate accumulation in the 0–90-cm soil profile. The adjusted N management practices effectively controlled those close to the acceptable soil nitrate-N level. Overall, our results suggest that efforts using optimized N treatment integrated with CRU or straw returning might be feasible for sustainable crop production in this region.

Data availability statement

The original contributions presented in the study are included in the article/Supplementary Material. Further inquiries can be directed to the corresponding authors.

Author contributions

LW: Conceptualization, Data curation, Investigation, Methodology, Writing – original draft. LM: Data curation, Writing – review & editing. YL: Software, Validation, Writing – review & editing. C-MG: Writing – review & editing. JW: Investigation, Writing – review & editing. FZ: Investigation, Writing – review & editing. ZL: Supervision, Writing – review & editing. DT: Software, Validation, Writing – review & editing.

Funding

The author(s) declare financial support was received for the research, authorship, and/or publication of this article. The research was financially supported by the National Natural Science Foundation of China (41877100), the National Key Research and Development Program of China (2021YFD1901003), the Agricultural Scientific and Technological Innovation Project of Shandong Academy of Agricultural Sciences (CXGC2023F03), the Earmarked Fund for China Agriculture Research System (CARS-03), the Key Research and Development Program (Science and technology demonstration project) of Shandong Province (2022SFGC0303) and the Smart Fertilization Project.

Conflict of interest

The authors declare that the research was conducted in the absence of any commercial or financial relationships that could be construed as a potential conflict of interest.

Publisher's note

All claims expressed in this article are solely those of the authors and do not necessarily represent those of their affiliated organizations, or those of the publisher, the editors and the reviewers. Any product that may be evaluated in this article, or claim that may be made by its manufacturer, is not guaranteed or endorsed by the publisher.

Supplementary material

The Supplementary Material for this article can be found online at: https://www.frontiersin.org/articles/10.3389/fpls.2023.1274943/full#supplementary-material

References

Bodirsky, B. L., Popp, A., Lotze-Campen, H., Dietrich, J. P., Rolinski, S., Weindl, I., et al. (2014). Reactive nitrogen requirements to feed the world in 2050 and potential to mitigate nitrogen pollution. *Nat. Commun.* 5, 3858. doi: 10.1038/ncomms4858

Chen, X., Cui, Z., Fan, M., Vitousek, P., Zhao, M., Ma, W., et al. (2014). Producing more grain with lower environmental costs. *Nature* 514, 486–489. doi: 10.1038/nature13609

Chen, X., Cui, Z. L., Vitousek, P. M., Cassman, K. G., Matson, P. A., Bai, J. S., et al. (2011). Integrated soil-crop system management for food security. *Proc. Natl. Acad. Sci. U.S.A.* 108, 6399–6404. doi: 10.1073/pnas.1101419108

Chen, Y., Liu, T., Tian, X., Wang, X., Li, M., Wang, S., et al. (2015). Effects of plastic film combined with straw mulch on grain yield and water use efficiency of winter wheat in Loess Plateau. *Field Crop Res.* 172, 53–58. doi: 10.1016/j.fcr.2014.11.016

Chivenge, P., Vanlauwe, B., and Six, J. (2010). Does the combined application of organic and mineral nutrient sources influence maize productivity? *A Meta-analysis. Plant Soil.* 342, 1–30. doi: 10.1007/s11104-010-0626-5

Cui, Z., Chen, X., Miao, Y., Zhang, F., Sun, Q., Schroder, J., et al. (2008a). On-farm evaluation of the improved soil N_{min}-based nitrogen management for summer maize in North China Plain. *Agron. J.* 100, 517–525. doi: 10.2134/agronj2007.0194

Cui, Z., Chen, X., and Zhang, F. (2010). Current nitrogen management status and measures to improve the intensive wheat-maize system in China. *Ambio* 39, 376–384. doi: 10.1007/s13280-010-0076-6

Cui, Z., Zhang, F., Chen, X., Miao, Y., Li, J., Shi, L., et al. (2008b). On-farm evaluation of an in-season nitrogen management strategy based on soil N-min test. *Field Crop Res.* 105, 48–55. doi: 10.1016/j.fcr.2007.07.008

Dai, J., Wang, Z. H., Li, M. H., He, G., Li, Q., Cao, H. B., et al. (2016). Winter wheat grain yield and summer nitrate leaching: long-term effects of nitrogen and phosphorus rates on the Loess Plateau of China. *Field Crop Res.* 196, 180–190. doi: 10.1016/j.fcr.2016.06.020

Das, S., and Adhya, T. K. (2014). Effect of combine application of organic manure and inorganic fertilizer on methane and nitrous oxide emissions from a tropical flooded soil planted to rice. *Geoderma* 213, 185–192. doi: 10.1016/j.geoderma.2013.08.011

Devevre, O. C., and Horwath, W. R. (2000). Decomposition of rice straw and microbial carbon use efficiency under different soil temperatures and moistures. *Soil Biol. Biochem.* 32, 1773–1785. doi: 10.1016/S0038-0717(00)00096-1

He, P., Li, S., Jin, J., Wang, H., Li, C., Wang, Y., et al. (2009). Performance of an optimized nutrient management system for double-cropped wheat-maize rotations in North-Central China. *Agron. J.* 101, 1489–1496. doi: 10.2134/agronj2009.0099

He, P., Sha, Z., Yao, D., Xing, S., and Zhou, W. (2013). Effect of nitrogen management on productivity, nitrogen use efficiency and nitrogen balance for a wheat-maize system. *J. Plant Nutr.* 36, 1258–1274. doi: 10.1080/01904167.2013.784982

Ju, X. (2014). Direct pathway of nitrate produced from surplus nitrogen inputs to the hydrosphere. *Proc. Natl. Acad. Sci. U.S.A.* 111, E416. doi: 10.1073/pnas.1321334111

Ju, X., Xing, G., Chen, X., Zhang, S., Zhang, L., Liu, X., et al. (2009). Reducing environmental risk by improving N management in intensive Chinese agricultural systems. *Proc. Natl. Acad. Sci. U.S.A.* 106, 3041–3046. doi: 10.1073/pnas.0813417106

Kanakidou, M. (2019). China's nitrogen management. *Nat. Geosci.* 12, 403–404. doi: 10.1038/s41561-019-0358-y

Li, H., Wang, L., Li, J., Gao, M., Zhang, J., Zhang, J., et al. (2017). The development of China-DNDC and review of its applications for sustaining Chinese agriculture. *Ecol. Model.* 348, 1–13. doi: 10.1016/j.ecolmodel.2017.01.003

Li, P., Lu, J., Wang, Y., Wang, S., Hussain, S., Ren, T., et al. (2018). Nitrogen losses, use efficiency, and productivity of early rice under controlled-release urea. *Agric. Ecosyst. Environ.* 251, 78–87. doi: 10.1016/j.agee.2017.09.020

Li, Z., Dong, S., Wang, K., Liu, P., Zhang, J., Wang, Q., et al. (2008). Soil nutrient leaching patterns in maize field under different fertilizations: an in *situ* study. *Chin. J. Appl. Ecol.* 19, 65–70. doi: 10.13287/j.1001-9332.2008.002

Liu, Z., Chen, Z., Ma, P., Meng, Y., and Zhou, J. (2017). Effects of tillage, mulching and N management on yield, water productivity, N uptake and residual soil nitrate in a long-term wheat-summer maize cropping system. *Field Crop Res.* 213, 154–164. doi: 10.1016/j.fcr.2017.08.006

Liu, Y., Tao, Y., Wan, K. Y., Zhang, G. S., Liu, D. B., Xiong, G. Y., et al. (2012). Runoff and nutrient losses in citrus orchards on sloping land subjected to different surface mulching practices in the Danjiangkou Reservoir area of China. *Agr. Water Manage.* 110, 34–40. doi: 10.1016/j.agwat.2012.03.011

Liu, B., Wang, X., Ma, L., Chadwick, D., and Chen, X. (2021). Combined applications of organic and synthetic nitrogen fertilizers for improving crop yield and reducing reactive nitrogen losses from China's vegetable systems: A meta-analysis. *Environ. Pollut.* 269, 116143. doi: 10.1016/j.envpol.2020.116143

Liu, C., and Zheng, H. (2002). South-to-North water transfer schemes for China. *Int. J. Water Resour. D.* 18, 453–471. doi: 10.1080/0790062022000006934

Meng, Q., Yue, S., Hou, P., Cui, Z., and Chen, X. (2016). Improving yield and nitrogen use efficiency simultaneously for maize and wheat in China: a review. *Pedosphere* 26, 137–147. doi: 10.1016/s1002-0160(15)60030-3

Peng, Z., Liu, Y., Li, Y., Abawi, Y., Wang, Y., Men, M., et al. (2017). Responses of nitrogen utilization and apparent nitrogen loss to different control measures in the wheat and maize rotation system. *Front. Plant Sci.* 8. doi: 10.3389/fpls.2017.00160

Qiu, S., Ju, X., Lu, X., Li, L., Ingwersen, J., Streck, T., et al. (2012). Improved nitrogen management for an intensive winter wheat/summer maize double-cropping system. *Soil Sci. Soc Am. J.* 76, 286–297. doi: 10.2136/sssaj2011.0156

Ren, K., Sun, Y., Zou, H., Li, D., Lu, C., Duan, Y., et al. (2023). Effect of replacing synthetic nitrogen fertilizer with animal manure on grain yield and nitrogen use efficiency in China: a meta-analysis. *Front. Plant Sci.* 14. doi: 10.3389/fpls.2023.1153235

Rodríguez, S. B., Alonso-Gaite, A., and Álvarez-Benedí, J. (2005). Characterization of nitrogen transformations, sorption and volatilization processes in urea fertilized soils. *Vadose. Zone. J.* 4, 329–336. doi: 10.2136/vzj2004.0102

Said-Pullicino, D., Cucu, M. A., Sodano, M., Birk, J. J., Glaser, B., and Celi, L. (2014). Nitrogen immobilization in paddy soils as affected by redox conditions and rice straw incorporation. *Geoderma* 228-229, 44–53. doi: 10.1016/j.geoderma.2013.06.020

Sparks, D. L., Page, A. L., Helmke, P. A., Loeppert, R. H., Soltanpour, P. N., Tabatabai, M. A., et al. (1996). Methods of soil analysis part 3: chemical methods. *Soil Sci. Soc. America America Soc. Agron.* doi: 10.2136/sssabookser5.3

Sun, H., Zhang, X., Chen, S., Pei, D., and Liu, C. (2007). Effects of harvest and sowing time on the performance of the rotation of winter wheat-summer maize in the North China Plain. *Ind. Crop Prod.* 25, 239–247. doi: 10.1016/j.indcrop.2006.12.003

Tan, D., Jiang, L., Tan, S., Zheng, F., Xu, Y., Cui, R., et al. (2013). An in *situ* study of inorganic nitrogen flow under different fertilization treatments on a wheat-maize rotation system surrounding Nansi Lake, China. *Agr. Water Manage.* 123, 45–54. doi: 10.1016/j.agwat.2013.03.011

Tang, Q., Ti, C., Xia, L., Xia, Y., Wei, Z., and Yan, X. (2019). Ecosystem services of partial organic substitution for chemical fertilizer in a peri-urban zone in China. *J. Clean. Prod.* 224, 779–788. doi: 10.1016/j.jclepro.2019.03.201

Wang, L., Lu, P., Ren, T., Liu, T., Geilfus, C.-M., and Lu, J. (2020). Improved nitrogen efficiency in winter oilseed rape hybrid compared with the parental lines under contrasting nitrogen supply. *Ind. Crop Prod.* 155, 112777. doi: 10.1016/j.indcrop.2020.112777

Wang, L., Tang, L., Wang, X., and Chen, F. (2010). Effects of alley crop planting on soil and nutrient losses in the citrus orchards of the Three Gorges Region. *Soil Till. Res.* 110, 243–250. doi: 10.1016/j.still.2010.08.012

Wang, L., Xue, C., Pan, X., Chen, F., and Liu, Y. (2018). Application of controlled-release urea enhances grain yield and nitrogen use efficiency in irrigated rice in the Yangtze River Basin, China. *Front. Plant Sci.* 9. doi: 10.3389/fpls.2018.00999

Wang, L., Yuan, X., Liu, C., Li, Z., Chen, F., Li, S., et al. (2019). Soil C and N dynamics and hydrological processes in a maize-wheat rotation field subjected to different tillage and straw management practices. *Agric. Ecosyst. Environ.* 285, 106616. doi: 10.1016/j.agee.2019.106616

Wei, Z., Hoffland, E., Zhuang, M., Hellegers, P., and Cui, Z. (2021). Organic inputs to reduce nitrogen export *via* leaching and runoff: a global meta-analysis. *Environ. Pollut.* 291, 118176. doi: 10.1016/j.envpol.2021.118176

Wei, W., Yan, Y., Cao, J., Christie, P., Zhang, F., and Fan, M. (2016). Effects of combined application of organic amendments and fertilizers on crop yield and soil organic matter: An integrated analysis of long-term experiments. *Agric. Ecosyst. Environ.* 225, 86–92. doi: 10.1016/j.agee.2016.04.004

Yang, X., Lu, Y., Ding, Y., Yin, X., Raza, S., and Tong, Y.a. (2017). Optimising nitrogen fertilisation: A key to improving nitrogen-use efficiency and minimising nitrate leaching losses in an intensive wheat/maize rotation, (2008–2014). *Field Crop Res.* 206, 1–10. doi: 10.1016/j.fcr.2017.02.016

Zhang, F., Cui, Z., Fan, M., Zhang, W., Chen, X., and Jiang, R. (2011). Integrated soil-crop system management: reducing environmental risk while increasing crop productivity and improving nutrient use efficiency in China. *J. Environ. Qual.* 40, 1051–1057. doi: 10.2134/jeq2010.0292

Zhang, X., Davidson, E. A., Mauzerall, D. L., Searchinger, T. D., Dumas, P., and Shen, Y. (2015). Managing nitrogen for sustainable development. *Nature* 528, 51–59. doi: 10.1038/nature15743

Zhang, J., He, P., Ding, W., Ullah, S., Abbas, T., Li, M., et al. (2021a). Identifying the critical nitrogen fertilizer rate for optimum yield and minimum nitrate leaching in a typical field radish cropping system in China. *Environ. Pollut.* 268, 115004. doi: 10.1016/j.envpol.2020.115004

Zhang, X., Sun, Z., Liu, J., Ouyang, Z., and Wu, L. (2018). Simulating greenhouse gas emissions and stocks of carbon and nitrogen in soil from a long-term no-till system in the North China Plain. *Soil Till. Res.* 178, 32–40. doi: 10.1016/j.still.2017.12.013

Zhang, S., Zhang, G., Wang, D., Liu, Q., and Xu, M. (2021b). Investigation into runoff nitrogen loss variations due to different crop residue retention modes and nitrogen fertilizer rates in rice-wheat cropping systems. *Agr. Water Manage.* 247, 106729. doi: 10.1016/j.agwat.2020.106729

Zheng, W., Wan, Y., Li, Y., Liu, Z., Chen, J., Zhou, H., et al. (2020). Developing water and nitrogen budgets of a wheat-maize rotation system using auto-weighing lysimeters: effects of blended application of controlled-release and un-coated urea. *Environ. Pollut.* 263, 114383. doi: 10.1016/j.envpol.2020.114383

frontiers | Frontiers in Plant Science

TYPE Original Research
PUBLISHED 19 January 2024
DOI 10.3389/fpls.2023.1276580

Check for updates

OPEN ACCESS

EDITED BY
Li Wang,
Shandong Academy of Agricultural Sciences, China

REVIEWED BY
Amitava Rakshit,
Banaras Hindu University, India
Oluwaseun Olayemi Aluko,
Henan University, China
Suhas P. Wani,
International Crops Research Institute for the Semi-Arid Tropics (ICRISAT), India

*CORRESPONDENCE
Qianbing Zhang
qbz102@163.com
Chunhui Ma
chunhuima@126.com

RECEIVED 12 August 2023
ACCEPTED 28 December 2023
PUBLISHED 19 January 2024

CITATION
Wei K, Zhao J, Sun Y, López IF, Ma C and Zhang Q (2024) Optimizing nitrogen and phosphorus application to improve soil organic carbon and alfalfa hay yield in alfalfa fields. *Front. Plant Sci.* 14:1276580. doi: 10.3389/fpls.2023.1276580

Optimizing nitrogen and phosphorus application to improve soil organic carbon and alfalfa hay yield in alfalfa fields

Kongqin Wei[1], Junwei Zhao[1], Yanliang Sun[1], Ignacio F. López[2], Chunhui Ma[1*] and Qianbing Zhang[1*]

[1]College of Animal Science and Technology, Shihezi University, Shihezi, Xinjiang, China, [2]School of Agriculture and Environment, Massey University, Palmerston North, New Zealand

Soil organic carbon (SOC) is the principal factor contributing to enhanced soil fertility and also functions as the major carbon sink within terrestrial ecosystems. Applying fertilizer is a crucial agricultural practice that enhances SOC and promotes crop yields. Nevertheless, the response of SOC, active organic carbon fraction and hay yield to nitrogen and phosphorus application is still unclear. The objective of this study was to investigate the impact of nitrogen-phosphorus interactions on SOC, active organic carbon fractions and hay yield in alfalfa fields. A two-factor randomized group design was employed in this study, with two nitrogen levels of 0 kg·ha^{-1} (N_0) and 120 kg·ha^{-1} (N_1) and four phosphorus levels of 0 kg·ha^{-1} (P_0), 50 kg·ha^{-1} (P_1), 100 kg·ha^{-1} (P_2) and 150 kg·ha^{-1} (P_3). The results showed that the nitrogen and phosphorus treatments increased SOC, easily oxidized organic carbon (EOC), dissolved organic carbon (DOC), particulate organic carbon (POC), microbial biomass carbon (MBC) and hay yield in alfalfa fields, and increased with the duration of fertilizer application, reaching a maximum under N_1P_2 or N_1P_3 treatments. The increases in SOC, EOC, DOC, POC, MBC content and hay yield in the 0–60 cm soil layer of the alfalfa field were 9.11%-21.85%, 1.07%-25.01%, 6.94%-22.03%, 10.36%-44.15%, 26.46%-62.61% and 5.51%-23.25% for the nitrogen and phosphorus treatments, respectively. The vertical distribution of SOC, EOC, DOC and POC contents under all nitrogen and phosphorus treatments was highest in the 0–20 cm soil layer and tended to decrease with increasing depth of the soil layer. The MBC content was highest in the 10–30 cm soil layer. DOC/SOC, MBC/SOC (excluding N_0P_1 treatment) and POC/SOC were all higher in the 0–40 cm soil layer of the alfalfa field compared to the N_0P_0 treatment, indicating that the nitrogen and phosphorus treatments effectively improved soil fertility, while EOC/SOC and DOC/SOC were both lower in the 40–60 cm soil layer than in the N_0P_0 treatment, indicating that the nitrogen and phosphorus treatments improved soil carbon sequestration potential. The soil layer between 0-30 cm exhibited the highest sensitivity index for MBC, whereas the soil layer between 30-60 cm had the highest sensitivity index for POC. This suggests that the indication for changes in SOC due to nitrogen and phosphorus treatment shifted from MBC to POC as the soil depth increased. Meanwhile, except the 20–30 cm layer of soil in the N_0P_1 treatment and the 20–50 cm layer in the N_1P_0 treatment, all fertilizers enhanced the soil Carbon management index (CMI) to varying degrees. Structural equation modeling shows that nitrogen and phosphorus indirectly affect SOC content by changing the content of the active organic carbon fraction, and that SOC is primarily impacted by POC and MBC. The comprehensive assessment indicated that the N_1P_2 treatment was the optimal fertilizer application pattern. In summary, the nitrogen and phosphorus treatments improved soil fertility in the 0–40 cm soil layer and soil carbon sequestration potential in the 40–60 cm soil layer of alfalfa fields. In agroecosystems, a recommended application rate of 120 kg·ha^{-1} for nitrogen and 100 kg·ha^{-1} for phosphorus is the most effective in increasing SOC content, soil carbon pool potential and alfalfa hay yield.

KEYWORDS

nitrogen fertilizer, phosphorus fertilizer, soil organic carbon, soil reactive organic carbon, alfalfa, hay yield

1 Introduction

Alfalfa (*Medicago sativa* L.) is a high quality perennial legume forage grass, known as the "king of forage grasses", which not only supports the development of animal husbandry but also plays an important role in ecological restoration and soil quality improvement (Zhang et al., 2009; Li et al., 2019). Nitrogen and phosphorus are the most important mineral elements limiting the growth and development of alfalfa (Gren et al., 2012; Yuan et al., 2020). In field management, fertilizer application is often used to improve alfalfa hay yield and utilization years, but imbalanced fertilization has resulted in lower alfalfa yields and reduced soil quality (Li et al., 2015). Soil organic carbon (SOC) content is not only an important indicator of soil health and fertility, but also plays a dual role as a carbon source and sink in the soil carbon cycle, which is important to the carbon balance of farmland ecosystems and the sustainable and stable use of farmland soils. Long-term inputs of nitrogen and phosphorus have been shown to increase the level of SOC content in alfalfa fields (Gu et al., 2023). Additionally, it has been shown that when nitrogen and phosphorus are applied in the establishment year only, the SOC content of alfalfa fields increases significantly in the second year. However, by the eighth year, the SOC content has decreased to a minimal level. (Wang et al., 2020). Furthermore, high nutrient inputs can impact the production performance of alfalfa (Wang et al., 2023). Therefore, it is necessary to establish appropriate fertilizer application methods to enhance the SOC content and hay yield in alfalfa fields.

The dynamics of SOC are influenced by several factors, including the quantity of nitrogen and phosphorus supplied (Li et al., 2022), the manner of fertilizer application (Govednik et al., 2023) and the type of soil (Yuan et al., 2022). Prior research has indicated that the use of nitrogen has a positive influence on SOC levels and soil fertility (Li et al., 2023). It has been observed that the application of nitrogen fertilizer leads to soil acidification, which hinders the breakdown process of organic carbon. However, it concurrently enhances the stability of SOC (Zeng et al., 2023). Nitrogen application promotes plant carbon input processes and increases SOC accumulation (Xu et al., 2021). The application of nitrogen also induces alterations in the composition of soil microbial communities, hence facilitating the build up of SOC (Tang et al., 2023). Concurrently, the utilization of nitrogen and phosphorus increased the levels of soil nutrients (with initial soil phosphorus levels of 0.45 g·kg^{-1} and 0.76 g·kg^{-1}), which led to the promotion of alfalfa growth and an increase in photosynthetic rates, consequently leading to elevated inputs of soil carbon (Hakl et al., 2021; Sun et al., 2022; Wang et al., 2023). It has been demonstrated that the application of phosphorus has an impact on the content of SOC, but not alter the geographical distribution of SOC fractions. (Hu et al., 2022). In contrast to the application of individual nutrients, the addition of nitrogen and phosphorus not only enhanced soil acidity but also mitigated the nitrogen and phosphorus deficiencies induced by single nutrient inputs. This combined approach had a beneficial synergistic impact on the build up of SOC (Tie et al., 2022). Previous research has demonstrated that the application of nitrogen and phosphorus has distinct effects on SOC content through separate mechanisms. Specifically, nitrogen input facilitates the input of carbon from litter matter, while phosphorus input hinders the decomposition of organic carbon. These processes synergistically contribute to the overall enhancement of SOC sequestration (Zhang et al., 2022a). However, it has also been found that the combination of nitrogen and phosphorus applications enhanced the abundance of SOC degradation genes and promoted the decomposition of SOC (Ye et al., 2023). Nitrogen and phosphorus additions also affect the stoichiometric ratios of carbon, nitrogen, and phosphorus in the soil, as well as the nutrient balance of soil microorganisms. These changes modify the decomposition of SOC by altering the intensity of the priming effect (Qin et al., 2024). Furthermore, the influence of

 10.3389/fpls.2023.1276580

co-applying nitrogen and phosphorus fertilizers on the amounts of SOC in various soil strata exhibits variability. Study has demonstrated that the concurrent utilization of nitrogen and phosphorus fertilizers leads to augment the proportion of SOC in both surface and deep soil layers (Xu et al., 2021). Nevertheless, research has also indicated that employing this approach results in a reduction in SOC content inside the uppermost layer. The decrease in carbon stocks can be ascribed to the rise in microbial biomass and the heightened functioning of carbon-degrading enzymes (Luo et al., 2019). In conclusion, the findings pertaining to the impact of nutrient inputs on SOC sequestration exhibit variability, with a predominant emphasis in prior research on the influence of nutrient inputs on organic carbon levels specifically within the surface soil layer. Previous research has indicated that subsoil has higher carbon stocks than Surface soil (Button et al., 2022), little is known about the changes in subsoil organic carbon due to nitrogen and phosphorus inputs. Therefore, this experiment investigated the changes in SOC content in the 0–60 cm soil layer of an alfalfa field as a result of nitrogen and phosphorus inputs.

SOC may be categorized into active and inert organic carbon based on its stability, where soil active organic carbon is sensitive to fertilizer management and can be a better indicator of early changes in soil quality than SOC (Li et al., 2021c). Soil active organic carbon includes soil microbial biomass carbon (MBC), easily oxidized organic carbon (EOC), dissolved organic carbon (DOC) and particulate organic carbon (POC) (Chen et al., 2016). Study has demonstrated that the application of nitrogen and phosphorus has the capacity to alter the carbon source preferences of soil microorganisms, resulting in an increase in the concentration of active organic carbon. (Li et al., 2021a). However, it has also been found that the use of fertilizer leads to an augmentation in nutrient turnover and expedites the depletion of active organic carbon in the soil (Shi et al., 2022). Previous researchers have developed a soil carbon pool management index (CMI) to assess changes in SOC and reactive organic carbon (Blair et al., 1995). The findings of this study indicate that the CMI exhibits a significant degree of sensitivity to various agricultural land management strategies (Zhu et al., 2015). Hence, it is important to comprehend the alterations in the active organic component of soil and the CMI resulting from various nitrogen and phosphorus treatments. This understanding has significance in the context of organic carbon sequestration and the pursuit of sustainable development in agricultural soils.

The arid region in Northwest China is expansive and ecologically delicate, containing a substantial amount of stored organic carbon. Nevertheless, recent research indicates a decline in the region's SOC content over the last three decades, resulting in diminished soil fertility and crop yields (Zhang et al., 2022b). Therefore, our objective was to establish a fertilization regime that promotes alfalfa hay production and improves SOC sequestration. A 2-year nutrient addition trial was conducted in Shihezi, Xinjiang to investigate (1) the response of SOC and active organic carbon fractions to nitrogen and phosphorus inputs in 0–60 cm soils of alfalfa fields; (2) the contribution of soil active organic carbon fractions to SOC accumulation; and (3) the relationship between alfalfa hay yield, SOC and soil active organic carbon fractions under nitrogen and phosphorus fertilizer supplementation.

2 Materials and methods

2.1 Experimental site

The experimental site is located at the Shihezi University Water-saving Irrigation Experimental Station in Shihezi, Xinjiang (44°20′ N, 88°30′ E), which belongs to the temperate continental arid climate. The average temperature during the growing season of alfalfa is 25°C, the average annual temperature is 8°C, the average annual sunshine duration is 2770 h, the annual frost-free period is 168–171 d, the annual precipitation is 113–170 mm, and the average precipitation during the growing season of alfalfa is 50 mm (mostly concentrated from June to late August). The soil type of the test field is gray desert soil with the following physical and chemical properties: total nitrogen 1.18 g·kg^{-1}, alkaline nitrogen 145.47 mg·kg^{-1}, total phosphorus 0.53 g·kg^{-1}, available phosphorus 19.30 mg·kg^{-1}, available potassium 119.80 mg·kg^{-1}, organic matter 21.56 g·kg^{-1}, bulk weight 1.54 g·cm^{-3}, pH=7.26.

2.2 Experimental design and crop management

The experiment was conducted in a two-factor randomized group design with two levels of nitrogen application: 0 kg·ha^{-1} (N_0) and 120 kg·ha^{-1} (N_1), and four levels of phosphorus application: 0 kg·ha^{-1} (P_0), 50 kg·ha^{-1} (P_1), 100 kg·ha^{-1} (P_2) and 150 kg·ha^{-1} (P_3), respectively. The determination of nitrogen and phosphorus fertilizer inputs was conducted using a field survey. The survey involved selecting fertilizer application rates (N_1 and P_2) that are commonly used in high-yielding local alfalfa fields. These rates were then adjusted by increasing and decreasing them by 50% to establish the appropriate fertilizer application rate. Alfalfa, a leguminous pasture, naturally produces rhizomes that provide nitrogen to the plant (Lagunas et al., 2019). Meanwhile, phosphorus application enhances the development of efficient rhizomes and boosts nitrogen-fixing enzyme activity, resulting in increased fixation of free nitrogen by rhizomes (Schulze et al., 2011). Studies have shown that applying nitrogen does not improve alfalfa yield and instead reduces the plant's nitrogen fixation capacity (Xie et al., 2015). Therefore, only two levels of nitrogen fertilizer were considered necessary. Fertilizer was applied in drips with water 3–5 days after mowing the first, second and third crops. The application of fertilizer occurred on the following dates: 19 April, 25 May, 4 July, and 14 August 2020, as well as 18 April, 27 May, 3 July, and 4 August 2021.

The test alfalfa variety was WL366HQ, which was manually sown in strips on 29 April 2019 with a row spacing of 20 cm, a sowing depth of 2 cm and a sowing rate of 18.0 kg·ha^{-1}. A 1 m wide pedestrian passage was set up between each plot to effectively isolate the fertilizer and water from each other between the plots. The trial employed subsurface drip irrigation as the chosen irrigation method. The drip tape was situated at a height of 10 cm above the ground, aligned with the direction of the alfalfa strips. The drip heads were evenly distributed at a spacing of 20 cm, while each drip strip was positioned at a spacing of 60 cm. The management practices in the field were mostly identical across all plots, with the exception of varying degrees of fertilizer application.

2.3 Sampling and measurements

2.3.1 Soil sample collection

On 30th September 2020 and 24th September 2021, soil samples were collected from the same layer of soil in each plot at 6 different soil depths (0–10 cm, 10–20 cm, 20–30 cm, 30–40 cm, 40–50 cm, 50–60 cm) using a 3 cm diameter soil auger in accordance with the “five-point sampling method”, and the same layer of soil in each plot was mixed evenly and divided into 2 parts to remove visible dead branches and gravel by hand, and then further removed the root system by using a 2 mm sieve. One portion was placed in a self-sealing bag and immediately stored at a low temperature for the determination of MBC and DOC; the other portion was brought back to the laboratory for air drying and used for the determination of SOC, POC and EOC.

2.3.2 Soil sample measurement

SOC content was determined using the potassium dichromate volumetric method with external heating; DOC was determined using the potassium dichromate method; MBC was determined using the chloroform fumigation-leaching method; EOC was determined using the $KMnO_4$ oxidation method; and POC was determined using the sodium hexametaphosphate separation method (Lu, 2000; Jiang et al., 2006; Vieira et al., 2007).

2.3.3 Hay yield measurement

Using the sample method, alfalfa plants of uniform growth were selected at the first flowering stage (around 5% of flowering), and alfalfa plants (1 m × 1 m) within the sample square (leaving a stubble height of 5 cm) were cut with scissors, weighed and recorded, and repeated three times. Three samples of 300 g of fresh alfalfa were taken back to the laboratory. Oven dried at 105°C for 30 min and then dried at 65°C to a constant weight to calculate the moisture content of the alfalfa and further convert the alfalfa dry matter yield.

2.3.4 Soil reactive organic carbon efficiency and sensitivity index

The equation for the effective rate of the soil active organic carbon fraction is (Yu et al., 2020):

$$\text{DOC efficiency rate} = \frac{\text{DOC content}}{\text{SOC content}} \times 100\,\%$$

$$\text{MBC efficiency rate} = \frac{\text{MBC content}}{\text{SOC content}} \times 100\,\%$$

$$\text{EOC efficiency rate} = \frac{\text{EOC content}}{\text{SOC content}} \times 100\,\%$$

$$\text{POC efficiency rate} = \frac{\text{POC content}}{\text{SOC content}} \times 100\,\%$$

Soil active organic carbon fraction sensitivity index was calculated as (Chaudhary et al., 2017):

$$\text{Sensitivity index} = \frac{\text{active organic carbon content} - \text{reference active organic carbon content}}{\text{reference active organic carbon content}} \times 100\,\%$$

Where the measured soil active organic carbon content under the N_0P_0 treatment is used as the reference active organic carbon content.

2.3.5 Carbon management index

The CMI was calculated based on the methods by Blair et al. (1995). In this study, N_0P_0 was used as the reference when calculating the CMI. The calculation is as follows:

$$L = \frac{\text{content of labile SOC}}{\text{content of non—labile SOC}}$$

where L refers to the carbon pool activity. The labile SOC content is expressed by the soil EOC content, and the non-labile SOC content is quantified by subtracting the content of EOC from the total SOC.

$$LI = \frac{\text{L in treatment}}{\text{L in reference}}$$

where LI is the lability index.

$$CPI = \frac{\text{SOC content of treatment}}{\text{SOC content of reference}}$$

where CPI is the carbon pool index.

$$CMI = CPI \times LI \times 100$$

2.4 Data analysis

Data were collated using Microsoft Excel 2021 and data were analyzed for significance using SPSS 26.0. A three-way ANOVA was used to analyze the effects of nitrogen level, phosphorus level and soil depth on SOC, MBC, DOC, EOC, POC, soil reactive organic carbon efficiency, sensitivity index and carbon management index. One-way ANOVA was used to determine the significance ($P< 0.05$) of different nitrogen application treatments at the same phosphorus level and different phosphorus application treatments at the same nitrogen level on the content of SOC, MBC, DOC, EOC and POC, plotted and correlated using Origin 2022. A structural equation model was fitted to the effects of nitrogen application level, phosphorus application level and soil depth on SOC, MBC, DOC, EOC and POC using Amos 24.0 software.

3 Results

3.1 Soil organic carbon content

The nitrogen and phosphorus treatments significantly increased SOC content and varied with soil depth ($P< 0.05$, Table 1; Figure 1). Compared to the N_0P_0 treatment, SOC content in the 0–60 cm soil layer increased by 0.70%-16.32%, 1.09%-17.38%, 1.86%-15.99%, 3.52%-23.42%, 24.89%-58.89% and 23.85%-57.23% under each nitrogen and phosphorus treatment, respectively (Figure 1; Figure 2A). SOC content was significantly greater under the P_2 and P_3 treatments than under the P_0 treatment at the same level of

TABLE 1 Analysis of variance (ANOVA) for the effect of nitrogen level, phosphorus level and soil depth on SOC and soil reactive organic carbon.

Variable	2020					2021				
	SOC ($g \cdot kg^{-1}$)	EOC ($g \cdot kg^{-1}$)	DOC ($g \cdot kg^{-1}$)	POC ($g \cdot kg^{-1}$)	MBC ($g \cdot kg^{-1}$)	SOC ($g \cdot kg^{-1}$)	EOC ($g \cdot kg^{-1}$)	DOC ($g \cdot kg^{-1}$)	POC ($g \cdot kg^{-1}$)	MBC ($g \cdot kg^{-1}$)
Nitrogen(N)	238.94**	0.07^{ns}	45.27**	4047.20**	206.80**	183.62**	293.40**	296.68**	1178.92**	1965.16**
Phosphoric(P)	345.51**	812.95**	86.49**	215.70**	480.03**	426.88**	1368.33**	322.68**	749.09**	1307.77**
Depth(D)	1982.02**	4056.18**	94.20**	4197.37**	2290.87**	3249.15**	3251.31**	554.72**	9074.16**	3607.97**
N×P	9.98**	8.76**	5.31**	35.75**	13.53**	15.91**	277.69**	4.47**	2.76*	69.43**
N×D	13.63**	100.09**	0.26^{ns}	12.91**	5.96**	12.85**	5.18**	0.65^{ns}	61.64**	63.33**
P×D	6.50**	12.32**	1.32^{ns}	9.76**	17.08**	20.22**	12.10**	4.59**	37.72**	20.35**
N×P×D	6.57**	6.15**	0.78^{ns}	14.73**	2.62**	15.67**	28.08**	4.50**	34.47**	19.36**

* denotes P< 0.05, ** denotes P< 0.01, ns denotes P > 0.05. Values in the table are ANOVA statistics (F values). N denotes nitrogen treatment, P denotes phosphorus treatment, D denotes soil depth, SOC denotes soil organic carbon, EOC denotes easily oxidized organic carbon, DOC denotes dissolved organic carbon, POC denotes particulate organic carbon, and MBC denotes microbial biomass carbon.

nitrogen application ($P< 0.05$). Under nitrogen and phosphorus treatments, SOC content was greatest in 2020 under treatment N_1P_2 and highest in 2021 under treatment N_1P_3. Except for the 50–60 cm soil layer in 2020 and the 30–40 cm soil layer in 2021, the differences in SOC content between the N_1P_2 and N_1P_3 treatments were not significant ($P > 0.05$) (Figure 1). The SOC content in 2021 was higher than that in 2020 (Figure 2A).

3.2 Soil reactive organic carbon fraction

3.2.1 Soil easily oxidized organic carbon content

The content of EOC was significantly influenced by nitrogen and phosphorus treatments, soil depth and their interactions ($P< 0.05$, Table 1). In comparison to the N_0P_0 treatment, EOC content in the 0–60 cm soil layer increased by 2.99%-32.93%, -4.85%-31.55%, -13.49%-29.51%, -6.38%-35.52%, -4.45%-48.30% and 0.75%-51.72% under each nitrogen and phosphorus treatment, respectively. Under the N_0 treatment, EOC content of the 0–60 cm soil layer tended to increase with increasing phosphorus application in 2020 and 2021 (except for the 20–30 cm soil layer in 2021), reaching a maximum under the P_3 treatment and significantly greater than the P_0 treatment ($P< 0.05$) (Figure 3). Under the N_1 treatment, EOC content in the 0–60 cm soil layer tended to increase with increasing phosphorus application in 2020, reaching a maximum in the P_3 treatment and significantly greater than in the P_1 and P_0 treatments ($P< 0.05$). The EOC content in all soil layers tended to increase and then decrease in 2021, reaching a maximum in the P_2 treatment and being significantly greater than in the other three treatments ($P< 0.05$). At the same level of phosphorus application, the differences in EOC content between the N_0 and N_1 treatments were significant (except for the P_0 treatment in 2021 and the P_3 treatment in 2020) in the 0–10 cm and 10–20 cm soil layers ($P< 0.05$). EOC content was higher in 2021 than in 2020 and highest in N_1P_2 (Figure 2B).

3.2.2 Soil dissolved organic carbon content

The concentration of DOC was influenced by nitrogen and phosphorus treatments and soil depth (Table 1). In 2020, the application of phosphorus under the N_0 treatment resulted in a pattern of rising and subsequently decreasing DOC content in each soil layer. The highest DOC content was seen under the P_2 treatment, which was substantially larger than the P0 treatment ($P< 0.05$) (Figure 4). The phosphorus application treatment was significantly greater than the P_0 treatment ($P< 0.05$). Furthermore, in the soil layer ranging from 40–60 cm, both the P_2 and P_3 treatments shown considerably higher values compared to the P_0 treatment ($P< 0.05$). Under the N_1 treatment, the P_2 and P_3 treatments significantly increased the soil DOC content of the alfalfa field in 2020 compared to the P_0 treatment ($P< 0.05$), but the difference between the phosphorus treatments was not significant ($P > 0.05$). In 2021, DOC content tended to increase with increasing phosphorus application, reaching a maximum under the P_3 treatment and in the 0–50 cm soil layer, the P_3 treatment was significantly higher than the P_2, P_1 and P_0 treatments ($P< 0.05$). Under the P_3 treatment, DOC content was significantly higher ($P< 0.05$) in the N_1 treatment than in the N_0 treatment in the 0–40 cm and 50–60 cm soil layers in 2020, while the difference between the N_1 and N_0 treatments was not significant ($P > 0.05$) in the 40–50 cm soil layer. Under the other phosphorus treatments, the differences between the nitrogen application treatments were not significant ($P > 0.05$). In the 0–20 cm soil layer in 2021, the differences between N_0 and N_1 treatments were significant ($P< 0.05$), except for the P_2 treatment where the differences between N_0 and N_1 treatments were not significant ($P > 0.05$), and in the 20–30 cm and 40–50 cm soil layers, the differences between N_0 and N_1 treatments were significant ($P< 0.05$) (Figure 4). The mean DOC content showed a trend of increasing, then decreasing and then increasing under the nitrogen and phosphorus treatments. Furthermore, the DOC concentration in 2021 surpassed that of 2020 (Figure 2C).

3.2.3 Soil particulate organic carbon content

The POC content was substantially influenced by the application of nitrogen and phosphorus treatments, as well as the soil depth, and their interaction ($P< 0.05$, Table 1). In the N_0 treatment, the levels of POC in the soil layers at depths of 10–20 cm and 40–50 cm exhibited a pattern of initial increase followed by decrease upon phosphorus

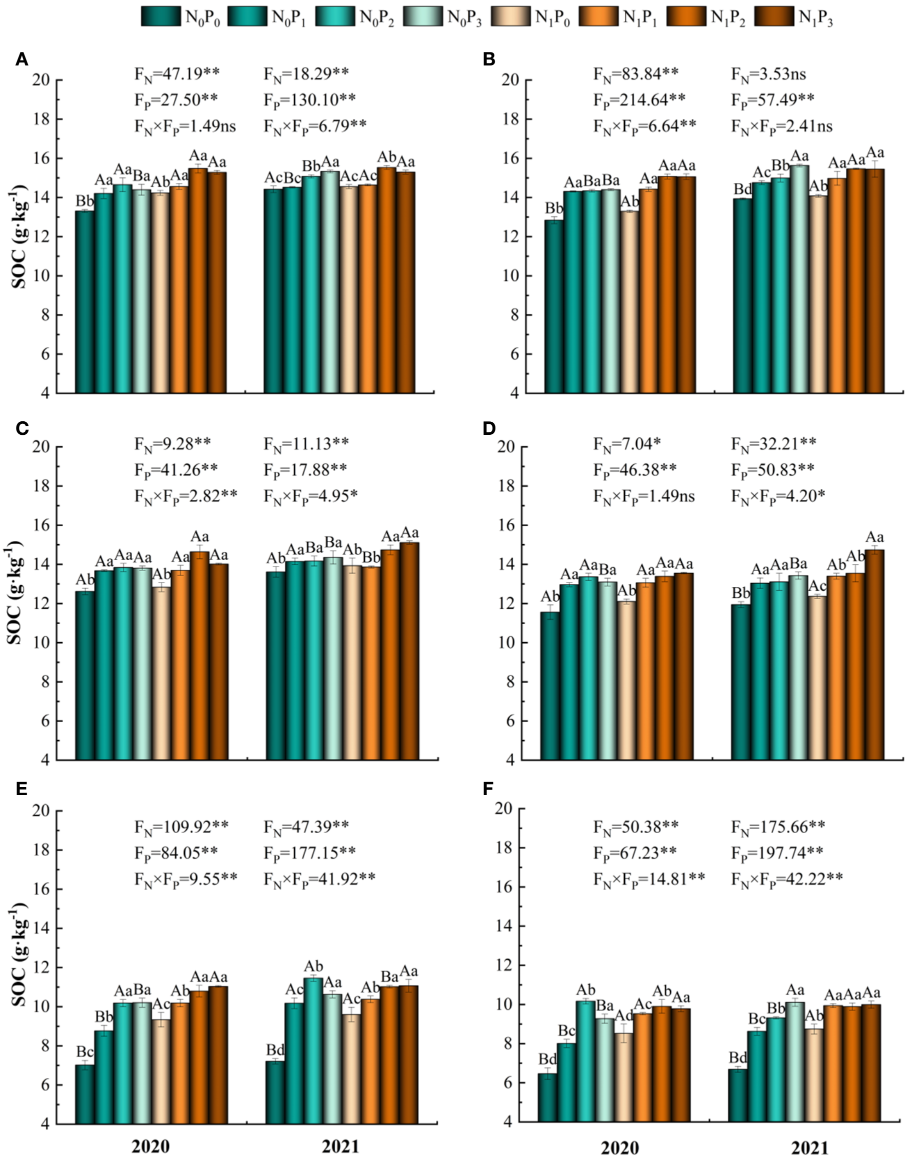

FIGURE 1
SOC content under different nitrogen and phosphorus treatments. Different lowercase letters indicate significant differences ($P< 0.05$) between different phosphorus application treatments at the same level of nitrogen application, and different capital letters indicate significant differences ($P< 0.05$) between different nitrogen application treatments at the same level of phosphorus application. * denotes $P< 0.05$, ** denotes $P< 0.01$ and ns denotes $P > 0.05$. **(A–F)** denote SOC content in the 0–10 cm, 10–20 cm, 20–30 cm, 30–40 cm, 40–50 cm and 50–60 cm soil layers, respectively.

application in both 2021 and 2020. The highest POC content was observed under the P_2 treatment. Conversely, in the other soil layers, POC content showed a gradual increase with phosphorus application, reaching its peak under the P_3 treatment (Figure 5). Under the N_0 treatment, the content of POC in all soil layers was significantly higher under the P_2 and P_3 treatments than under the P_0 treatment ($P< 0.05$). Under the N_1 treatment, the content of POC in the 0–20 cm, 30–40 cm, 50–60 cm, 0–10 cm and 30–40 cm soil layers in 2020 tended to increase and then decrease with increasing phosphorus application in 2021, with the highest content under the P_2 treatment. POC content in the 10–30 cm, 50–60 cm and 40–50 cm soil layers in 2021 and 2020 tended to increase gradually with increasing phosphorus application. Under the N_1 treatment, POC content was significantly higher ($P< 0.05$) in all soil layers under the P_2 and P_3 treatments than under the P_0 treatment, except for the 20–30 cm and 40–50 cm layers in 2020 and 2021. Under the same phosphorus application treatment, POC content was significantly higher ($P< 0.05$) in the 0–60 cm soil layer in 2020 and in the 30–60 cm soil layer in 2021 under treatment N_1 than under treatment N_0. POC content increased, then decreased and then increased again in both years under all nitrogen and phosphorus treatments and was higher in 2021 than in 2020 (Figure 2D).

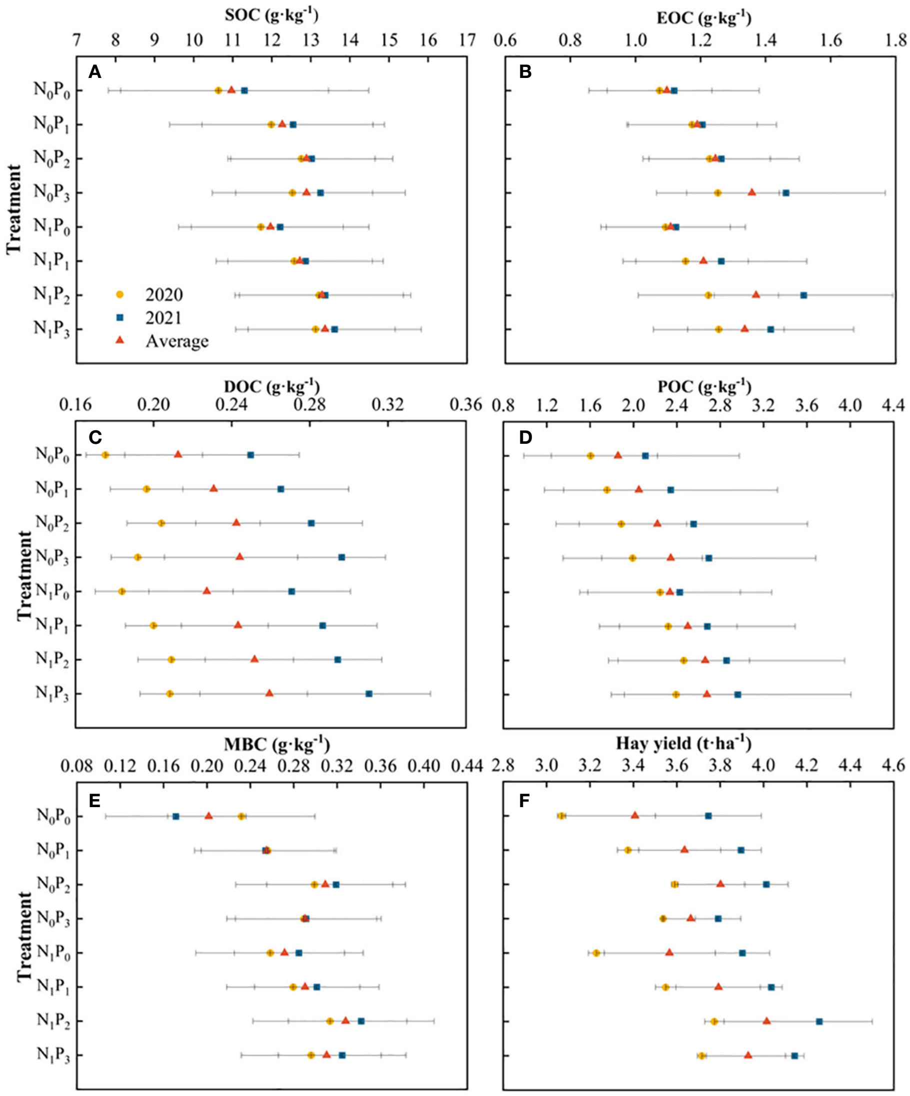

FIGURE 2
Soil organic carbon (SOC), active organic carbon fraction content (EOC、DOC、POC and MBC) and hay yield under different nitrogen and phosphorus treatments. **(A–F)** are represented separately SOC、EOC、DOC、POC、MBC and hay yield. SOC denotes soil organic carbon, EOC denotes readily oxidizable organic carbon, DOC denotes dissolved organic carbon, POC denotes particulate organic carbon, and MBC denotes quantity carbon.

3.2.4 Soil microbial biomass carbon content

Nitrogen and phosphorus treatments, soil depth and their interactions significantly affected MBC content ($P< 0.05$, Table 1). Under the N_0 and N_1 treatments, MBC content in the 0–60 cm soil layer tended to increase and then decrease with increasing phosphorus application (except for the 30–40 cm soil layer in 2020), reaching a maximum under the P_2 treatment, which was significantly greater than the P_0 treatment ($P< 0.05$) (Figure 6). Under the same phosphorus application treatment, MBC content was significantly different between the N_1 and N_0 treatments in 2020 ($P< 0.05$) and was significantly higher in the N_1 treatment than in the N_0 treatment in the 30–60 cm soil layer in 2021 ($P< 0.05$). MBC content in all soil layers was highest in the 10–20 cm soil layer and lowest in the 50–60 cm soil layer. The MBC content tended to increase, then decrease, then increase and then decrease under the nitrogen and phosphorus treatments, with the highest content in the N_1P_2 treatment. Except for the N_0P_0 treatment, MBC content was higher in 2021 than in 2020 (Figure 2E).

3.3 Soil reactive organic carbon efficiency and sensitivity index

Nitrogen application level, phosphorus application level and soil depth significantly affected the effective rate of soil reactive

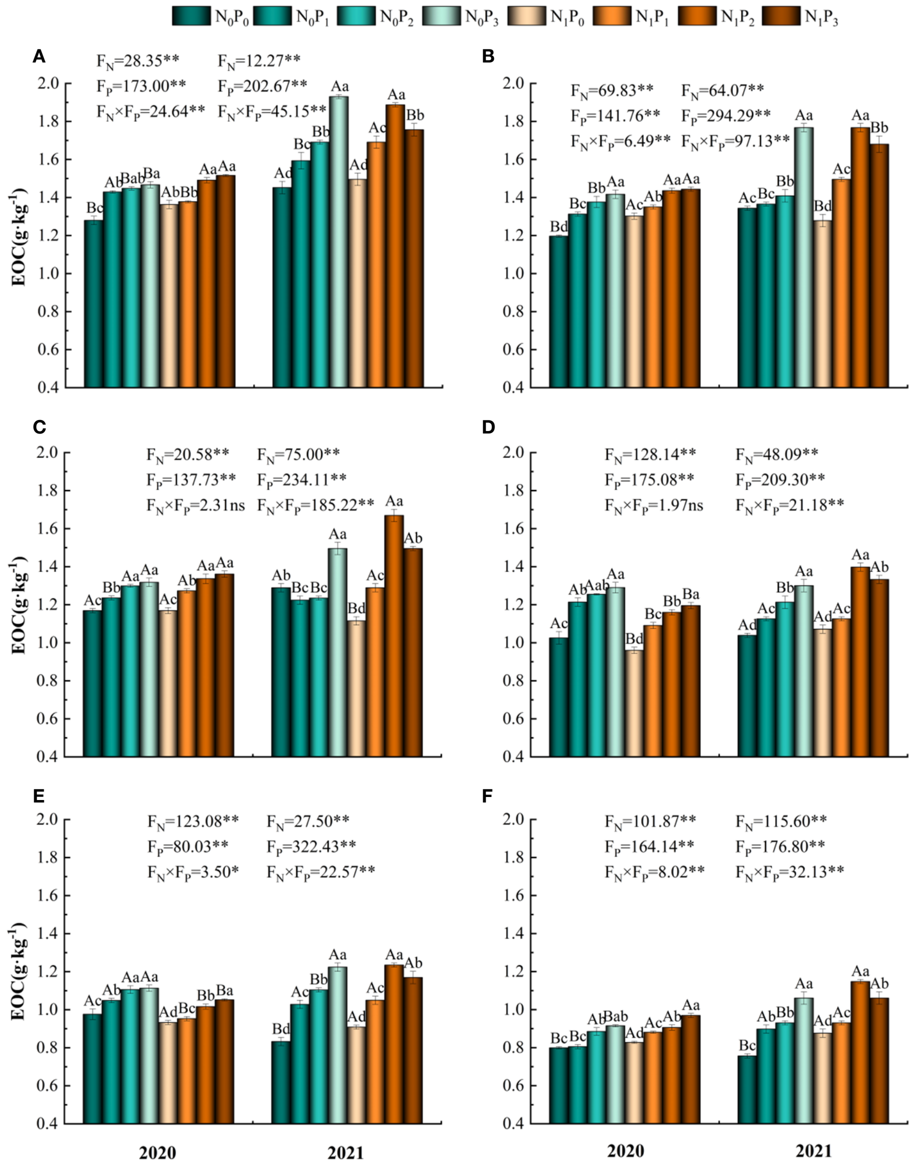

FIGURE 3
Soil easily oxidized organic carbon under different nitrogen and phosphorus treatments. **(A–F)** indicate the easily oxidized organic carbon content of soils in the 0–10 cm, 10–20 cm, 20–30 cm, 30–40 cm, 40–50 cm and 50–60 cm soil layers, respectively. * denotes $P < 0.05$, ** denotes $P < 0.01$ and ns denotes $P > 0.05$.

organic carbon ($P< 0.05$, Table 2), except for the non-significant effect of nitrogen application level on the effective rate of EOC in 2021 and MBC in 2020 ($P > 0.05$). Overall, EOC/SOC, DOC/SOC, POC/SOC and MBC/SOC were higher in the 0–40 cm soil layer than in the N_0P_0 treatment under all nitrogen and phosphorus treatments. In the 40–60 cm soil layer, EOC/SOC and DOC/SOC were lower under nitrogen and phosphorus treatments than under the N_0P_0 treatment (Figure 7). The highest MBC sensitivity index or POC sensitivity index was found under each nitrogen and phosphorus treatment. The soil layers that exhibited the highest sensitivity index for MBC were the 0–10 cm and 20–30 cm layers, whereas the soil layers with the highest sensitivity index for POC were the 10–20 cm and 30–60 cm levels (Figure 8).

3.4 Carbon management index

The carbon pool management index (CPI) was significantly affected by the rate of nitrogen application, phosphorus application, and soil depth ($P< 0.05$, Table 3). Nevertheless, the nitrogen application rate did not have a significant effect on L in 2021 ($P > 0.05$). The L and LI increased in the 0–10 cm soil layer but decreased in the 40–60 cm layer under all fertilizer treatments compared to the N_0P_0 treatment. The CPI was higher in the 0–60 cm soil layer under all fertilizer treatments than in the N_0P_0 treatment. Similarly, the CMI increased to varying degrees under all fertilizer treatments, except for N_0P_1 in the 20–30 cm layer and N_1P_0 in the 20–50 cm layer. The highest CMI was observed under N_1P_2 treatment. Correlation analysis revealed that the

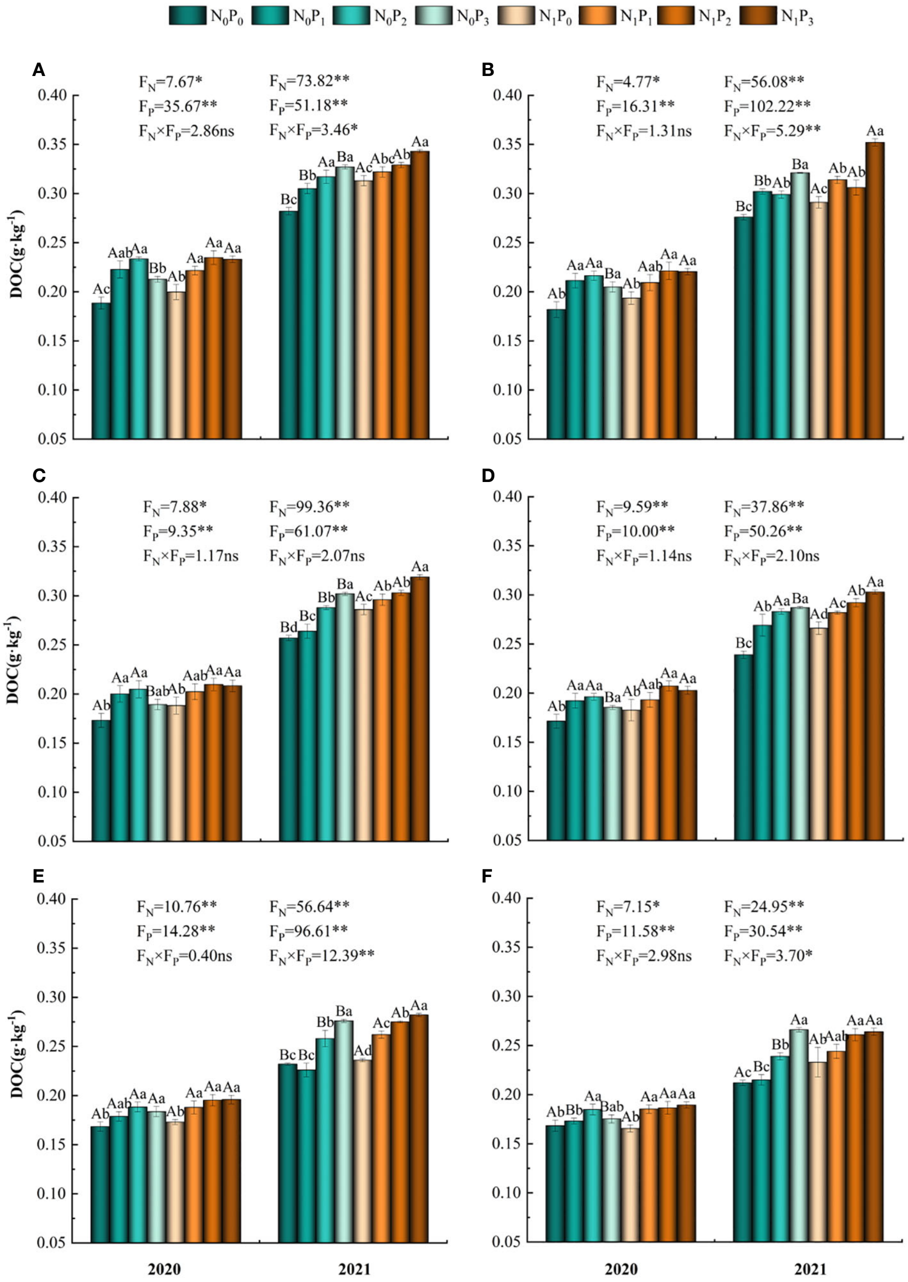

FIGURE 4
Soil dissolved organic carbon content under different nitrogen and phosphorus treatments. **(A-F)** indicate soil dissolved organic carbon content in the 0–10 cm, 10–20 cm, 20–30 cm, 30–40 cm, 40–50 cm and 50–60 cm soil layers, respectively. * denotes $P < 0.05$, ** denotes $P < 0.01$ and ns denotes $P > 0.05$.

L and LI were significantly correlated with EOC, while the CPI and CMI were significantly correlated with SOC (Figure 9).

3.5 Structural equation modeling analysis

The structural equation model shows that the effect of nitrogen and phosphorus on SOC is mainly indirect, and the content of POC and MBC in different soil layers are the main factors affecting its change (Figure 10). In particular, there was no significant effect of nitrogen application on EOC in 2020 ($P > 0.05$), a result consistent with the analysis of variance results. Compared to 2020, the effect of POC content on SOC content increased in 2021, from 0.34 to 0.48, but reduced the effect of MBC content on SOC content, from 0.23 to 0.17.

3.6 Correlation analysis of alfalfa hay yield and measurement indicators

Nitrogen and phosphorus inputs increased hay yield in alfalfa, with the highest hay yield under the N_1P_2 treatment (Figure 2F). Compared to the N_0P_0 treatment, alfalfa hay yield increased by 5.51%, 10.12%, 6.68%, 9.36%, 12.29%, 23.23% and 23.25% under each treatment, respectively (Figure 11). Regression analysis

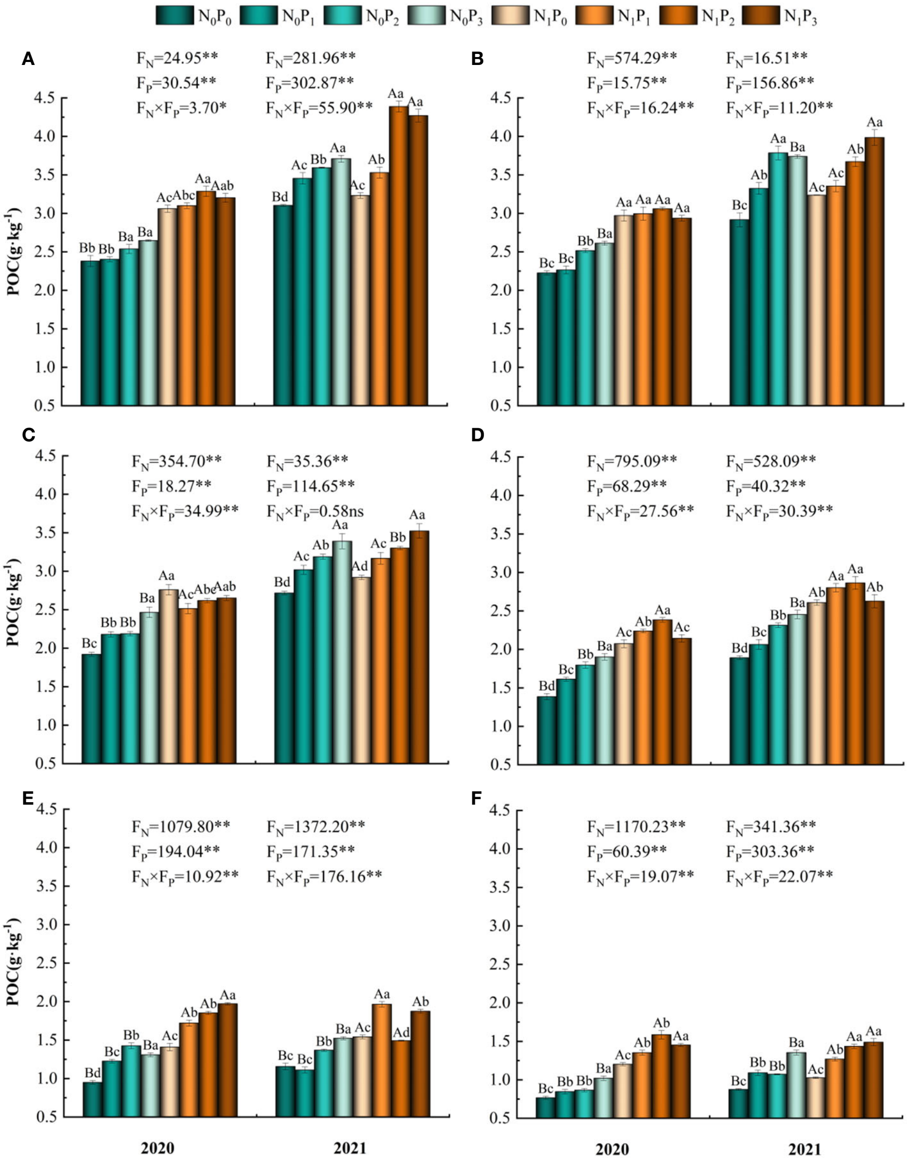

FIGURE 5
Particulate organic carbon content of soil under different nitrogen and phosphorus treatments. **(A-F)** indicate the particulate organic carbon content of soil in the 0–10 cm, 10–20 cm, 20–30 cm, 30–40 cm, 40–50 cm and 50–60 cm soil layers, respectively. * denotes $P < 0.05$, ** denotes $P < 0.01$ and ns denotes $P > 0.05$.

showed that SOC (R^2 = 0.555), DOC (R^2 = 0.791), EOC (R^2 = 0.487), POC (R^2 = 0.727) and MBC (R^2 = 0.310) were each significantly correlated with hay yield (Figure 11).

3.7 Principal component analysis and comprehensive evaluation of measurement indicators

SOC, active organic carbon fractions, CMI and alfalfa hay yield under nitrogen and phosphorus treatments were comprehensively evaluated by principal component analysis, and two principal components with eigenvalues greater than one were extracted, with a cumulative contribution of 83.7%. The principal component analysis showed that the combined scores of each nitrogen and phosphorus treatment were N_1P_2 (2.44) > N_1P_3 (2.01) > N_0P_3 (0.80) > N_0P_2 (0.45) > N_1P_1 (0.30) > N_1P_0 (-1.25) > N_0P_1 (-1.33) > N_0P_0 (-3.43) in order (Figure 12). Therefore, the N_1P_2 treatment was the optimal treatment to improve soil carbon sequestration and alfalfa hay production in alfalfa fields.

4 Discussion

4.1 Effect of nitrogen and phosphorus application on soil organic carbon and alfalfa hay yield in alfalfa fields

The primary contributor to SOC is the carbon inputs from plants, both above and below ground. The application of fertilizers

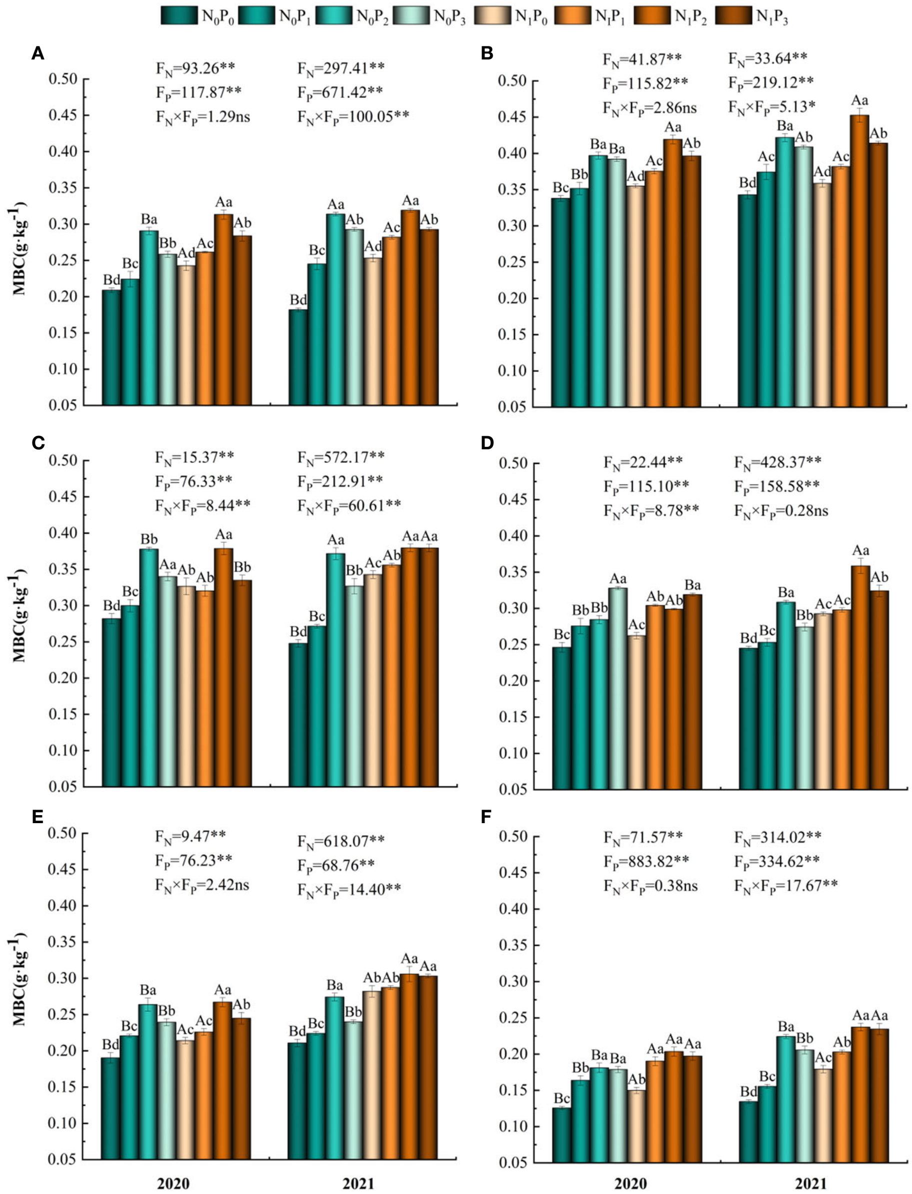

FIGURE 6
Soil microbial biomass carbon content under different nitrogen and phosphorus treatments. **(A–F)** indicate soil microbial carbon content in the 0–10 cm, 10–20 cm, 20–30 cm, 30–40 cm, 40–50 cm and 50–60 cm soil layers, respectively. * denotes $P < 0.05$, ** denotes $P < 0.01$ and ns denotes $P > 0.05$.

has the potential to influence the patterns and processes associated with plant carbon inputs (Ali Shah et al., 2021). The results of this study showed that nitrogen and phosphorus applications increased SOC content. The primary reason may be attributed to the synergistic effect of nitrogen and phosphorus administration, resulting in a significant augmentation of both above-ground and root biomass in plants. Consequently, there is an amplified influx of plant litter and root secretions, thereby facilitating the process of plant carbon input (Shi et al., 2022). Under phosphorus application alone, SOC content tended to increase and then decrease with increasing phosphorus application, whereas under nitrogen and phosphorus combination conditions, SOC content tended to increase gradually. This may be due to the toxic effect of excessive phosphorus input to the soil, which exacerbates soil nitrogen limitation, inhibits plant growth activity and reduces SOC content (Ziehn et al., 2021). Phosphorus alone also exacerbates soil microbial nitrogen limitation and reduces soil microbial abundance, which in turn reduces SOC content (Liu et al., 2023). The application of both nitrogen and phosphorus can alleviate the nutrient limitation resulting from phosphorus alone, increase extracellular enzyme activity, accelerate the rate of decomposition of litter, and increase plant carbon input (Zhang et al., 2022a). Consequently, the sequestration of SOC is increased. However, it has also indicated that nitrogen and phosphorus inputs lead to a decrease in SOC content (Li et al., 2021b). The primary factor is the introduction of nitrogen and phosphorus inputs accelerates the decomposition of SOC by soil microorganisms, resulting in an imbalance between carbon decomposition and accumulation.

TABLE 2 Analysis of variance (ANOVA) on the effect of nitrogen application level, phosphorus application level and soil depth on the efficiency of active organic carbon.

Variable	2020				2021			
	EOC/SOC	DOC/SOC	POC/SOC	MBC/SOC	EOC/SOC	DOC/SOC	POC/SOC	MBC/SOC
Nitrogen(N)	237.77**	18.69**	1601.15**	0.80^{ns}	3.36^{ns}	4.79*	414.13**	406.11**
Phosphoric(P)	26.21**	14.30**	6.90**	58.01**	165.03**	32.93**	82.64**	159.94**
Depth(D)	1125.91**	297.81**	580.83**	621.53**	246.08**	489.02**	1962.65**	495.30**
N×P	16.81**	15.38**	15.43**	3.29*	185.65**	22.74**	9.21**	15.42**
N×D	64.60**	13.91**	4.82**	20.04**	8.65**	14.58**	36.60**	18.71**
P×D	23.08**	11.10**	6.22**	19.22**	15.43**	25.71**	31.00**	31.30**
N×P×D	10.90**	6.95**	16.87**	9.15**	12.13**	24.07**	31.94**	13.44**

* indicates $P< 0.05$, ** indicates $P< 0.01$, ns indicates $P > 0.05$. Values in the table are ANOVA statistics (F values). N represents nitrogen treatment, P represents phosphorus treatment, D represents soil depth, SOC represents soil organic carbon, EOC represents easily oxidized organic carbon, DOC represents dissolved organic carbon, POC represents particulate organic carbon, and MBC represents microbial biomass carbon.

Consequently, this alters the function of the soil carbon pool, shifting it from a carbon sink to a carbon source (Luo et al., 2019). The findings of this study indicate that the 0–20 cm soil layer exhibited the highest SOC content, while the 50–60 cm soil layer had the lowest SOC content. This disparity can be attributed to the accumulation of decomposed plant litter primarily in the surface layer, as well as the limited nutrient input with increasing soil depth. Additionally, the reduced activity of soil microorganisms in the lower layer contributed to a noticeable aggregation of SOC in the vertical distribution (Gao et al., 2021). The results of this study showed that the surface SOC content was higher under the N_1P_2 treatment compared to the other treatments. One aspect to consider is that the N_1P_2 treatment led to the greatest yield of alfalfa, resulting in an increased litter input into the soil, conversely, a balanced nitrogen to phosphorus ratio also enhanced the quality of the litter and promoted its decomposition (Tie et al., 2022). Consequently, this treatment exhibited the highest organic carbon content in the surface soil. This study also revealed that the SOC content was higher in 2021 compared to 2020, mainly due to the increase in SOC content with increasing fertilizer application time (Xu et al., 2021), while the periodic input of litter from alfalfa, a perennial forage grass, also increased SOC content (Wei et al.,

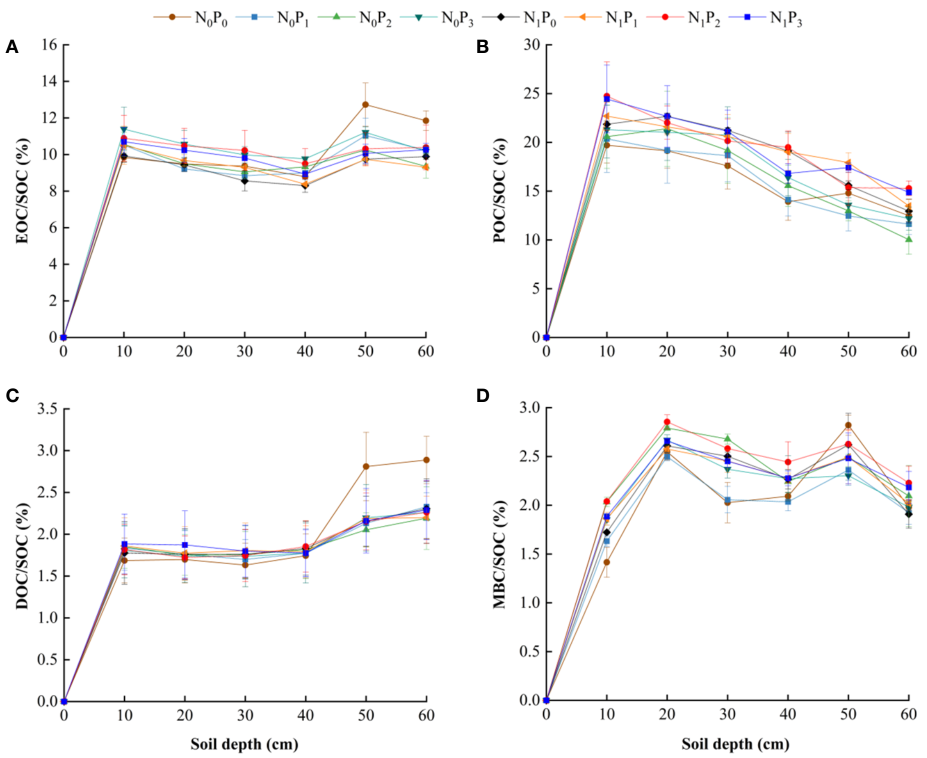

FIGURE 7
Effective rate of soil reactive organic carbon under different nitrogen and phosphorus treatments.

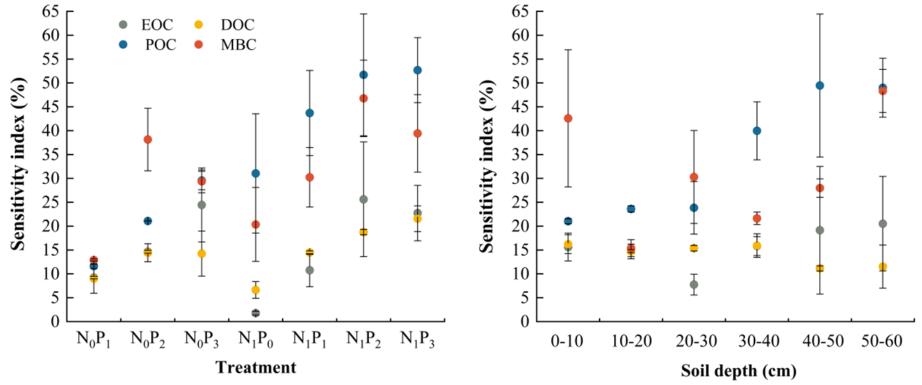

FIGURE 8
Sensitivity indices for soil reactive organic carbon under different nitrogen and phosphorus treatments. EOC indicates easily oxidized organic carbon, DOC indicates dissolved organic carbon, POC indicates particulate organic carbon and MBC indicates microbial biomass carbon.

2022). Therefore, the judicious application of nitrogen and phosphorus significantly affects the spatial and temporal distribution of SOC in alfalfa fields, effectively increasing SOC content and carbon sequestration potential.

In the present study, it was shown that SOC content was significantly correlated with the hay yield of alfalfa (R^2 = 0.555). This is mainly due to the fact that fertilization plays a crucial role in enhancing plant biomass, resulting in an increase in carbon input in both plant roots and shoots. This, in turn, leads to an elevation in SOC (Xu et al., 2021). Moreover, the fluctuations in SOC levels impact the availability of soil nutrients, pH levels, and microbial activity, all of which ultimately influence crop yields (Waqas et al., 2020). In this study, the N_1P_3 treatment exhibited the highest SOC content, while the N_1P_2 treatment resulted in the highest hay yield. These findings align with previous research indicating that a sustained increase in SOC levels may lead to a slight decrease in crop yield (Lin et al., 2023). To maximize SOC sequestration and increase crop yield, the combined analysis showed that the N_1P_2 treatment provided a better balance between SOC content and alfalfa hay yield. Simultaneously, the SOC content is influenced by multiple factors such as management system, soil properties and natural conditions (Lal, 2020), and the best fertilizer application method should be determined according to the specific cropping system.

4.2 Effect of nitrogen and phosphorus application on soil active organic carbon in alfalfa fields

Soil active organic carbon is characterized by high activity, a rapid turnover rate, facile mineralization and decomposition, and the capacity to provide nutrients directly to crops. Its content is influenced by a combination of carbon input processes, such as plant and animal residues and root secretions, and carbon decomposition processes by microorganisms (He et al., 2022). The results of this study showed that the introduction of nitrogen and phosphorus significantly increased the active organic carbon content of the soil, probably because nitrogen and phosphorus addition influenced the decomposition of SOC by changing the diversity and abundance of microorganisms (Li et al., 2021a). In this research, it was found that soil EOC, DOC and POC contents

TABLE 3 Analysis of variance (ANOVA) on the effect of nitrogen application level, phosphorus application level and soil depth on the carbon management index.

Variable	2020				2021			
	L	LI	CPI	CMI	L	LI	CPI	CMI
Nitrogen(N)	239.25**	106.47**	69.23**	4.85*	3.49^{ns}	3.98*	148.55**	136.62**
Phosphoric(P)	27.30**	10.42**	90.01**	240.10**	165.01**	126.23**	316.17**	619.70**
Depth(D)	126.17**	292.81**	160.50**	67.61**	245.80**	183.73**	940.30**	135.81**
N×P	17.97**	5.67**	4.87**	1.66^{ns}	187.14**	130.64**	22.23**	128.87**
N×D	66.27**	23.41**	8.85**	41.79**	8.76**	5.88**	21.63**	4.82**
P×D	23.57**	10.55**	6.58**	5.71**	15.62**	11.98**	35.94**	5.14**
N×P×D	11.43**	4.74**	2.69**	2.16*	12.05**	8.11**	16.07**	8.42**

* denotes $P < 0.05$, ** denotes $P < 0.01$ and ns denotes $P > 0.05$. L represents the carbon pool activity, LI represents the lability index, CPI represents the carbon pool index, CMI represents carbon management index.

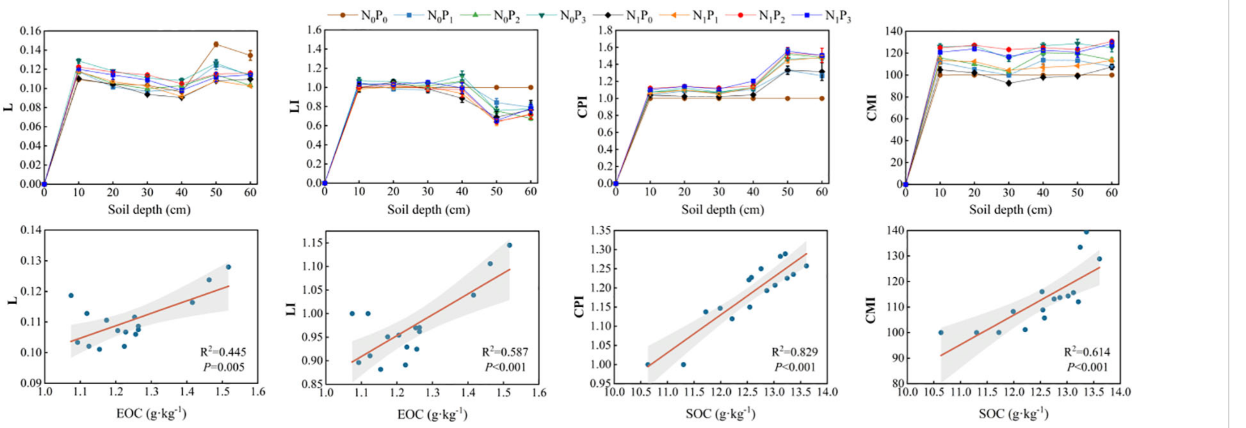

FIGURE 9
Soil carbon pool management index and correlation between carbon pool management index and EOC and SOC under different nitrogen and phosphorus treatments.

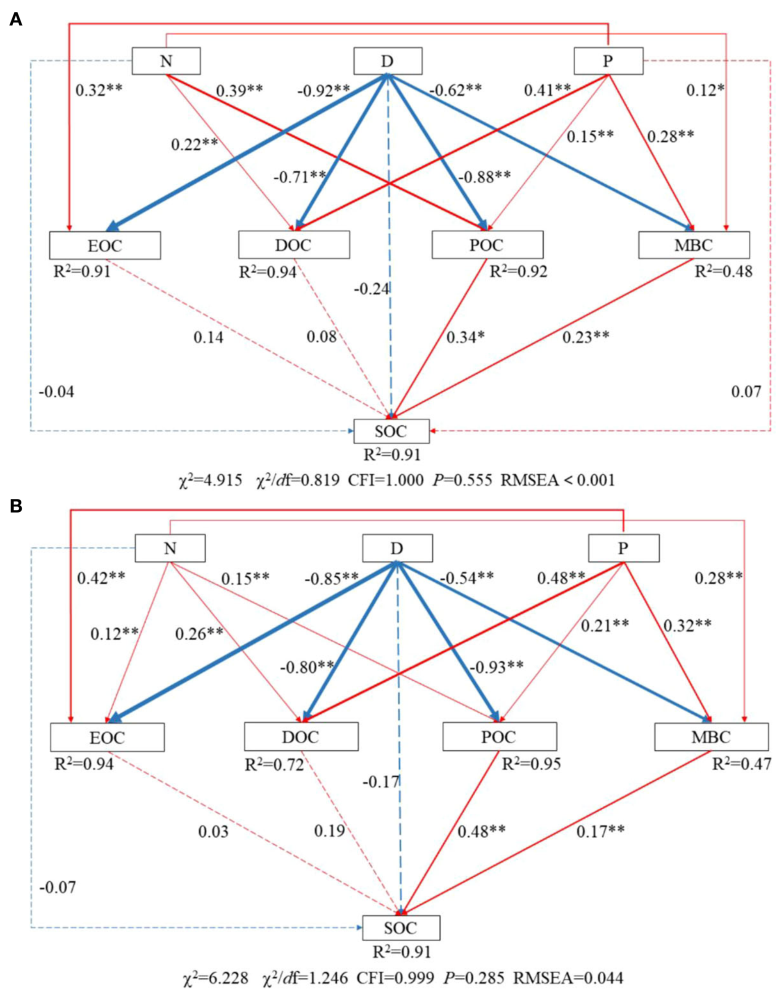

FIGURE 10
Structural equation modeling of the effect of nitrogen and phosphorus treatments on SOC and active organic carbon. **(A)** 2020, **(B)** 2021. The numbers next to the lines are normalized path coefficients, and the thickness of the lines indicates the size of the path coefficients. Red indicates a positive correlation, blue indicates a negative correlation, dashed lines indicate non-significant, and solid lines indicate significant. * indicates $P < 0.05$; ** indicates $P < 0.01$.

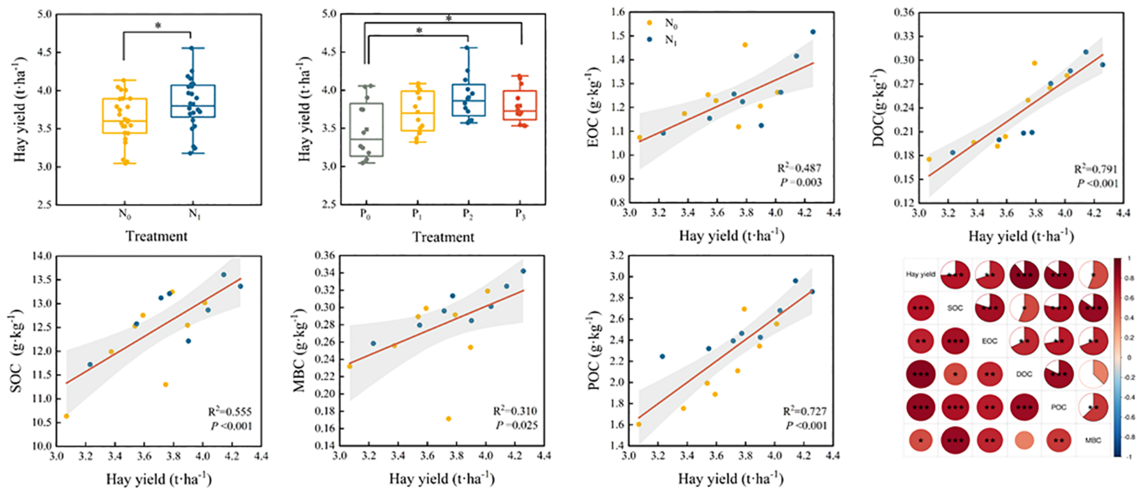

FIGURE 11
Effect of fertilization on hay yield and correlation analysis between hay yield and SOC, DOC, EOC, POC and MBC with hay yield. * indicates a significant level of *P*< 0.05, ** indicates a significant level of *P*< 0.01, *** indicates a significant level of *P*< 0.001.

exhibited their greatest values within the 0–20 cm soil layer when subjected to the same treatment. In addition, these contents exhibited a decreasing trend as the soil depth increased. This is mainly due to the phenomenon that the 0–20 cm soil layer has greater concentration of humus by litter and root secretions, which forms the fixation effect of organic colloids and makes the soil active organic carbon content higher. However, as the soil depth increases, the fixation effect rapidly diminishes (Juhos et al., 2021). MBC is the most active part of soil active organic carbon and is a highly responsive indicator of early soil changes, which originate from soil microorganisms (Patoine et al., 2022). In this research, the highest MBC content was exhibited only in the 10–20 cm soil layer. It can be attributed to the potential influence of climatic conditions on the biomass and activity of soil microorganisms (Jansson and Hofmockel, 2020). Furthermore, the 0–10 cm soil layer was subject to disturbances from the external environment, characterized by persistent dryness and low annual rainfall (Yao et al., 2018). Consequently, the soil microbial population in this layer was found to be relatively low. Simultaneously, the constraining elements for MBC content shifted with increasing soil depth. The study showed that microbial biomass in the upper soil layer was primarily influenced by nitrogen fertilizer and carbon sources. Additionally, the introduction of nitrogen and phosphorus resulted in enhanced nutrient effectiveness and litter input within the 10–20 cm layer, therefore leading to an increase in the abundance and variety of soil microorganisms (Tang et al., 2023). This outcome explains the highest MBC content under the N_1P_2 treatment. In contrast, subsoil microbial biomass was more influenced by soil factors and decreased with increasing soil depth (Sun et al., 2021). The content of soil active organic carbon was

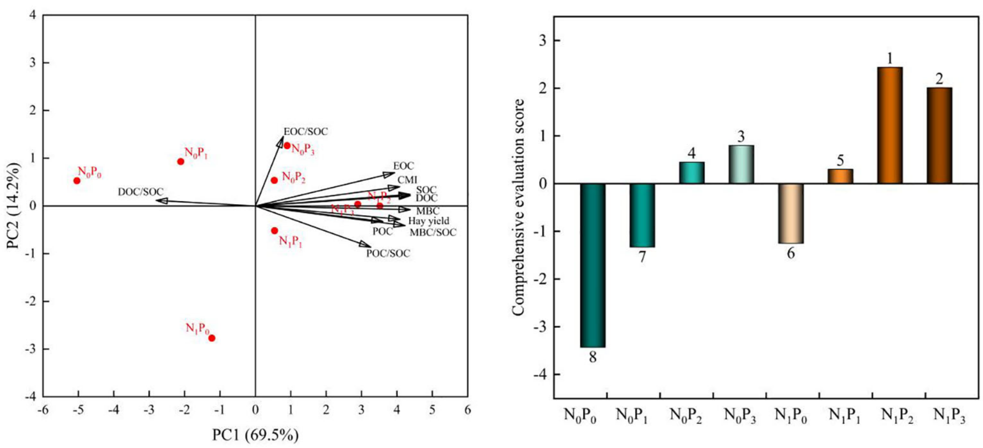

FIGURE 12
Principal component analysis and comprehensive evaluation of the measured indicators under nitrogen and phosphorus treatment. Principal component analysis showed that the eigenvalues of SOC (PC1 = 0.350, PC2 = 0.122) and DOC (PC1 = 0.350, PC2 = 0.108) were similar, so leading to the overlap of the two arrows.

increased to varying degrees by the addition amount and proportion of nitrogen and phosphorus. Furthermore, the extent of this increase was shown to be influenced by the time of fertilizer application.

4.3 Effect of nitrogen and phosphorus application on soil organic carbon efficiency, sensitivity index and carbon management index

The usage of the ratio between soil active organic carbon and SOC provides a more accurate representation of the SOC trend (Qu et al., 2021). The stability of SOC may be inferred by examining the ratio of POC to SOC, likewise, the activity of SOC can be assessed by analyzing the ratio of MBC to SOC (Zhao et al., 2023). The relationship between the ratio of EOC to SOC and the decomposition capacity of SOC can be established. Additionally, the ratio of DOC to SOC may serve as an indicator of the extent of SOC loss (Tang et al., 2010). The results of this study showed that nitrogen and phosphorus inputs increased the ratio of POC to SOC. However, phosphorus application reduced the proportion of POC, in the 40–60 cm soil layer, mainly because the effect of phosphorus fertilization on soil carbon was primarily occurs within the 0–30 cm soil layer, while nitrogen fertilization could affect SOC content in the 0–120 cm soil layer (Zhong et al., 2015). Similarly, it proved that phosphorus fertilization can increase POC content but does not affect its spatial distribution (Hu et al., 2022). The proportion of POC to SOC exhibited the highest values, suggesting that POC made the greatest contribution to SOC. The structural equation modeling also revealed that POC had the highest cumulative effect on SOC. This is consistent with previous findings that POC plays a dominant role in the accumulation of SOC (Qu et al., 2021). Nitrogen and phosphorus inputs increased the ratio of EOC to SOC in the 0–10 cm soil layer, resulting in enhanced SOC activity in the 0–10 cm soil layer, while the ratio of EOC to SOC was lower in the 40–60 cm soil layer than in the N_0P_0 treatment, indicating that nitrogen and phosphorus inputs slowed the decomposition of SOC in the 40–60 cm soil layer, thereby increasing the potential for soil carbon sequestration. Similarly, the proportion of soil DOC to SOC in the 40–60 cm soil layer was also lower than in the N_0P_0 treatment, which further proved that the nitrogen and phosphorus input gave the subsoil a higher carbon sequestration potential (Tang et al., 2010). The sensitivity index is a measure of the soil reactive organic carbon component that exhibits the greatest responsiveness to various nitrogen and phosphorus treatments (Chaudhary et al., 2017). we revealed that the amount and rate of nitrogen and phosphorus additions did not have an equivalent influence on the sensitivity index of soil reactive organic carbon. In the alfalfa field, it was shown that MBC exhibited the greatest degree of responsiveness to nitrogen and phosphorus treatments within the 0–30 cm soil layer. Conversely, the POC was found to be highest in the 30–60 cm soil layer.

Compared with single indicators for evaluating soil fertility, such as SOC, the CMI index can provide a more sensitive evaluation of changes in SOC and serve as a valuable indicator for assessing soil fertility (Mandal et al., 2020; Rai et al., 2023). In this study, the application of nitrogen and phosphorus resulted in an increase in the CMI index within the 0–60 cm soil layer, except for the 20–30 cm soil layer under the N_0P_1 treatment and the 20–50 cm soil layer under the N_1P_0 treatment. This finding further supports the notion that fertilizer application contributes to the accumulation of SOC throughout all soil layers (Zhang et al., 2021). Additionally, the research revealed that L and LI index were higher in the 0–10 cm soil layer compared to the N_0P_0 treatment, while they were lower in the 40–60 cm soil layer under all fertilization treatments. This observation aligns with the previous discussion, indicating that nitrogen and phosphorus inputs enhance the decomposition of organic matter and nutrient cycling in the shallow soil layer (0–10 cm), while promoting the stability of the soil carbon pool in the deeper soil layer (Wang et al., 2015).

5 Conclusion

Nitrogen and phosphorus treatments increased SOC, MBC, POC, DOC, EOC and alfalfa hay yield, and this process increased with the duration of fertilization. However, the effect of different nitrogen and phosphorus treatments varied, with SOC, EOC, DOC, POC, MBC content and alfalfa hay yield all being highest under N_1P_2 or N_1P_3 treatments, increasing by 21.85%, 25.01%, 22.03%, 44.15%, 62.61% and 23.25%, respectively. Meanwhile, the CMI of different soil layers was sensitive to nitrogen and phosphorus additions, with the highest carbon pool management index under the N_1P_2 treatment. The comprehensive evaluation results indicated that the N_1P_2 treatment was the optimal fertilizer application. Structural equation analysis showed that MBC and POC content significantly influenced the accumulation of SOC. Compared with N_0P_0, the nitrogen and phosphorus treatments increased the efficiency of the soil active organic carbon fraction in the 0–40 cm soil layer but decreased the efficiency of the EOC and DOC in the 40–60 cm soil layer, indicating that the nitrogen and phosphorus treatments improved the soil fertility in the 0–40 cm soil layer and the soil carbon sequestration potential in the 40–60 cm soil layer. The highest MBC sensitivity index was found in the 0–30 cm soil layer, and the highest POC sensitivity index was found in the 30–60 cm soil layer. This indicates that as the depth of the soil layer increases, the indicator of SOC change from MBC to POC is changed by nitrogen and phosphorus. In conclusion, the application of appropriate nitrogen and phosphorus treatments in agroecosystems has proven to be a viable strategy for enhancing SOC levels and increasing alfalfa hay yield. Optimal outcomes have been seen when utilizing nitrogen at a rate of 120 kg·ha^{-1} and phosphorus at a rate of 100 kg·ha^{-1}.

Data availability statement

The original contributions presented in the study are included in the article/supplementary material. Further inquiries can be directed to the corresponding authors.

Author contributions

KW: Conceptualization, Data curation, Formal analysis, Investigation, Methodology, Software, Validation, Visualization, Writing – original draft. JZ: Conceptualization, Data curation, Investigation, Writing – review & editing. YS: Conceptualization, Formal analysis, Software, Writing – review & editing. IL: Conceptualization, Writing – review & editing. CM: Conceptualization, Writing – review & editing. QZ: Conceptualization, Funding acquisition, Project administration, Resources, Supervision, Validation, Writing – review & editing.

Funding

The author(s) declare financial support was received for the research, authorship, and/or publication of this article. The work was supported by the National Natural Science Foundation of China (NO. 31660693) and China Agriculture Research System of MOF and MARA.

Conflict of interest

The authors declare that the research was conducted in the absence of any commercial or financial relationships that could be construed as a potential conflict of interest.

Publisher's note

All claims expressed in this article are solely those of the authors and do not necessarily represent those of their affiliated organizations, or those of the publisher, the editors and the reviewers. Any product that may be evaluated in this article, or claim that may be made by its manufacturer, is not guaranteed or endorsed by the publisher.

References

Ali Shah, S. A., Xu, M., Abrar, M. M., Mustafa, A., Fahad, S., Shah, T., et al. (2021). Long-term fertilization affects functional soil organic carbon protection mechanisms in a profile of Chinese loess plateau soil. *Chemosphere* 267, 128897. doi: 10.1016/j.chemosphere.2020.128897

Blair, G., Lefroy, R., and Lisle, L. (1995). Soil carbon fractions based on their degree of oxidation, and the development of a carbon management index for agricultural systems. *Aust. J. Agric. Res.* 46 (7), 1459–1466. doi: 10.1071/AR9951459

Button, E. S., Pett-Ridge, J., Murphy, D. V., Kuzyakov, Y., Chadwick, D. R., and Jones, D. L. (2022). Deep-C storage: Biological, chemical and physical strategies to enhance carbon stocks in agricultural subsoils. *Soil Biol. Biochem.* 170, 108697. doi: 10.1016/j.soilbio.2022.108697

Chaudhary, S., Dheri, G. S., and Brar, B. S. (2017). Long-term effects of NPK fertilizers and organic manures on carbon stabilization and management index under rice-wheat cropping system. *Soil Tillage Res.* 166, 59–66. doi: 10.1016/j.still.2016.10.005

Chen, S., Xu, C., Yan, J., Zhang, X., Zhang, X., and Wang, D. (2016). The influence of the type of crop residue on soil organic carbon fractions: An 11-year field study of rice-based cropping systems in southeast China. *Agric. Ecosyst. Environ.* 223, 261–269. doi: 10.1016/j.agee.2016.03.009

Gao, W., Wang, Q., Zhu, X., Liu, Z., Li, N., Xiao, J., et al. (2021). The vertical distribution pattern of microbial- and plant-derived carbon in the rhizosphere in alpine coniferous forests. *Rhizosphere* 20, 100436. doi: 10.1016/j.rhisph.2021.100436

Govednik, A., Potočnik, Ž., Eler, K., Mihelič, R., and Suhadolc, M. (2023). Combined effects of long-term tillage and fertilisation regimes on soil organic carbon, microbial biomass, and abundance of the total microbial communities and N-functional guilds. *Appl. Soil Ecol.* 188, 104876. doi: 10.1016/j.apsoil.2023.104876

Gren, G. I., Wetterstedt, J. M., and Billberger, M. F. K. (2012). Nutrient limitation on terrestrial plant growth–modeling the interaction between nitrogen and phosphorus. *New Phytol.* 194, 953–960. doi: 10.1111/j.1469-8137.2012.04116.x

Gu, X., Zhang, F., Xie, X., Cheng, Y., and Xu, X. (2023). Effects of N and P addition on nutrient and stoichiometry of rhizosphere and non–rhizosphere soils of alfalfa in alkaline soil. *Sci. Rep.* 13 (1), 12119. doi: 10.1038/s41598-023-39030-8

Hakl, J., Kunzová, E., Tocauerová, Š., Menšík, L., Mrázková, M., and Pozdíšek, J. (2021). Impact of long-term manure and mineral fertilization on yield and nutritive value of lucerne (Medicago sativa) in relation to changes in canopy structure. *Eur. J. Agronomy.* 123, 126219. doi: 10.1016/j.eja.2020.126219

He, X., Sheng, M., Wang, L., Zhang, S., and Luo, N. (2022). Effects on soil organic carbon accumulation and mineralization of long-term vegetation restoration in Southwest China karst. *Ecol. Indic.* 145, 109622. doi: 10.1016/j.ecolind.2022.109622

Hu, A., Huang, R., Liu, G., Huang, D., and Huan, H. (2022). Effects of green manure combined with phosphate fertilizer on movement of soil organic carbon fractions in tropical sown pasture. *Agronomy* 12 (5), 1101. doi: 10.3390/agronomy12051101

Jansson, J. K., and Hofmockel, K. S. (2020). Soil microbiomes and climate change. *Nat. Rev. Microbiol.* 18, 35–46. doi: 10.1038/s41579-019-0265-7

Jiang, P. K., Xu, Q. F., Xu, Z. H., and Cao, Z. H. (2006). Seasonal changes in soil labile organic carbon pools within a Phyllostachys praecox stand under high rate fertilization and winter mulch in subtropical China. *For. Ecol. Management.* 236 (1), 30–36. doi: 10.1016/j.foreco.2006.06.010

Juhos, K., Madarász, B., Kotroczó, Z., Béni, Á., Makádi, M., and Fekete, I. (2021). Carbon sequestration of forest soils is reflected by changes in physicochemical soil indicators — A comprehensive discussion of a long-term experiment on a detritus manipulation. *Geoderma* 385, 114918. doi: 10.1016/j.geoderma.2020.114918

Lagunas, B., Achom, M., Bonyadi-Pour, R., Pardal, A. J., Richmond, B. L., Sergaki, C., et al. (2019). Regulation of resource partitioning coordinates nitrogen and rhizobia responses and autoregulation of nodulation in Medicago truncatula. *Mol. Plant* 12 (6), 833–846. doi: 10.1016/j.molp.2019.03.014

Lal, R. (2020). Food security impacts of the "4 per Thousand". *initiative Geoderma* 374, 114427. doi: 10.1016/j.geoderma.2020.114427

Li, C., Aluko, O. O., Yuan, G., Li, J., and Liu, H. (2023). The responses of soil organic carbon and total nitrogen to chemical nitrogen fertilizers reduction base on a meta-analysis. *Sci. Rep.* 12 (1), 12326. doi: 10.1038/s41598-022-18684-w

Li, J., Han, G., Wang, G., Liu, X., Zhang, Q., Chen, Y., et al. (2022). Imbalanced nitrogen–phosphorus input alters soil organic carbon storage and mineralisation in a salt marsh. *Catena* 208, 105720. doi: 10.1016/j.catena.2021.105720

Li, J. H., Cheng, B. H., Zhang, R., Li, W. J., Shi, X. M., Han, Y. W., et al. (2021a). Nitrogen and phosphorus additions accelerate decomposition of slow carbon pool and lower total soil organic carbon pool in alpine meadows. *Land Degrad. Dev.* 32 (4), 1761–1772. doi: 10.1002/ldr.3824

Li, J. H., Zhang, R., Cheng, B. H., Ye, L. F., Li, W. J., and Shi, X. M. (2021b). Effects of nitrogen and phosphorus additions on decomposition and accumulation of soil organic carbon in alpine meadows on the Tibetan Plateau. *Land Degrad. Dev.* 32 (3), 1467–1477. doi: 10.1002/ldr.3792

Li, Q., Zhou, D., Denton, M. D., and Cong, S. (2019). Alfalfa monocultures promote soil organic carbon accumulation to a greater extent than perennial grass monocultures or grass-alfalfa mixtures. *Ecol. Eng.* 131, 53–62. doi: 10.1016/j.ecoleng.2019.03.002

Li, Y., Li, Z., Cui, S., Liang, G., and Zhang, Q. (2021c). Microbial-derived carbon components are critical for enhancing soil organic carbon in no-tillage croplands: A global perspective. *Soil Tillage Res.* 205, 104758. doi: 10.1016/j.still.2020.104758

Li, Z., Zhao, B., Wang, Q., Qin, X., Zhang, J., and Mao, J. (2015). Differences in chemical composition of soil organic carbon resulting from long-term fertilization strategies. *PloS One* 10 (4), e0124359. doi: 10.1371/journal.pone.0124359

Lin, B., Li, R., Liu, K., Pelumi Oladele, O., Xu, Z., Lal, R., et al. (2023). Management-induced changes in soil organic carbon and related crop yield dynamics in China's cropland. *Glob. Change Biol.* 29 (13), 3575–3590. doi: 10.1111/gcb.16703

Liu, H., Hao, Z., Yuan, Y., Li, C., and Zhang, J. (2023). Application of mineral phosphorus fertilizer influences rhizosphere chemical and biological characteristics. *Arch. Agron. Soil Sci.* 69 (5), 771–784. doi: 10.1080/03650340.2022.2034792

Lu, R. (2000). *Soil Chemical Analysis Method for Agriculture* (Beijing: China Agriculture Science and Technique Press).

Luo, R., Fan, J., Wang, W., Luo, J., Kuzyakov, Y., He, J. S., et al. (2019). Nitrogen and phosphorus enrichment accelerates soil organic carbon loss in alpine grassland on the Qinghai-Tibetan Plateau. *Sci. Total Environ.* 650, 303–312. doi: 10.1016/j.scitotenv.2018.09.038

Mandal, M., Prajnyamayee, K., and Muneshwar, S. (2020). Effect of long term manuring on carbon sequestration potential and dynamics of soil organic carbon labile pool under tropical rice-rice agro-ecosystem. *Commun. Soil Sci. Plant Anal.* 51 (4), 468–480. doi: 10.1080/00103624.2020.1718690

Patoine, G., Eisenhauer, N., Cesarz, S., Phillips, H. R. P., Xu, X., Zhang, L., et al. (2022). Drivers and trends of global soil microbial carbon over two decades. *Nat. Commun.* 13 (1), 4195. doi: 10.1038/s41467-022-31833-z

Qin, W., Feng, J., Zhang, Q., Yuan, X., Zhou, H., and Zhu, B. (2024). Nitrogen and phosphorus addition mediate soil priming effects via affecting microbial stoichiometric balance in an alpine meadow. *Sci. Total Environ.* 908, 168350. doi: 10.1016/j.scitotenv.2023.168350

Qu, X., Wang, X., Wu, J., and He, P. (2021). Both carbon sequestration and yield are related to particulate organic carbon stability affected by organic amendment origins in mollisol. *Journal of Soils and Sediments* 21, 3044–3056. doi: 10.1007/s11368-021-03010-0

Rai, A. K., Basak, N., Dixit, A. K., Rai, S. K., Das, S. K., Singh, J. B., et al. (2023). Changes in soil microbial biomass and organic C pools improve the sustainability of perennial grass and legume system under organic nutrient management. *Front. Microbiol.* 14. doi: 10.3389/fmicb.2023.1173986

Schulze, J., Mohamed, M. A. N., Carlsson, G., and Drevon, J. J. (2011). Phosphorous deficiency decreases nitrogenase activity but increases proton efflux in N_2-fixing Medicago truncatula. *Plant Physiol. Biochem.* 49 (4), 458–460. doi: 10.1016/j.plaphy.2011.01.022

Shi, J., Gong, J., Li, X., Zhang, Z., Zhang, W., Li, Y., et al. (2022). Plant–microbial linkages regulate soil organic carbon dynamics under phosphorus application in a typical temperate grassland in northern China. *Agric. Ecosyst. Environ.* 335, 108006. doi: 10.1016/j.agee.2022.108006

Sun, T., Wang, Y., Lucas-Borja, M. E., Jing, X., and Feng, W. (2021). Divergent vertical distributions of microbial biomass with soil depth among groups and land uses. *J. Environ. Management.* 292, 112755. doi: 10.1016/j.jenvman.2021.112755

Sun, Y., Wang, X., Ma, C., and Zhang, Q. (2022). Effects of nitrogen and phosphorus addition on agronomic characters, photosynthetic performance and anatomical structure of alfalfa in Northern Xinjiang, China. *Agronomy* 12 (7), 1613. doi: 10.3390/agronomy12071613

Tang, G., Li, K., Sun, Y., and Zhang, C. (2010). Soil labile organic carbon contents and their allocation characteristics under different land uses at dry-hot valley. *Environ. Sci.* 31 (5), 1365–1371. doi: 10.13227/j.hjkx.2010.05.041

Tang, S., Ma, Q., Marsden, K. A., Chadwick, D. R., Luo, Y., Kuzyakov, Y., et al. (2023). Microbial community succession in soil is mainly driven by carbon and nitrogen contents rather than phosphorus and sulphur contents. *Soil Biol. Biochem.* 180, 109019. doi: 10.1016/j.soilbio.2023.109019

Tie, L., Hu, J., Peñuelas, J., Sardans, J., Wei, S., Liu, X., et al. (2022). The amounts and ratio of nitrogen and phosphorus addition drive the rate of litter decomposition in a subtropical forest. *Sci. Total Environ.* 833, 155163. doi: 10.1016/j.scitotenv.2022.155163

Vieira, F. C. B., Bayer, C., Zanatta, J. A., Dieckow, J., Mielniczuk, J., and He, Z. L. (2007). Carbon management index based on physical fractionation of soil organic matter in an Acrisol under long-term no-till cropping systems. *Soil Tillage Res.* 96 (1-2), 195–204. doi: 10.1016/j.still.2007.06.007

Wang, W., Cheng, Z. G., Li, M. Y., Wang, B. Z., Li, J. Y., Wang, W., et al. (2020). Increasing periods after seeding under twice-annually harvested alfalfa reduces soil carbon and nitrogen stocks in a semiarid environment. *Land Degradation Dev.* 31 (18), 2872–2882. doi: 10.1002/ldr.3592

Wang, W., Lai, D. Y. F., Wang, C., Pan, T., and Zeng, C. (2015). Effects of rice straw incorporation on active soil organic carbon pools in a subtropical paddy field. *Soil Tillage Res.* 152, 8–16. doi: 10.1016/j.still.2015.03.011

Wang, Y., Tian, S., Shuai, H., Jin, B., Zhang, Y., Wei, J., et al. (2023). Effects of fertilization gradient on the production performance and nutritional quality of cultivated grasslands in karst areas. *Front. Plant Sci.* 14. doi: 10.3389/fpls.2023.1228621

Waqas, M. A., Li, Y., Lal, R., Wang, X., Shi, S., Zhu, Y., et al. (2020). When does nutrient management sequester more carbon in soils and produce high and stable grain yields in China? *Land Degradation Dev.* 31 (15), 1926–1941. doi: 10.1002/ldr.3567

Wei, Y., Xiong, X., Ryo, M., Badgery, W. B., Bi, Y., Yang, G., et al. (2022). Repeated litter inputs promoted stable soil organic carbon formation by increasing fungal dominance and carbon use efficiency. *Biol. Fertil. Soils.* 58 (6), 619–631. doi: 10.1007/s00374-022-01647-8

Xie, K. Y., Li, X. L., He, F., Zhang, Y. J., Wan, L. Q., David, B. H., et al. (2015). Effect of nitrogen fertilization on yield, N content, and nitrogen fixation of alfalfa and smooth bromegrass grown alone or in mixture in greenhouse pots. *J. Integr. Agric.* 14 (9), 1864–1876. doi: 10.1016/S2095-3119(15)61150-9

Xu, C. H., Xu, X., Ju, C. H., Chen, H. Y. H., Wilsey, B. J., Luo, Y. Q., et al. (2021). Long-term, amplified responses of soil organic carbon to nitrogen addition worldwide. *Glob. Change Biol.* 27 (6), 1170–1180. doi: 10.1111/gcb.15489

Yao, X., Zhang, N., Zeng, H., and Wang, W. (2018). Effects of soil depth and plant–soil interaction on microbial community in temperate grasslands of northern China. *Sci. Total Environ.* 630, 96–102. doi: 10.1016/j.scitotenv.2018.02.155

Ye, L. F., Liu, H. Y., Dan Deng, H., Zheng, Y. P., Han, Y. W., Gao, X. T., et al. (2023). Effects of decadal nitrogen and phosphorus fertilization on microbial taxonomic and functional attributes associated with soil organic carbon decomposition and concentration in an alpine meadow. *Ecol. Indic.* 146, 109790. doi: 10.1016/j.ecolind.2022.109790

Yu, Q., Hu, X., Ma, J., Ye, J., Sun, W., Wang, Q., et al. (2020). Effects of long-term organic material applications on soil carbon and nitrogen fractions in paddy fields. *Soil Tillage Res.* 196, 104483. doi: 10.1016/j.still.2019.104483

Yuan, X., Qin, W., Xu, H., Zhang, Z., and Zhu, B. (2020). Sensitivity of soil carbon dynamics to nitrogen and phosphorus enrichment in an alpine meadow. *Soil Biol. Biochem.* 150, 107984. doi: 10.1016/j.soilbio.2020.107984

Yuan, Z. Q., Feng, X. G., Tian, J. Y., Song, X., Li, G. Y., and Fang, C. (2022). Controlling factors of soil organic carbon and nitrogen in lucerne grasslands in a semiarid environment. *Catena* 211, 105983. doi: 10.1016/j.catena.2021.105983

Zeng, W., Wang, Z., Chen, X., Yao, X., Ma, Z., and Wang, W. (2023). Nitrogen deficiency accelerates soil organic carbon decomposition in temperate degraded grasslands. *Sci. Total Environ.* 881, 163424. doi: 10.1016/j.scitotenv.2023.163424

Zhang, T., Wang, Y., Wang, X., Wang, Q., and Han, J. (2009). Organic carbon and nitrogen stocks in reed meadow soils converted to alfalfa fields. *Soil Tillage Res.* 105 (1), 143–148. doi: 10.1016/j.still.2009.06.007

Zhang, X., Lu, S., Wang, C., Zhang, A., and Wang, X. (2021). Optimization of tillage rotation and fertilization increased the soil organic carbon pool and crop yield in a semiarid region. *Land Degrad. Dev.* 32 (18), 5241–5252. doi: 10.1002/ldr.4105

Zhang, J., Zhou, J., Lambers, H., Li, Y., Qin, G., Wang, M., et al. (2022a). Nitrogen and phosphorus addition exerted different influences on litter and soil carbon release in a tropical forest. *Sci. Total Environ.* 832, 155049. doi: 10.1016/j.scitotenv.2022.155049

Zhang, Z., Ding, J., Zhu, C., Shi, H., Chen, X., Han, L., et al. (2022b). Changes in soil organic carbon stocks from 1980-1990 and 2010-2020 in the northwest arid zone of China. *Land Degrad. Dev.* 33 (15), 2713–2727. doi: 10.1002/ldr.4293

Zhao, M., Li, Y., Wang, Y., Sun, Y., and Chen, Y. (2023). High stand density promotes soil organic carbon sequestration in Robinia pseudoacacia plantations in the hilly and gully region of the Loess Plateau in China. *Agric. Ecosyst. Environ.* 343, 108256. doi: 10.1016/j.agee.2022.108256

Zhong, Y., Yan, W., and Shangguan, Z. (2015). Soil organic carbon, nitrogen, and phosphorus levels and stocks after long-term nitrogen fertilization. *CLEAN-Soil Air Water.* 43 (11), 1538–1546. doi: 10.1002/clen.201400872

Zhu, L., Hu, N., Zhang, Z., Xu, J., Tao, B., and Meng, Y. (2015). Short-term responses of soil organic carbon and carbon pool management index to different annual straw return rates in a rice–wheat cropping system. *Catena* 135, 283–289. doi: 10.1016/j.catena.2015.08.008

Ziehn, T., Wang, Y. P., and Huang, Y. (2021). Land carbon-concentration and carbon-climate feedbacks are significantly reduced by nitrogen and phosphorus limitation. *Environ. Res. Lett.* 16 (7), 074043. doi: 10.1088/1748-9326/ac0e62

Frontiers in
Plant Science

Cultivates the science of plant biology and its applications

The most cited plant science journal, which advances our understanding of plant biology for sustainable food security, functional ecosystems and human health.

Discover the latest Research Topics

See more →

Frontiers

Avenue du Tribunal-Fédéral 34
1005 Lausanne, Switzerland
frontiersin.org

Contact us

+41 (0)21 510 17 00
frontiersin.org/about/contact